Southwest Region University Transportation Center

Modeling Driver Behavior During Merge Maneuvers

SWUTC/98/472840-00064-1

Center for Transportation Research
University of Texas at Austin
3208 Red River, Suite 200
Austin, Texas 78705-2650

Technical Report Documentation Page

1. Report No.	2. Government Accession No.	3. Recipient's Catalog No.
SWUTC/98/472840-00064-1		

4. Title and Subtitle	5. Report Date
Modeling Driver Behavior During Merge Maneuvers	September 1997
	6. Performing Organization Code

7. Author(s)	8. Performing Organization Report No.
Cheng-Chen Kou and Randy B. Machemehl	

9. Performing Organization Name and Address	10. Work Unit No. (TRAIS)
Center for Transportation Research The University of Texas at Austin 3208 Red River, Suite 200 Austin, Texas 78705-2650	11. Contract or Grant No. DTOS88-G-0006

12. Sponsoring Agency Name and Address	13. Type of Report and Period Covered
Southwest Region University Transportation Center Texas Transportation Institute The Texas A&M University System College Station, Texas 77843-3135	14. Sponsoring Agency Code

15. Supplementary Notes

Supported by a grant from the U.S. Department of Transportation, University Transportation Centers Program

16. Abstract

The major objective of this study is to develop empirical methodologies for modeling ramp driver acceleration-deceleration and gap acceptance behavior during freeway merge maneuvers. A large quantity of freeway merge data were collected from several entrance ramps including both parallel and taper type acceleration lanes capturing a wide traffic flow range to suite different analysis purposes. Comprehensive freeway merge traffic analyses were conducted using the collected data. Both graphical presentations and independence tests in contingency tables indicated that ramp vehicle approach speeds, freeway flow levels, and speed differentials as well as time or distance gaps between ramp vehicles. Combination forms of these traffic parameters were found to be better indicators for modeling freeway merge driver behavior.

17. Key Words	18. Distribution Statement
Acceleration, Deceleration, Ramp Vehicles, Freeway Merge Process, Merge Position, Merge Acceleration Rate, Lag Vehicles, Lead Vehicles, Speed Differential, Angular Velocity, Calibration	No Restrictions. This document is available to the public through NTIS: National Technical Information Service 5285 Port Royal Road Springfield, Virginia 22161

19. Security Classif.(of this report)	20. Security Classif.(of this page)	21. No. of Pages	22. Price
Unclassified	Unclassified	305	

MODELING DRIVER BEHAVIOR DURING MERGE MANEUVERS

by

Cheng-Chen Kou
Randy Machemehl

Research Report SWUTC/97/472840-00064

Southwest Region University Transportation Center
Center for Transportation Research
The University of Texas at Austin
Austin, Texas 78712

September 1997

Disclaimer

The contents of this report reflect the views of the authors, who are responsible for the facts and the accuracy of the information presented herein. This document is disseminated under the sponsorship of the Department of Transportation, University Transportation Centers Program, in the interest of information exchange. Mention of trade names or commercial products does not constitute endorsement or recommendation for use.

EXECUTIVE SUMMARY

Freeway entrance ramp accelerations and merging processes are complex and have significant impacts upon freeway traffic operations and ramp junction geometric designs. The complexity is a result of the fact that driver psychological components have multiple dimensions affecting freeway merge decisions.

The major objective of this study is to develop empirical methodologies for modeling ramp driver acceleration-deceleration and gap acceptance behavior during freeway merge maneuvers. A large quantity of freeway merge data were collected from several entrance ramps including both parallel and taper type acceleration lanes capturing a wide traffic flow range to suit different analysis purposes. Comprehensive freeway merge traffic analyses were conducted using the collected data. Both graphical presentations and independence tests in contingency tables indicated that ramp vehicle merge behavior is insignificantly related to any single traffic parameter, such as ramp vehicle approach speeds, freeway flow levels, and speed differentials as well as time or distance gaps between ramp vehicles and surrounding freeway and ramp vehicles. Combination forms of these traffic parameters were found to be better indicators for modeling freeway merge driver behavior.

Initially, ramp vehicle acceleration-deceleration behavior models were conceptually formulated as extended forms of conventional nonlinear car-following models incorporating joint freeway and ramp vehicle effects. These sophisticated nonlinear specifications, although theoretically attractive, have been proven to be infeasible to predict dynamic ramp vehicle acceleration-deceleration rates. A bi-level calibration framework, however, successfully provided good calibration results. A multinomial probit model, using speed differentials, distance separations of ramp vehicles to corresponding freeway and ramp vehicles, distance to the acceleration lane terminus, and Markov indexes as attributes, predicted ramp driver acceleration, deceleration, or constant speed choice behavior. The resulting acceleration or deceleration rate magnitudes were predicted by a family of exponential curves using ramp vehicle speed as an explanatory variable. Calibration results of a binary logit gap acceptance function indicated that perceived ramp driver angular velocity to a corresponding freeway lag vehicle and remaining distance to the acceleration lane end are the best gap acceptance decision criteria.

ACKNOWLEDGMENTS

The authors recognize that support was provided by a grant from the U.S. Department of Transportation, University Transportation Centers Program to the Southwest Region University Transportation Center.

ABSTRACT

Methodologies for modeling ramp driver acceleration-deceleration and gap acceptance behavior during freeway merge maneuvers are presented. This study serves an important purpose by pointing to the limitations of current freeway merge models which treat the ramp driver acceleration-deceleration and gap acceptance behavior as deterministic phenomena. In addition, the interdependence of freeway merge behavior and surrounding traffic conditions has been proven to be significant indicating that one should not ignore the linkage of driver behavior and traffic dynamics. Successful calibration of methodologies for modeling freeway merge driver behavior makes this study a valuable asset for further applications.

TABLE OF CONTENTS

LIST OF FIGURES

LIST OF TABLES

CHAPTER 1. INTRODUCTION

PROBLEM STATEMENT

The combination of driver behavior and vehicle capabilities produce observed traffic stream performance. Acceleration-deceleration performance of vehicles in a mixed traffic stream are of great importance. The general classes of acceleration-deceleration phenomena affect the design and analysis of auxiliary lanes adjacent to at-grade intersections, the duration of yellow traffic signal intervals, the analysis of traffic performance at stop sign controlled intersections, and traffic operations at freeway entrance-exit ramps. Appropriate characterization of driver acceleration-deceleration behavior is critical not only for design of traffic facilities but also for traffic operations analysis. Design values of acceleration-deceleration should be updated to reflect the normal capability and behavior of today's vehicle fleet and driver population. Previous research on vehicle acceleration-deceleration performance focused largely on relating vehicle acceleration-deceleration to operational effects. A fundamental behavior oriented approach is not found in the literature.

Acceleration-deceleration driver vehicle behavior has been found to vary depending on the stimulus. That is, if an at-grade intersection traffic signal and a freeway entrance ramp are considered as features causing acceleration, different driver-vehicle performance would naturally be expected. The proposed research will be primarily focused on only one class of the many acceleration-deceleration situations, namely freeway entrance ramp driver-vehicle behavior. This involves acceleration-deceleration characteristics and gap acceptance behavior of ramp drivers on acceleration lanes.

The acceleration and merging process from an entrance ramp to the freeway lanes constitutes an important aspect of freeway traffic operations and ramp junction geometric design. Competing traffic demands for space cause the operational efficiency to influence not only the ramp-freeway junction but also the area upstream of the junction. A ramp driver is required to make a series of decisions and carry out control tasks, all within the capability of the driver to process the information from the roadway and traffic and translate that information into speed and position control responses. It is believed that if the immediately available "gap-structure" is acceptable, the driver of the ramp vehicle accelerates and merges directly. If no gap is immediately available, however, the driver may accelerate to create a merge opportunity, or decelerate and wait for an acceptable later gap. Factors influencing this kind of complex driver behavior consist of both internal factors, such as driver attitude and vehicle characteristics, and external factors, which may

include speed and flow in the freeway stream, lane changing maneuvers in the freeway stream, relative positions of merging vehicles, and proximity of the merging vehicle to the ramp end.

Many studies have been done on gap acceptance models in the last few decades for the purposes of studying delay and capacity at priority intersections and freeway entrance ramps. However, surprisingly few fundamental quantitative investigations address the ramp vehicle's acceleration characteristics in conjunction with gap acceptance behavior in the acceleration lane; therefore challenges exist.

CONCEPTUAL FRAMEWORK

Interactions between freeway vehicles and ramp vehicles which may include lane-changing, unstable car-following , acceleration, possibly deceleration, and gap acceptance have made the operational characteristics of ramp-freeway junctions the most complex issue among overall freeway operations. However, limitations, both in time and budget, prevent this research from performing comprehensive investigations of the complete ramp-freeway junction. Instead, only the ramp vehicle merging behavior along the acceleration lane is of primary concern. The conceptual frameworks to approach this complex issue are illustrated in Figures 1.1 - 1.3.

Figure 1.1 shows a general diagram of the systematic components of the development of a freeway entrance ramp merging behavior model and its possible applications. The environmental factors expected to have effects in calibrating appropriate models can be largely divided into two categories, driver-vehicle factors and roadway factors. The detailed description of environmental factors is discussed in Figure 1.2. Constrained by those environmental factors, the driver decision process can be modeled empirically, analytically, or mathematically corresponding to predetermined decision criteria. Figure 1.3 shows the major components of the driver decision process. Applications of freeway entrance ramp merging behavior models are many. They could range from establishing geometric design issues, such as acceleration lane length, to evaluating overall freeway entrance ramp operations and controls, such as delay incurred by ramp vehicles.

Figure 1.2 depicts some of the environmental factors that are usually used to describe freeway entrance ramp operations. The factors that may have influence on the ramp driver's decision are enormous and cannot be completely included here. The variability of driver-vehicle factors in the merging behavior model is probably one of the most difficult issues. The difficulties stem from the fact that the psychological components of a driver have multiple dimensions and are extremely difficult to analyze quantitatively. Though it is not impossible, studying merging behavior exclusively from the driver-vehicle standpoint normally requires collecting data in

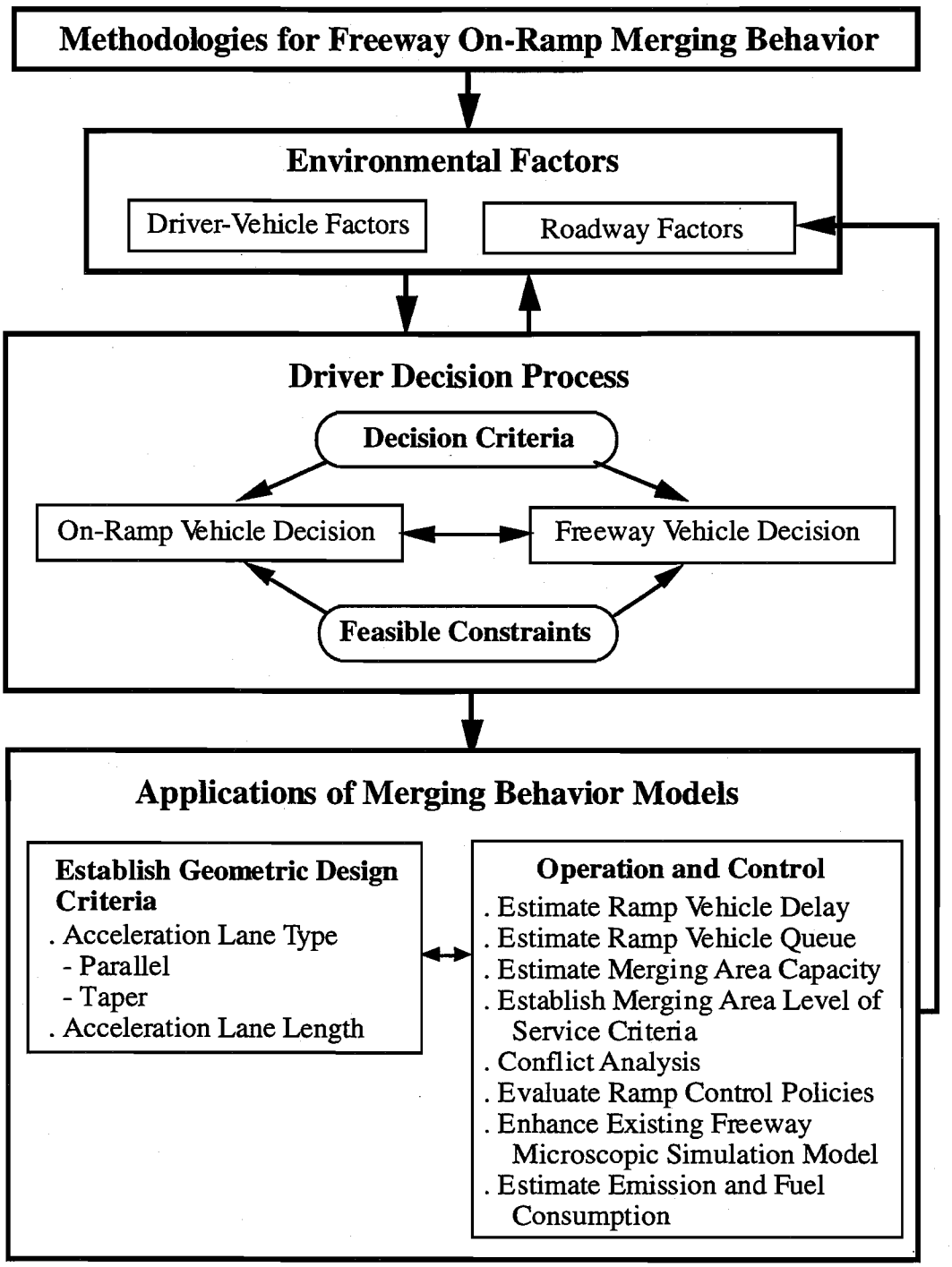

Figure 1.1 Conceptual framework for freeway merge behavior model

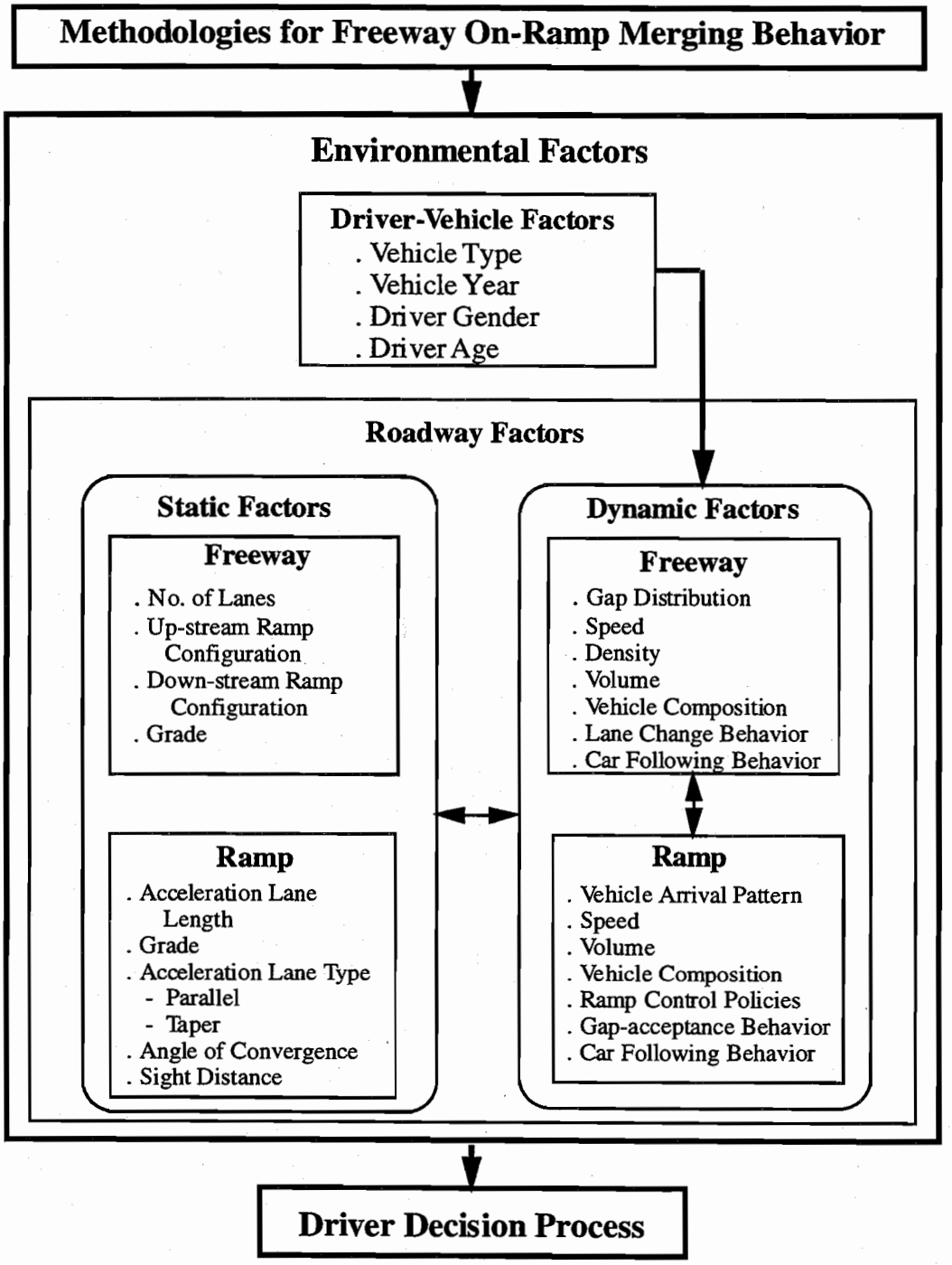

Figure 1.2 Conceptual framework for environmental factors module

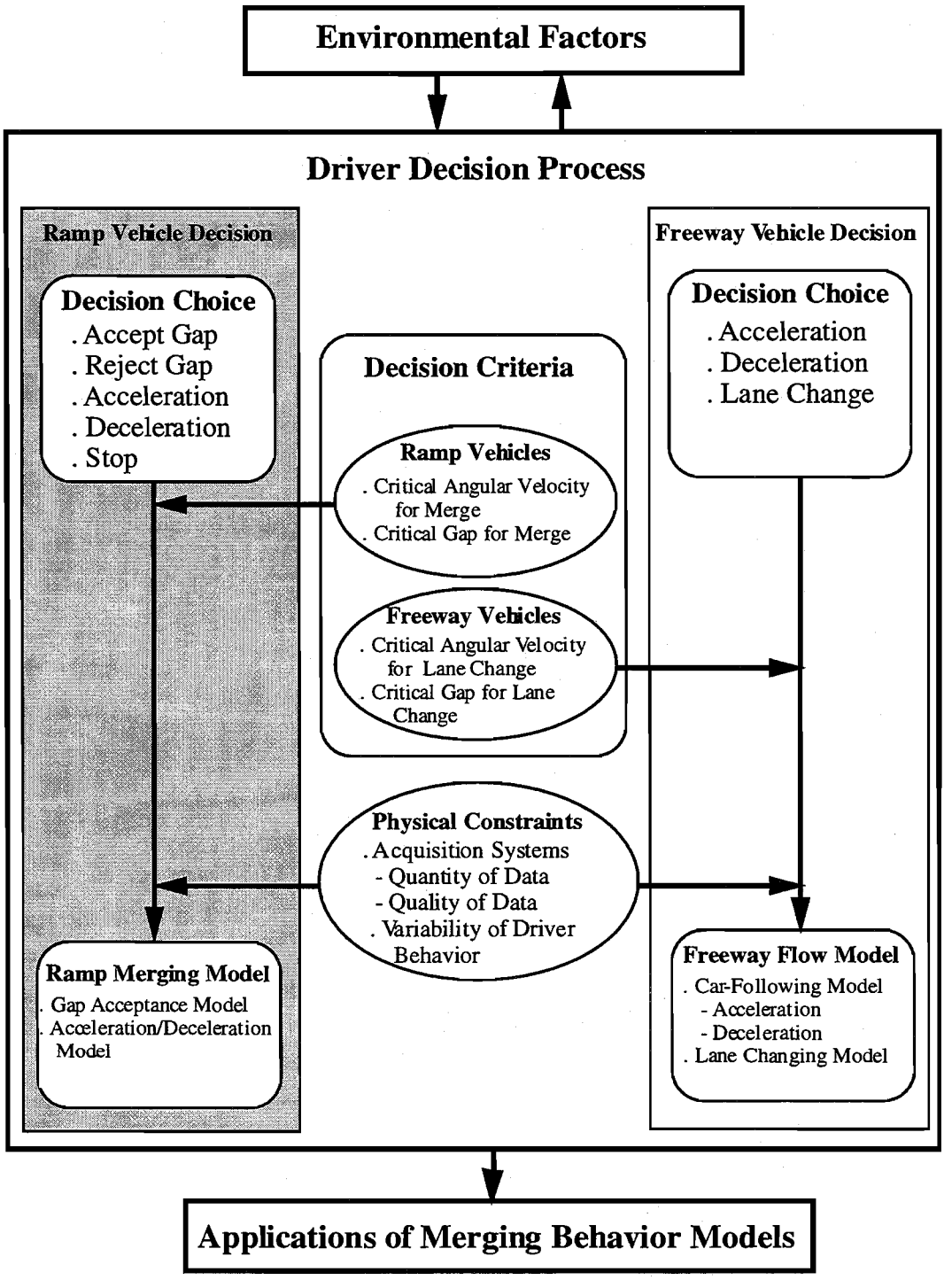

Figure 1.3 Conceptual framework of driver decision process module

conjunction with controlled experiments on the road or with laboratory simulators and is not the subject of the research.

The roadway factors, on the other hand, are those things that a driver can actually see or sense while driving on the entrance ramp. A driver processes information from the roadway and traffic and responds in terms of speed and position control. Although theoretically feasible it is practically impossible to incorporate all the factors depicted in Figure 1.2 into the calibration of a merging behavior model. A more important fundamental issue is how to specify critical information, under a reasonable framework, which a ramp vehicle driver needs, to safely and efficiently accomplish the required lateral and longitudinal positioning, both in space and time.

A driver processes the information, both in roadway and traffic, and responds accordingly based on some decision process which may vary from one driver to another. Details of the decision process for both ramp and freeway vehicle drivers, as well as, associated behavior models that can be derived are shown in Figure 1.3. Normally, ramp drivers and freeway drivers process different information and respond to the vehicle control differently. The decision choices of a ramp driver in the acceleration lane are acceptance or rejection of gaps, acceleration or possibly deceleration, and finally a forced stop if he is approaching the acceleration lane end. Freeway drivers, on the other hand, can detect and evaluate vehicles on the acceleration lane. They can respond by either slowing down to allow the merge or speeding up to prevent the merge. They can also choose to change lanes to reduce the ambiguity. A concept of angular velocity is proposed as the criterion that a ramp driver uses to determine whether a specific gap size is acceptable or not. Adding physical constraints, one can derive the behavior models for ramp drivers and freeway drivers. This research will primarily focus on the study of ramp driver behavior during freeway merge maneuvers.

RESEARCH OBJECTIVE AND STUDY APPROACH

Research Objective

The main objective of this research is to develop empirical methodologies for modeling ramp driver merging behavior in acceleration lanes and provide fundamental elements for analytical or simulation models designed for analyzing freeway entrance ramp operational performance. Items which will be incorporated into this research include traffic volumes, travel speeds of freeway and ramp vehicles, acceleration lane length, and driver-roadway-vehicle interaction.

Key issues to be addressed are as follows:

1) Collect freeway merge traffic and driver behavior data.

Traffic data provide the most fundamental and essential information for insights into the underlying traffic operational phenomena. Since freeway merge maneuvers involve strong vehicle interaction, data collection and reduction procedures applied in this study should be able to capture these dynamic traffic characteristics. These collected data will serve as major input in later freeway merge behavior analyses and model calibration procedures.

2) Develop an in-depth understanding toward the complex freeway merge driver-vehicle behavior.

A ramp driver normally must continuously adjust his/her speed or position with respect to corresponding freeway and ramp vehicles. Furthermore, the natural dynamics of ramp driver merge behavior may cause every driver to respond differently even if exposed to the same freeway-ramp vehicle relationship. Thoroughly understanding this complex driver-vehicle interrelation is essential for developing any meaningful freeway merge behavior model. To achieve this objective, a comprehensive analysis of freeway merge behavior using collected data should be performed.

3) Evolve conceptual methodologies for modeling ramp driver behavior during freeway merge maneuvers

Historically, dynamic ramp driver merge behavior has not been well incorporated in both freeway entrance ramp geometric design and freeway merge analytical as well as simulation models. Even though many researches have recognized the complex nature of merging behavior, they have been forced to make simple assumptions with regard to driver merge behavior because a sophisticated freeway merge behavior model is not available. Therefore, a major objective is to develop methodologies that are potentially applicable to calibrate freeway merge behavior models for different traffic and geometric configurations. This study will focus on developing methodologies for modeling ramp driver acceleration-deceleration and gap acceptance behavior during freeway merge maneuvers.

4) Calibrate conceptual methodologies for modeling driver behavior during freeway merge maneuvers.

Developing a conceptual methodology is not the ultimate end of this study. To ensure the proposed methodologies do catch the freeway merge driver-vehicle dynamics, this study will calibrate respectively the proposed acceleration-deceleration model and gap acceptance model using collected data. The final calibrated models should be simple in their mathematical forms and could be amenable to integration in freeway merge analytical and simulation models. However, the calibrated models are only applicable for the situation observed in the data. A model applicable to other geometric configurations or traffic conditions may be estimated with other suitable data set.

Considerable effort will be placed on actual field data collection and reduction in order to provide clear data to be used in developing reliable models. Due to time considerations of the data collection and reduction process and the need for good data, this research will primarily concentrate on obtaining a reasonable amount of accurate and clear data rather than large quantities.

Study Approach

The study approach follows the structure shown in Figure 1.4. Basically, this study will develop empirically methodologies to model ramp driver acceleration-deceleration and gap acceptance behavior during freeway merge maneuvers. It begins with two fundamental elements: 1) an extensive field survey that results in an unique observation data set describing freeway merge behavior, and 2) the development of a conceptual methodology for modeling ramp driver merge behavior. Freeway merge models which incorporate freeway-ramp driver-vehicle dynamics in the mathematical frameworks are specified and estimated based on these two elements. The major tasks in this approach are as follows:

1) Develop and conduct an extensive data collection plan to capture actual freeway merge behavior.

To collect dynamic traffic data, video taping is the major technique adapted in this study . However, where vehicle trajectory tracking is not required, manual survey methods are used. Considering the resource limitations, data collected in this study will include at least traffic volume, ramp vehicle merge positions, vehicle trajectory data which are used to calculate vehicle speed, acceleration-deceleration as well as angular velocity, and ramp driver gap acceptance/rejection behavior data.

2) Develop conceptual methodologies for modeling freeway merge driver behavior.

Two major freeway merge behaviors are addressed. They are ramp driver acceleration-deceleration and gap acceptance behaviors during merge maneuvers. Mathematical framework of the methodologies for modeling these behaviors should be able to reflect the dynamic nature of vehicle interaction during freeway merge maneuvers. In general, in addition to physical geometric constraints, the ramp vehicle maneuver is mainly influenced by corresponding freeway lag, freeway lead, and ramp lead vehicles if they exist. Therefore, the conceptual methodologies should combine all these potential elements in some mathematical form. These conceptual mathematical frameworks serve as bases for later model calibration. Modifications will be necessary during the model calibration process to best fit the unique data set.

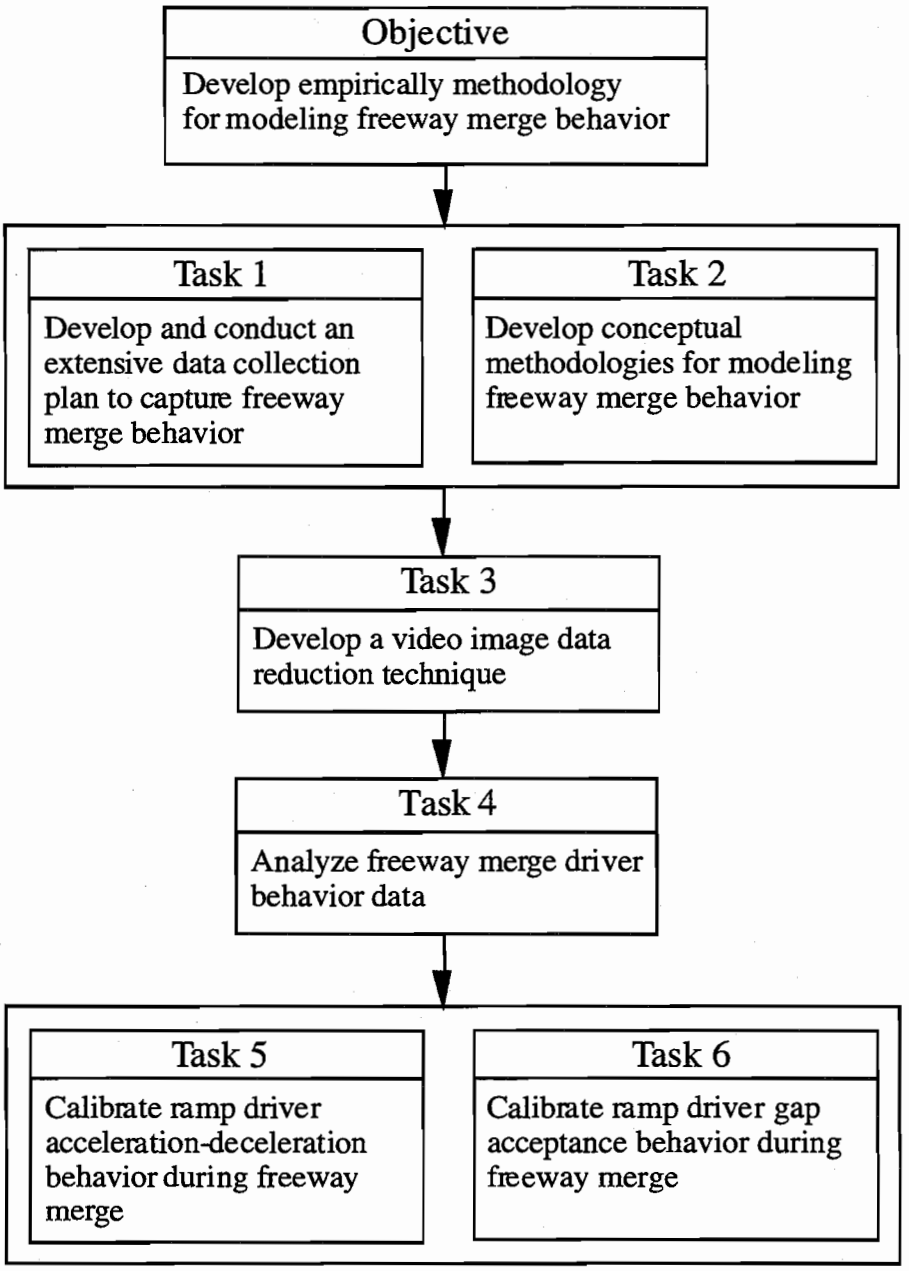

Figure 1.4 The study approach

3) Develop a video image data reduction technique.

To precisely catch dynamic vehicle interaction during freeway merging, one must obtain simultaneous freeway and ramp vehicle trajectory data along the merge area. Reducing vehicle trajectory data from video images is tedious and time consuming because one must playback the videotapes many times to track an individual vehicle. Careful data reduction will be implemented to ensure obtaining good and clear data. Potential speed data measurement errors which are embedded in the video image data reduction technique will also be investigated.

4) Analyze freeway merge driver behavior data.

To develop general dynamic freeway merge behavior knowledge, ramp vehicle merging positions for different freeway and ramp flow levels will be analyzed for various entrance ramp types. For the ramp where vehicle trajectory data are available, merging position with respect to ramp vehicle speed, as well as relative speed and time gap between the ramp vehicle and corresponding freeway vehicles will also be examined. Ramp drivers gap acceptance behavior with respect to merging speed, speed differential between ramp vehicles and corresponding freeway vehicles, and longitudinal distance between ramp vehicles and corresponding freeway vehicles will be investigated. Graphical presentations and statistical tests will be extensively used. Results should provide an in-depth understanding toward the complex freeway merge phenomenon. In addition, this analysis can also serve as a preliminary examination of the conceptual methodology described above.

5) Calibrate ramp driver acceleration-deceleration behavior during freeway merging.

Results from previous efforts should provide evidence for evolving the driver behavior models. Calibration of the freeway merging acceleration-deceleration as well as gap acceptance behavior models is the ultimate objective. Depending on the acceleration-deceleration behavior model structure, techniques applied in this calibration procedure may include classic regression methods for continuous model specification or random utility methods for discrete choice model specification. A pilot study will be performed using a small number of observations. The pilot study can provide feedback to the data collection, data reduction, and model development tasks. The calibrated freeway merge acceleration-deceleration behavior model should have statistical meaning and be easily applied to practical works such as microscopic freeway simulation models.

6) Calibrate a ramp driver freeway merge gap acceptance behavioral model.

When considering a specific freeway gap, a ramp driver will either accept or reject it. Therefore, gap acceptance behavior is readily specified as a binary choice behavioral model. Interaction between freeway and ramp vehicles and entrance ramp geometric configuration, e.g. proximity of the merging vehicle to the ramp end, should be incorporated in the model

specifications. The calibrated gap acceptance model should have statistical meaning and be appropriate for application to freeway merge operational evaluation.

REPORT OVERVIEW

This report is structured as follows. First, the introduction chapter gives an overview of the problem statement, research conceptual framework, research objective and study approach; and principal contributions. A background review of related research in this field is summarized in the second chapter which starts with a glossary of terms used; and is followed by a discussion of the following three topics: 1) freeway merging processes, 2) gap acceptance modeling, and 3) acceleration-deceleration characteristics of ramp vehicles in acceleration lanes. The chapter concludes with the limitations and deficiencies of previous studies.

In the third chapter, the proposed methodology for modeling freeway merge behavior is described. The research methodology includes data collection and reduction techniques, freeway merge behavior data analysis, and methodologies for modeling ramp driver acceleration-deceleration as well as gap acceptance behavior. These three elements are fundamental to the model development. The field data collection is designed to capture detailed dynamic freeway merge driver behavior. The data obtained form the principal observational basis for the behavioral models developed. Potential vehicle speed measurement errors associated with video image data reduction techniques are investigated. Probabilistic functions of time and speed measurement errors are developed to quantify the measurement error magnitude. Ramp vehicle merge positions with respect to freeway and entrance ramp flow levels and corresponding freeway vehicle movements are analyzed. Ramp driver gap acceptance behavior is investigated relating accepted gap size, accepted angular velocity, and merging speed differential with freeway vehicles to the merging positions. Statistical analysis and graphical presentation are extensively used. These analyses allow one to examine the ramp driver merging decision mechanisms in response to the variability of dynamic vehicle interaction and provide fundamental knowledge for evolution of the mathematical freeway merge behavior model frameworks.

The fundamental stimulus-response rule of conventional car following models is extended to formulate ramp vehicle acceleration-deceleration behavior during freeway merging. The response is specified as vehicle acceleration-deceleration performance while the stimulus could be a combination of speed differential, longitudinal distance, and speed. Recognizing the serial correlation property associated with successive acceleration-deceleration observations, a Generalized Least Square(GLS) technique is proposed as a calibration tool. The theoretical framework of the GLS technique is developed by specifying the within driver observational error

terms follow a first-order autoregressive equation. Ramp driver gap acceptance behavior is formulated as a binary choice equation which incorporates relative vehicle movement, or more precisely, angular velocity, and proximity of the merging vehicle to the ramp end. This formulation leads to the development of a critical angular velocity equation as a function of the number of gaps being rejected and remaining distance to ramp end. The mathematical framework developed in this chapter is provided as a basis for later model calibration.

Based on the proposed research methodology, a pilot preliminary calibration is performed using a small number of observations collected at a short parallel type entrance ramp. The results are presented in the fourth chapter and they serve as evidence of the suitability of the proposed methodology.

Chapter five is devoted to calibration of the ramp vehicle acceleration-deceleration behavior model. More freeway merge behavior data are collected at a long taper type entrance ramp in Houston Texas and are used in this calibration task. Similar to the works of the pilot study, a nonlinear regression technique is used as a calibration tool for various function specifications. Discouraging nonlinear regression results, however, guide one to an alternative bi-level methodology framework. This approach is believed to be more practically applicable since a driver will make an acceleration/deceleration decision in response to surrounding freeway and ramp vehicle movement. The actual acceleration or deceleration rates, however, may depend on other driver-vehicle characteristics, e.g. vehicle speed. Consequently, the first level of this approach formulates ramp driver acceleration-deceleration decisions using a discrete choice behavioral framework with three choice alternatives which are acceleration, maintain current speed, and deceleration. A recently developed multinomial probit (MNP) model parameter estimation program (Lam, 1991; Liu, 1996), allowing more general specifications, is used. The second level, on the other hand, develops continuous acceleration and deceleration models respectively which can be used to predict acceleration and deceleration rates. A regression technique is applied in this level to obtain the parameter estimates.

Calibration of the ramp driver gap acceptance behavior model is presented in the sixth chapter. Because the data sets contain very few gap rejections, the original model which incorporated the number of gaps being rejected in the mathematical framework is modified. Binary probit and logit models are used respectively to find the best fit model.

The last chapter summarizes the major findings and conclusions of this study together with future research directions.

PRINCIPAL CONTRIBUTIONS

The principal contributions of this research are briefly highlighted as follows:

1) Development of probability density functions to quantify recording time and speed data accuracy when reduced from video images. These functions provide a very useful tool which allows surveyors to evaluate in advance the probability of occurrence of certain measurement error magnitudes associated with a data survey scheme and to adjust the data collection plan accordingly.

2) Provision of an in-depth understanding of dynamic freeway merge behavior. This knowledge is fundamental to any advanced study on freeway merge driver behavior.

3) Provision of ramp driver behavior information which is potentially applicable to verify AASHTO freeway entrance ramp design criteria.

4) Successful discrete and continuous models application for calibrating ramp driver acceleration-deceleration behavior. This approach is believed to be more practical in terms of describing driver decision mechanisms.

5) Development of methodologies for modeling ramp driver acceleration-deceleration as well as gap acceptance behavior applicable to enhance existing micro level freeway simulation models. Significant contributions in the following subjects could be achieved by using these enhanced simulation models:

- establishment of new design criteria for freeway entrance ramp design speed and acceleration lane length;
- estimation of ramp vehicle merging delay;
- estimation of merging area fuel consumption and emission;
- evaluation of freeway entrance ramp operational performance;
- design of freeway entrance ramp control strategies.

CHAPTER 2. BACKGROUND AND LITERATURE REVIEW

INTRODUCTION

The freeway on-ramp merging process has been studied since the 1940's. Research on several elements of ramp driver behavior during the merging process has been performed, but has focused mainly on gap acceptance/rejection and its applications, such as merging vehicle delay or queue length. Few efforts have examined other driver behavior aspects, such as ramp vehicle acceleration during the merging process. This chapter is designed to give a systematic and comprehensive review of the subjects related to freeway ramp driver behavior during merging.

In this chapter, the following topics will be reviewed and discussed. First, the definitions of major terms that will be frequently used are given. Second, the general description of the merging process along freeway on-ramps will be reviewed. Third, ramp vehicle gap acceptance models along with their applications will be discussed, followed by reviews of ramp vehicle acceleration characteristics. Finally, deficiencies and limitations of previous studies will be addressed.

GLOSSARY OF TERMS

AASHTO - American Association of State Highway and Transportation Officials.

AASHTO Guide - A Policy on Geometric Design of Highways and Streets published by the AASHTO.

Acceleration Lane - The length of pavement between a freeway entrance ramp and the freeway mainlane in which a vehicle transitions from the ramp speed to a speed appropriate for entry onto the freeway. In this research, acceleration lane is the study area which is defined as the section from merging end to the end of ramp traveled way where the right edge of the ramp traveled way intersects the right edge of the freeway through lane.

Angular Velocity - The rate of change of the angle which is bounded by the path of the vehicle and the imaginary line connecting the vehicle and an object, either fixed or moving. For the freeway merging process, for example, the gap seeking driver will view the oncoming traffic in the adjacent lane of the freeway using the rear-view mirror or by turning his head and evaluate the rate of change of the angle, which is the angular velocity, produced by the rear of his vehicle and the path of the freeway lag vehicle to determine whether the oncoming gap is large enough to perform a safe merge.

Critical Angular Velocity - A ramp driver will evaluate the angular velocity of a freeway vehicle relative to his/her vehicle. The driver will only take action, such as merging into a freeway gap, when the angular velocity is at or below a threshold value. The threshold value is called the critical angular velocity of the driver.

Critical Gap - The minimum gap which a ramp driver will consider as acceptable.

Critical Gap Distribution - The probability density function of the critical gap which may be distributed across drivers or within drivers.

Freeway Lag Vehicle - The freeway right lane vehicle that is behind the ramp vehicle when viewed from the ramp vehicle.

Freeway Lead Vehicle - The freeway right lane vehicle that is in front of the ramp vehicle when viewed from the ramp vehicle.

Freeway Right Lane - The freeway rightmost lane to which the ramp vehicle will eventually merge. For those countries where people drive on the left, e.g., UK, this definition should be applied to freeway leftmost lane.

Gap - The time interval between successive freeway vehicles moving in the same lane with respect to some reference point.

Gap Acceptance Function - The probability function that associates with each time gap a gap acceptance probability, $\alpha(t)$, such that the merging driver merges into the main stream with probability $\alpha(t)$ when confronted with a gap of duration t.

Lag - The time interval after arrival of a ramp vehicle at the merging end until arrival of the first freeway right lane vehicle at the same point.

Merging - The process by which vehicles in two separate traffic streams moving in the same direction form a single stream.

Merging End - The physical nose at which the ramp driver can begin the gap search and acceptance process.

Multiple Merge - Two or more ramp vehicles merge into a single freeway time gap.

Ramp - A connecting roadway between two intersecting or parallel roadways, one end of which joins in such a way as to produce merging.

Ramp Lead Vehicle - For a ramp vehicle, the other ramp vehicle that is immediately in front of it is specified as its ramp lead vehicle.

Figure 2.1 gives a graphical representation of a typical freeway merging area. Freeway vehicles f1 and f2, for example, are the freeway lag and lead vehicles respectively for ramp vehicle r1. For ramp vehicle r3, the freeway lag and lead vehicles are f2 and f3 respectively. At the time

depicted in the figure, ramp vehicle r2 is the ramp lead vehicle for ramp vehicle r1 and ramp vehicle r3 is the ramp lead vehicle for ramp vehicle r2.

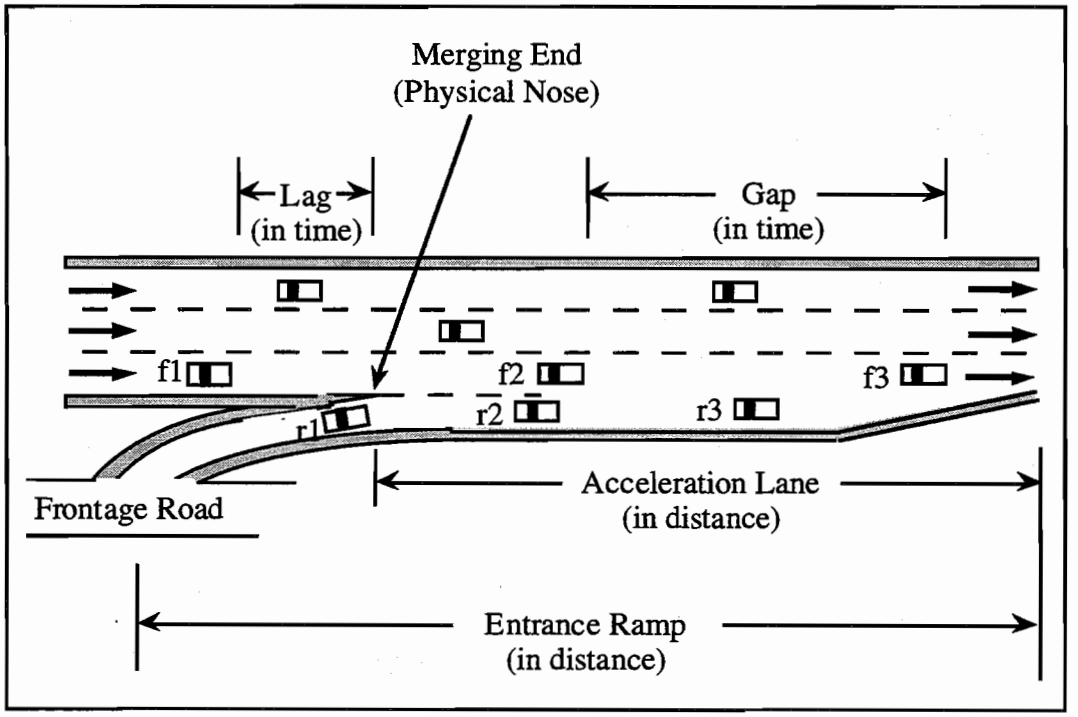

Figure 2.1 Typical configuration of freeway entrance ramp (not to scale)

FREEWAY MERGING OPERATION PROCESS

The ramp vehicle merging process is a complex pattern of driver behavior. A driver performs several different tasks during the merging process. Michaels and Fazio (1989) defined these tasks as follows: 1) tracking of the ramp curvature, 2) steering from the ramp curvature onto a tangent acceleration lane, 3) accelerating from the ramp controlling speed up to a speed closer to the freeway speed, 4) searching for an acceptable gap, and 5) steering from the acceleration lane onto the freeway lane or aborting. Essentially, drivers tend not to concentrate upon two

different tasks simultaneously. They, however, will time-share between tasks. For example, a driver on the acceleration lane may alternate attention between accelerating/decelerating and gap searching.

By painting the same on-ramp to represent three different designs, Ichiro and Moskowitz (1960) studied traffic behavior on 50:1 and 30:1 tapered, and a parallel ramp. In general, all three designs resulted in similar vehicle paths; however, at low ramp and freeway volumes, vehicles entering the freeway need to use as much as or even more distance than those entering at higher volumes. Jarzy and Michael (1963), on the other hand, reported that for both parallel and taper type acceleration lanes, most ramp drivers tended to merge soon after entering the acceleration lane and at too low a speed. A longer length of the parallel portion of the acceleration lane did not show better usage than a shorter one.

Worrall, et al. (1967) discussed a purely empirical analysis of merging behavior at a freeway entrance ramp and pointed out that the relative merging speed exerts a significant influence on the ramp driver's merging decision, in which the proportion of vehicles accepting a small lag size decreases rapidly as the relative speed increases. A similar result was also obtained theoretically by Drew (1968). The freeway volume was found to have a relatively insignificant influence on merging behavior. Furthermore, the point of merge is independent of the relative merging speed.

In order to include a fairly wide range of geometric configurations, Wattleworth, et al. (1967) collected data at 29 entrance ramps coast to coast and border to border. The acceleration lanes of the ramps ranged from 240 to 1500 feet long and the convergence angle ranged from 1 to 14 degrees. From the results of these studies, it is quite apparent that operation in the merging area is to a great extent a function of the geometry of the entrance ramp and acceleration lane. Four variables including length of acceleration lane, angle of convergence, ramp grade, and width of acceleration lane, were found to have a pronounced effect on the merging operation. In general, larger speed changes take place on entrance ramps which have a larger angle of convergence for an equal acceleration lane length. Furthermore, it appears that for a given angle of convergence, vehicles accelerate more rapidly on short acceleration lanes than on long acceleration lanes. For gap acceptance behavior, drivers on ramps with a small convergence angle and long acceleration lane, in general, reject fewer gaps before merging onto the freeway than drivers on ramps with a large convergence angle and short acceleration lane. This result, however, cannot be accepted conclusively. The probability distribution of the merge point was shown to closely follow the Gamma distribution. Statistical tests show good agreement. Such probability distributions are useful in checking and validating computer simulation programs which are designed to study the ramp merging phenomena.

The studies reviewed above are emphasized mainly for the description of ramp driver general merging phenomena or empirical behavior. One should be cautious about treating these results as absolutely conclusive.

Historically, AASHTO emphasized that the acceleration lane is used by ramp vehicles to accelerate from an initial speed associated with the entrance curve design speed to the desired merging speed which is normally defined as the freeway running speed less 5 mph. A recent study, Reilly, et al. (1989), however, indicated that more than 40% of the ramp vehicles have a speed differential at merge greater than 5 mph. In Israel, Polus, et al. (1985) also reported that no great increases in speeds occurred on the acceleration lanes, and the speed difference between through and merging vehicles at merge ranged from 6.5 mph to 10.2 mph. They further concluded that the entire merging process is controlled by gap acceptance behavior since the majority of ramp drivers do not seem to use the acceleration lane strictly for acceleration purposes. The evidence found in different research indicates that the principles adopted by AASHTO to determine acceleration lane length depart somewhat from real situations. The current AASHTO guide states:

> A speed-change lane should, as a minimum requirement, have sufficient length to enable the driver to make the necessary change between the speed of operation on the highway and the speed on the turning roadway in a safe and comfortable manner. Moreover, in the case of an acceleration lane, there should be additional length sufficient to permit adjustments in speeds of both through vehicles and entering vehicles so that the driver of the entering vehicle can position himself opposite a gap in the through traffic stream and maneuver into it before reaching the end of the acceleration lane. The latter requirement has much to do with both the configuration and length of acceleration lane(1990).

However, this design criterion is abstract. The effect of gap acceptance behavior on the design of acceleration lane length has still not seen quantitatively addressed.

GAP ACCEPTANCE MODEL

The interaction of vehicles within a single traffic stream or the interaction of two separate traffic streams are two of the most important traffic operation aspects. Merging, for example, into a freeway stream from an on-ramp acceleration lane is one type of interaction. The theory behind the traffic interaction associated with this merging maneuver is the gap acceptance concept. A number of traffic flow researchers have developed both deterministic and stochastic theories for

gap acceptance at unsignalized intersections and freeway entrance ramps. Most of the researches, however, are empirical, leading to design and operational procedures. Only a few mathematical approaches are found due to the vehicle interactions complexity.

There are two major theoretical approaches for studying gap acceptance phenomena. The first one derives the gap acceptance function of a randomly chosen driver when he/she confronts a specific gap size and merges onto or crosses a traffic stream. The other approach develops the critical gap distribution of a group of drivers. It is assumed that ramp drivers evaluate each oncoming freeway right lane gap and choose to merge if the gap is greater than some critical time gap. The gap acceptance function is conceptually equivalent to the critical gap distribution (Drew, 1971) although they are essentially different. For instance, the probability of a randomly chosen driver accepting a gap of size t is the same as the probability of that driver having a critical gap less than t. A detailed review of gap acceptance functions is presented in the following section followed by a review of critical gap distributions.

Gap Acceptance Function

The simplest form of gap acceptance function is the step function. It is assumed that all drivers will accept a gap, t, if it is greater than their common critical gap, T_c, or reject if it is not. The gap acceptance function is shown as follows:

$$\alpha(t) = 1 \qquad t \geq T_c \qquad (2.1)$$

$$= 0 \qquad t < T_c \qquad (2.2)$$

However, almost all direct measurements of $\alpha(t)$ indicate that the gap acceptance function is not of the simple step form but rather a monotonic non-decreasing function of the gap (Herman and Weiss, 1961; Solberg and Oppenlander, 1960; Drew et al., 1967). Blumenfeld and Weiss(1970) commented on the step gap acceptance function indicating that even if individual gap acceptance functions were of the step functional form, there might still be an overall distribution of T_c, not to say that individual gap acceptance functions were not the step functional form.

Herman and Weiss (1961) performed a controlled experiment at the General Motors Research Laboratories to investigate the individual drivers' gap acceptance function for crossing a single lane road from a standing start at a stop sign. The results lead to the exponential form of $\alpha(t)$ as follows:

$$\alpha(t) = 0 \qquad t \leq 3.3 \text{ sec.} \qquad (2.3)$$

$$= 1 - \exp[\,-2.7(\,t - 3.3\,)\,] \qquad t > 3.3 \text{ sec.} \qquad (2.4)$$

Using other data collected by the Midwest Research Institute in collaboration with the Texas Transportation Institute (Perchonok and Levy, 1960), Herman and Weiss further calibrated the gap acceptance function for a vehicle moving on an actual highway ramp and yielded an approximate $\alpha(t)$ as follows:

$$\alpha(t) = 0 \qquad t \leq 0.7 \text{ sec.} \qquad (2.5)$$

$$= 1 - \exp[\,-0.78(\,t - 0.7\,)\,] \qquad t > 0.7 \text{ sec.} \qquad (2.6)$$

Even though the general idea of $\alpha(t)$ is preferred to the step function in the description of reality, it still represents a drastic idealization in that the gap acceptance function is also a function of the road conditions, speed of the oncoming vehicle, condition of the car, and other essentially psychological factors. One just simply assumes that these factors have been averaged out in the specification of $\alpha(t)$, commented Herman and Weiss (1961).

There is some evidence from queuing models that using the step gap acceptance function leads to a good approximation, at least for low flows (Evans and Herman, 1964; Weiss, 1967; Blumenfeld and Weiss, 1970). By assuming that the gap acceptance function depends on the speed of the next car to arrive at the intersection, Weiss (1967) concluded that under light traffic conditions, differences in the mean delay time when calculated with velocity dependence are small, and can be negligible from the practical point of view.

Blunden, Clissold, and Fisher (1962) attempted to estimate the distribution of critical gaps for drivers turning into a free-flowing stream at an intersection. However, they were actually looking at the proportion of gaps of a given size which are accepted. In fact, they were modeling an accepted gap distribution rather than a critical gap distribution. Finally, the cumulative Erlang distribution was fitted to the measurement data of the proportion of drivers who would accept a gap of size t.

Probit analysis, a standard statistical technique for fitting a weighted linear regression line to the gap acceptance data has been proposed by Solberg and Oppenlander (1966), Drew, et al. (1967), and Miller (1972). In these studies a probit functional form was used to model the cumulative probability of accepting gaps of varying lengths. The proportions are transformed to probits. The probit corresponding to any proportion is the number of standard deviations away

from the mean such that the cumulative normal probability at that point equals the proportion. The probit and the logarithm of gap size can then be fitted to a simple linear form.

Instead of using gap length as an independent variable, Maze (1981) used the ratio of mean time length of all gaps accepted to gap length as an independent variable and used the logit functional form to calibrate the gap acceptance function of drivers at an unsignalized intersection.

The behavior of drivers evaluating oncoming gaps in a major stream is very complex. Obviously, gap length is not the only criterion that drivers use to determine whether to accept a specific gap. Other factors contribute to the whole decision process as well. More precisely, drivers adopt different decision behavior in different situations even though they are evaluating a gap of the same size. For example, the longer the time that a driver waits to merge into a freeway stream, the higher the probability that he or she will accept a smaller gap length. The effect of these impatient drivers was first investigated theoretically by Weiss and Maradudin (1962) who estimated waiting time distributions of minor road vehicles at a stop sign. Adebisi and Sama (1989) pointed out that a driver's gap acceptance behavior reacts to delays by accepting shorter gaps as the duration of delay for executing a left-turn maneuver increases. Madanat, Cassidy, and Wang (1994) claimed that queuing delay, a parameter describing the elapsed time between joining the queue and arriving at the intersection stop bar, has significant effect on a driver's gap acceptance behavior at stop-controlled intersections. The probability of gap acceptance increases with increasing gap length and total delay accrued at the intersection.

Pant and Balakrishnan (1994) applied the neural network technique to derive gap acceptance function using data collected at rural, low-volume, two-way stop-controlled intersections. They found that the type of control, the turning movements in both the major and minor directions, size of gap, service time, stop type (rolling or complete), vehicular speed, queue in the minor direction, and existence of vehicles in the opposite approach have a significant effect on the driver's decision to accept or reject a gap. They also claimed that the neural network performed better than the logit model by correctly estimating a higher percentage of accepting or rejecting a gap.

For freeway merging, ramp drivers are in the acceleration lane and looking for acceptable gaps to complete the merge maneuver. Therefore, the effect of delay for merging on gap acceptance behavior is not as significant as it would be in the case of a stop-controlled intersection. Kita (1993) indicated that the probability of a ramp vehicle accepting a specific gap for merging varies with the position in the acceleration lane or more precisely the remaining distance to the end of the acceleration lane, and the relative speed of the corresponding freeway vehicle. A binary logit model was adopted to calibrate the gap acceptance function. It was found that ramp

drivers have a tendency to accept smaller gaps when approaching the end of the acceleration lane.

Mine and Mimura (1969) extended Weiss and Maradudin's method (1962) to derive the probability density function of the delay to the merging vehicle. The gap acceptance function is assumed to be a function of the time gap and the velocity of the merging vehicle at the time when it confronts the gap. An assumption of infinite acceleration lane length incorporated into the calculation prevents the results from being further applied. Blumenfeld and Weiss (1971) later revised Mine and Mimura's model by assuming a finite length of acceleration lane and defined the delay as the relative time difference between a vehicle on the main stream and a merging vehicle. Polus and Livneh (1987) made further modification by suggesting a method to adjust the travel time on the acceleration lane and considering the influence of ramp vehicles on the computed delay. However, the assumption of constant speed for both freeway and ramp vehicles causes both their models to depart somewhat from reality. Nevertheless, the model proposed by Polus and Livneh (1987) was still adopted by NCHRP 3-35 (Reilly, et al., 1989) in the evaluation and revision of the AASHTO design guideline for freeway speed-change lanes.

Fitzpatrick (1991) found that passenger car drivers had a 50 percent probability of accepting a gap of 6.5 second for both left and right turns and an 85 percent probability of accepting a gap of 8.25 second at a moderate- to high- volume stop-controlled intersection. Truck drivers' 50 percent probability of accepting a gap was 8.5 seconds. In general, at a high volume location, 85 percent of the truck drivers accepted a 10.0 second gap; at a low volume location, 15.0 seconds was the accepted gap value.

Lyons, et al., (1988) in their simulation model designed for estimation of fuel and time penalties associated with merging traffic used a totally different concept to describe merging behavior. They assumed that the merging traffic does not have defined gap-acceptance criteria for merging with the freeway traffic but rather forces a merge. They introduced a correction factor to the effective headway between the merging vehicle and freeway vehicle to allow a smooth transition from the entrance ramp to the freeway through lane. They claimed that the correction factor simulates how the freeway shoulder lane traffic will eventually generate an acceptable gap because it will recognize the merging traffic and interact to avoid collision. However, the theoretical background of how to derive the correction factor was not discussed by the authors. This method approaches the merging phenomenon exclusively from the standpoint of the vehicle operation mechanism and ignores the component of driver behavior imbedded in this complex decision process.

Critical Gap Distribution

The size of the critical gap is determined by the driver's characteristics and style of driving, but varies with the design of the junction, the type and speed of the trailing vehicle forming the gap, and other factors such as weather. In addition, the critical gap may be affected by frustration caused by delay or position of the gap seeking vehicle in the acceleration lane. There is no consistency in its definition; however, critical gap has often been treated as a single average value by many researchers.

Raff (1950) defined critical lag to be "the size lag which has the property that the number of accepted lags shorter than it is the same as the number of rejected lags longer than it". Such a definition can be viewed as the intersection of the two cumulative curves depicted in Figure 2.2. In order not to over-represent cautious drivers who reject many gaps before final acceptance, Raff only considered accepted or rejected lags in the definition of critical lag. This approach produces, in theory, an unbiased result but it is statistically inefficient due to the fact that it disregards much useful information (Miller, 1972). However, Raff's critical lag is still very commonly used by researchers (Polus, et al., 1985; Polus and Livneh, 1987; Makigami, Adachi, and Sueda, 1988; Makigami and Matsuo, 1991) because it is simple to obtain.

Drew (1967) proposed an alternative method to eliminate gap acceptance bias. The method takes into account only those vehicles which reject at least the initial lag and uses only the largest rejected gap per vehicle. Drew further assumed that the critical gaps of a particular ramp driver lie within the range of the largest rejected gap and the gap finally accepted. A histogram can be constructed by summation of these ranges for all ramp drivers to give the estimation of the critical gap distribution. Ashworth (1968) validated Drew's method through simulation and found that it seriously over-estimates the distribution parameters. The reason seems to be the discounting of accepted lags from the calculations. Ashworth then proposed a theoretical approach using all accepted and rejected gaps to eliminate this bias. He showed that with a normal distribution of critical gaps and a negative exponential headway distribution of major flow, the resulting gap acceptance curve obtained is shifted by an amount s^2q from its original position; where s^2 is the variance of the critical gap distribution and q is the major flow rate. Miller (1972) extended Ashworth's work by relaxing the constraint of normal critical gap distribution and found similar results.

McNeil and Morgan (1968) used a concept similar to Drew's but obtained the moment of the minimum gap acceptance distribution and the complete distribution through very complicated mathematical efforts. They claimed that as long as the joint distribution of the largest rejected gap and the gap finally accepted is known, then the information for the number of gaps rejected is not

important. Ramsey and Routledge (1973) proposed a method for estimating the probability structure of critical gaps across the population of drivers by utilizing the histograms of all accepted and rejected gaps. This method is simple to apply but difficult to interpret because it produces a discrete critical gap distribution consisting of point estimates at the boundaries of the classes used in the analysis. Hewitt (1983) derived a method which estimates the critical gap distribution of those drivers entering a main road at a priority intersection who have rejected the initial lag offered to them. A satisfactory result was obtained based on the assumption that each driver has the same value of critical lag and critical gap.

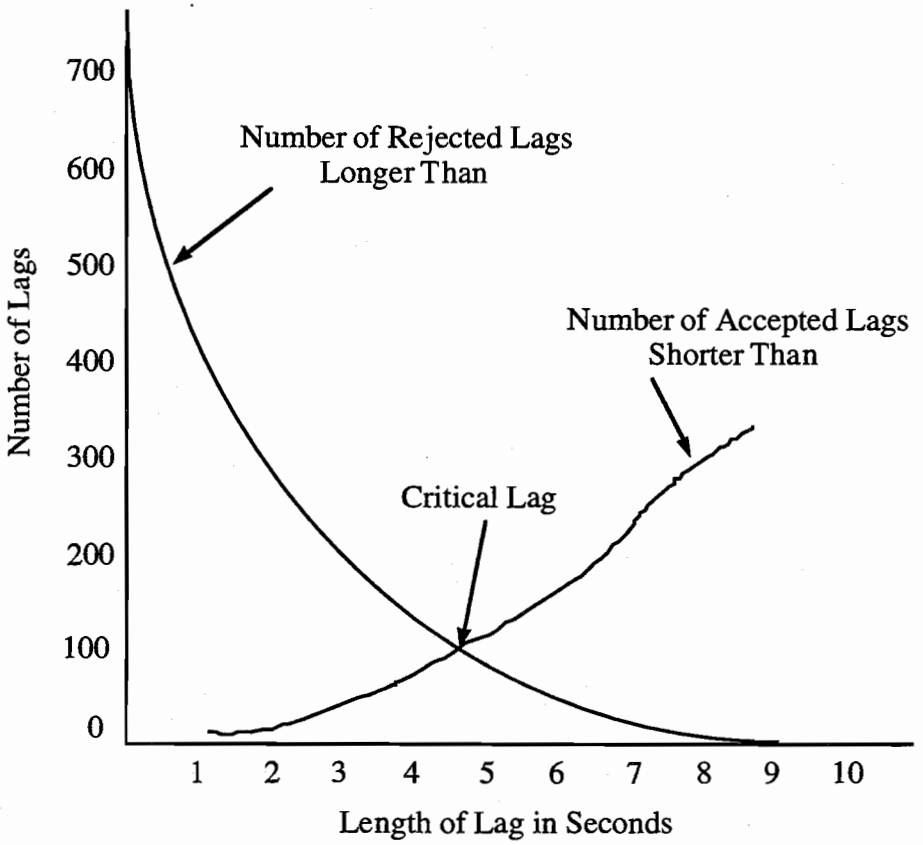

Figure 2.2 Distribution of accepted and rejected lags at intersection (Raff's method)

Hewitt (1985) later made a comparison between the methods of Ashworth (1968), those discussed in Miller (1972), Ramsey and Routledge (1973), and Hewitt (1983) and concluded that the most important factor determining the goodness of the estimated mean critical gap is the type of data used in calibrating the value, rather than the method employed. In general, methods using both lag and all gaps produced better estimates than those using lag only. Of the methods compared, Hewitt commented that the Ashworth method has the advantage of simplicity in calculation; the maximum likelihood method is the most complicated, but gives the most accurate estimates of mean and standard deviation; and the Hewitt and Ramsey-Routledge methods give a reasonable estimate of the actual shape of the distribution even though no assumptions about the critical gap distribution are made.

Clearly, the assumption of an identical critical gap across drivers is somewhat unrealistic. The critical gap for a certain maneuver should vary across drivers and even within drivers. Therefore, it should be modeled as a random variable. Several techniques (Ashworth, 1970; Golias and Kanellaidis, 1990; Hewitt, 1983) have been used to describe the critical gap distribution assuming that every driver has a fixed critical gap; however, the critical gap is distributed across drivers. This kind of behavior is called consistent behavior. Many researchers, on the other hand, have proposed inconsistent gap acceptance behavior in which the critical gap for an individual is no longer treated as a constant, but as a random variable. Different probability density functions have been derived using either controlled experiment or actual field data to represent inconsistent critical gap distributions. For instance, Herman and Weiss (1961) used the shifted negative exponential distribution; Blumden, et al. (1962) used the Gamma distribution; Solberg and Oppenlander (1966) and Drew, et al. (1967) used the lognormal distribution; and Miller (1972) used the normal distribution.

Daganzo (1981) extended Miller's method (1972) by using a multinomial probit model to estimate the critical gap parameters which are considered to vary across as well as within gaps for a given driver. Empirical work conducted by Bottom and Ashworth (1978) showed that over 85% of the variance in gap acceptance behavior may result from variations within gaps for given drivers. Due to estimability problems, Daganzo didn't actually distinguish between the two above-mentioned components of stochastic variation, as argued by Mahmassani and Sheffi (1981). Palamarthy (1993) followed exactly the same approach as Daganzo in modeling pedestrian crossing gap acceptance behavior. Mahmassani and Sheffi (1981) proposed a model trying to explain within driver variations by explicitly specifying the dependence of the mean critical gap on the number of rejected gaps. Using the same data set reported by Daganzo (1981), Mahmassani

and Sheffi obtained results suggesting that the critical gap for given drivers does decrease as more gaps pass by.

Drew (1971) applied the multiple regression technique to derive a statistical relationship for predicting the critical gap of merging vehicles based upon the length of the acceleration lane and the angle of convergence for both parallel and taper type acceleration lanes respectively. The results are shown as follows:

$$T = 5.547 + 0.828\theta - 1.043L + 0.045L^2 - 0.042\theta^2 - 0.874S \qquad (2.7)$$

where

T = critical gap in second

θ = angle of convergence in degrees

L = length of acceleration lane in 100-ft stations

S = shape factor = 1 for taper type, 0 for parallel type

It can be seen from the equation that a driver traveling on a taper type entrance ramp will have a smaller critical gap than its parallel type entrance ramp counterpart given the same length and the same angle of convergence.

In addition to the concept of gap acceptance, angular velocity as a freeway merge criterion has been proposed since the early 1970's (Drew, 1971). However, this concept has not been well recognized by most researchers since then. The reasons causing this situation are not clear to the author. The most probable explanation might be due to the fact that it is relatively much more cumbersome to reduce angular velocity than to just reduce time gaps. The theory behind angular velocity can be best described using Figure 2.3. As a ramp vehicle is merging, the ramp driver evaluates the angular velocity, which is the first order motion vector relative to the ramp vehicle, created by the freeway lag vehicle. As the freeway lag vehicle is closing on the gap seeking driver, the angle q, as viewed by the merging driver becomes larger or becomes smaller if the freeway lag vehicle is falling behind relative to the merging vehicle. Mathematically, angular velocity is defined as the change in the angle q over time or dq/dt (Gordon and Michaels, 1963; Michaels and Cozan, 1963; Drew, 1971). Approximately, the angular velocity can be quantitatively expressed by a simple first order differential equation:

Source : Reilly, et al., 1989

Figure 2.3 Typical component of angular velocity

$$\omega = \frac{(D + O)(V_f - V_r)}{L^2} \quad (2.8)$$

Where

ω = angular velocity, rads/sec;

D = width of freeway lag vehicle, ft;

O = lateral offset between freeway vehicle and ramp vehicle, ft;

V_f = speed of freeway lag vehicle, ft/sec;

V_r = speed of ramp vehicle, ft/sec;

L = longitudinal distance between ramp and freeway lag vehicles, ft.

This method is superior to any other model considering only the time or distance gap as the basis for the gap acceptance decision since it takes into consideration the distance to the approaching freeway lag vehicle and the relative speed of these two vehicles. Because of the theory behind angular velocity, it is obvious that using angular velocity to describe the merging process is closer to real driver behavior. Empirical evidence(Michaels and Cozan, 1963) showed that the angular velocity threshold is in the range of 0.01 to 0.001 rads/sec with a normal value of 0.004 rads/sec. Michaels and Fazio (1989) adopted the angular velocity methodology to determine acceleration lane length. The results indicated that the nominal acceleration lane length to insure 85 percent or more merge opportunities for ramp vehicles was no more than 800 ft. Reilly, et al. (1989) incorporated angular velocity into the calculation of minimum entry length which must be provided downstream of the merging end and found different values from those recommended in the AASHTO (1990).

The gap acceptance model, either from the perspective of gap acceptance function or of critical gap distribution, has been recognized as a core component in many traffic engineering studies. They are non-signalized intersection operations (Ashworth, 1969; Catchpole and Plank, 1986; Golias, 1981; Kimber, 1989; Madanat, Cassidy, and Wang, 1994; McNeil and Smith, 1969; Weiss, 1967), freeway entrance ramp operations (Blumenfeld and Weiss, 1971; Drew, et al., 1968; Evans and Herman, 1964; Herman and Weiss, 1961; Makigami and Matsuo, 1990, 1991; Michaels and Fazio, 1989; Mine and Mimura, 1969; Reilly, et al., 1989; Weiss and Maradudin, 1962), freeway merging simulation models (Dawson, 1964; Glickstein, Findley, and Levy, 1961; Perchonok and Levy, 1960; Salter and El-Hanna, 1976; Skabardonis, 1985; Szwed and Smith,

1972; Wallman, 1976), and emission as well as fuel consumption prediction in freeway merging area (Lyons, et al., 1988).

ACCELERATION/DECELERATION CHARACTERISTICS OF RAMP VEHICLES IN THE ACCELERATION LANE

Historically, AASHTO has suggested that the freeway acceleration lane length be exclusively based on ramp vehicle acceleration-deceleration performance. It is believed that drivers begin to merge when the relative speed between the freeway vehicle and ramp vehicle is less than 5 mph. Unfortunately, there have been relatively few articles devoted to the study of acceleration characteristics of vehicles in the acceleration lane. The earliest investigation of acceleration characteristics was conducted in the late 1930's (Beakey, 1938; Loutzenheiser, 1938) and was used by AASHO for its calculation of highway entrance ramp length until the early 1980's. Although Olson, et al. (1984) made slight modifications to the survey conducted in the late 1930's, the acceleration performance proposed by Olson, et al. on which AASHTO(1990) based the calculation of needed acceleration lane length is still not realistic due to its oversimplification of the operational characteristics of ramp vehicles in acceleration lanes.

Huberman (1982) used a radar speedometer technique to measure vehicle acceleration on highway entrance ramps in Canada. However, the radar units were set up at the upstream portion of the physical nose of the entrance ramp and precluded observation of acceleration characteristics of ramp vehicles in the acceleration lanes which is the most challenging part of the vehicle operational performance model. Michaels and Fazio (1989) found that there seems to be a series of steps associated with ramp vehicle acceleration during freeway merge. There is a decline in speed between successive accelerations rather than the hypothesized constant speed or continuously increasing speed. Polus (1985) claimed that the entire merging process is controlled by gap-acceptance behavior.

A recent study by Sullivan, Chatziioanou, and Devadoss (1995) used individual vehicle's time-space trajectory data collected from a sample of freeway on-ramps with a wide variety of physical and operational characteristics to derive ramp vehicle speed and acceleration functions. The time-space data points (T_i, S_i) for each individual vehicle were fitted to an 8th order polynomial of the form:

$$S = f(T) = a_0 + a_1T + a_2T^2 + a_3T^3 + \ldots + a_7T^7 + a_8T^8 \qquad (2.9)$$

Using each fitted trajectory, speed, V, and acceleration, A, profiles for individual vehicles were derived analytically as the first and second derivatives of location S with respect to time T and were shown as follows:

$$V = f'(T) = a_1 + 2a_2T + 3a_3T^2 + \ldots + 7a_7T^6 + 8a_8T^7 \quad (2.10)$$

$$A = f''(T) = 2a_2 + 6a_3T + 12a_4T^2 + \ldots + 42a_7T^5 + 56a_8T^6 \quad (2.11)$$

The final polynomial coefficients for Eqs(2.10) and (2.11) were obtained by averaging respective coefficients over all individual vehicles. Although superior to previous studies from the viewpoint of describing acceleration performance, this study, however, still didn't incorporate the dynamic vehicle interaction in the acceleration behavior modeling.

Due to a lack of applicable models to describe complex acceleration characteristics in acceleration lanes, most analytical or simulation models simply make use of several assumptions including: constant speed for merging vehicles(Blumenfeld and Weiss, 1971; Szwed and Smith, 1974; Polus, 1987; Makigami, 1988, 1991); constant acceleration rates (Glickstein, 1961; Perchonok and Levy, 1960; Dawson, 1964); or conventional follow-the-leader car-following techniques (Salter and El-Hanna, 1976). Skabardonis (1985) in his simulation model used a slightly complicated procedure based on the ramp vehicle speed approaching the acceleration lane and the assumption that acceleration rates are approximated normally distributed to generate the ramp vehicle acceleration rates. The relation between acceleration characteristics and the gap acceptance process, however, was not addressed.

LIMITATIONS AND DEFICIENCIES OF PREVIOUS STUDIES

Mathematical models have been extensively used by many researchers to study driver behavior when merging into or crossing major streams at freeway entrance ramps or street intersections without signals. Their main focus is the prediction or derivation of the mathematical forms of merging delay or queue length to minor stream vehicles. Many distinguished accomplishments have been reported providing quantitative descriptions of this complex process, among others are Herman and Weiss, 1961; Weiss and Maraderdia, 1962; Evant, et al., 1964; Weiss, 1967; Drew, 1967; Ashworth, 1969; Blumenfeld and Weiss, 1970. Certain simplified assumptions made to the fundamental driver merging behavior process, however, limit those mathematical models to be less than totally realistic. In addition, as long as the fundamental

assumptions are relaxed, complexity associated with the derivation of closed mathematical forms limits mathematical approaches.

Previous empirical studies (Ashworth, 1970; Buhr, 1967; Drew, et al., 1967; Fukutome and Moskowitz, 1959; Worral, et al., 1967), on the other hand, have not related the effects of the acceleration lane to overall merging process operation because they focus on the general ramp vehicle behavior. Unlike street intersection operations where vehicles stop and look for an acceptable gap, the acceleration lane plays an important role in modeling freeway entrance ramp merging behavior (Kita, 1993). Acceleration lane characteristics provide the flexibility to incorporate effects of relative speed and physical length constraints in the merging behavior model. As a consequence, the methodologies developed for street intersections normally cannot be directly applied to freeway entrance ramps. The effects of the acceleration lane in modeling merging behavior deserve more detailed investigation.

The concept of angular velocity has been recognized (Michaels and Cozan, 1963, 1989; Drew, 1971; Reilly, et al., 1989) as a good criterion to describe driver behavior during freeway merge maneuver. Reilly, et al. (1989) commented that "...using the threshold of angular velocity leads to a simplified accept-reject criterion...which is generally a more stable decision basis than some other criteria for human control". In order to let the entrance ramp merging behavior models include real-world phenomena, the angular velocity concept should be appropriately incorporated into the formulation.

Acceleration characteristics of ramp vehicles in acceleration lanes is an essential component in all microscopic simulation models designed for simulating freeway entrance ramp merging. When ramp vehicles are running in the acceleration lane, they interact with vehicles in the freeway right lane and with other ramp vehicles as well. Therefore, their acceleration characteristics cannot be modeled by simply assuming no other vehicles exist. No literature has been found with quantitative discussions of this complex interaction phenomena. Adoption of the car-following concept to model ramp vehicle acceleration performance is applausive. However, simple forms such as follow-the-leader car-following models do not include effects of freeway vehicles and are not appropriate for direct application to merging vehicle flow. Interactions between ramp vehicles and freeway right lane vehicles are believed to play an important role in determining merging vehicle acceleration characteristics. Michaels and Fazio (1989) found that there is a decline in speed between successive accelerations when ramp drivers are gap searching. This phenomena implies that freeway vehicles have a pronounced influence on ramp vehicle acceleration behavior and cannot be excluded from the formulation of ramp vehicle acceleration characteristics during merging.

SUMMARY

The major components of the freeway entrance ramp merging process including operational characteristics, gap acceptance behavior, angular velocity concept, and ramp vehicle acceleration characteristics along with their applications have been reviewed. The limitations and deficiencies of previous studies, which are partly due to simplifying assumptions and partly due to exclusion of critical model components, are discussed. Finally, conceptual approaches to overcome those limitations and deficiencies are described. The methodolgies applied in this study are discussed in the next chapter.

CHAPTER 3. RESEARCH METHODOLOGY

INTRODUCTION

Fundamental studies of freeway entrance ramp merging behavior have been proceeded mainly by means of either mathematical methods or empirical approaches depending on the assumptions made regarding driver behavior, data used to develop the models, and final results obtained. Different levels of success have been achieved over the last few decades. This study will focus on collecting field data at freeway entrance ramps, and developing methodologies that are appropriate to calibrate freeway merge behavior models, including acceleration-deceleration characteristics and gap acceptance phenomena. There are four general elements included in the research approach. They are 1) examination of current freeway merging behavior models and deficiencies that may exist; 2) identification of possible approaches to make up for deficiencies of previous research; 3) establishment of a thorough understanding of the freeway merging process, particularly with respect to driver behavior and traffic flow characteristics; and 4) development of calibration methodologies for modeling freeway merge driver behavior. A set of detailed activities are defined and followed to achieve the general elements. Figure 3.1 shows a conceptual flowchart of the activities to be included, and a more detailed description of each is presented in the following section.

CONCEPTUAL APPROACH TO PROBLEM

To gain a clear understanding of previous research deficiencies and to search for possible directions of further improvements, pertinent literature was comprehensively reviewed. Observations of vehicle operational characteristics in freeway entrance ramps were conducted at several locations to establish a solid idea of traffic flow characteristics during freeway merging. Preliminary methodologies for calibrating freeway entrance ramp merge behavior models were developed conceptually based on knowledge gained from the literature review and on-site observations as well as the objectives to be achieved. These preliminary methodologies were not only used as a guideline to develop data collection and later data reduction procedures but also served as the basis for performing preliminary data analysis and model calibration. Basically, these preliminary methodologies are proposed as hypotheses to be examined and refined.

In order to best describe the interaction between ramp vehicle acceleration-deceleration characteristics and gap acceptance behavior, traffic data were collected when freeway flow levels range from medium to high and flow was stable. During periods of heavy freeway congestion,

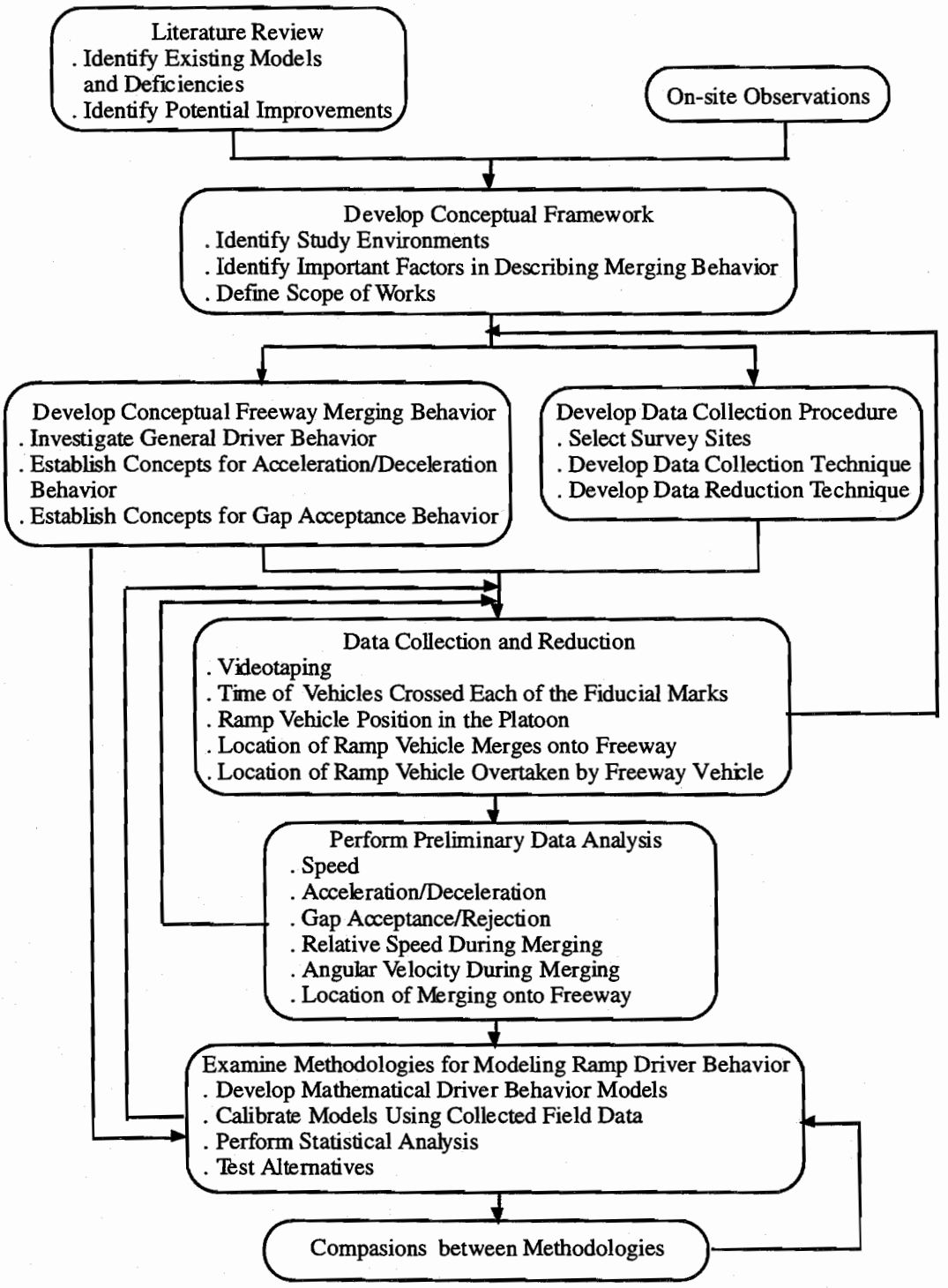

Figure 3.1 Conceptual research flowchart

unstable or stop-and-go traffic flow appears and makes the "gap structure" unstable and extremely difficult to interpret. In such a situation, a ramp driver enters the freeway either by forcing a merge or by the accommodation of a freeway lag vehicle. Consequently, ramp vehicle acceleration-deceleration characteristics and gap acceptance behavior cannot be treated as normal and stable behavior. During very light freeway traffic conditions, on the other hand, a ramp driver normally does not have any difficulty finding an acceptable gap. Ramp vehicle acceleration-deceleration characteristics are therefore mainly determined by the freeway entrance ramp geometry and the ramp vehicle mechanical capacity. Little interaction between acceleration-deceleration characteristics and gap acceptance behavior is expected in light traffic flow conditions. When a freeway has a moderate to high flow level, a ramp driver normally adjusts speed while performing gap searches and merging maneuver by accelerating and decelerating. At this flow level, strong interaction happens between ramp driver acceleration-deceleration and gap acceptance behavior. To verify proposed methodologies, the collected field data, such as freeway and ramp vehicle speeds, acceleration-deceleration rates, merge positions, and gaps finally accepted etc., were used to identify and quantify key variables for use in freeway merging model calibration. Detailed data collection and reduction techniques are described in the next section.

Preliminary analyses were conducted to detect possible conceptual methodology deficiencies. Feedback loops, as shown in Figure 3.1, were actuated if modifications to the previous steps were desired. Finally, the collected field data were applied to the established driver behavior concepts to examine the proposed methodologies for freeway merging behavior. Statistical tests or other comparisons to alternative methodologies are needed to select the most appropriate methodologies. The final models expected in this research are the most appropriate methodologies for modeling ramp vehicle acceleration-deceleration as well as gap acceptance behavior during merging.

DATA COLLECTION AND REDUCTION TECHNIQUES

One of the major tasks of this research is the collection and reduction of field data to be used in calibrating freeway entrance ramp merging behavior models. These data include vehicle speed, acceleration and deceleration, gap acceptance or rejection, steering maneuvers, and any other data necessary to define and model the merging process. Described below are the data collection methods and data reduction procedures as well as the potential measurement errors associated with these procedures.

Data Collection Methods

In this research traffic data were collected by either manual or video recording method. An important advantage of the video recording method is that videotaping traffic provides a permanent record of the data which can be later analyzed at various levels of detail or re-checked during data reduction as necessary. In order to perform videotaping, the selected sites must have a near by vantage point from which the operation of the entire merging area can be videotaped. Yashiro and Kotani (1986) used a kite balloon to overcome the problem when no natural viewing point could be found. The data characteristics of this research requires that the camera should be positioned in such a way that the vehicle movements along the longitudinal direction can be clearly tracked. Experience gained from preliminary video recording at some candidate locations indicated that roadway or pedestrian overpasses immediately upstream or downstream of the merging area do not fulfill this necessary condition. These overpasses normally cannot provide a vantage point from which the longitudinal movements along the acceleration lane can be precisely tracked. In fact, overpasses are good locations for videotaping lateral movements but are inappropriate for videotaping longitudinal movements. This finding excludes many candidate locations from further consideration and makes it extremely difficult to find a good location in the Austin area. Considerable time and effort were expended in finding a videotaping site.

For the purpose of calculating speeds and acceleration-deceleration rates from the video image, the acceleration lane was divided into specified distance intervals by either directly painting lines on the pavement or placing visible objects along the ramp shoulder as reference points. The former is better, theoretically, because it allows the time-base of a vehicle crossing each of the fiducial marks to be precisely read off the video image. This method, however, is practically infeasible because drivers will respond to these unexpected pavement marks by reducing their speeds. This unusual response causes the measurements to depart somewhat from reality. Placing visible objects along the ramp shoulder as reference points seems to be more appropriate if these objects can be placed in such a way that they do not disturb drivers.

In this research, in order not to attract drivers' attention, wide and long lines were painted, at regular distance intervals, on the grass beside the ramp shoulder along the acceleration lane with one line painted near the physical nose. All lines were perpendicular to the pavement edge and are almost invisible to drivers. The distance between lines was determined partially by distance from the video camera and partially by the required measurement accuracy. A typical data collection site layout is shown in Figure 3.2. In addition to the lines, distances between fixed objects, for example light posts or traffic signs, were measured. These can serve as reference distances in later data reduction processes.

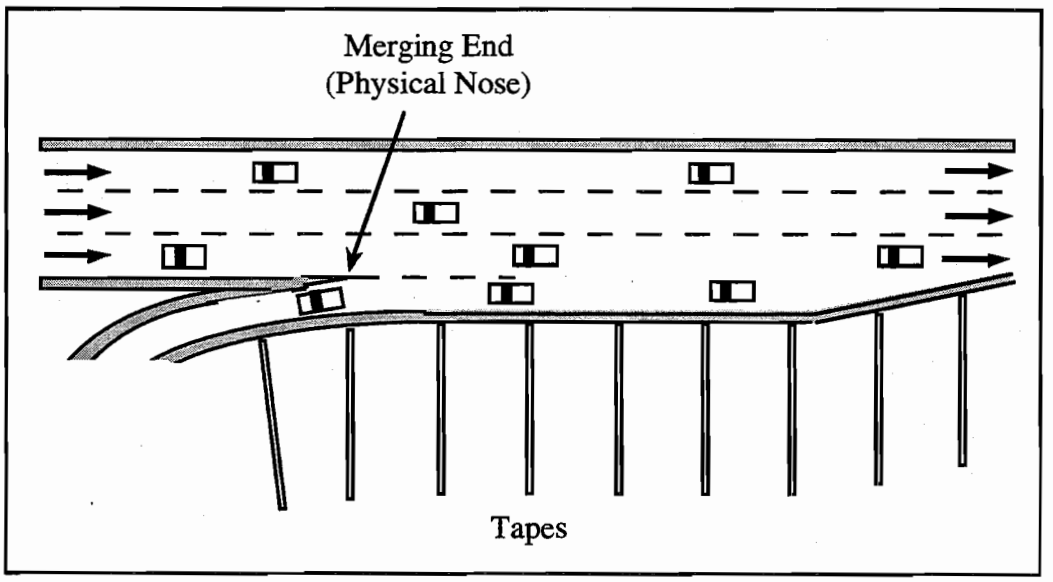

Figure 3.2 Typical fiducial mark layout of data collection site

In order to calculate vehicle speed and acceleration-deceleration rates along the acceleration lane, the time-base of a vehicle crossing successive fiducial marks must be precisely read off the video image. A video camera with built-in time code generator with satisfactory time-base resolution was not available so the video recording were made without the time-base superimposed. Assistance from the Mechanical Engineering Media Services and the Supercomputer Center of The University of Texas at Austin made it possible to play back the original tapes in the laboratory and rerecord(with some marginal loss of accuracy due to possible recording and playback speed differences) with a crystal-controlled digital clock(hours, minutes, seconds, and frame number), superimposed. The time-base can be synchronized to any clock time before starting.

Data Reduction Procedure

Considerable efforts are required to reduce data from the videotapes manually. There are three primary tasks in the video data reduction. First, traffic counts are made by reviewing the videotapes in real time. The second task and probably the most time consuming work is the tracking of individual vehicles along the merging area. The third part of the process is to record

where ramp vehicles are overtaken by freeway lag vehicles and where the ramp vehicles eventually merge into the freeway. Locations of these occurrences are specified by the fiducial marks where they took place. Fiducial marks are lines drawn across the acceleration lane and freeway lanes directly on a transparency superimposed on the video monitor.

The vehicle tracking process requires the videotapes to be played back at slow speed, or frame-by-frame, to ensure precise recording of the time vehicles cross each of the fiducial marks, in sequence. In this research, the resolution of the time-base permits tracking vehicles at 0.03-sec. intervals(30 frames/sec).

The primary data reduced from the videotapes are a set of times that each ramp vehicle, with corresponding(if any) freeway lag, freeway lead, and ramp lead vehicles, cross each fiducial mark. This is done by tracking a specific ramp vehicle and at the same time identifying its corresponding freeway lag, freeway lead, and ramp lead vehicles. It is then possible to rewind the tape and follow each individual vehicle accordingly. For a specific ramp vehicle, only those freeway lag and lead vehicles which are within a reasonable distance are considered. A reasonable distance, in this research, is assumed as the distance at which a ramp vehicle can detect the movements of freeway right lane vehicles. This distance, however, is somewhat arbitrarily chosen and is difficult to be precisely defined. Three hundred feet has been reported as the distance that a driver of a merging vehicle, when stopping on the roadside, can detect movements of an oncoming freeway vehicle(Levin, 1970), and could be an useful reference. To incorporate more freeway merge traffic operational data, this study uses 400 feet and 300 feet with respect to freeway lag and freeway as well as ramp lead vehicles respectively as data reduction reasonable distances. Table 3.1 shows a typical data reduction form.

Most traffic characteristic parameters can be calculated from the time-base data of each vehicle crossing the fiducial marks. First, the average speed of a vehicle between each pair of fiducial marks is calculated simply by dividing the distance between fiducial marks by the travel time. Acceleration and deceleration rates are then calculated from the speed data. The longitudinal distance and angular velocity between a specific ramp vehicle and its corresponding freeway lag vehicle, freeway lead vehicle, and ramp lead vehicle at the time when the ramp vehicle crosses each fiducial mark can also be calculated. This analysis procedure allows the tracing of time-distance relations, or speed profiles, of ramp vehicles along the acceleration lane as well as these same relations for the freeway vehicles that bounded the gaps.

Other useful data in terms of driver behavior are also reduced during the vehicle tracking process. These data include:

- The position of a ramp vehicle in a ramp vehicle platoon. For example, a tracked ramp vehicle is a single vehicle, the leader of a platoon, the second vehicle of a platoon, or the third vehicle of a platoon.

- The location, as specified by fiducial marks where the ramp vehicle was overtaken by freeway lag vehicles.

- The location, as specified by fiducial marks where the ramp vehicle merged into the freeway right lane.

- Whether the merge is forced.

- Whether the specified ramp vehicle merged before its corresponding ramp lead vehicle.

Sources of Potential Measurement Errors

Obtaining accurate data is an important aspect of this research. Quality control is implemented throughout the data collection and reduction process. Measurement errors, however, are still significant in analyzing the video recording, especially in the vehicle tracking process. Difficulties in reducing data result from several inevitable factors. These factors are due to the imbedded limitations of data collection devices, the visual blocking of vehicles by other vehicles, human errors, or the natural deficiencies of the adopted data reduction techniques.

In order to ensure obtaining consistent and accurate data for use in later model development, data were reduced from video images by the author alone to avoid possible inconsistent measurement resulted from different observers. Even though, inconsistent measurement may still exist due to author's inherent human inconsistency, physical conditions at the time of data reduction, or incautiousness. At a very early stage of this study, an experiment was performed to examine the reduced data consistency to ensure this potential problem can be compromised. Video taping was conducted at a three-lane one way street, Balcones Drive. A video camera featuring 0.1- sec.(10 frames/sec) time-base resolution was used in this specific experiment. Two groups of vehicles, with twelve vehicles in each group, were sampled from video images. The times each vehicle passed two fiducial marks, 50 feet apart, were recorded respectively and average travel speeds were then calculated accordingly. This process was repeated five times for each group. For each repetition, exactly the same twelve vehicles were sampled. The reduced average travel speeds, in mph, of each vehicle in each repetition are shown in Tables 3.2 and 3.3 respectively. Essentially, if author is reliable in reducing data from video images, the average travel speeds for each vehicle in each repetition should be similar. In other words, the standard deviations shown in the last column of each table should be small. Results demonstrated in both Tables 3.2 and 3.3 show that most standard deviations are either

TABLE 3.1 TYPICAL FORM DESIGNED FOR DATA REDUCTION

Ramp Vehicle #:	Vehicle Type:	Ramp Type:	Location:	Date: / /

Fiducial Mark #	Time of Each Vehicle Crossed Each of the Fiducial Marks				Position in Platoon	Overtaken by Freeway Vehicle?	Merge into Freeway?	Force a Merge?	Merge before Ramp Lead?
	Ramp Vehicle	Freeway Lag	Ramp Lead	Freeway Lead					
1									
2									
3									
4									
5									
6									
7									
8									
9									
10									
11									
12									
13									
14									
15									

zero or fairly small indicating the author reduced from video images identical data during each repetition. This evidence supports the fact that the author can reduce reliable video image data.

Another possible speed estimation measurement error results from embedded video equipment limitations. In this study, data were video-taped using a video camera; the video image is played back in a video camera recorder(VCR) featuring a jog-shuffer function to allow video images to be moved forward/backward frame-by-frame; the time each vehicle crossed each fiducial mark in sequence is recorded; and the average travel speed between fiducial marks is calculated. As a consequence, these calculated speeds will always have measurement errors due to embedded video camera time-base resolution limitations. Ideally, if the time-base resolution is the only cause of measurement errors, the probability density functions(pdf) of this kind of measurement error, ε, associated with calculated average travel speed between fiducial marks is given in Eqs(3.1) and (3.2). Derivation of the pdf is detailed in Appendix I.

TABLE 3.2 REDUCED AVERAGE TRAVEL SPEED OF EACH VEHICLE IN EACH REPETITION (GROUP 1)

	Repetition						
Vehicle	1	2	3	4	5	Mean	Std. Dev.
1	24.30	24.30	26.16	24.30	24.30	24.67	0.83
2	28.34	28.34	28.34	28.34	28.34	28.34	0.00
3	28.34	28.34	28.34	28.34	28.34	28.34	0.00
4	28.34	28.34	28.34	28.34	28.34	28.34	0.00
5	30.92	30.92	30.92	30.92	30.92	30.92	0.00
6	28.34	28.34	28.34	28.34	28.34	28.34	0.00
7	26.16	26.16	26.16	26.16	26.16	26.16	0.00
8	28.34	26.16	26.16	26.16	28.34	27.03	1.19
9	28.34	28.34	28.34	28.34	28.34	28.34	0.00
10	28.34	28.34	26.16	28.34	28.34	27.90	0.97
11	24.30	24.30	24.30	24.30	24.30	24.30	0.00
12	28.34	28.34	28.34	26.16	28.34	27.90	0.97
Mean	27.70	27.52	27.49	27.34	27.70		
Std. Dev.	1.89	1.92	1.74	1.94	1.89		

TABLE 3.3 REDUCED AVERAGE TRAVEL SPEED OF EACH VEHICLE IN EACH REPETITION (GROUP 2)

	Repetition						
Vehicle	1	2	3	4	5	Mean	Std. Dev.
1	34.01	37.79	37.79	34.01	37.79	36.28	2.07
2	34.01	34.01	34.01	34.01	34.01	34.01	0.00
3	30.92	30.92	30.92	30.92	30.92	30.92	0.00
4	42.52	42.52	42.52	42.52	42.52	42.52	0.00
5	34.01	34.01	34.01	34.01	34.01	34.01	0.00
6	37.79	37.79	37.79	37.79	37.79	37.79	0.00
7	37.79	37.79	37.79	37.79	37.79	37.79	0.00
8	37.79	34.01	37.79	37.79	37.79	37.03	1.69
9	34.01	34.01	34.01	34.01	34.01	34.01	0.00
10	34.01	34.01	34.01	34.01	34.01	34.01	0.00
11	34.01	34.01	34.01	34.01	34.01	34.01	0.00
12	37.79	37.79	37.79	37.79	37.79	37.79	0.00
Mean	35.72	35.72	36.04	35.72	36.04		
Std. Dev.	3.07	3.07	3.08	3.07	3.08		

$$f(\varepsilon) = [\, \kappa - \frac{\kappa^2}{v_{act}} (\frac{\varepsilon D}{v_{act} + \varepsilon}) \,] \frac{D}{(v_{act} + \varepsilon)^2} \qquad (3.1)$$

$$0 \le \varepsilon \le \frac{v_{act}^2}{\kappa D - v_{act}}$$

$$f(\varepsilon) = [\, \kappa + \frac{\kappa^2}{v_{act}} (\frac{\varepsilon D}{v_{act} + \varepsilon}) \,] \frac{D}{(v_{act} + \varepsilon)^2} \qquad (3.2)$$

$$\frac{-v_{act}^2}{\kappa D + v_{act}} \le \varepsilon \le 0$$

where

κ video camera time-base resolution, in frame/sec;

v_{act} actual speed of a vehicle approaching the fiducial mark, in ft/sec;

D distance between each fiducial marks, in feet.

As expected, the faster the actual speed and the shorter the fiducial mark intervals, the larger the probability of having a large measurement error in estimating average travel speed between fiducial marks. As can be seen in Figures 3.3 and 3.4, however, the measurement error which results from the limitation of the time-base resolution is not significant for a 30 frames/sec resolution. The probability density function of measurement error can be derived from either time scale orientation or distance scale orientation. The results from these two approaches have been proven to be identical. In addition, a Monte-Carol simulation technique was applied to verify the pdf's derived mathematically. The goodness-of-fit chi-square test shows very good agreement.

However, the time-base resolution is not the only cause of measurement errors. To perform vehicle tracking, each frame is projected on a video display terminal with a perspective grid overlay. Parallax error inevitably occurs in determining when vehicles actually cross fiducial marks. The further down the acceleration lane the vehicle proceeds, for a given perspective distortion, the greater the errors are likely to be. The time-location errors propagate in the calculation of speeds, accelerations, and angular velocities. The parallax error is difficult to remove unless the fiducial marks can be painted directly on the road pavement. Measurement errors and the enormous variability among drivers in the vehicle-highway system account for the variability of calculated traffic parameters.

Travel Time Experiment

This controlled experiment was designed to investigate the effects of fiducial mark distance on the consistency of estimated travel speeds. The distance interval between each pair of fiducial marks was 10 feet and the total marked area was 50 feet. Three experienced drivers were instructed to maintain constant speed at 30 mph, 40 mph, 50 mph, and 60 mph respectively when passing the marked area. For each driving speed, 10 to 15 runs were performed by each driver. The experiment for 50 mph and 60 mph was performed in a freeway section with three through lanes, while the experiment for 30 mph and 40 mph was performed on the frontage road. All experiments were performed and videotaped during weekend off-peak times to be sure the drivers received minimum disturbance from other vehicles and could easily maintain constant speed. The time code resolution of the video recording is 0.1 sec/frame. Data were reduced for the cases of fiducial mark distances 30 feet, 40 feet, and 50 feet respectively, and results are

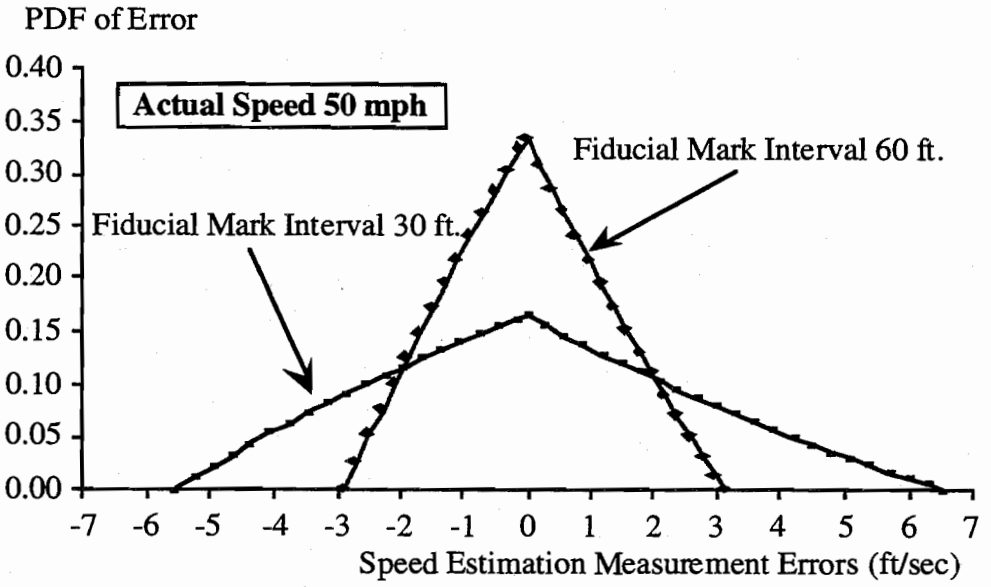

Figure 3.3 Probability density functions of speed estimation measurement errors (actual speed 50 mph, fiducial mark intervals 30 ft and 60 ft)

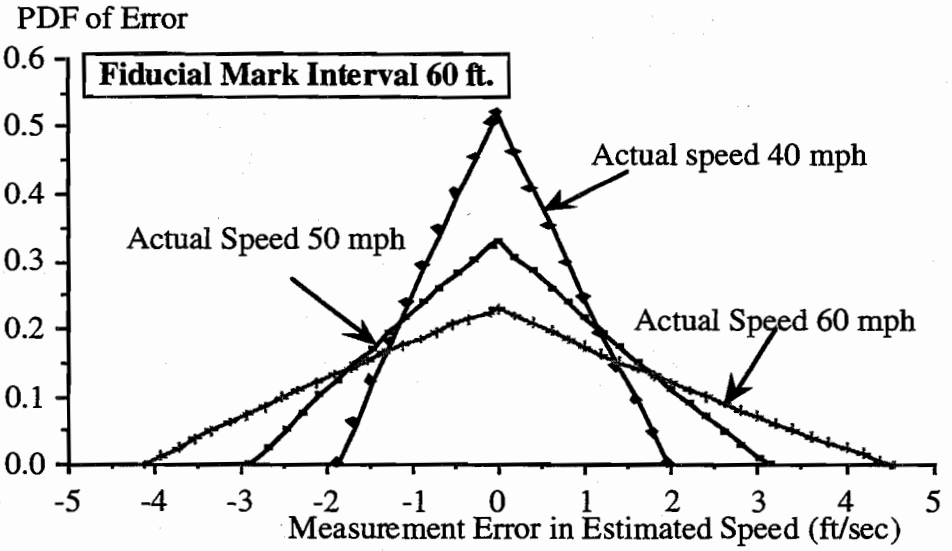

Figure 3.4 Probability density functions of speed estimation measurement error (fiducial mark intervals 60 ft., actual speed 40 mph, 50 mph, 60 mph)

shown in Table 3.4. A graphical presentation of the standard deviation of estimated speeds for different fiducial mark distances and speed is shown in Figure 3.5.

TABLE 3.4 RESULTS OF TRAVEL SPEED EXPERIMENTS

Test car Speed (mph)	Mean and Std. Dev. of Estimated Speed (mph) Fiducial Mark Distance (feet)		
	30	40	50
30	28.58 (3.13)	27.26 (2.50)	27.26 (2.30)
40	35.75 (5.80)	35.66 (4.44)	36.06 (4.22)
50	48.27 (10.22)	50.93 (8.23)	52.66 (7.70)
60	54.22 (10.29)	54.32 (7.93)	54.56 (7.76)

Note: the value in parenthesis is Std. Dev.

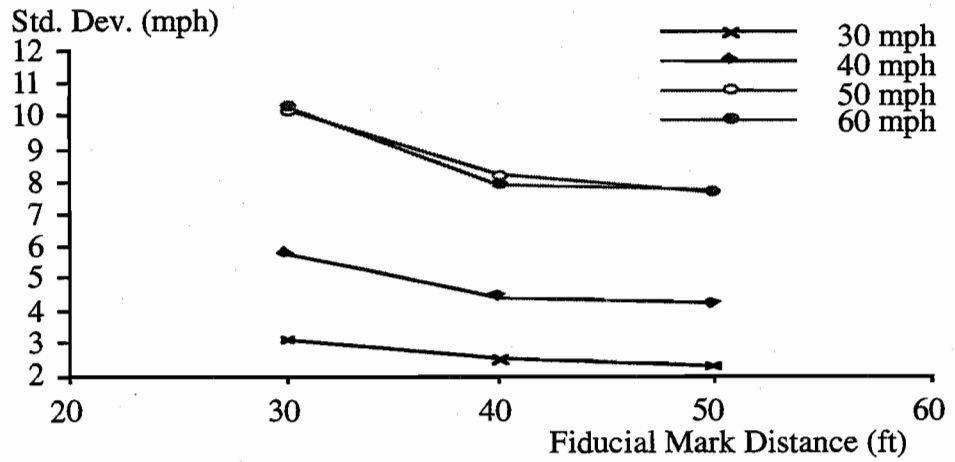

Figure 3.5 Std. dev. of estimated speeds with respect to different test car speeds and mark distances

Although the standard deviations of test car speeds of 50 mph and 60 mph are almost the same, the trends, however, are consistent with those of Figures 3.3 and 3.4 indicating that the larger the approach speed and the smaller the fiducial mark distance, the larger the estimated speed variance. Nevertheless, it is not appropriate to lengthen the fiducial mark distance to reduce the estimated speed variance. Not only because valuable information will be lost but also the probability that ramp vehicles will maintain constant speed will be decreased.

FREEWAY MERGE PROCESS ANALYSIS

A driver performs several different tasks during the merging process. Michaels and Fazio (1989) defined these tasks as follows: 1) tracking of the ramp curvature, 2) steering from the ramp curvature onto a tangent acceleration lane, 3) accelerating from the ramp controlling speed up to a speed closer to the freeway speed, 4) searching for an acceptable gap, and 5) steering from the acceleration lane onto the freeway lane or aborting. Essentially, drivers tend not to concentrate upon two different tasks simultaneously. They, however, will time-share between tasks. It is believed that ramp driver merge behavior is significantly influenced by the geometric configurations of the entrance ramp and the surrounding freeway and ramp vehicles. Despite the abstractness of ramp driver behavior, the merge position and gap acceptance can be clearly defined and observed in the field. In addition, knowing the merge position is useful in recognizing the use of acceleration lanes and in evaluating the goodness of ramp junction designs. Therefore, this study conducted a comprehensive field survey to investigate the role of prevailing traffic conditions and acceleration lane geometric features on ramp vehicle merge position as well as gap acceptance. Both parallel and taper type acceleration lanes were included. Each ramp type was further divided into long and short acceleration lanes. Long acceleration lanes refer to those whose lengths meet AASHTO design criterion. Short acceleration lanes, on the other hand, refer to those not meeting AASHTO design criteria. Sketchs of each entrance ramp along with average merge percentages in each section are shown in Figures 3.6 to 3.9. The long taper type entrance ramp is located in Houston Texas and the other three locations are in Austin Texas. These surveys covered both off-peak and peak periods to capture a wide traffic flow range. Congested traffic was not considered because ramp drivers behave unpredictably and execute forced merges. Among the locations under investigation, the long taper type acceleration lane is the only one for which vehicle trajectory data were captured; and therefore corresponding analyses related to vehicle speeds, speed differentials, and time lags were available. Ramp vehicle merge position analyses are presented in the next section followed by gap acceptance behavior analyses.

1. Short Parallel Type Entrance Ramp

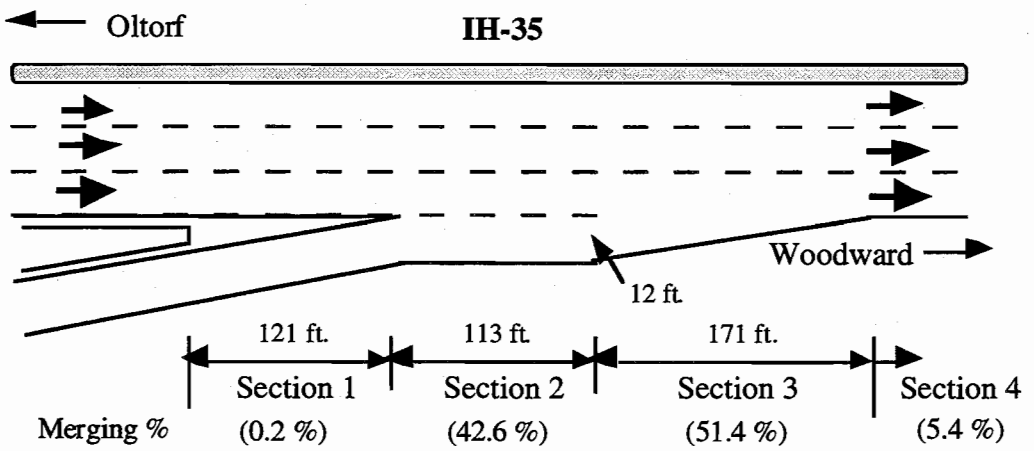

Figure 3.6 Sketch of short parallel type entrance ramp

2. Short Taper Type Entrance Ramp

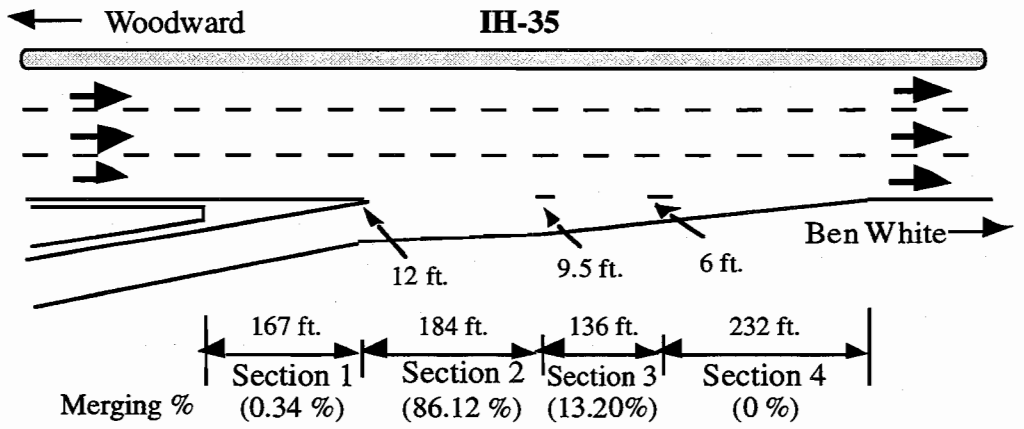

Figure 3.7 Sketch of short taper type entrance ramp

3. Long Parallel Type Entrance Ramp

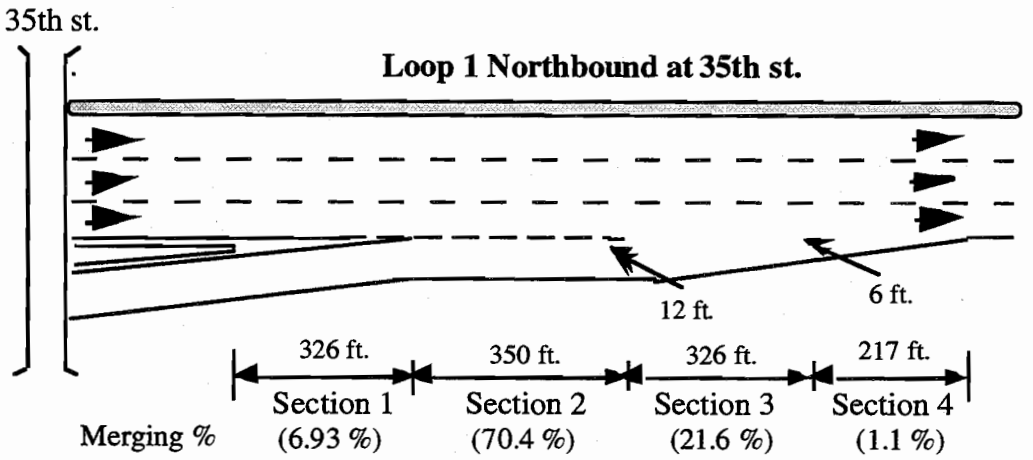

Figure 3.8 Sketch of long parallel type entrance ramp

4. Long Taper Type Entrance Ramp

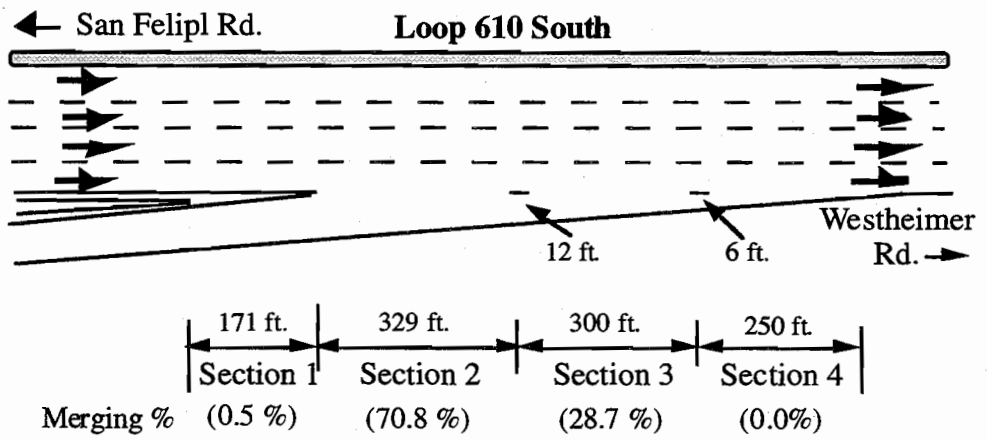

Figure 3.9 Sketch of long taper type entrance ramp

On the average, except for the short parallel type acceleration lane, more than 70% of the ramp vehicles merged where ramp has a width of 12 feet. Except for the long parallel type acceleration lane, very few merges occurred in section 1. Almost all vehicles merged before the last taper section where the ramp width is less than 6 feet. On the short parallel type acceleration lane, there is a 12 feet paved shoulder in section 4 which some drivers used as an acceleration lane extension. This explains why comparatively higher percentages of vehicles merged in sections 3 and 4 of this location. The short taper type location has a guardrail along sections 3 and 4 which seems to discourage drivers from using those sections. In other words, drivers tried to merge as soon as possible in order to avoid the guardrail resulting in 86.46% of the ramp vehicles merging before section 3. Section 1 of the long parallel type acceleration lane is 326 feet in length and drivers easily mistake it as a normal merging area resulting in 6.93% merging in that section.

The relationship of sectional merge percentages with respect to different acceleration lane lengths was graphically examined using the data collected at limited locations. Hypothetically, the longer the entrance ramp, the sooner the ramp vehicle merge. If this hypothesis holds, the data should demonstrate such a trend. However, the graphical results, as shown in Figure 3.10, visibly do not strongly support the conceptual hypothesis partly due to insufficient data collection sites. Nevertheless, it is still feasible to develop a general model describing the relationship of the sectional merge percentage as a function of attributes of the merge such as acceleration lane length and entrance ramp type. This kind of model would be useful in freeway entrance ramp design practices. In this study, however, it is impossible to conduct such analysis because data were collected at only one location for each entrance ramp type. More data collected from different sites would be needed to develop such a relationship.

Merge Position Analysis

Acceleration lanes are designed as safety facilities allowing ramp vehicles to make a smooth merge without causing dramatic interference to freeway streams. A well designed acceleration lane should permit ramp drivers to perform a safe merge within the effective acceleration lane length. Due to the dynamic nature of freeway merge traffic flows, many elements influence ramp vehicle merge positions. Among others, the more important elements are entrance ramp geometric configurations, ramp vehicle speeds, relative speeds as well as relative positions with respect to freeway vehicles, and ramp driver attributes and preferences. Establishing an in-depth understanding of freeway merge position phenomenon is useful in developing a freeway merge behavior mathematical framework. Quantitative examinations of this freeway merge phenomenon, however, are not well documented in literature. Fairly general investigations of freeway merge

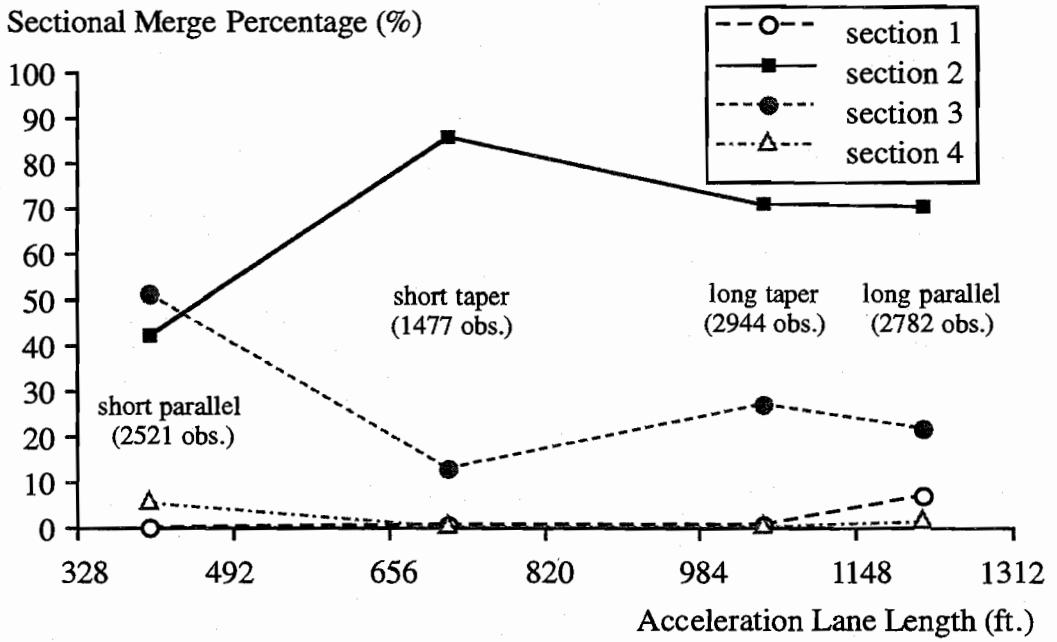

Figure 3.10 Sectional merge percentage vs. acceleration lane length

positions with respect to different entrance ramp types were presented in the previous section. This section, on the other hand, will examine the relationships between freeway merge positions and prevailing traffic flow conditions. Details of graphical presentations along with tests of independence in contingency tables of merge positions with respect to traffic flow levels, ramp vehicle speeds, time gaps to freeway vehicles, and speed differentials to freeway vehicles are shown in Figures 3.11 to 3.19 and Tables 3.6 to 3.14, respectively.

The major objective of using contingency table is to test the null hypothesis that merge positions are independent of prevailing traffic conditions against the alternative that the two categories are dependent. That is , one wishes to test

H_0 : column classification is independent of row classification.

Theoretically, if the two classifications are independent of each other, a cell probability will equal the product of its respective row and column probabilities in accordance with the multiplicative law of probability. Accordingly, under the null hypothesis, the maximum-likelihood estimate of the expected frequency of cell (i, j), n_{ij}, is given as follows(Mendenhall et al., 1986) :

$$\hat{E}(n_{ij}) = \frac{r_i c_j}{n} \tag{3.3}$$

Where

r_i is the number of observations in row i

c_j is the number of observations in column j

n is the total number of observations

One can use the expected and observed cell frequencies to calculate the test statistic:

$$\chi^2 = \sum_{j=1}^{c}\sum_{i=1}^{r} \frac{[\, n_{ij} - \hat{E}(n_{ij})\,]^2}{\hat{E}(n_{ij})} \tag{3.4}$$

Where

r is the number of row classifications

c is the number of column classifications

The test statistic, χ^2, follows the chi-square distribution with $(r\text{-}1)(c\text{-}1)$ degree of freedom. Therefore, if one use α=0.05, one will reject the null hypothesis that the two categories are independent if $\chi^2 > \chi^2_{0.05,\,(r-1)(c-1)}$.

Merge Positions with Respect to Freeway and Ramp Flow Levels. Merge percentages in this analysis are the average values over five minute intervals; and the traffic flow is a five minute flow rate. The flow rate boundaries used in the contingency table independence tests were calculated based on the level of service criteria for ramp-freeway junction areas in the Highway Capacity Manual (1994). The hourly flow rate for each level of service is simply the product of that level's maximum density and maximum speed. Table 3.5 demonstrates the hourly flow rate for levels of service B to E.

TABLE 3.5 LEVEL OF SERVICE AND CORRESPONDING HOURLY FLOW RATES

Level of Service	Hourly Flow Rate (vph)
B	1160
C	1568
D	1820
E	2200

1. Short Parallel Type Acceleration Lane

Across all flow ranges, compared to the other ramp types, higher percentages, 35% to 70%, of ramp vehicles merged in section 3. This may be explained by the shortness of sections 1 and 2 and the fact that there is a 12 feet paved shoulder in section 4 serving as an entrance ramp continuation. In addition, on a short acceleration lane, drivers normally have little time to make decisions. Therefore, this result might be the direct consequence of driver behavior randomness. The statistical test result shown in Table 3.6 coincides with that of the graphical presentation in Figure 3.11.

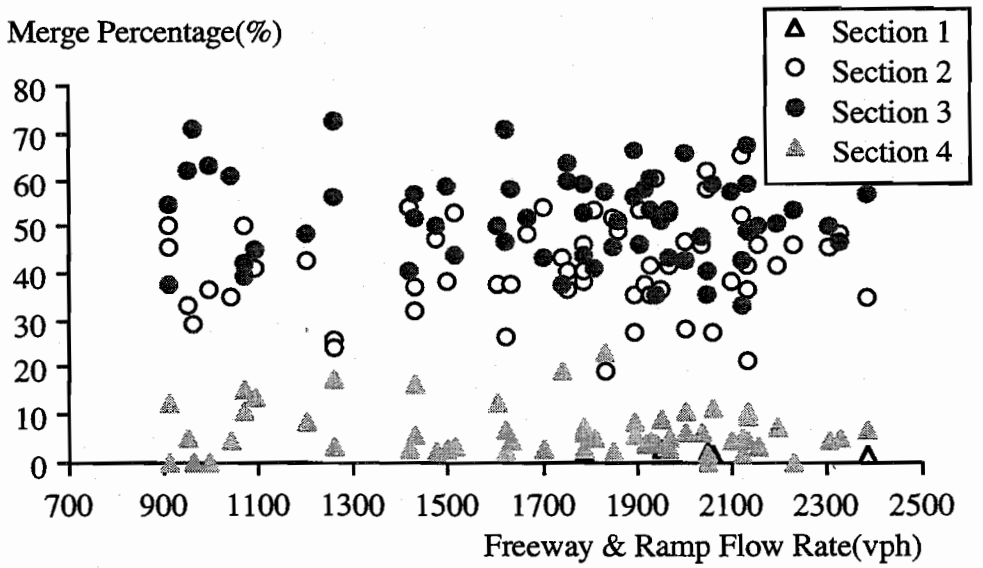

Figure 3.11 Merge percentage vs. total freeway right lane and ramp flows (short parallel type entrance ramp)

TABLE 3.6 TEST OF INDEPENDENCE FOR MERGE POSITIONS VS. TOTAL FREEWAY RIGHT LANE AND RAMP FLOWS(SHORT PARALLEL TYPE ENTRANCE RAMP)

	Numbers of Merges			
Hourly Flow Rate (vph)	Section 2	Section 3	Section 4	Total
< 1568	205 (216.3)	266 (261.1)	34 (27.6)	505
1568 < < 1820	204 (207.8)	256 (250.7)	25 (26.5)	485
1820 < < 2200	550 (538.4)	639 (649.8)	68 (68.8)	1257
2200 <	114 (110.5)	134 (133.4)	10 (14.1)	258
Total	1073	1295	137	2505

(Note: Numbers in parentheses are the estimated expected cell frequencies.)
The test statistic value is 4.173 and the critical value is $\chi^2_{6,\ 0.95} = 12.59$.

Conclusion : Accept the null hypothesis that merge positions are independent of freeway right lane and ramp total flow rates at a 5% significance level.

2. Short Taper Type Acceleration Lane

For this ramp type and all traffic flow values, more than 70% of the ramp vehicles merged in section 2. This result is not surprising for the acceleration lane width decreases from 12 feet at the section 2 beginning to 9.5 feet at the section 2 end and section 4 has a guardrail and no shoulder. In order not to stop before merging, ramp drivers will try to merge earlier. In other words, the geometry tends to force merging. The result of Figure 3.12 coincides with that of the statistical test in Table 3.7.

3. Long Parallel Type Acceleration Lane

Intuitively, it was hypothesized that the larger the freeway and ramp flow rates, the longer the distance ramp vehicles travel in the acceleration lane because of few large freeway traffic gaps. However, the data of Figure 3.13 do not show this trend but indicate that no matter how large the flow rates, 60% to 80% and 10% to 30% of the ramp vehicles merge in sections 2 and 3, respectively. This might partially result from the fact that at large freeway flow rates, aggressive ramp drivers take advantage of slow freeway traffic speeds and merge earlier while passive drivers stay in the acceleration lane waiting for larger gaps. A high percentage of ramp vehicles illegally merged in section 1 where the length is 326 feet. The Table 3.8 result supports that of Figure

3.13. The percentage of ramp vehicles merging in section 4 were very small; and therefore it was not included in the statistical test.

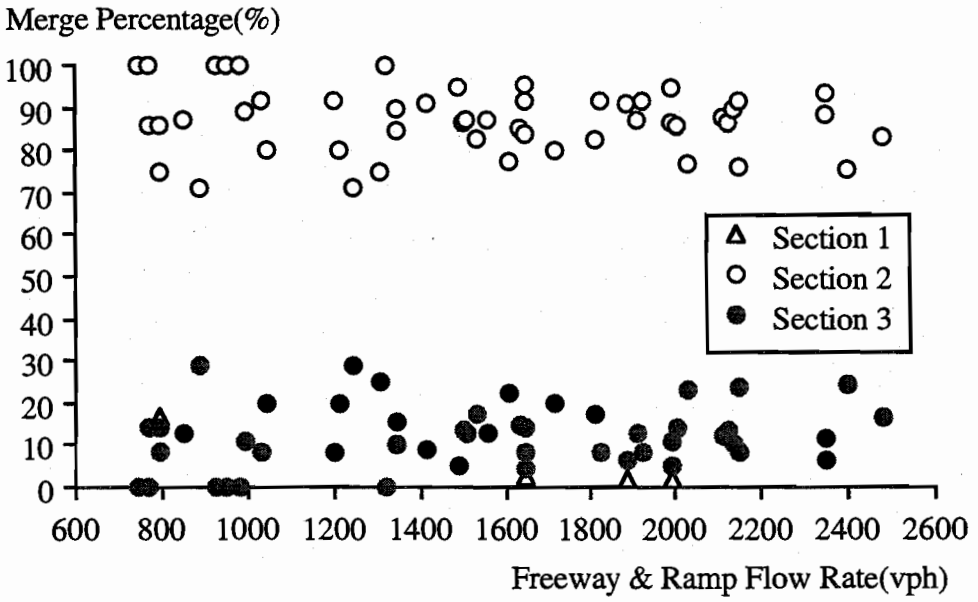

Figure 3.12 Merge percentage vs. total freeway right lane and ramp flows (short taper type entrance ramp)

TABLE 3.7 TEST OF INDEPENDENCE FOR MERGE POSITIONS VS. TOTAL FREEWAY RIGHT LANE AND RAMP FLOWS (SHORT TAPER TYPE ENTRANCE RAMP)

	Numbers of Merges		
Hourly Flow Rate (vph)	Section 2	Section 3	Total
< 1568	329 (326.9)	48 (50.1)	377
1568 < < 1820	201 (205.5)	36 (31.5)	237
1820 < < 2200	532 (525.4)	74 (80.6)	606
2200 <	210 (214.2)	37 (32.8)	247
Total	1272	195	1467

The test statistic value is 2.068 and the critical value is $\chi^2_{3,\ 0.95} = 7.81$.

Conclusion : Accept the null hypothesis that merge positions are independent of freeway right lane and entrance ramp total flow rates at the 5% significance level.

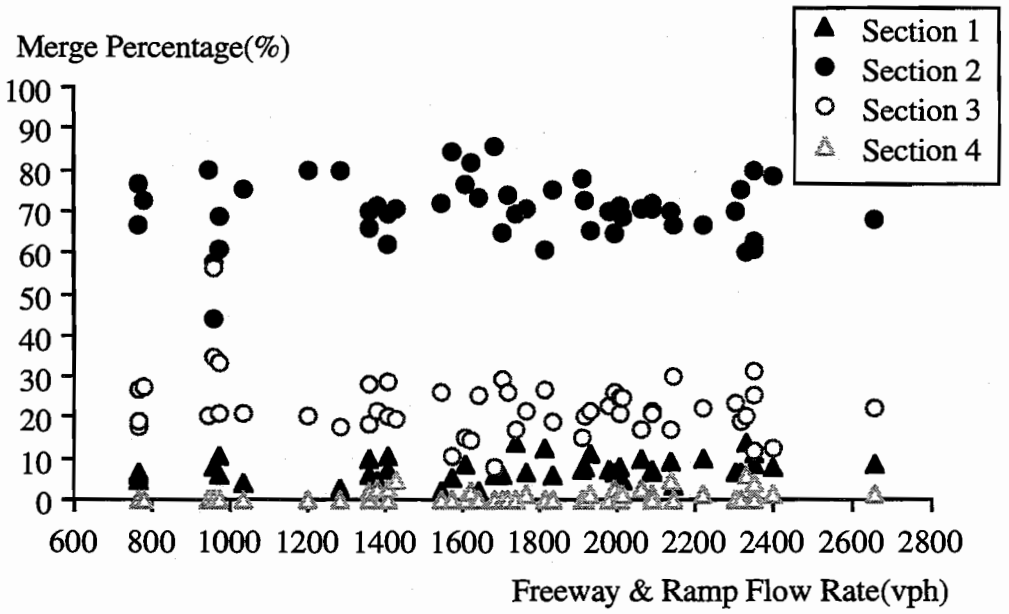

Figure 3.13 Merge percentages vs. total freeway right lane and ramp flows (long parallel type entrance ramp)

TABLE 3.8 TEST OF INDEPENDENCE FOR MERGE POSITIONS VS. TOTAL FREEWAY RIGHT LANE AND RAMP FLOWS (LONG PARALLEL TYPE ENTRANCE RAMP)

	Numbers of Merges			
Hourly Flow Rate (vph)	Section 1	Section 2	Section 3	Total
< 1568	30 (40.1)	403 (407.2)	139 (124.7)	572
1568 < < 1820	34 (38.2)	402 (387.2)	108 (118.6)	544
1820 < < 2200	66 (64.7)	655 (656.3)	201 (201.0)	922
2200 <	63 (50.1)	499 (508.3)	152 (155.7)	714
Total	193	1959	600	2752

Test statistic value is 9.816 and the critical value is $\chi^2_{6,\ 0.95} = 12.59$.

Conclusion : Accept the null hypothesis that merge positions are independent of freeway right lane and entrance ramp total flow rates at the 5% significance level.

4. Long Taper Type Acceleration Lane

The data of Figure 3.14 also show that merge positions are not very different across all flow rate ranges. For all flow rates, 50% to 80% of the ramp vehicles merged in section 2 where the acceleration lane width is greater than 12 feet. The reasons are similar to those explained for the long parallel type acceleration lane. The Figure 3.14 result coincides with the statistical test result in Table 3.9. In general, for both long parallel and taper type acceleration lanes, across all flow rate ranges, higher percentages of ramp vehicles merge in section 2. This seems to reveal that drivers prefer to merge earlier whenever a merge chance exists.

Merge Positions with Respect to Ramp Vehicle Approach Speeds. Ramp vehicle approach speeds were measured at the section 1 end point. It was hypothesized that the higher the ramp vehicle speed, the shorter the distance needed to complete the merge maneuver due to smaller speed differentials relative to freeway vehicles. The data of Figure 3.15, however, do not visibly support this hypothesis. The merge percentages in section 2 do not increase with higher approach speeds. This result might be due to the natural vehicle merge trajectory and driver-vehicle randomness. The results given in Table 3.10 also indicate that ramp vehicle merge positions are independent of approach speeds.

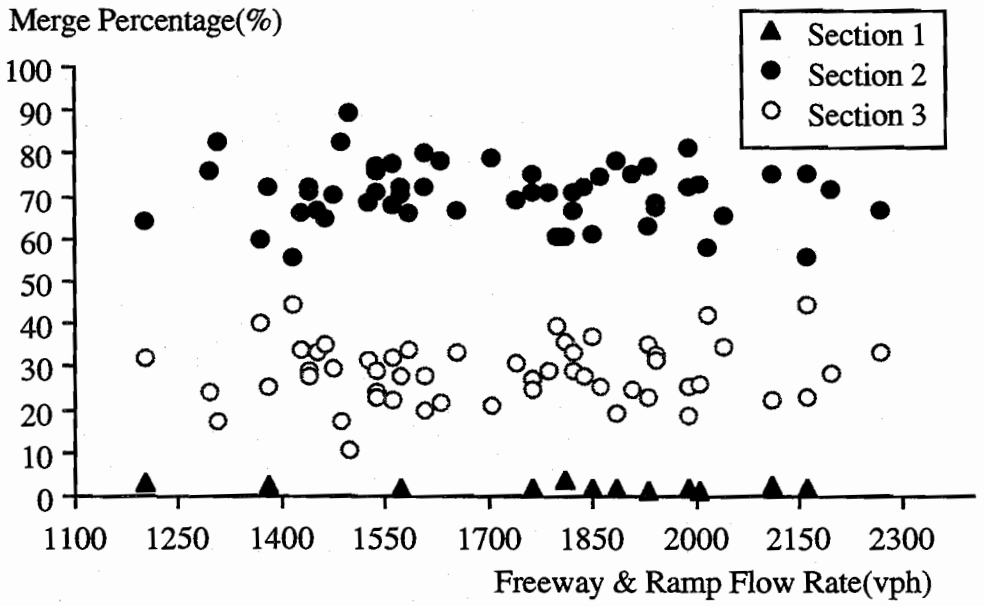

Figure 3.14 Merge percentage vs. total freeway right lane and ramp flows (long taper type entrance ramp)

TABLE 3.9 TEST OF INDEPENDENCE FOR MERGE POSITIONS VS. TOTAL FREEWAY RIGHT LANE AND RAMP FLOWS (LONG TAPER TYPE ENTRANCE RAMP)

	Numbers of Merges		
Hourly Flow Rate (vph)	Section 2	Section 3	Total
< 1568	630 (627.6)	252 (254.4)	882
1568 < < 1820	548 (545.1)	218 (220.9)	766
1820 < < 2200	867 (869.6)	355 (352.4)	1222
2200 <	40 (42.7)	20 (17.3)	60
Total	2085	845	2930

Test statistic value is 0.702 and the critical value is $\chi^2_{3,\ 0.95} = 7.81$.

Conclusion : Accept the null hypothesis that merging positions are independent of freeway right lane and entrance ramp total flow rates at the 5% significance level.

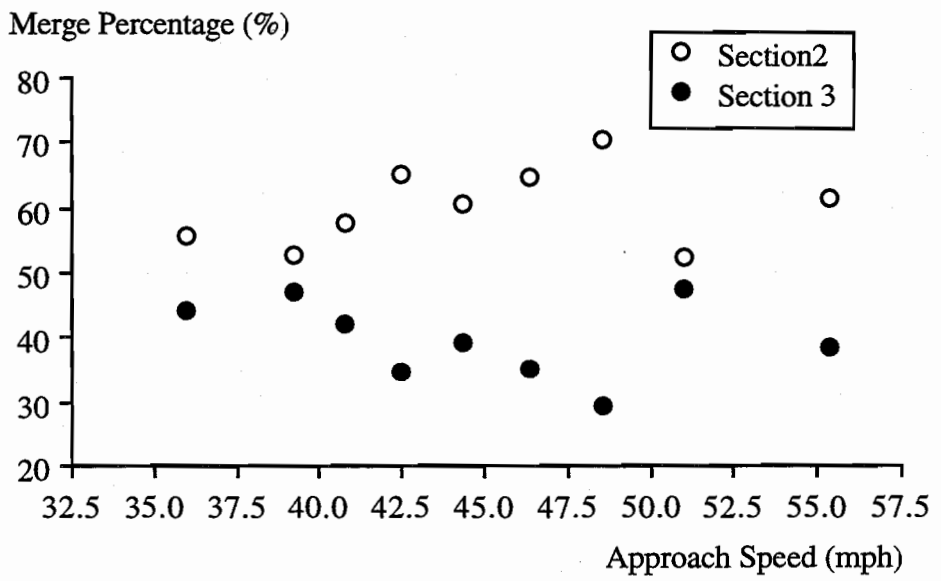

Figure 3.15 Merge percentage vs. ramp vehicle approach speed (long taper type entrance ramp)

TABLE 3.10 TEST OF INDEPENDENCE FOR MERGE POSITIONS VS. RAMP VEHICLE APPROACH SPEEDS (LONG TAPER TYPE ENTRANCE RAMP)

	Numbers of Merges		
Approach Speed (mph)	Section 2	Section 3	Total
speed < 40.0	19 (21.7)	16 (13.3)	35
40.0 <= speed < 45.0	55 (55.8)	35 (34.2)	90
45.0 <= speed < 50.0	62 (56.4)	29 (34.6)	91
50.0 <= speed	19 (21.1)	15 (12.9)	34
Total	155	95	250

Test statistic value is 2.907 an the critical value is $\chi^2_{3,\ 0.95} = 7.81.$

Conclusion : Accept the null hypothesis that merge positions are independent of ramp vehicle approach speeds at the 5% significance level.

Merge Positions with Respect to Time Lags between Ramp Vehicles and Corresponding Freeway Lag Vehicles. Time lags were measured at the section 1 end point. The freeway lag vehicle is defined in this study as the freeway right lane vehicle that is immediately behind the ramp vehicle when viewed by the ramp driver. It was hypothesized that the larger the time lag, the easier the ramp vehicle merge into the freeway stream. In other words, an increasing percentage of ramp vehicles should merge in section 2 when large time lags are presented. Whereas, trends shown in Figure 3.16 do not fully support this expectation. This result might be due to the fact that some ramp drivers would like to stay in the acceleration lane longer and comfortably merge with the freeway stream having a higher speed in the later portion of the acceleration lane even though a large acceptable gap is presented. The result of Table 3.11 also concludes that merge positions are independent of time lags to freeway lag vehicles.

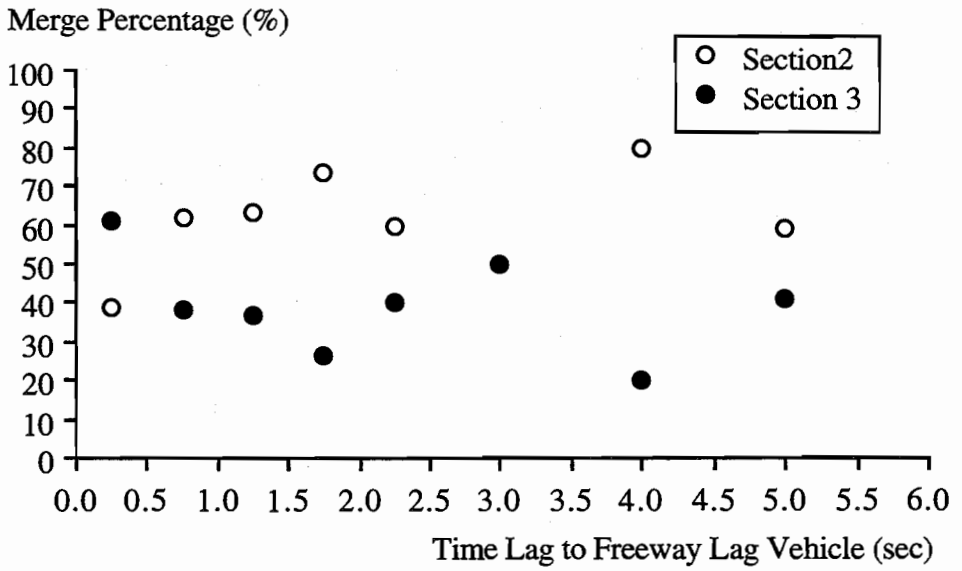

Figure 3.16 Merge percentage vs. time lag to freeway lag vehicle (long taper type entrance ramp)

TABLE 3.11 TEST OF INDEPENDENCE FOR MERGE POSITIONS VS. TIME LAGS TO FREEWAY LAG VEHICLES (LONG TAPER TYPE ENTRANCE RAMP)

	Numbers of Merges		
Time Lag (sec)	Section 2	Section 3	Total
lag < 1.0	38 (43.4)	32 (26.6)	70
1.0 <= lag < 2.0	60 (53.9)	27 (33.1)	87
2.0 <= lag < 3.5	31 (34.7)	25 (21.3)	56
3.5 <= lag	26 (22.9)	11 (14.1)	37
total	155	95	250

Test statistic value is 5.683 and the critical value is $\chi^2_{3,\ 0.95} = 7.81$.

Conclusion : Accept the null hypothesis that merging positions are independent of the time lags between the ramp vehicles and their corresponding freeway lag vehicles at the 5% significance level.

Merge Positions with Respect to Time Lags between Ramp Vehicles and Corresponding Freeway Lead Vehicles. Time lags were measured at the section 1 end point and the freeway lead vehicle is defined as the freeway right lane vehicle that is immediately in front of the ramp vehicle when viewed by the ramp driver. Similar to the previous case, one can hypothesize that there should be a higher percentage of ramp vehicles merging in section 2 when large time lags are presented. However, trends shown in Figure 3.17 are not strong enough to support the intuitive hypothesis. The conclusion drawn from Table 3.12 coincides with that of Figure 3.17.

Merge Positions with Respect to Speed Differentials between Ramp Vehicles and Corresponding Freeway Lag Vehicles. Speed Differentials, measured at the section 1 end point, with respect to freeway lag vehicles were defined as follows:

speed differential(V_{flagr}) = freeway lag vehicle speed - ramp vehicle speed

Unlike those elements considered in at-graded intersection merging, relative speed is one of the most important elements that influence freeway merge behavior. Intuitively, if relative speed is the sole factor that a ramp driver considers for merging, a ramp vehicle having a higher speed than its freeway lag vehicle, a negative speed differential according to above definition, should merge earlier. On the contrary, if a ramp vehicle has a lower speed than its freeway lag vehicle, a positive speed differential, the ramp vehicle will possibly yield to the freeway lag vehicle and wait for later acceptable gaps. Under this circumstance, the ramp vehicle will tend to merge in the later portion of the acceleration lane. Although Figure 3.18 indicates a slightly declining trend of merging percentages in section 2 as relative speed increases, the statistical test shown in Table 3.13, however, does not support the intuitive hypothesis that the faster the ramp vehicles relative to corresponding freeway lag vehicles, the earlier the freeway merge. Nevertheless, the result in Table 3.13 reveals that the test statistic will be significant at the 15 percent level implying that relative speed might have an effect on ramp vehicle merge positions.

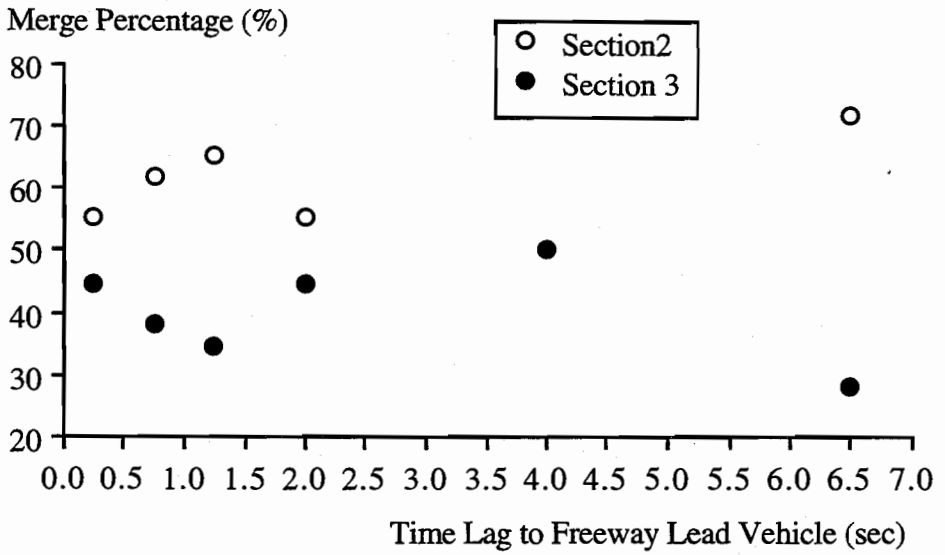

Figure 3.17 Merge percentage vs. time lag to freeway lead vehicle (long taper type entrance ramp)

TABLE 3.12 TEST OF INDEPENDENCE FOR MERGE POSITIONS VS. TIME LAGS TO FREEWAY LEAD VEHICLES (LONG TAPER TYPE ENTRANCE RAMP)

	Numbers of Merges		
Time Lag (sec)	Section 2	Section 3	Total
lag < 1.0	51 (54.6)	37 (33.4)	88
1.0 <= lag < 2.5	45 (45.3)	28 (27.7)	73
2.5 <= lag < 5.5	11 (13.6)	11 (8.4)	22
5.5 <= lag	48 (41.5)	19 (25.5)	67
total	155	95	250

Test statistic value is 4.604 and the critical value is $\chi^2_{3,\ 0.95} = 7.81$.

Conclusion : Accept the null hypothesis that merge positions are independent of the time lag between the ramp vehicles and their freeway lead vehicles at the 5% significance level.

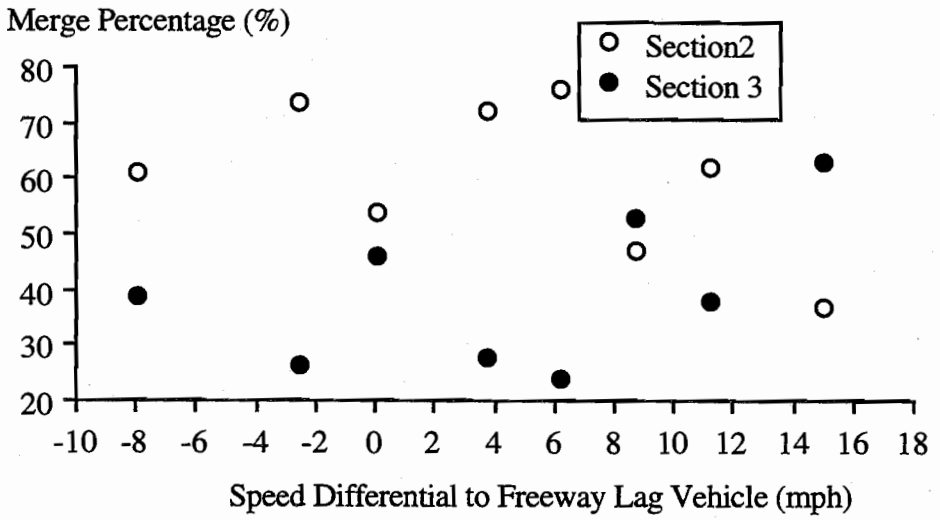

Figure 3.18 Merge percentage vs. speed differential to freeway lag vehicle (long taper type entrance ramp)

TABLE 3.13 TEST OF INDEPENDENCE FOR MERGE POSITIONS VS. SPEED DIFFERENTIALS TO FREEWAY LAG VEHICLES (LONG TAPER TYPE ENTRANCE RAMP)

	Numbers of Merges		
Speed Differentials (mph)	Section 2	Section 3	Total
speed diff. < 0.0	42 (37.1)	18 (22.9)	60
0.0 <= speed diff. < 5.0	47 (50.1)	34 (30.9)	81
5.0 <= speed diff. < 10.0	37 (34.0)	18 (21.0)	55
10.0 <= speed diff.	20 (24.8)	20 (15.2)	40
total	146	90	236

Test statistic value is 5.258 and the critical value is $\chi^2_{3,\ 0.95} = 7.81$.

Conclusion : Accept the null hypothesis that merge positions are independent of the speed differential between ramp vehicles and their freeway lag vehicles at the 5% significance level.

Merge Positions with Respect to Speed Differentials between Ramp Vehicles and Corresponding Freeway Lead Vehicles. The speed differentials, measured at the section 1 end point, with respect to freeway lead vehicles were defined as follows:

$$\text{speed differential}(V_{rflead}) = \text{ramp vehicle speed} - \text{freeway lead vehicle speed}$$

Hypothetically, when a ramp vehicle enters the acceleration ramp with a higher speed than the corresponding freeway lead vehicle, a positive speed differential according to above definition, the ramp driver can either accelerate to overtake the freeway lead vehicle and merge in front of it or decelerate to look for later gaps. In either situation, the ramp vehicle should have a higher probability to merge in the later portion of the acceleration lane. The larger the speed differential, the larger the probability. Except for the data point when the speed differential is greater than 12.5 mph, the data shown in Figure 3.19 do not strongly support the intuitive hypothesis. The statistical test in Table 3.14 also indicates that the test statistic is not significant at the 5 percent significance level.

In conclusion, for all entrance ramp types, ramp drivers behave differently with regard to merge positions. Both the graphical presentations and the independence tests in the contingency tables show that the ramp vehicle merge position is not significantly related to any single traffic parameter. It is reasonable to conclude that driver-vehicle behavior during merge maneuvers can only be better modeled using some combinations of the above traffic parameters.

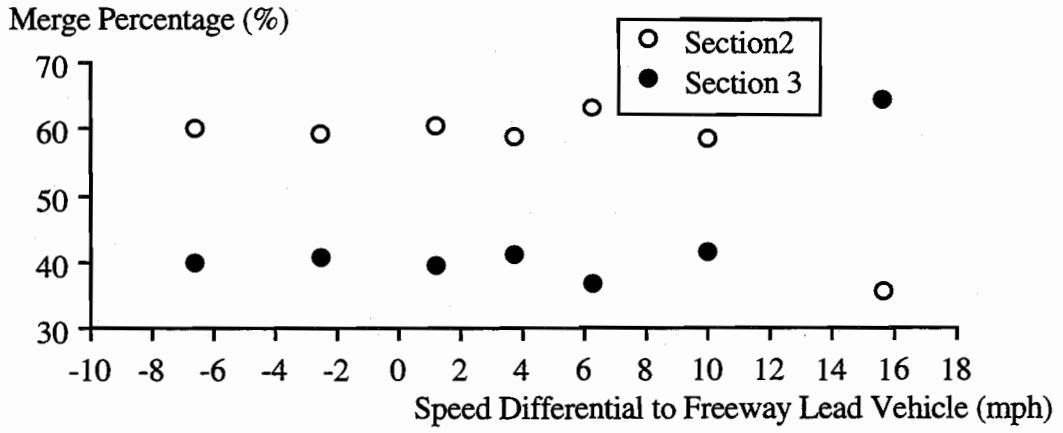

Figure 3.19 Merge percentage vs. speed differential to freeway lead vehicle (long taper type entrance ramp)

TABLE 3.14 TEST OF INDEPENDENCE FOR MERGE POSITIONS VS. SPEED DIFFERENTIALS TO FREEWAY LEAD VEHICLES (LONG TAPER TYPE ENTRANCE RAMP)

	Numbers of Merges		
Speed Differential (mph)	Section 2	Section 3	Total
speed diff. < 0.0	25 (24.6)	17 (17.4)	42
0.0 <= speed diff. < 5.0	39 (38.0)	26 (27.0)	65
5.0 <= speed diff. < 10.0	31 (29.8)	20 (21.2)	51
10.0 <= speed diff.	12 (14.6)	13 (10.4)	25
total	107	76	183

Test statistic value is 1.323 and the critical value is $\chi^2_{3,\ 0.95} = 7.81$.

Conclusion : Accept the null hypothesis that merge positions are independent of the speed differentials between ramp vehicles and their freeway lead vehicles at the 5% significance level.

Merge Gap Acceptance Behavior Analysis

Many elements affect ramp driver gap acceptance behavior. Aggressive drivers may accept a small gap early in the acceleration lane and at a small speed differential relative to the corresponding freeway lag vehicle while passive drivers may not. In the literature, freeway merge gap acceptance analyses were mainly focused on examination of accepted gap or accepted speed differential magnitudes. This approach, however, is too simple to catch freeway merge gap acceptance dynamics, for hypothetically, a ramp driver may behave differently at different acceleration lane locations even facing a similar "gap structure". In this study, gap structure refers to those elements that compose freeway gaps, e.g. time gap, distance gap, and speed differential as well as angular velocity between the ramp and corresponding freeway lag and lead vehicles. To develop an in-depth understanding of freeway merge gap acceptance behavior, this study investigated the driver-vehicle phenomena, i.e. acceleration rate, speed, and relative speed to surrounding freeway vehicles, at the location where ramp drivers accepted a gap and performed a merge. This analysis tries to examine whether ramp drivers evaluate "gap structure" differently at different entrance ramp locations. For example, one might want to find out if ramp drivers will accelerate strongly when they merge early in the acceleration lane or if ramp drivers will accept a smaller gap when they merge in the later portion of the acceleration lane. Knowing this ramp driver gap acceptance behavior is useful in developing conceptual gap acceptance behavior models. Due to observation data availability, this analysis is focused on the long taper type entrance ramp

only. Scatter plots of various accepted gap structure elements *versus* merge locations, in terms of fiducial marks, along with the mean, median, and standard deviation were shown in Figures 3.20 to 3.29 respectively.

Merge Acceleration Rate *versus* Merge Position. Acceleration lanes are designed to allow ramp vehicles to accelerate to a speed comparable to freeway vehicles before performing a safe merge. Hypothetically, if ramp vehicles merge early in the acceleration lanes, they may use large acceleration rates in order to quickly match freeway vehicle speeds. However, ramp vehicles traveling in the later portion of the acceleration lane while waiting for a larger acceptable gap may also use large acceleration rates during merge maneuvers to avoid stopping at the acceleration lane end. Although both the median and the mean lines shown in the Figure 3.20 do not strongly demonstrate such trends, the scatter plot, however, seems to partially support this intuitive hypothesis. Most points for fiducial marks 11 and 13 show larger acceleration rates than other fiducial marks. On average, vehicles merging in the later portion of the acceleration lane use larger acceleration rates during the merge maneuver than those merging early. Merging acceleration rate distributions for each fiducial mark are similar due to similar standard deviation magnitudes.

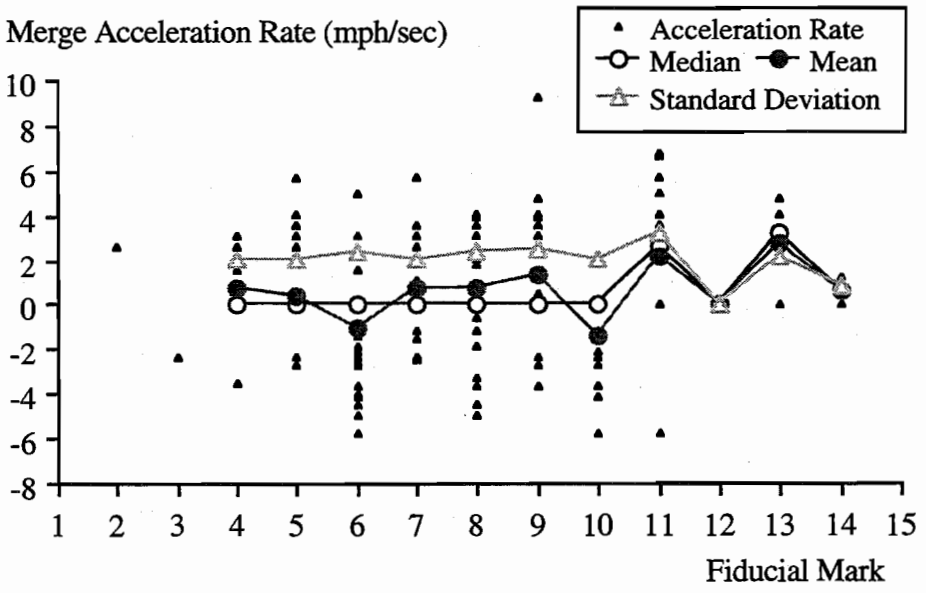

Figure 3.20 Ramp vehicle merge acceleration rate vs. merge position (fiducial mark)

Merge Speed *versus* Merge Position. Intuitively, ramp vehicles should have a higher merge speed if they merge in the later portions of the acceleration lane. Actually, due to gap search dynamics during the merge maneuvers, ramp drivers normally adjust speed in response to surrounding freeway traffic gap structures. As a result, ramp vehicles do not necessarily have higher merge speeds as they proceed further down the acceleration lane. Figure 3.21 shows that, except for those of fiducial mark 14, mean and median merge speeds across all fiducial marks do not visibly change significantly. Low merge speeds from fiducial mark 14 indicate that ramp vehicles potentially tend to reduce speed while they are approaching the acceleration lane end. Due to only two ramp vehicles were observed to merge from fiducial mark 14, these results are tentative. In spite of almost equal mean and median magnitudes across all fiducial marks, the scatter of points range from as low as 25 mph to as high as 60 mph indicating that individual ramp drivers do behave differently. A high standard deviation magnitude also supports this evidence.

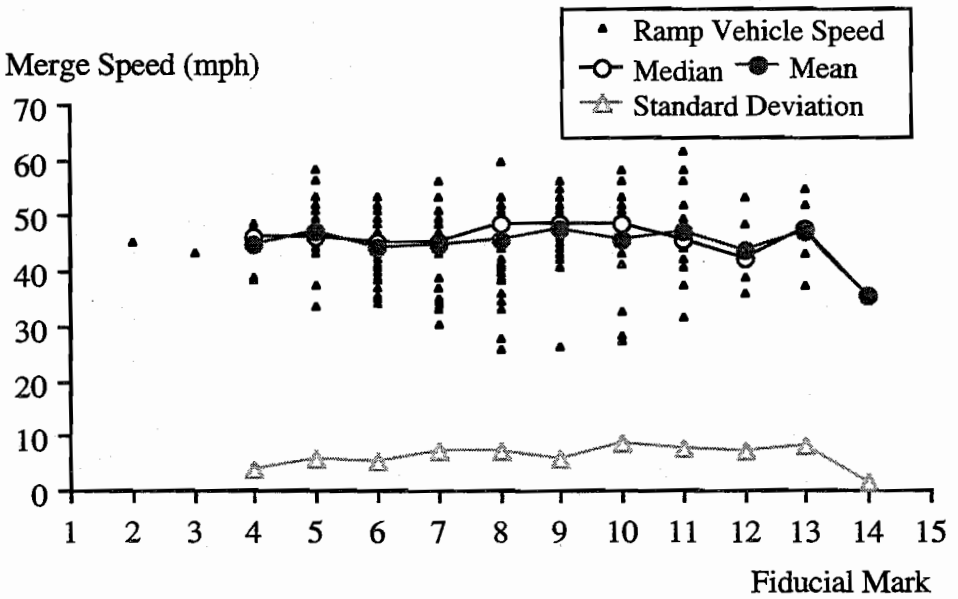

Figure 3.21 Ramp vehicle merge speed vs. merge position (fiducial mark)

Merge Speed Differential to Freeway Lag Vehicle *versus* Merge Position. Merge speed differentials to freeway lag vehicles were measured at the time when ramp vehicles were performing a merge maneuver and are defined as follows:

merge speed differential to freeway lag vehicle
= freeway lag vehicle speed at ramp vehicle merging time - ramp vehicle speed

On average, as shown in Figure 3.22, ramp vehicles had only a slightly lower speed than corresponding freeway lag vehicles when they merged between fiducial marks 4 and 11. The difference, however, is not significant. Negative merge relative speeds observed at fiducial marks 12 and 13 indicate that in the later portion of the acceleration lane, ramp vehicles merged with a higher speed than corresponding freeway lag vehicles. This phenomenon is probably due to the fact that when approaching the entrance ramp merge area, freeway vehicles will yield to corresponding ramp lead vehicles by reducing speed or making a lane change to create a larger gap for ramp vehicles. Dramatic scatter plot ranges associate with each fiducial mark, however, reveal that significant gap acceptance behavior differences, in terms of speed differential during the merge maneuver, exist among ramp drivers.

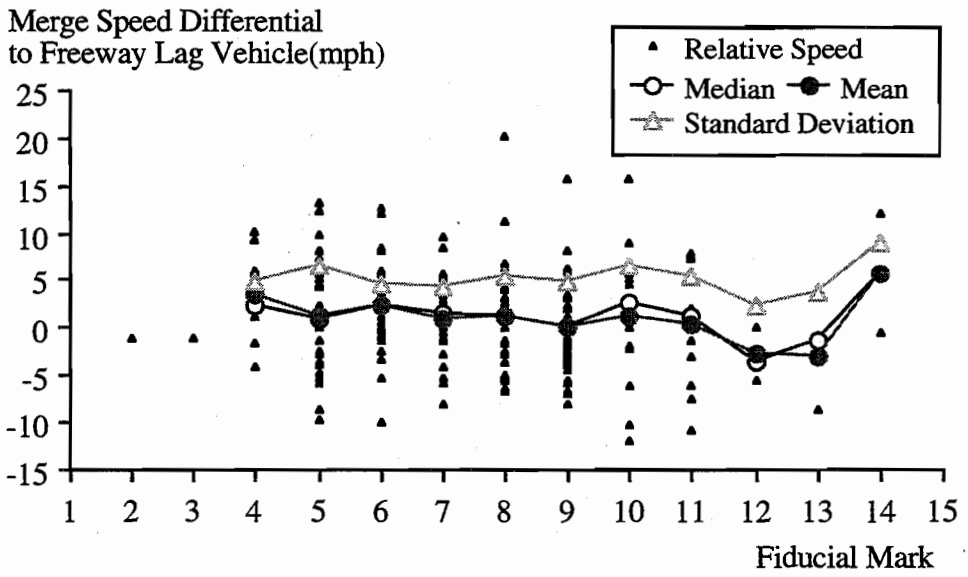

Figure 3.22 Merge speed differential to freeway lag vehicle vs. merge position (fiducial mark)

Merge Time Gap to Freeway Lag Vehicle *versus* Merge Position. In the last section, one of the important gap structure elements, relative speed between ramp vehicles and their corresponding freeway lag vehicles, was discussed. However, treating relative speed as a sole gap structure element will mislead the freeway merge gap acceptance behavior analysis. Theoretically, zero speed differential between a ramp vehicle and its corresponding freeway lag vehicle implies an infinite time gap between these two vehicles. Obviously, facing a zero or even negative speed differential to its freeway lag vehicle, a ramp driver will not carelessly merge to the freeway stream despite the physical separation to the freeway lag vehicle. Consequently, the effect of the time gap to the freeway lag vehicle on ramp driver gap evaluation behavior should be investigated. In this analysis, each ramp vehicle merge time gap to its freeway lag vehicle was dynamically measured at the location, represented by fiducial marks, where each ramp vehicle actually merged and was defined as the time difference between ramp vehicle passage and corresponding freeway lag vehicle passage of that specific fiducial mark. Results shown in Figure 3.23 demonstrates that the median visibly has a slightly decreasing trend. This phenomenon, although insignificant, implicitly reveals that most ramp drivers may tend to accept a smaller gap as they proceed further down the acceleration lane. The increasing trend at fiducial marks 12, 13 and 14 might be due to the fact that freeway lag vehicles yield the right of way to anxious ramp vehicles to prevent a merge accident. This result, however, is not conclusive due to the small data quantity. Mean freeway merge accepted gap magnitudes, ranging from 1 to 2 seconds, were considerably smaller than those found at at-graded stop-controlled intersections (Fitzpatrick 1991, Raff 1950, and Solberg and Oppenlander 1966) indicating that in addition to time gap, relative speed between ramp and freeway vehicles also plays an important role in determining ramp driver gap acceptance behavior.

Merge Distance Gap to Freeway Lag Vehicle *versus* Merge Position. In this analysis, merge distance gaps are the longitudinal distances between ramp vehicles and their corresponding freeway lag vehicles measured at the locations where ramp vehicles merged. Similar to time gap, distance gap is another important freeway merge gap acceptance element. Intuitively, time gap and distance gap are positively correlated. The larger the time gap, the longer the distance gap. However, these two gap structure elements might have different impacts on ramp driver gap acceptance behavior; especially when speed differential effects are involved. Theoretically, ramp drivers should be able to estimate distance gaps easier than time gaps while traveling in the acceleration lane and consequently use it as a merge decision criterion. Therefore, a ramp driver might accept a very small distance gap which is an inconceivably small time gap, as

long as this ramp vehicle has a higher speed than its corresponding freeway lag vehicle and the distance gap is physically large enough to avoid a merge collision. Figure 3.24 shows that aggressive ramp drivers accepted small merge distance gaps when they merged immediately right after entering the acceleration lane, e.g. marks 2, 3, and 4. Ramp drivers who merged in the later portion of acceleration lane, e.g. marks 12, 13, and 14, were also accepted small distance gaps. This phenomenon might be partially due to the fact that ramp drivers were willing to accept small gaps to avoid stopping at the acceleration lane end. These conclusions, however, are tentative for few observations were obtained from marks 2, 3, 12, 13, and 14. Average merge distance gaps for all fiducial marks range between 100 feet and 150 feet and visibly have few significant differences except near the ramp end. The scatter plots, however, indicate widely varying driver merge behavior.

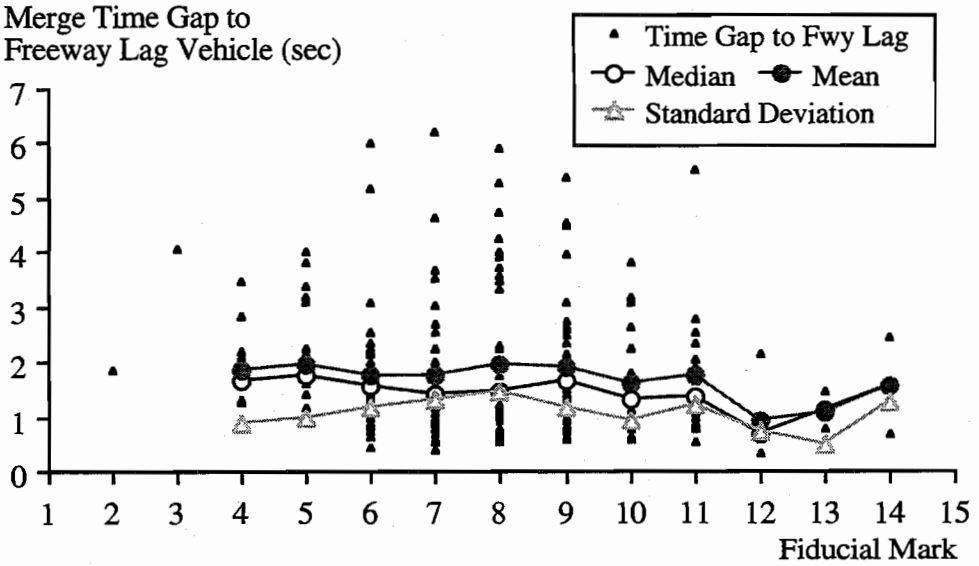

Figure 3.23 Merge time gap to freeway lag vehicle vs. merge position (fiducial mark)

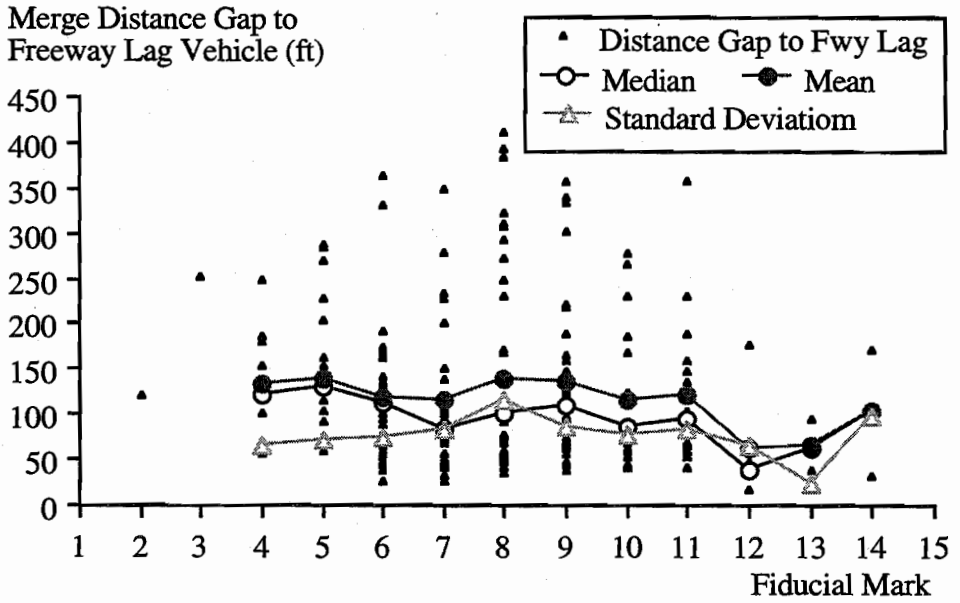

Figure 3.24 Merge distance gap to freeway lag vehicle vs. merge position (fiducial mark)

Merge Angular Velocity to Freeway Lag Vehicle *versus* Merge Position. The previous analyses treated each gap structure element as an unique gap acceptance decision criterion. Experience from one's daily driving, however, indicates that such an approach may not be sufficient to describe complex freeway merge behavior. The actual gap acceptance criteria used by ramp drivers during freeway merge maneuver are mixed and are difficult to clearly define. Nevertheless, it is believed that ramp drivers must use some combination of the above mentioned gap structure elements as freeway merge criteria. Among others, angular velocity, created by the relative movement of a ramp vehicle and its corresponding freeway lag vehicle, has been recognized as a good freeway merge gap acceptance decision criterion (Gordon and Michaels, 1963; Drew, 1971; Michaels and Fazio, 1989; Reilly, et al., 1989). Mathematically, angular velocity incorporates relative speed and longitudinal distance separation into one single formulation. As the freeway lag vehicle is closing on the gap seeking driver, the angular velocity becomes larger or smaller if the freeway lag vehicle is falling behind relative to the merging vehicle. Intuitively, using angular velocity as a gap acceptance decision criterion is superior to any model considering only the time or distance gap although it is extremely difficult to experimentally prove. Figure 3.25 shows the angular velocities actually accepted by ramp drivers *versus* the merge positions, in

terms of fiducial marks. Similar to those of Figure 3.22, the means and medians of merging angular velocity are close to zero because angular velocity is a function of relative speed. The scatter ranges in Figure 3.25 are visibly smaller than those of Figures 3.22, 3.23, and 3.24. Most merge angular velocities fall within the range of ± 0.025 rads/sec. This evidence implicitly reveals that angular velocity might be a better gap acceptance decision criterion than others for it reflects a more consistent driver behavior. Driver merging at fiducial marks 12, 13, and 14 seem to accept a negative angular velocity. This conclusion, however, is tentative because of small number of observations.

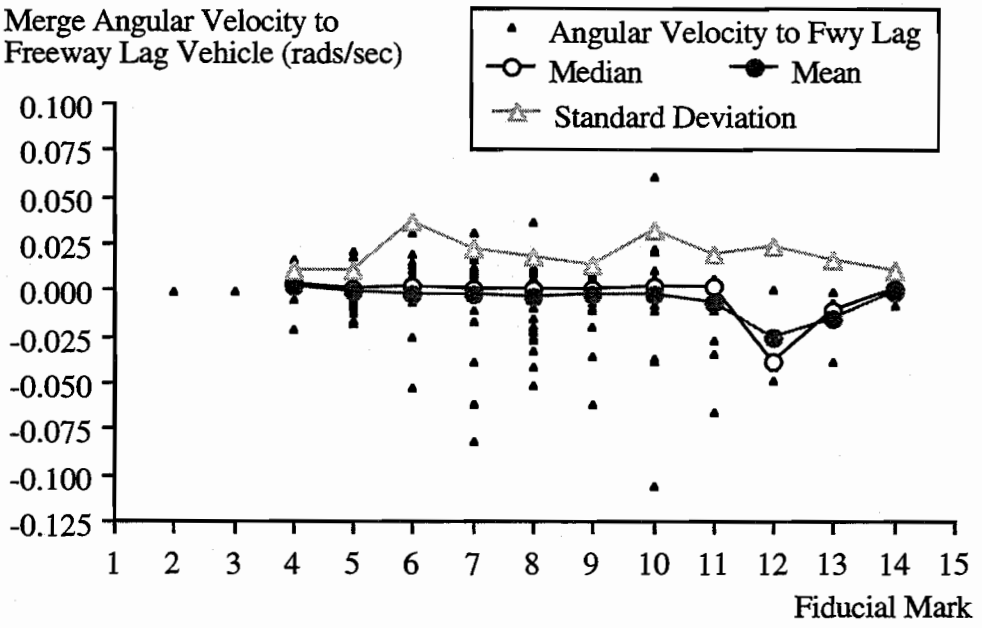

Figure 3.25 Merge angular velocity to freeway lag vehicle vs. merge position (fiducial mark)

Merge Speed Differential to Freeway Lead Vehicle *versus* Merge Position. When ramp drivers are performing a freeway merge maneuver, they will consider relative movements to corresponding not only freeway lag vehicles but also freeway lead vehicles. Due to viewing angle differences in evaluating relative vehicle movement, effects of these two vehicles are different. Ramp drivers must use rear view mirrors or turn their heads to detect freeway lag vehicle movement, while neither action is needed for viewing freeway lead vehicles. The effects

of gap structure elements, with respect to freeway lag vehicles, on ramp driver gap acceptance behavior have been discussed in sections 3.4.2.3 to 3.4.2.6. Similar analyses but focused on freeway lead vehicle gap structure effects are presented in the following sections.

In this section, speed differential, with respect to the corresponding freeway lead vehicle, associated with the actual accepted gap *versus* merge positions is discussed. Merge speed differentials to the freeway lead vehicle were measured at the time when ramp vehicles were performing a merge maneuver and are defined as follows:

merge speed differential to freeway lead vehicle
= ramp vehicle speed - freeway lead vehicle speed at ramp vehicle merging time

Demonstrations in Figure 3.26 indicate that, on average, ramp vehicles have a lower speed than their corresponding freeway lead vehicles no matter where they merge into the freeway. This result is in conformity with one's intuitive expectation since most ramp drivers will keep a lower speed than their freeway lead vehicles to avoid a potential merge collision. Dramatic mean and median magnitude changes at fiducial marks 12, 13, and 14 might be due to the small number of observations. Investigating gap acceptance behavior solely from the speed differential perspective is not sophisticated enough to explain complex freeway merge behavior. Ramp drivers having different time or distance gaps with their freeway lead vehicles might behave differently even though they all have the same speed differential magnitude with their freeway lead vehicles. The time and distance gap effects, between ramp vehicles and their corresponding freeway lead vehicles, on ramp driver gap acceptance behavior will be discussed in the following sections.

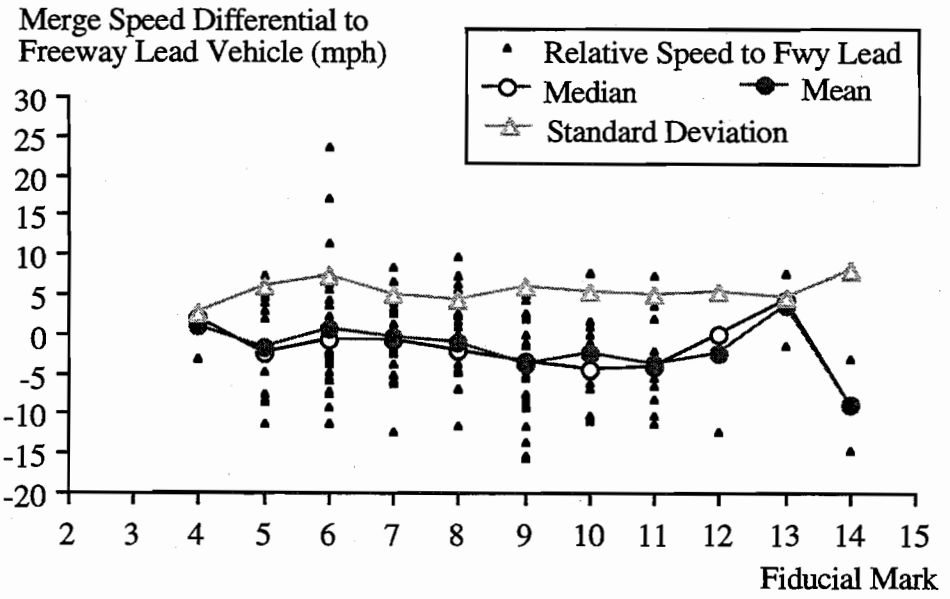

Figure 3.26 Merge speed differential to freeway lead vehicle vs. merge position (fiducial mark)

Merge Time Gap to Freeway Lead Vehicle *versus* Merge Position. In this analysis, each ramp vehicle's merge time gap to its freeway lead vehicle was measured at the location, represented by fiducial marks, where each ramp vehicle actually merged and was defined as the time difference between the ramp vehicle and the corresponding freeway lead vehicle fiducial mark passage. Results shown in Figure 3.27 indicate that most median and mean merge time gaps fall within 1.0 to 1.5 seconds. These values are considerably smaller than those minimum safe time headways proposed by Pipes' and Forbes' theories (May, 1990) which were developed using freeway stream flow. This merge characteristic makes freeway entrance ramps a potential hazard area. The means and medians depicted in Figure 3.27 are smaller than those demonstrated in Figure 3.23 revealing that most ramp drivers tend to accept a freeway lead merge gaps that are smaller than freeway lag merge gaps. This phenomenon is reasonable since without turning their heads, ramp drivers can easily evaluate freeway lead vehicle movements and consequently have a smaller PIJR (Perception, Identification, Judgment, and Reaction) time than for evaluating freeway lag vehicle movements. Essentially, ramp drivers must pay more attention to corresponding freeway lag vehicles during the gap search process.

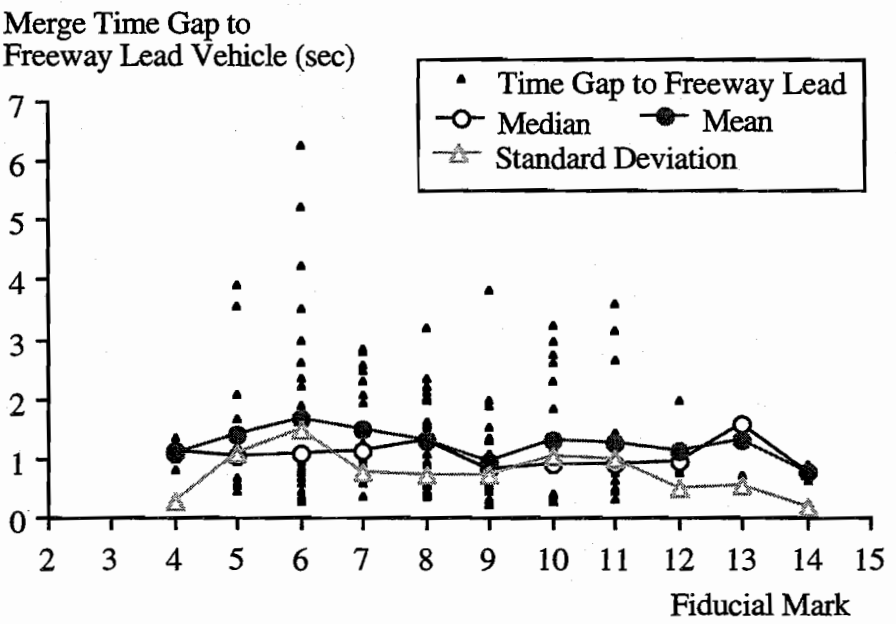

Figure 3.27 Merge time gap to freeway lead vehicle vs. merge position (fiducial mark)

Merge Distance Gaps to Freeway Lead Vehicle *versus* Merge Position. In this analysis, merge distance gaps are the longitudinal distance separation between ramp vehicles and their corresponding freeway lead vehicles measured at the locations where ramp vehicles merged. Results shown in Figure 3.28 indicate that the majority of ramp vehicles had a short, less than 60 feet, longitudinal separation with the corresponding freeway lead vehicle during merge maneuver. This phenomenon is not surprising when freeway lead vehicles have a higher speed because under such situations, ramp drivers can safely merge despite a short freeway lead distance gap. Nevertheless, the merge distance gaps found in this study are considerably smaller than that suggested in the California Motor Vehicle Code(May, 1990), namely: "A good rule for following another vehicle at a safe distance is to allow yourself at least the length of a car between your vehicle and the vehicle ahead for every ten miles per hour of speed at which you are traveling." This short merge distance gap characteristics increase the probability of merge collisions.

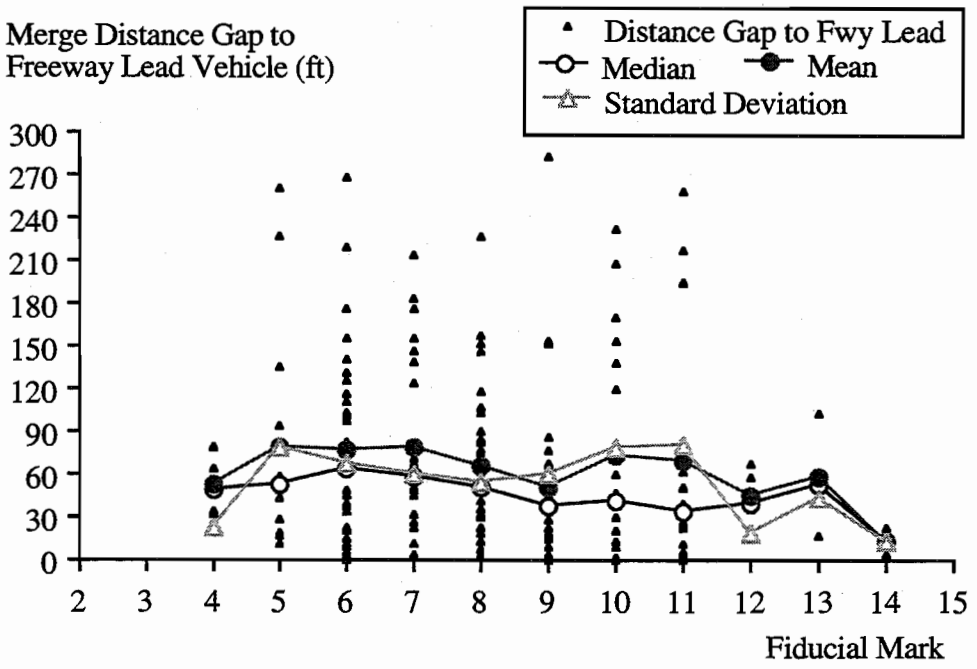

Figure 3.28 Merge distance gap to freeway lead vehicle vs. merge position (fiducial mark)

Merge Angular Velocity to Freeway Lead Vehicle *versus* Merge Position. Intuitively, one might assume that ramp drivers simultaneously evaluate different gap structure elements during the freeway merge gap search process. The results shown in Figures 3.26, 3.27, and 3.28 demonstrate great scatter associated with each individual gap structure element. This evidence implicitly reveals that a single gap structure element might not be sufficient to describe gap acceptance behavior. Angular velocity is a combination of factors incorporating speed differential and longitudinal separation into one mathematical form. The scatter depicted in Figure 3.29 illustrates a smaller range implying that angular velocity might be a more consistent gap acceptance decision criterion than any single gap structure element. This result is consistent with that of Figure 3.25. Drastic mean and standard deviation changes in fiducial marks 13 and 14 may be partially due to small numbers of observations.

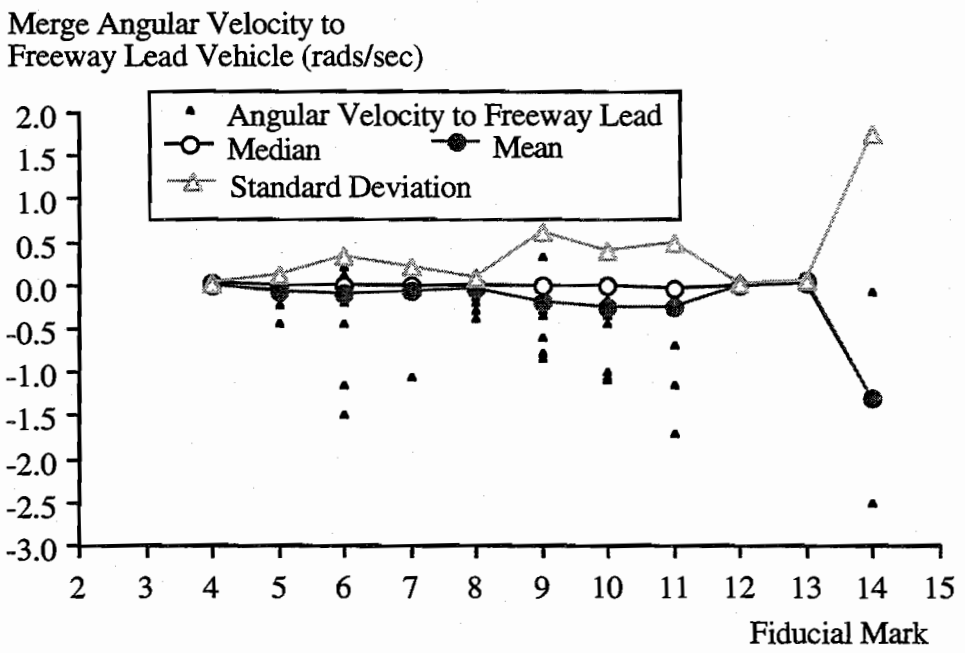

Figure 3.29 Merge angular velocity to freeway lead vehicle vs. merge position (fiducial mark)

Test for Equality of Means. Graphical presentations of gap structure elements actually accepted by ramp drivers *versus* merge positions, in terms of fiducial marks, have been illustrated in Figures 3.20 to 3.29. For all figures, the mean values across fiducial marks have visibly insignificant differences except near the acceleration lane end, e.g. marks 12, 13, and 14, where few observations were obtained. A statistical test for equality of means was performed and is presented in this section, however, fiducial marks where less than 5 observations were obtained were not included in this test.

The null and alternative hypotheses are denoted as

H_0 : All means are equal

H_1 : All means are not equal

The test statistic, r, is given by

$$r = \frac{\sum_{j=1}^{k} n_j (\bar{x}_{j\bullet} - \bar{\bar{x}})^2 / (k - 1)}{\sum_{j=1}^{k} \sum_{i=1}^{n_j} (x_{ji} - \bar{x}_{j\bullet})^2 / (n - k)} \qquad (3.5)$$

Where

n_j observation number of group j;

$\bar{x}_{j\bullet}$ mean value of group j;

$\bar{\bar{x}}$ grand mean;

k group number;

n total observation, $n = \sum_{j=1}^{k} n_j$;

If the null hypothesis is true, then r has an F distribution with k-1 and n-k degrees of freedom. One should reject the null hypothesis if r falls within the rejection region. In other words, for a given significance level α, reject the null hypothesis when $r > F_{(k-1,\, n-k,\, \alpha\%)}$. Statistical test results are summarized in Table 3.15. Among the gap structure elements, only merge acceleration rate is shown to have significant mean differences, at the 0.05 significance level, across the fiducial marks. These results are consistent with those mean trends depicted in the corresponding figures. This test, however, provides only numerical mean equality information among groups. In addition to mean and standard deviation, other distribution information associated with each fiducial mark is not well incorporated in the calculated statistic. Consequently, the test results might be misleading if the data distribution is skewed because under such circumstance, few extreme observations will make a great contribution to the calculated means. Figures 3.22 to 3.29 show great scatter spread and significant skewing which limits the statistical test result applications. These data characteristics also reveal that freeway merge gap acceptance behavior should be examined using disaggregate rather than aggregate data to accurately capture dynamic driver behavior.

TABLE 3.15 SUMMARY OF TEST FOR EQUALITY OF MEANS

Gap Structure Element	r	k	n	$F_{(k-1, n-k, 5\%)}$	Result
Ramp vehicle merge acceleration rate	5.439	8	206	2.05	Reject
Ramp vehicle merge speed	0.977	8	206	2.05	Accept
Merge speed differential to freeway lag vehicle	0.716	8	206	2.05	Accept
Merge time gap to freeway lag vehicle	0.276	8	206	2.05	Accept
Merge distance separation to freeway lag vehicle	0.458	8	206	2.05	Accept
Merge angular velocity to freeway lag vehicle	0.161	8	206	2.05	Accept
Merge speed differential to freeway lead vehicle	2.152	7	160	2.16	Accept
Merge time gap to freeway lead vehicle	1.432	7	160	2.16	Accept
Merge distance separation to freeway lead vehicle	0.598	7	160	2.16	Accept
Merge angular velocity to freeway lead vehicle	1.326	7	160	2.16	Accept

METHODOLOGIES FOR MODELING RAMP DRIVER ACCELERATION-DECELERATION BEHAVIOR

Ramp vehicle drivers process information from the roadway and traffic and respond in terms of speed and position control, or more precisely, acceleration-deceleration and merging. Analyses presented in the previous sections serve as fundamental information in the development of freeway merge driver behavior models. In this section, discussion will focus on the derivation of a methodology for modeling ramp driver acceleration-deceleration behavior. Merging, or gap acceptance, behavior will be addressed in the next section.

Essentially, a ramp driver does not have as much flexibility as a freeway driver to perform a desired acceleration-deceleration maneuver. Dynamic factors which come from physical geometric constraints such as the length of acceleration lane and relative movements of surrounding freeway and ramp vehicles mix together to determine ramp vehicle acceleration-deceleration behavior. Personal intention or desire seem to play a less important role in the ramp vehicle driver decision process. However, the derivation of the ramp vehicle acceleration-

deceleration mathematical model should not be as simple as that suggested by Huberman (1982) in which the ramp vehicle acceleration rate was simply modeled as a function of speed. Conceptually, the methodology developed to model ramp vehicle acceleration-deceleration behavior should take the geometric features of the acceleration lane and the freeway and ramp traffic characteristics into account. The most important elements that directly affect a ramp driver's acceleration or deceleration decision would be the position of the ramp vehicle in the acceleration lane and the relative positions and speeds of the ramp vehicle to the corresponding freeway lag, lead, and ramp lead vehicles. Considering the inherent characteristics of ramp vehicle behavior, the concept of car-following which was originally developed for the case of single-lane follow-the-leader may be adopted as a basis to model the ramp vehicle acceleration-deceleration behavior. Appropriate modifications to the original models are required to suit the unique characteristics of ramp vehicle acceleration-deceleration behavior. A brief discussion of the conventional car-following model is presented in the following subsection.

Conventional Car-Following Model

The General Motors research group, led by Dr. Robert Herman, made the greatest contribution to the development of the car-following theories through their comprehensive field experiments and the discovery of the mathematical bridge between microscopic and macroscopic theories of traffic flow. The fundamental concept behind the car-following model is a form of stimulus-response equation, where the response is the reaction of a driver to the motion of the vehicle immediately preceding him in a single lane traffic stream. In its simplest terms, proposed by Chandler et al. (1958), it represents driver psychology expressed in the form

$$\text{Response}(t+T) = \text{Sensitivity} * \text{Stimulus}(t) \tag{3.6}$$

Where

T is the time lag of response to the stimulus

A graphical presentation of two-vehicle car-following is shown in Figure 3.30. The terms $x_{n+1}(t)$ and $x_n(t)$ are the locations of vehicle n+1 and n respectively at time t. The response is normally taken as the acceleration($\ddot{x}_{n+1}$) of the following vehicle n+1 at time t+T. The stimulus, on the other hand, could be a function of the positions of a number of cars and their time derivatives, and perhaps also other parameters. The sensitivity is a factor that represents the magnitude of response per unit of stimulus. The larger the sensitivity the following driver has, the larger the response magnitude with respect to the same unit of stimulus. In other words, the driver

is more sensitive to the stimulus. If λ represents the sensitivity and the stimulus is assumed to be the relative speed between successive vehicles at time t, $\dot{x}_n(t) - \dot{x}_{n+1}(t)$, the Eq.(3.6) becomes

$$\ddot{x}_{n+1}(t+T) = \lambda[\dot{x}_n(t) - \dot{x}_{n+1}(t)] \tag{3.7}$$

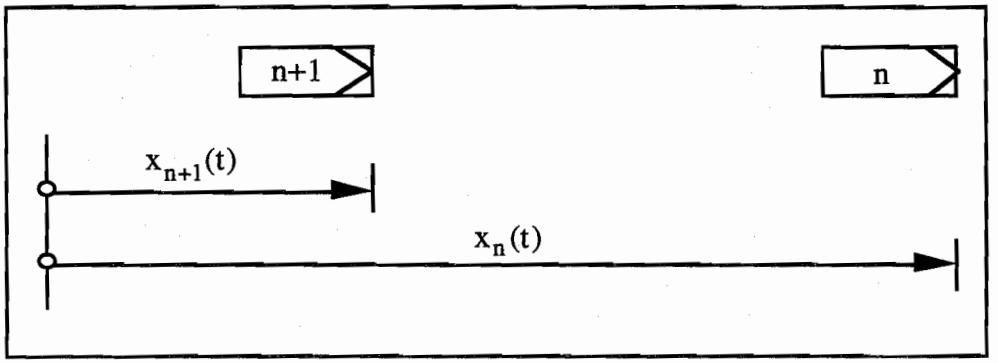

Figure 3.30 Basic diagram of single lane car-following behavior

Gazis et al. (1959) proposed that the sensitivity was inversely proportional to the space headway, i.e.

$$\lambda = \frac{\alpha_1}{x_n(t) - x_{n+1}(t)} \tag{3.8}$$

Eq.(3.7) can then be rewritten as follows:

$$\ddot{x}_{n+1}(t+T) = \frac{\alpha_1}{x_n(t) - x_{n+1}(t)}[\dot{x}_n(t) - \dot{x}_{n+1}(t)] \tag{3.9}$$

One of the limitations of this model is its lack of realism at low densities, particularly exhibited in the limiting case where there is no upper bound on stream velocity. Edie (1961) proposed a modified model to overcome the above limitation by hypothesizing that the sensitivity varies with the absolute velocity of the following driver. That is

$$\lambda = \alpha_2 \frac{\dot{x}_{n+1}(t + T)}{[\, x_n(t) - x_{n+1}(t) \,]^2} \tag{3.10}$$

Gazis et al. (1961) proposed a more general nonlinear expression for the sensitivity:

$$\lambda = \alpha_0 \frac{\dot{x}_{n+1}{}^m(t + T)}{[\, x_n(t) - x_{n+1}(t) \,]^l} \tag{3.11}$$

The general expression for these car-following theories thus becomes

$$\ddot{x}_{n+1}(t+T) = \alpha_0 \frac{\dot{x}_{n+1}{}^m(t + T)}{[\, x_n(t) - x_{n+1}(t) \,]^l} [\, \dot{x}_n(t) - \dot{x}_{n+1}(t) \,] \tag{3.12}$$

May and Keller (1967) derived best-fit nonlinear indices to simulate observed freeway data and recommended m=0.8 and l=2.8.

In the above dynamic car-following models the relative speed between lead and following vehicles has been assumed to be the only stimulus. In practice, it is very questionable whether a driver is able to precisely gauge such a parameter or not. Michaels (1965), reporting on human perception of motion, stated that the dominant perceptual factor, or the stimulus, in a car-following situation is the rate of change of visual angle. Figure 3.31 shows the visual angle in the car-following scheme.

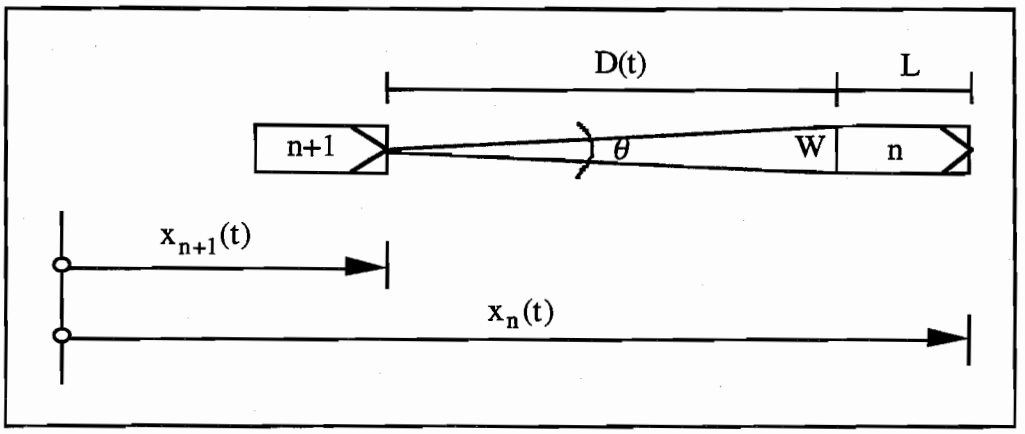

Figure 3.31 Diagram of visual angle θ in car-following situation

The rate of change of visual angle, dθ/dt, is derived as follows:

$$\tan(\frac{\theta}{2}) = \frac{\frac{W}{2}}{D(t)} \tag{3.13}$$

Solving Eq.(3.13) for θ,

$$\theta = 2\tan^{-1}[\frac{W}{2D(t)}] \tag{3.14}$$

Differentiating both sides of Eq.(3.14) with respect to t,

$$\frac{d\theta}{dt} = \frac{2}{1+\frac{W^2}{4D^2(t)}} \cdot \frac{-W}{2D^2(t)} \cdot \frac{d[D(t)]}{dt}$$

$$= \frac{-4W}{4D^2(t)+W^2} \cdot \frac{d[X_n(t) - L - X_{n+1}(t)]}{dt}$$

$$= \frac{-W}{D^2(t)+(\frac{W}{2})^2} \cdot [\dot{X}_n(t) - \dot{X}_{n+1}(t)] \tag{3.15}$$

In any practical case, $(\frac{W}{2})^2 << D^2(t)$ and $L << X_n(t) - X_{n+1}(t)$ so that Eq.(3.15) approximates to

$$\frac{d\theta}{dt} \cong \frac{W}{[X_n(t) - X_{n+1}(t)]^2} \cdot [\dot{X}_{n+1}(t) - \dot{X}_n(t)] \tag{3.16}$$

If the rate of change of the visual angle is the stimulus of the following driver's response, the dynamic car-following equation becomes

$$\ddot{X}_{n+1}(t+T) = \lambda \frac{W}{[X_n(t) - X_{n+1}(t)]^2} \cdot [\dot{X}_{n+1}(t) - \dot{X}_n(t)] \tag{3.17}$$

Where λ' is the new sensitivity.

Equation (3.17) is therefore the car-following law that results from the assumption that the following driver performs acceleration in proportion to the magnitude of the rate of change of the visual angle. If the sensitivity is proportional to the absolute velocity of the following vehicle, Eq.(3.17) is equivalent to that proposed by Edie, as shown in Eq.(3.10). Several researchers have proposed the visual angle car-following model to be a more appropriate approach, among others, Michaels, 1965; Fox and Lehman, 1967; Lee and Jones, 1967; Pipes, 1967; and Heyes and Ashworth, 1972.

Conceptual Methodology Frameworks for Ramp Vehicle Acceleration-Deceleration Behavior

The movements of a vehicle along a freeway entrance ramp involve successive navigational decisions, pursuit tracking, positional control relative to other vehicles and roadway elements, gap search and acceptance operations, and steering into the freeway stream. The acceleration-deceleration characteristics for each task are different. At the section of entrance ramp before the merging end, drivers normally have to adjust speed to accommodate the controlling conditions of the ramp curvature and superelevation on the basis of both visual and kinesthetic cues. At this stage, interactions between vehicles are so insignificant as to have little influence on the ramp driver's acceleration-deceleration behavior. As the ramp vehicle approaches the merging end, the traffic in the freeway right lane becomes visible and at an angle and speed differential that allows the ramp driver to begin to evaluate the gap situation. While the ramp vehicle is traveling in the acceleration lane, the driver searches gaps and determines whether they are sufficient for merging. This procedure may involve deceleration, reduction of acceleration, maintaining a constant speed, maintaining current acceleration, or increasing acceleration, as the conditions (primarily distance separation and speed differential) may dictate. Obviously, the acceleration-deceleration performance of ramp vehicles in acceleration lanes are much more complicated than what the conventional car-following models can describe since more traffic and geometric factors should be considered. Essentially, the central basis for modeling ramp vehicle acceleration-deceleration behavior is different from that of the conventional car-following model. Nevertheless, the fundamental concept, Response = Sensitivity * Stimulus, of the car-following models can still be appropriately adopted as long as the stimulus can be well specified.

In general, the maneuver of a ramp vehicle is mainly influenced by its corresponding freeway lag, freeway lead, and ramp lead vehicles if they exist. Significant differences due to acceleration-deceleration behavior at different traffic conditions are expected. For example, where no freeway vehicles are present, the ramp driver can travel near his desired speed. However, where there is a freeway lag or lead vehicle present, the ramp driver is forced to stay in the acceleration lane and probably change speed to create an acceptable gap. Therefore, different ramp vehicle acceleration-deceleration models should be considered for different situations depending on the presence of other corresponding vehicles. Ideally, the following two major categories as well as their associated models should be considered and developed to verify proposed methodologies.

Category 1: The ramp vehicle is a single vehicle or is the leader of a platoon of ramp vehicles in the acceleration lane. In other words, there is no ramp lead vehicle in front of it.
Category 2: The ramp vehicle is a member, not the leader, of a platoon of ramp vehicles. In other words, at least one ramp lead vehicle is in front of it.

Each category should be further divided into four cases based on the presence of corresponding freeway vehicles. They are:

(1) both freeway lag and lead vehicles are present within a specific distance; 300 feet assumed in this study;
(2) only freeway lag vehicle is present;
(3) only freeway lead vehicle is present; and
(4) neither freeway lag nor lead vehicle is present, in other words, no freeway vehicles in sight.

The hypothesized methodologies for the ramp vehicle acceleration-deceleration models retain the conventional car-following concept that the relative speeds between the ramp vehicle and its corresponding vehicles are the stimulus and the associated response is the ramp vehicle acceleration-deceleration rates. The equation for the follow-the-leader car-following model, namely Eq.(3.12), is expanded linearly to incorporate the influence of both freeway vehicles and other ramp vehicles. A similar concept has been proposed by Herman and Rothery (1965) with regard to a three-car car-following situation.

The hypothesized expression of ramp vehicle acceleration-deceleration behavior for category 1, single or leader of a platoon, is given as follows:

$$\ddot{X}_{r_i}(d_j + D) = \beta_0 + \beta_1 \frac{\dot{X}_{r_i}(d_j + D)^{\gamma}}{[X_{r_i}(d_j) - X_{flag_i}(d_j)]^{\alpha_1}} [\dot{X}_{flag_i}(d_j) - \dot{X}_{r_i}(d_j)]$$

$$+ \beta_2 \frac{\dot{X}_{r_i}(d_j + D)^{\gamma}}{[X_{flead_i}(d_j) - X_{r_i}(d_j)]^{\alpha_2}} [\dot{X}_{r_i}(d_j) - \dot{X}_{flead_i}(d_j)]$$

$$+ \beta_3 \frac{\dot{X}_{r_i}(d_j + D)^{\gamma}}{[L - X_{r_i}(d_j)]^{\alpha_3}} [\dot{X}_{r_i}(d_j)]$$

$$+ u_{r_i d_j} \qquad (3.18)$$

Where:

$X_{r_i}(d_j)$: location of ramp vehicle i when it passed the fiducial mark j; alternatively, it is the location of fiducial mark j measured from merging end, j=1, 2,..., m_i;

$X_{flag_i}(d_j)$: location of ramp vehicle i's corresponding freeway lag vehicle when vehicle i passed the fiducial mark j;

$X_{flead_i}(d_j)$: location of ramp vehicle i's corresponding freeway lead vehicle when vehicle i passed the fiducial mark j;

$\dot{X}_{r_i}(d_j)$: velocity of ramp vehicle i when it passed the fiducial mark j; alternatively, it is the velocity of ramp vehicle i at location d_j;

$\dot{X}_{flag_i}(d_j)$: velocity of ramp vehicle i's corresponding freeway lag vehicle when vehicle i passed the fiducial mark j;

$\dot{X}_{flead_i}(d_j)$: velocity of ramp vehicle i's corresponding freeway lead vehicle when vehicle i passed the fiducial mark j;

$\ddot{X}_{r_i}(d_j + D)$: acceleration rate of ramp vehicle i at location d_j+D;

$u_{r_i d_j}$: disturbance of the estimated acceleration rates for the observation of ramp vehicle i when it passed the fiducial mark j;

d_j : position of the fiducial mark j measured from the merging end;

L : length of the acceleration lane;

D : distance lag;

m_i : the total number of observations of estimated acceleration-deceleration rates of ramp vehicle i.

β_0, β_1, β_2, β_3, α_1, α_2, α_3, and γ are parameters to be estimated.

The forth term of Eq.(3.18) reflects the effect of the terminus of the acceleration lane on the ramp vehicle's acceleration-deceleration behavior. D, analogical to the parameter T in Eq.(3.7), is the distance lag of the response to the stimulus. The reason for using distance lag D instead of using time lag T in the formulation is because the data in this study were reduced and recorded in terms of the fiducial marks representing where they took place. The use of distance lag, however, is essentially equivalent to the use of time lag since the equivalent time lag can be directly obtained simply by dividing the distance lag by the ramp vehicle's travel speed.

Following the same argument, the general formula of category 2 is similar to Eq.(3.18) except the effect of the ramp lead vehicle should be taken into account. The general equation is shown as follows:

$$\begin{aligned}\ddot{X}_{r_i}(d_j+D) = \beta_0 &+ \beta_1 \frac{\dot{X}_{r_i}(d_j+D)^{\gamma}}{[X_{r_i}(d_j)-X_{flag_i}(d_j)]^{\alpha_1}}[\dot{X}_{flag_i}(d_j)-\dot{X}_{r_i}(d_j)] \\ &+ \beta_2 \frac{\dot{X}_{r_i}(d_j+D)^{\gamma}}{[X_{flead_i}(d_j)-X_{r_i}(d_j)]^{\alpha_2}}[\dot{X}_{r_i}(d_j)-\dot{X}_{flead_i}(d_j)] \\ &+ \beta_3 \frac{\dot{X}_{r_i}(d_j+D)^{\gamma}}{[X_{rlead_i}(d_j)-X_{r_i}(d_j)]^{\alpha_3}}[\dot{X}_{r_i}(d_j)-\dot{X}_{rlead_i}(d_j)] \\ &+ u_{r_i d_j} \end{aligned} \quad (3.19)$$

Where

$X_{rlead_i}(d_j)$: location of ramp vehicle i's corresponding ramp lead vehicle when vehicle i passes the fiducial mark j;

$\dot{X}_{rlead_i}(d_j)$: velocity of ramp vehicle i's corresponding ramp lead vehicle when vehicle i passes the fiducial mark j.

The other variables are as defined above.

Each case in categories 1 and 2 can be modeled as a special case of Eqs.(3.18) and (3.19). For example, when a ramp vehicle is a single vehicle in the acceleration lane and has no freeway lead vehicle in front of it, then the acceleration-deceleration model is simply obtained by removing the third term of Eq.(3.18) from the general formula. The procedure adopted in this study to calibrate the parameters of Eqs.(3.18) and (3.19) is shown in Figure 3.32.

As a first step of the calibration, the disturbance of each observation is assumed to be

$$u_{r_i d_j} \sim \text{iid}(0, \sigma_u^2) \qquad \text{for all i and j} \qquad (3.20)$$

where iid means independently and identically distributed. Thus, there is no serial correlation in the disturbance for any individual ramp vehicle and there is no dependence between the disturbances for different ramp vehicles, either contemporaneous or lagged are assumed, and the disturbance has a constant variance at all observations.

Essentially, Eqs(3.18) and (3.19) are nonlinear forms because of the existence of nonlinearity in the parameters and therefore cannot be directly transformed to linear forms. As a consequence, the conventional Ordinary Least Squares(OLS) technique is not appropriate for estimating the regression coefficients of Eqs.(3.18) and (3.19). However, by assigning constant values to some of the parameters, Eqs.(3.18) and (3.19) are readily transformed to linear forms to which OLS can be applied. Assuming $\alpha_1 = \alpha_2 = \alpha_3 = 2$, Eq.(3.18) can be rewritten as follows:

$$\begin{aligned}
\ddot{X}_{r_i}(d_j + D) \;=\; & \beta_0 \\
& + \beta_1 \frac{\dot{X}_{r_i}(d_j + D)^{\gamma}}{[X_{r_i}(d_j) - X_{\text{flag}_i}(d_j)]^2} [\dot{X}_{\text{flag}_i}(d_j) - \dot{X}_{r_i}(d_j)] \\
& + \beta_2 \frac{\dot{X}_{r_i}(d_j + D)^{\gamma}}{[X_{\text{flead}_i}(d_j) - X_{r_i}(d_j)]^2} [\dot{X}_{r_i}(d_j) - \dot{X}_{\text{flead}_i}(d_j)] \\
& + \beta_3 \frac{\dot{X}_{r_i}(d_j + D)^{\gamma}}{[L - X_{r_i}(d_j)]^2} [\dot{X}_{r_i}(d_j)] \\
& + u_{r_i d_j}
\end{aligned} \qquad (3.21)$$

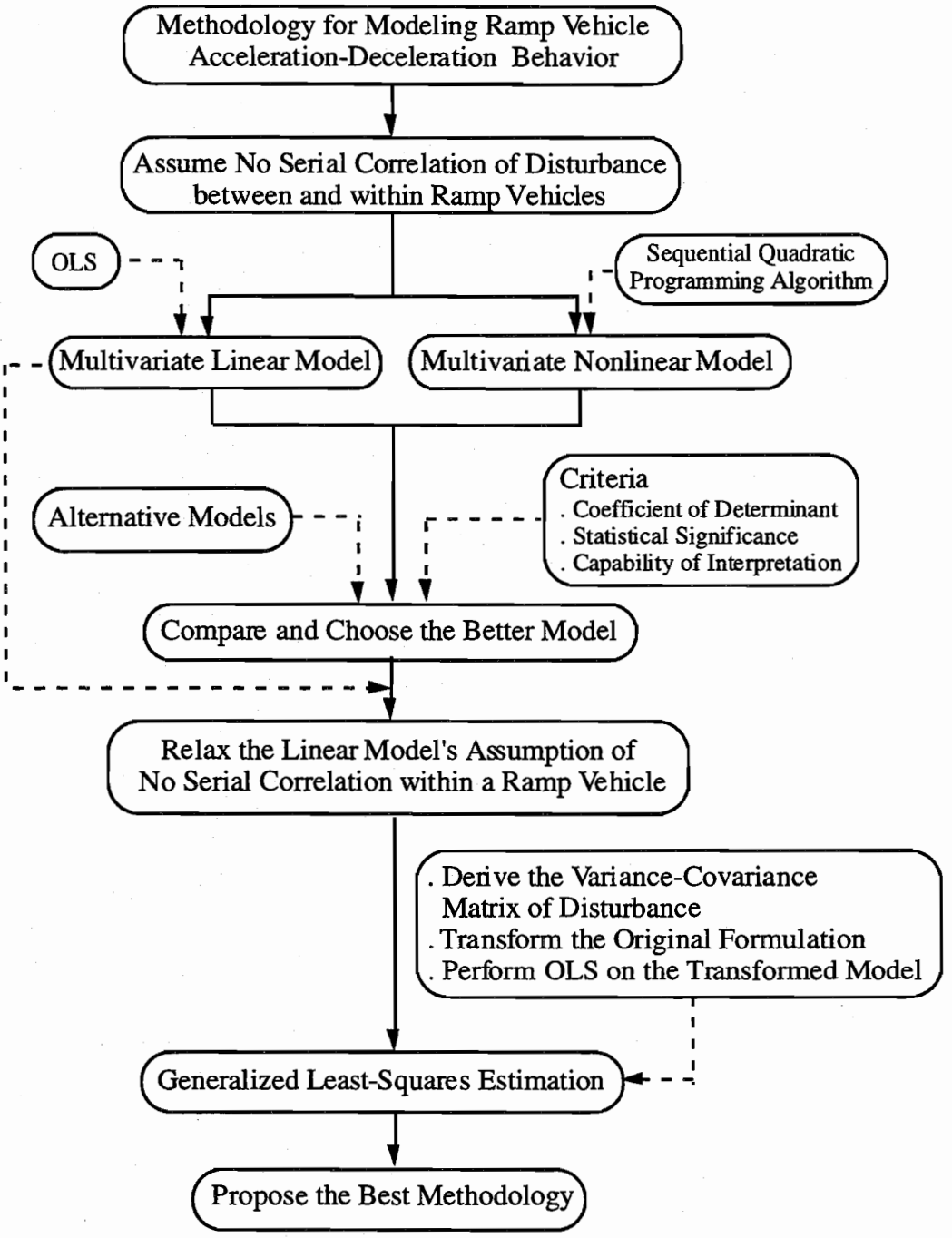

Figure 3.32 Flowchart of developing methodologies for ramp vehicle acceleration-deceleration behavior

Partitioning the regression coefficients, β_1, β_2, β_3, into two parts, Eq.(3.21) can then be rearranged as follows:

$$\ddot{X}_{r_i}(d_j + D) = \beta_0 + \beta_1' \dot{X}_{r_i}(d_j + D)^{\gamma} \frac{W_{rflag}[\dot{X}_{flag_i}(d_j) - \dot{X}_{r_i}(d_j)]}{[X_{r_i}(d_j) - X_{flag_i}(d_j)]^2}$$

$$+ \beta_2' \dot{X}_{r_i}(d_j + D)^{\gamma} \frac{W_{rflead}[\dot{X}_{r_i}(d_j) - \dot{X}_{flead_i}(d_j)]}{[X_{flead_i}(d_j) - X_{r_i}(d_j)]^2}$$

$$+ \beta_3' \dot{X}_{r_i}(d_j + D)^{\gamma} \frac{W_{rend}[\dot{X}_{r_i}(d_j)]}{[L - X_{r_i}(d_j)]^2}$$

$$+ u_{r_i d_j} \qquad (3.22)$$

Where

W_{rflag} : the lateral distance between the ramp vehicle and its corresponding freeway lag vehicle;

W_{rflead} : the lateral distance between the ramp vehicle and its corresponding freeway lead vehicle;

W_{rend} : an imaginary lateral distance that can accommodate a ramp vehicle to stop at the terminus of the acceleration lane.

By definition,

$$\omega_{rflag_i}(d_j) = \frac{W_{rflag}[\dot{X}_{flag_i}(d_j) - \dot{X}_{r_i}(d_j)]}{[X_{r_i}(d_j) - X_{flag_i}(d_j)]^2} \qquad (3.23)$$

is the angular velocity, viewed by ramp driver i at location d_j, produced by the ramp vehicle's corresponding freeway lag vehicle;

$$\omega_{rflead_i}(d_j) = \frac{W_{rflead}[\dot{X}_{r_i}(d_j) - \dot{X}_{flead_i}(d_j)]}{[X_{flead_i}(d_j) - X_{r_i}(d_j)]^2} \qquad (3.24)$$

is the angular velocity between ramp vehicle i, viewed at location d_j, and its corresponding freeway lead vehicle; and

$$\omega_{rend_i}(d_j) = \frac{W_{rend}[\dot{X}_{r_i}(d_j)]}{[L - X_{r_i}(d_j)]^2} \tag{3.25}$$

is the angular velocity between ramp vehicle i, viewed at location d_j, and the terminus of the acceleration lane.

Substituting Eqs.(3.23), (3.24), and (3.25) in Eq.(3.22),

$$\begin{aligned} \ddot{X}_{r_i}(d_j + D) = \beta_0 &+ \beta_1' \dot{X}_{r_i}(d_j + D)^{\gamma} \omega_{rflag_i}(d_j) \\ &+ \beta_2' \dot{X}_{r_i}(d_j + D)^{\gamma} \omega_{rflead_i}(d_j) \\ &+ \beta_3' \dot{X}_{r_i}(d_j + D)^{\gamma} \omega_{rend_i}(d_j) \\ &+ u_{r_i d_j} \end{aligned} \tag{3.26}$$

Parameter γ is a factor used to reflect the significance of a ramp vehicle's current travel speed in contributing to its acceleration-deceleration performance. The larger the value of γ, the more significant the current speed is to describe the acceleration-deceleration performance. Thus, by assigning constant values to γ, Eq.(3.26) simply turns out to be a multivariate linear model to which OLS can apply. Through the transformation of the original model, the only parameters left to be estimated are the constant term, β_0, and the regression coefficients, β_1', β_2', and β_3'. The same arguments also apply to the calibration of Eq.(3.19); the acceleration-deceleration model is given as follows:

$$\begin{aligned} \ddot{X}_{r_i}(d_j + D) = \beta_0 &+ \beta_1' \dot{X}_{r_i}(d_j + D)^{\gamma} \omega_{rflag_i}(d_j) \\ &+ \beta_2' \dot{X}_{r_i}(d_j + D)^{\gamma} \omega_{rflead_i}(d_j) \\ &+ \beta_3' \dot{X}_{r_i}(d_j + D)^{\gamma} \omega_{rlead_i}(d_j) \\ &+ u_{r_i d_j} \end{aligned} \tag{3.27}$$

Where

$\omega_{rlead_i}(d_j)$ is the angular velocity between ramp vehicle i, viewed at location d_j, and its corresponding ramp lead vehicle.

A typical diagram of the angular velocity components of a ramp vehicle in the acceleration lane is shown in Figure 3.33.

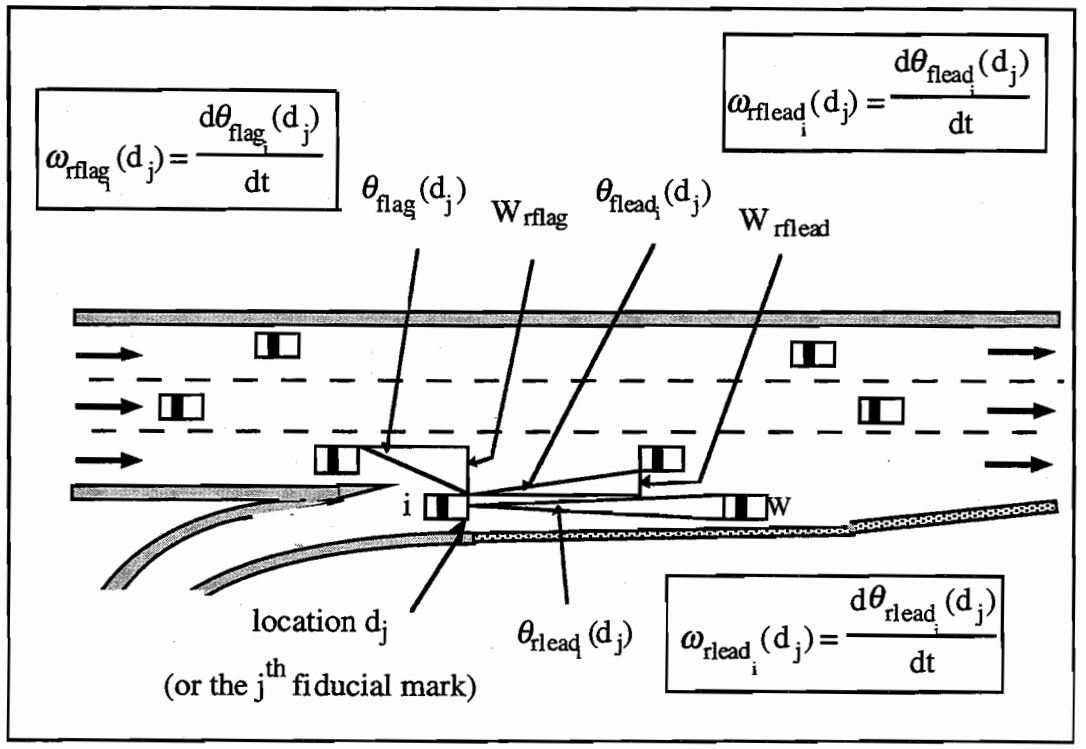

Figure 3.33 Diagram of ramp vehicle angular velocity components

Transforming the original nonlinear formulations to linear forms, such as Eqs.(3.26) and (3.27), has some applausive advantages. Most significantly, the linear model can simply interpret the complex acceleration-deceleration decision behavior. In the linear model, the angular velocity components were implicitly treated as stimuli for ramp vehicles to perform acceleration or deceleration. This hypothesis is closer to true human perception behavior. Michaels (1965) postulated that from the standpoint of human perception of motion, the rate of change of visual angle is the dominant perceptual factor that determines the driver's maneuver. It is a well

recognized fact that when a ramp vehicle is traveling in the acceleration lane, the driver will intend to adjust speed to maintain the angular velocities of the corresponding freeway lag, lead and corresponding ramp lead vehicles or the terminus of acceleration lane at or below their thresholds respectively in order to create a sufficient size of gap to perform the merge maneuver. This evidence supports angular velocity as an appropriate stimulus or cue to explain ramp vehicle acceleration-deceleration behavior.

Although the linear model, or more precisely the angular velocity model, is an appropriate approach to model ramp vehicle acceleration-deceleration behavior, the nonlinear nature of the relations must be considered and deserves further investigation. A nonlinear regression technique will be performed to calibrate the parameters in Eqs.(3.18) and (3.19) where all the parameters are not restricted to certain constants. These results will be compared with those obtained from linear regressions. The better models or some combinations of these two models will be determined based on decision criteria, such as the coefficient of determination, the significance of regression coefficients, and the capability of interpretation of complex situations. As a rule of thumb, the larger the coefficient of determination, the better the model. The capability or ease of the proposed models to interpret the fundamental relations behind complex acceleration-deceleration behavior is also an important criterion to determine the appropriate model. A model that has nice statistical properties but has difficulties describing fundamental phenomena should be treated cautiously.

Because of the embedded assumptions made to the conventional regression models, the above procedures for calibrating ramp vehicle acceleration-deceleration behavior models are applicable only when there is no serial correlation in the disturbances for any individual ramp vehicle, there is no dependence between the disturbances for different ramp vehicles, and the disturbance has a constant variance. These assumptions, however, are not always true in light of the inherent characteristics of the observations. The acceleration-deceleration rates for ramp vehicles were calculated based on speeds calculated at successive fiducial marks. Because of short distance intervals between successive fiducial marks, there is a very high likelihood of a potential serial correlation problem associated with successively calculated acceleration-deceleration data. In other words, the assumption of Eq. (3.20) is not valid.

For example, a ramp vehicle continuously accelerates in the acceleration lane and its acceleration rates are calculated successively at each fiducial mark. Inevitably, these observations are serially correlated. The shorter the distance between fiducial marks, the more significant is the serial correlation problem associated with successive observations. If a ramp vehicle's acceleration-deceleration rates are calculated at every foot, very accurate historical data can be

obtained as long as the exact time of crossing each fiducial mark can be precisely obtained. At the same time, the data will have perfect serial correlation. On the contrary, if the distance between successive fiducial marks is lengthened to eliminate the potential serial correlation problem, much valuable information is lost. For instance, only one grand average acceleration-deceleration rate could be calculated for each ramp vehicle and it is assumed that there is no dependence between vehicles, the perfectly independent observations could be obtained and used to calibrate the acceleration-deceleration models. However, the models derived from this kind of grand average data provide nothing to describe complex driver behavior.

It is necessary to recognize that the calculated ramp vehicle acceleration-deceleration historical data are serial correlated to some extent and that appropriate corrections should be considered. If the serial correlation problem is ignored and the conventional OLS is directly applied to solve the problems, such as Eqs. (3.26) and (3.27), then any application of the OLS estimators is potentially misleading. More importantly, the substitution of these numbers in the conventional t statistic and confidence interval calculations is strictly invalid since the assumptions used in deriving these inference procedures no longer apply. For the same reason the optimal minimum variance property of OLS no longer holds.

Generalized Least Squares Technique

An alternative estimation procedure, namely Generalized Least-Squares (GLS), which explicitly incorporates the serial correlation characteristics in its parameter estimation procedures can be used to calibrate the acceleration-deceleration model. The derivation of GLS estimations is described as follows(Johnston, 1984):

Assume the basic model is now

$$\mathbf{y} = \mathbf{X}\beta + \mathbf{u} \tag{3.28}$$

Where

$$E(\mathbf{uu}') = \Omega \tag{3.29}$$

Premultiplying the assumed model, Eq.(3.28), by some nonsingular transformation matrix **T** to obtain

$$\mathbf{Ty} = (\mathbf{TX})\beta + \mathbf{Tu} \tag{3.30}$$

Each element in the vector **Ty** is then some linear combination of the elements in **y**. The variance matrix for the disturbance in Eq.(3.30) is

$$E(\mathbf{Tuu'T}) = \mathbf{T}\Omega\mathbf{T}' \tag{3.31}$$

since $E(\mathbf{Tu}) = 0$.

If it were possible to specify $\mathbf{T}$ such that

$$\mathbf{T}\Omega\mathbf{T}' = \mathbf{I} \tag{3.32}$$

then the OLS could be applied to the transformation variables $\mathbf{Ty}$ and $\mathbf{TX}$ in Eq.(3.30) and the resultant estimates would have all the optimal properties of OLS and could be validly subjected to the usual inference procedures.

It is, in fact, possible to find a matrix $\mathbf{T}$ which will satisfy Eq.(3.32). If Ω is a symmetric positive definite matrix, a nonsingular matrix $\mathbf{P}$ can be found such that

$$\Omega = \mathbf{PP}' \tag{3.33}$$

and therefore

$$\mathbf{P}^{-1}\Omega\mathbf{P}'^{-1} = \mathbf{I} \tag{3.34}$$

Comparison of Eqs.(3.32) and (3.34) shows that the appropriate $\mathbf{T}$ is given by

$$\mathbf{T} = \mathbf{P}^{-1} \tag{3.35}$$

and it easily follows that

$$\begin{aligned} \Omega^{-1} &= \mathbf{P}'^{-1}\mathbf{P}^{-1} \\ &= (\mathbf{P}^{-1})'\mathbf{P}^{-1} \\ &= \mathbf{T}'\mathbf{T} \end{aligned} \tag{3.36}$$

Applying OLS to Eq.(3.30) then gives

$$\begin{aligned} \mathbf{b}_* &= (\mathbf{X'T'TX})^{-1}\mathbf{X'T'Ty} \\ &= (\mathbf{X}'\Omega^{-1}\mathbf{X})^{-1}\mathbf{X}'\Omega^{-1}\mathbf{y} \end{aligned} \tag{3.37}$$

with the variance-covariance matrix given by

$$Var(\mathbf{b}_*) = (\mathbf{X}'\Omega^{-1}\mathbf{X})^{-1} \tag{3.38}$$

Since Eqs.(3.31) and (3.32) imply that Eq.(3.30) satisfies the assumptions required for the application of OLS, it follows that $\mathbf{b}_*$ is a best linear unbiased estimator of β in the model of $\mathbf{y} = \mathbf{X}\beta + \mathbf{u}$ with $E(\mathbf{uu}') = \Omega$.

According to the data characteristics of this study, Eq.(3.28) can be rewritten as follows:

$$\begin{bmatrix} \mathbf{y}_{r_1} \\ \mathbf{y}_{r_2} \\ \vdots \\ \mathbf{y}_{r_i} \\ \vdots \\ \mathbf{y}_{r_n} \end{bmatrix} = \begin{bmatrix} \mathbf{i}_{r_1} & \mathbf{X}_{r_1} \\ \mathbf{i}_{r_2} & \mathbf{X}_{r_2} \\ \vdots & \vdots \\ \mathbf{i}_{r_i} & \mathbf{X}_{r_i} \\ \vdots & \vdots \\ \mathbf{i}_{r_n} & \mathbf{X}_{r_n} \end{bmatrix} \begin{bmatrix} \beta_0 \\ \beta_1 \\ \beta_2 \\ \vdots \\ \beta_k \end{bmatrix} + \begin{bmatrix} \mathbf{u}_{r_1} \\ \mathbf{u}_{r_2} \\ \vdots \\ \mathbf{u}_{r_i} \\ \vdots \\ \mathbf{u}_{r_n} \end{bmatrix} \tag{3.39}$$

Where

n is the total number of ramp vehicles included in the data set;

k is the number of explanatory variables.

$\mathbf{y}_{r_i}$, $\mathbf{X}_{r_i}$, $\mathbf{u}_{r_i}$, and $\mathbf{i}_{r_i}$ can be further detailed as follows:

$$\mathbf{y}_{r_i} = \left[y_{r_i}(d_1) \quad y_{r_i}(d_2) \quad \cdots \quad y_{r_i}(d_j) \quad \cdots \quad y_{r_i}(d_{m_i}) \right]' \tag{3.40}$$

Where

$y_{r_i}(d_j)$ is ramp vehicle i's acceleration-deceleration rate calculated at location d_j, or fiducial mark j, j=1, 2 ... m_i;

m_i is the total number of acceleration-deceleration rates collected for ramp vehicle i.

$$\mathbf{X}_{r_i} = \begin{bmatrix} X_{i1d_1} & X_{i2d_1} & \cdots & X_{ikd_1} \\ \cdots & \cdots & \cdots & \cdots \\ X_{i1d_j} & X_{i2d_j} & \cdots & X_{ikd_j} \\ \cdots & \cdots & \cdots & \cdots \\ X_{i1d_{m_i}} & X_{i2d_{m_i}} & \cdots & X_{ikd_{m_i}} \end{bmatrix} \tag{3.41}$$

Where

X_{ikd_j} is the i^{th} ramp vehicle's k^{th} explanatory variable at location d_j.

$$\mathbf{u}_{r_i} = \left[u_{r_i}(d_1) \quad u_{r_i}(d_2) \quad \cdots \quad u_{r_i}(d_j) \quad \cdots \quad u_{r_i}(d_{m_i})\right]' \tag{3.42}$$

Where

$u_{r_i}(d_j)$ is ramp vehicle i's acceleration-deceleration rate calculated at location d_j, or fiducial mark j, j=1, 2, ..., m_i

The matrix $\mathbf{i}_{r_i}$ is an m_i * 1 column vector for ramp vehicle i with all elements equal to 1. That is

$$\mathbf{i}_{r_i} = (1 \quad 1 \quad \cdots \quad 1)'_{1*m_i} \tag{3.43}$$

Essentially, all the efforts are to find a consistent estimator of Ω. From the definition of Ω, one knows that the Ω matrix involves $(\sum_{i=1}^{n} m_i)(1 + \sum_{i=1}^{n} m_i)/2$ unknown parameters if there are no prior restrictions on any elements. Clearly, estimation, under such circumstances, becomes impossible using only $\sum_{i=1}^{n} m_i$ observations. Therefore, one should make some assumptions about the elements of Ω. According to the nature of the collected data, it is reasonable to assume that the acceleration-deceleration rates calculated at successive fiducial marks for a specific ramp vehicle are correlated, namely within driver correlation, or time-series observations. On the other hand, the calculated acceleration-deceleration rates between different ramp vehicles, namely across driver correlation, are assumed independent, or cross-sectional independence. In other words, there is no correlation across drivers. Thus the specification of the disturbance variance-covariance matrix of basic model $\mathbf{y} = \mathbf{X}\beta + \mathbf{u}$ has a block-diagonal form.

$$\text{Var}(\mathbf{u}) = E(\mathbf{uu}')$$

$$= \begin{bmatrix} \Sigma_{r_1} & 0 & \cdots & \cdots & \cdots & 0 \\ 0 & \Sigma_{r_2} & 0 & \cdots & \cdots & \vdots \\ \vdots & 0 & \ddots & 0 & \cdots & \vdots \\ \vdots & \vdots & 0 & \Sigma_{r_i} & 0 & \vdots \\ \vdots & \vdots & \vdots & 0 & \ddots & 0 \\ 0 & \cdots & \cdots & \cdots & 0 & \Sigma_{r_n} \end{bmatrix} \tag{3.44}$$

Where

Σ_{r_i} is the disturbance variance-covariance matrix of ramp vehicle i.

Because there exists serial correlation within successive calculated acceleration-deceleration rates for a specific ramp vehicle, the resultant variance-covariance matrix, Σ_{r_i}, would then be

$$\begin{aligned}\Sigma_{r_i} &= \text{Var}(\mathbf{u}_{r_i}) \\ &= E(\mathbf{u}_{r_i}\mathbf{u}_{r_i}') \\ &= \begin{bmatrix} \sigma^2_{i_{11}} & \sigma^2_{i_{12}} & \cdots & \sigma^2_{i_{1j}} & \cdots & \sigma^2_{i_{1m_i}} \\ \sigma^2_{i_{21}} & \sigma^2_{i_{22}} & \cdots & \cdots & \cdots & \sigma^2_{i_{2m_i}} \\ \vdots & \vdots & \ddots & \cdots & \cdots & \cdots \\ \sigma^2_{i_{j1}} & \vdots & \vdots & \sigma^2_{i_{jj}} & \cdots & \sigma^2_{i_{jm_i}} \\ \vdots & \vdots & \vdots & \vdots & \ddots & \cdots \\ \sigma^2_{i_{m_i1}} & \sigma^2_{i_{m_i2}} & \vdots & \sigma^2_{i_{m_ij}} & \vdots & \sigma^2_{i_{m_im_i}} \end{bmatrix}\end{aligned} \tag{3.45}$$

Where

$$\sigma^2_{i_{jj}} = \text{var}[u_{r_i}(d_j)] = E[u^2_{r_i}(d_j)] \qquad \text{for } j=1, 2, \ldots, m_i \tag{3.46}$$

$$\sigma^2_{i_{jk}} = \text{Cov}[u_{r_i}(d_j), u_{r_i}(d_k)] = E[u_{r_i}(d_j)u_{r_i}(d_k)]$$

$$\text{for } j=1, 2, \ldots, m_i,\ k=1, 2, \ldots, m_i, \text{ and } j \neq k \tag{3.47}$$

With the specification of Eq.(3.42), neighboring disturbance terms might be strongly correlated. It can be hypothesized that

$$u_{r_i}(d_j) = \rho_{r_i} u_{r_i}(d_{j-1}) + \varepsilon_{r_i}(d_j) \tag{3.48}$$

Where

ρ_{r_i} is known as the first-order coefficient of autocorrelation for ramp vehicle i, and the series $\{\varepsilon_{r_i}(d_j)\}$ has the following properties

$$E(\varepsilon_{\mathbf{r}_i}) = \mathbf{0} \tag{3.49}$$

$$E(\varepsilon_{\mathbf{r}_i}\varepsilon_{\mathbf{r}_i}') = \sigma^2_{\varepsilon_{r_i}}\mathbf{I} \tag{3.50}$$

$$\mathrm{Cov}[\,\varepsilon_{r_i}(d_j),\ \varepsilon_{r_i}(d_{j+s})\,] = 0 \qquad \text{for all i, } s \neq 0 \tag{3.51}$$

Equation (3.48) specifies a first-order autoregressive (Markov) series. Let L denote the lag operator such that when applied to any variable X_t

$$L X_t = X_{t-1}$$
$$L^2 X_t = X_{t-2}$$
$$\vdots$$

Thus Eq.(3.48) may be rewritten as

$$(1 - \rho_{r_i} L)u_{r_i}(d_j) = \varepsilon_{r_i}(d_j) \tag{3.52}$$

or
$$u_{r_i}(d_j) = \frac{1}{(1 - \rho_{r_i} L)}\varepsilon_{r_i}(d_j)$$
$$= (1 + \rho_{r_i} L + \rho^2_{r_i} L^2 + \ldots)\varepsilon_{r_i}(d_j)$$
$$= \varepsilon_{r_i}(d_j) + \rho_{r_i}\varepsilon_{r_i}(d_{j-1}) + \rho^2_{r_i}\varepsilon_{r_i}(d_{j-2}) + \ldots \tag{3.53}$$

Squaring both sides of Eq.(3.53) and taking the expectation,

$$\mathrm{var}[\,u_{r_i}(d_j)\,] = E[\,u_{r_i}{}^2(d_j)\,] = \frac{\sigma^2_{\varepsilon_{r_i}}}{1 - \rho^2_{r_i}} \qquad |\rho_{r_i}| < 1 \tag{3.54}$$

The right hand side does not include j, thus the $\{u_{r_i}(d_j)\}$ series has a constant variance, specified as

$$\sigma^2_{r_i} = \frac{\sigma^2_{\varepsilon_{r_i}}}{1 - \rho^2_{r_i}} \tag{3.55}$$

Using the definition of $u_{r_i}(d_j)$ in Eq.(3.53) and the properties of $\varepsilon_{r_i}(d_j)$ assumed in Eqs.(3.49) to (3.51), it is simple to establish that

$$E[\, u_{r_i}(d_j)u_{r_i}(d_{j-1}) \,] = \rho_{r_i}\sigma^2_{r_i} \tag{3.56}$$

$$E[\, u_{r_i}(d_j)u_{r_i}(d_{j-2}) \,] = \rho^2_{r_i}\sigma^2_{r_i} \tag{3.57}$$

and in general

$$E[\, u_{r_i}(d_j)u_{r_i}(d_{j-s}) \,] = \rho^s_{r_i}\sigma^2_{r_i} \tag{3.58}$$

Substituting Eq.(3.58) into Eq.(3.45), the disturbance variance-covariance matrix of ramp vehicle i, $\Sigma_{\mathbf{r_i}}$, is readily written as follows:

$$\Sigma_{\mathbf{r_i}} = \begin{bmatrix} \sigma^2_{r_i} & \rho_{r_i}\sigma^2_{r_i} & \cdots & \rho^{m_i-1}_{r_i}\sigma^2_{r_i} \\ \rho_{r_i}\sigma^2_{r_i} & \sigma^2_{r_i} & \cdots & \rho^{m_i-2}_{r_i}\sigma^2_{r_i} \\ \cdots & \cdots & \cdots & \cdots \\ \rho^{m_i-1}_{r_i}\sigma^2_{r_i} & \rho^{m_i-2}_{r_i}\sigma^2_{r_i} & \cdots & \sigma^2_{r_i} \end{bmatrix}$$

$$= \sigma^2_{r_i}\begin{bmatrix} 1 & \rho_{r_i} & \cdots & \rho^{m_i-1}_{r_i} \\ \rho_{r_i} & 1 & \cdots & \rho^{m_i-2}_{r_i} \\ \cdots & \cdots & \cdots & \cdots \\ \rho^{m_i-1}_{r_i} & \rho^{m_i-2}_{r_i} & \cdots & 1 \end{bmatrix}$$

$$= \sigma^2_{r_i}\Omega_{r_i} \tag{3.59}$$

Where

$$\Omega_{r_i} = \begin{bmatrix} 1 & \rho_{r_i} & \cdots & \rho^{m_i-1}_{r_i} \\ \rho_{r_i} & 1 & \cdots & \rho^{m_i-2}_{r_i} \\ \cdots & \cdots & \cdots & \cdots \\ \rho^{m_i-1}_{r_i} & \rho^{m_i-2}_{r_i} & \cdots & 1 \end{bmatrix} \tag{3.60}$$

Substituting Eq.(3.59) into Eq.(3.44), the variance-covariance matrix of the basic model assuming the disturbance follows a first-order autoregressive scheme is thus given as follows:

$$\text{var}(\mathbf{u}) = \begin{bmatrix} \sigma_{r_1}^2\Omega_{r_1} & 0 & \cdots & 0 & \cdots & 0 \\ 0 & \sigma_{r_2}^2\Omega_{r_2} & \cdots & \cdots & \cdots & 0 \\ \cdots & \cdots & \cdots & \cdots & \cdots & \cdots \\ 0 & \cdots & \cdots & \sigma_{r_i}^2\Omega_{r_i} & \cdots & 0 \\ \cdots & \cdots & \cdots & \cdots & \cdots & \cdots \\ 0 & 0 & \cdots & 0 & \cdots & \sigma_{r_n}^2\Omega_{r_n} \end{bmatrix} \tag{3.61}$$

and therefore

$$\Omega = \begin{bmatrix} \sigma_{r_1}^2\Omega_{r_1} & 0 & \cdots & 0 & \cdots & 0 \\ 0 & \sigma_{r_2}^2\Omega_{r_2} & \cdots & \cdots & \cdots & 0 \\ \cdots & \cdots & \cdots & \cdots & \cdots & \cdots \\ 0 & \cdots & \cdots & \sigma_{r_i}^2\Omega_{r_i} & \cdots & 0 \\ \cdots & \cdots & \cdots & \cdots & \cdots & \cdots \\ 0 & 0 & \cdots & 0 & \cdots & \sigma_{r_n}^2\Omega_{r_n} \end{bmatrix} \tag{3.62}$$

Consequently, to complete the task of deriving Ω, all one needs to know are the values of $\sigma_{r_i}^2$'s and Ω_{r_i}'s, or equivalently ρ_{r_i}'s and $\sigma_{\varepsilon_{r_i}}^2$'s.

One can proceed in the following way to find the consistent estimates of the elements of Eq(3.62). First, apply the ordinary least squares method to all $\sum_{i=1}^{n} m_i$ observations. The resulting regression coefficient estimates are unbiased and consistent. Therefore, they can be applied to calculate the regression residuals $e_{r_i}(d_j)$. Using these residuals, one can obtain estimates of ρ_{r_i}, say, $\hat{\rho}_{r_i}$, by the following equation,

$$\hat{\rho}_{r_i} = \frac{\sum_{j=2}^{m_i} e_{r_i}(d_j)e_{r_i}(d_{j-1})}{\sum_{j=2}^{m_i} e_{r_i}^2(d_j)} \tag{3.63}$$

After obtaining $\hat{\rho}_{r_i}$, one can use it to transform the observation data and rewrite the original model into another form

$$\mathbf{y}^* = \mathbf{X}^*\beta^* + \varepsilon^* \tag{3.64}$$

or more specifically,

$$y^*_{r_i}(d_j) = \beta^*_0 + \beta^*_1 X^*_{i1d_j} + \beta^*_2 X^*_{i2d_j} + \ldots + \beta^*_k X^*_{ikd_j} + \varepsilon^*_{r_i}(d_j) \tag{3.65}$$

where

$$y^*_{r_i}(d_j) = y_{r_i}(d_j) - \hat{\rho}_{r_i} y_{r_i}(d_{j-1}) \qquad (j = 2, 3, \ldots, m_i) \tag{3.66}$$

$$X^*_{i\kappa d_j} = X_{i\kappa d_j} - \hat{\rho}_{r_i} X_{i\kappa d_{j-1}} \tag{3.67}$$

$$\varepsilon^*_{r_i}(d_j) = u_{r_i}(d_j) - \hat{\rho}_{r_i} u_{r_i}(d_{j-1}) \tag{3.68}$$

$i = 1, 2, \ldots, n,$

$\kappa = 1, 2, \ldots, k$

The purpose of the transformation is to obtain observations that are at least asymptotically nonautoregressive, and, therefore, the basic assumptions of the classical normal linear regression model are satisfied. To this end, one can apply the ordinary least squares method to Eq.(3.65) for which one has $\sum_{i=1}^{n}(m_i - 1)$ observations. The resulting regression residuals, $\hat{\varepsilon}^*_{r_i}(d_j)$, can be used to estimate the variance of $\varepsilon_{r_i}(d_j)$, $\sigma^2_{\varepsilon_{r_i}}$, by the following expression

$$\hat{\sigma}^2_{\varepsilon_{r_i}} = \frac{1}{m_i - k - 1}\sum_{j=2}^{m_i} \hat{\varepsilon}^*_{r_i}(d_j)^2 \tag{3.69}$$

Substituting Eqs.(3.63) and (3.69) in Eq.(3.55), one can obtain the consistent estimator of $\sigma^2_{r_i}$. Having obtained consistent estimators of ρ_{r_i} and $\sigma^2_{r_i}$, one complete the task of deriving consistent estimators of the element of Ω. With the accomplishment of obtaining Ω, or more precisely, $\hat{\Omega}$, the generalized least-squares method can then be applied to the basic model of Eq.(3.28). The best linear unbiased estimators of the regression coefficient and their associated variances can be obtained using Eqs.(3.37) and (3.38) respectively. This approach, however, is applicable only when Ω is a symmetric positive definite matrix. A necessary and sufficient condition for $\hat{\Omega}$ to be positive definite is that all the eigenvalues of $\hat{\Omega}$ be positive, or the determinant of every principal submatrix be positive. This test can be easily performed using state-of-the-art matrix operation software, e.g. MATLAB.

Calibration Procedures

The GLS formulation derivations have been presented in above section. This section will discuss the procedures, as shown in Figure 3.34, of calibrating the proposed methodology for modeling ramp vehicle acceleration-deceleration behavior during the freeway merge maneuvers. Only the procedures for calibrating category 1, as defined in section 3.5.2, or the associated model, Eq.(3.18), are presented in this section. Exactly the same calibration procedures are applied to the category 2, or Eq.(3.19) calibration. One must point out that this proposed method was developed for the case when vehicle trajectories were recorded at regular fiducial mark intervals. One revelation from the derivations of the GLS formulations is that GLS is applicable to linear regression models only. Therefore, one cannot calibrate this specific traffic flow model by directly applying GLS to Eq.(3.18) which is a nonlinear model. Modifications to Eq.(3.18) are required to make it suitable for GLS application. Essentially, Eq.(3.18) cannot be directly transformed to a linear form because of nonlinearity in the parameters. As a consequence, one should try to fix the values of those parameters, namely α_1, α_2, α_3, and γ, to transform Eq.(3.18) into a linear model. First, one can simply apply a nonlinear regression technique to Eq.(3.18) using the pooling of cross-section and time-series observations and obtain the regression coefficient estimators of $\hat{\beta}_0$, $\hat{\beta}_1$, $\hat{\beta}_2$, $\hat{\beta}_3$, $\hat{\alpha}_1$, $\hat{\alpha}_2$, $\hat{\alpha}_3$, and $\hat{\gamma}$ respectively. This task can be easily accomplished using statistical software, e.g. SPSS. This process should be repeated for different D values in order to find the best model. For example, if the fiducial mark interval is 50 feet, one may want to try those cases of D equal to 0 feet, 50 feet, or 100 feet etc.. The case of D equal to 0 feet simply implies that there is no distance, or time, lag between the stimulus the driver received and the response he/she made. The D that gives the best estimation results is chosen as the best model and used in later GLS calibration. By substituting the $\hat{\alpha}_1$, $\hat{\alpha}_2$, $\hat{\alpha}_3$, and $\hat{\gamma}$ in Eq.(3.18), one can rewrite Eq.(3.18) into Eq.(3.70).

$$
\begin{aligned}
\ddot{X}_{r_i}(d_j+D) \;=\; & \beta_0' + \beta_1' \frac{\dot{X}_{r_i}(d_j+D)^{\hat{\gamma}}}{[X_{r_i}(d_j)-X_{flag_i}(d_j)]^{\hat{\alpha}_1}}[\dot{X}_{flag_i}(d_j)-\dot{X}_{r_i}(d_j)] \\
& + \beta_2' \frac{\dot{X}_{r_i}(d_j+D)^{\hat{\gamma}}}{[X_{flead_i}(d_j)-X_{r_i}(d_j)]^{\hat{\alpha}_2}}[\dot{X}_{r_i}(d_j)-\dot{X}_{flead_i}(d_j)] \\
& + \beta_3' \frac{\dot{X}_{r_i}(d_j+D)^{\hat{\gamma}}}{[L-X_{r_i}(d_j)]^{\hat{\alpha}_3}}[\dot{X}_{r_i}(d_j)] \\
& + u_{r_i}(d_j)' \qquad (3.70)
\end{aligned}
$$

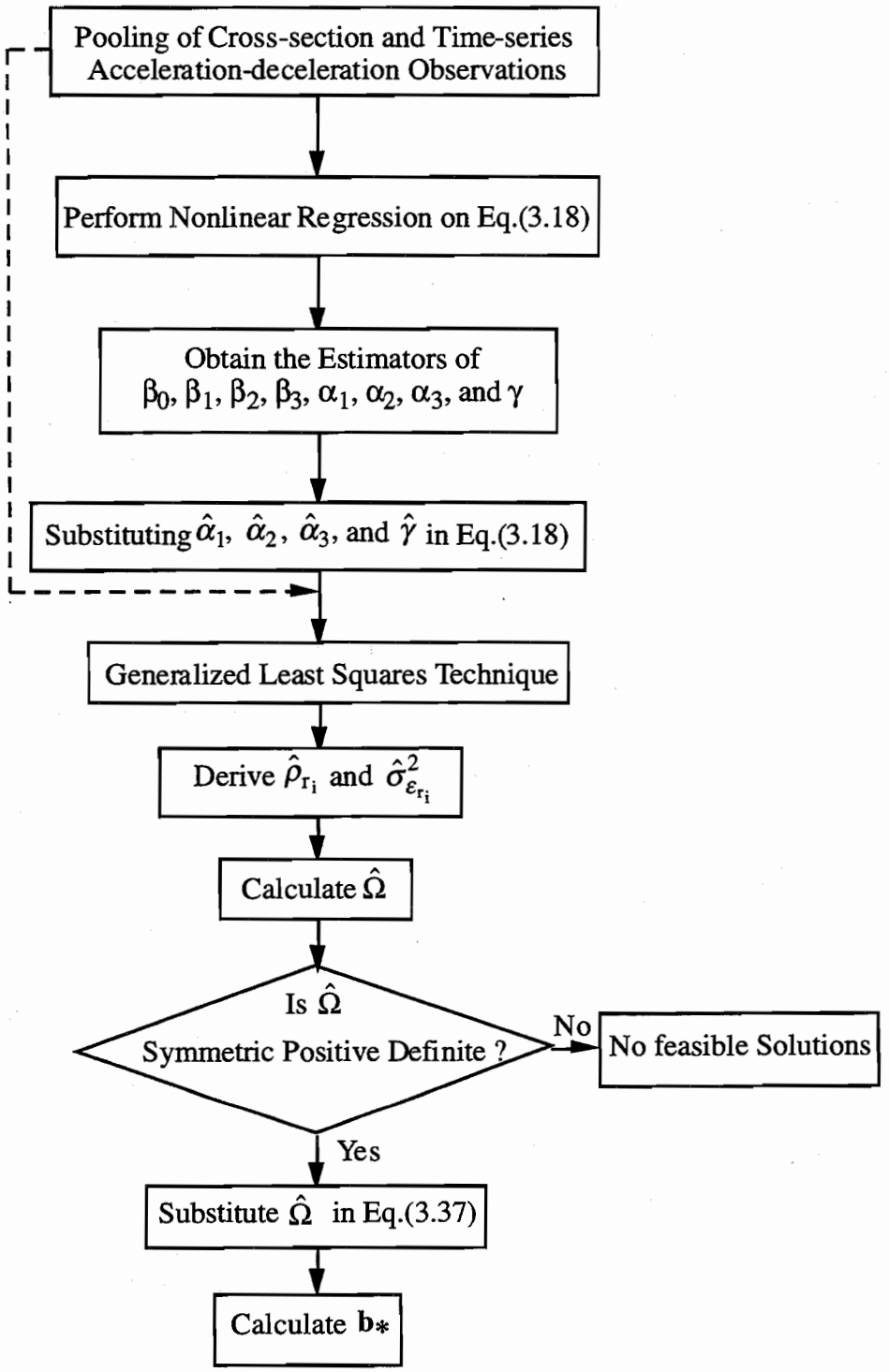

Figure 3.34 Flowchart of performing the generalized least squares technique

Clearly, Equation(3.70) is a linear form with only $\beta_0^{'}$, $\beta_1^{'}$, $\beta_2^{'}$, and $\beta_3^{'}$ to be estimated. The remaining tasks are to find their consistent and unbiased estimators using the GLS technique.

Applying OLS to Eq.(3.70) using pooling of cross-section and time-series observations, one can calculate $\hat{\rho}_{r_i}$ by means of Eq.(3.63). Substituting $\hat{\rho}_{r_i}$ in Eqs.(3.66), (3.67), and (3.68) respectively, one can rewrite Eq.(3.70) into Eq.(3.71).

$$Y_i^* = \beta_0^{''} + \beta_1^{''} X_{i1}^* + \beta_2^{''} X_{i2}^* + \beta_3^{''} X_{i3}^* + \varepsilon_i^* \tag{3.71}$$

Where

$$Y_i^* = \ddot{X}_{r_i}(d_j + D) - \hat{\rho}_{r_i} \ddot{X}_{r_i}(d_{j-1} + D) \tag{3.72}$$

$$\begin{aligned} X_{i1}^* = {} & \frac{\dot{X}_{r_i}(d_j + D)^{\hat{\gamma}}}{[X_{r_i}(d_j) - X_{flag_i}(d_j)]^{\hat{\alpha}_1}} [\dot{X}_{flag_i}(d_j) - \dot{X}_{r_i}(d_j)] \\ & - \hat{\rho}_{r_i} \frac{\dot{X}_{r_i}(d_{j-1} + D)^{\hat{\gamma}}}{[X_{r_i}(d_{j-1}) - X_{flag_i}(d_{j-1})]^{\hat{\alpha}_1}} [\dot{X}_{flag_i}(d_{j-1}) - \dot{X}_{r_i}(d_{j-1})] \end{aligned} \tag{3.73}$$

$$\begin{aligned} X_{i2}^* = {} & \frac{\dot{X}_{r_i}(d_j + D)^{\hat{\gamma}}}{[X_{flead_i}(d_j) - X_{r_i}(d_j)]^{\hat{\alpha}_2}} [\dot{X}_{r_i}(d_j) - \dot{X}_{flead_i}(d_j)] \\ & - \hat{\rho}_{r_i} \frac{\dot{X}_{r_i}(d_{j-1} + D)^{\hat{\gamma}}}{[X_{flead_i}(d_{j-1}) - X_{r_i}(d_{j-1})]^{\hat{\alpha}_2}} [\dot{X}_{r_i}(d_{j-1}) - \dot{X}_{flead_i}(d_{j-1})] \end{aligned} \tag{3.74}$$

$$\begin{aligned} X_{i3}^* = {} & \frac{\dot{X}_{r_i}(d_j + D)^{\hat{\gamma}}}{[L - X_{r_i}(d_j)]^{\hat{\alpha}_3}} [\dot{X}_{r_i}(d_j)] \\ & - \hat{\rho}_{r_i} \frac{\dot{X}_{r_i}(d_{j-1} + D)^{\hat{\gamma}}}{[L - X_{r_i}(d_{j-1})]^{\hat{\alpha}_3}} [\dot{X}_{r_i}(d_{j-1})] \end{aligned} \tag{3.75}$$

$$\varepsilon_i^* = u_{r_i}(d_j)' - \hat{\rho}_{r_i} u_{r_i}(d_{j-1})' \tag{3.76}$$

Applying OLS to the transformation of Eq.(3.71), one can calculate $\hat{\sigma}^2_{\varepsilon_{r_i}}$ using Eq(3.69). Substituting $\hat{\rho}_{r_i}$ and $\hat{\sigma}^2_{\varepsilon_{r_i}}$ in Eq.(3.55) to obtain $\hat{\sigma}^2_{r_i}$ and then substituting $\hat{\rho}_{r_i}$ and $\hat{\sigma}^2_{r_i}$ in

Eq.(3.59) to obtain $\hat{\Sigma}_{\mathbf{r}_i}$, one can calculate $\hat{\Omega}$ using Eq.(3.44). To ensure GLS is appropriately applicable to this specific acceleration-deceleration model, one must confirm that $\hat{\Omega}$ is a symmetric positive definite matrix. By the derivations described in Eq.(3.59), $\hat{\Omega}$ must be a symmetric matrix. A necessary and sufficient condition for $\hat{\Omega}$ to be positive definite is that all the eigenvalues of $\hat{\Omega}$ be positive, or the determinant of every principal submatrix be positive. These tests can be easily performed using matrix operation software, e.g. MATLAB. Finally, substituting $\hat{\Omega}$ in Eq.(3.37), one gets consistent and unbiased estimators of Eq.(3.70). Equivalently, the estimators of the original model, Eq.(3.18), are also obtained.

GAP ACCEPTANCE MODEL

The gap acceptance process is one of the most complicated components in the freeway merge model. A gap acceptance model which precisely describes driver behavior in the acceleration lane and appropriately incorporates roadway and traffic conditions into the driver's decision process is important in the analysis of freeway entrance ramp traffic operations and control schemes. From this standpoint, a sophisticated gap acceptance model that can be applied to analyze traffic operations in the freeway merge process, evaluate acceleration lane geometric designs, and enhance freeway simulation model capabilities is a major task of this study.

Critical Angular Velocity Specification

In attempting to enter a freeway from an acceleration lane, a ramp driver observes nearby freeway vehicles which make up the gap into which the driver will eventually merge. Most evidence in the psychological literature suggests that the ramp driver is only capable of processing a first order motion vector when analyzing an adjacent freeway vehicle. Essentially, the ramp driver evaluates the angular velocity created by the corresponding freeway lag vehicle to determine whether a specific gap size is sufficient.

Based on driver behavior, it is hypothesized that ramp drivers operate at some angular velocity thresholds. From the ramp driver standpoint, a freeway lag vehicle in the adjacent freeway lane will have either of two angular velocity components. Angular velocity will either be increasing if the freeway lag vehicle is closing on the gap seeking driver or decreasing if the lag vehicle is falling behind relative to the gap seeking driver. The ramp driver can establish a criterion for accepting or rejecting any detected gap. If the angular velocity is greater than the ramp driver's threshold, the lag vehicle must be closing and the perceived gap is too small to be accepted.

Conversely, if the angular velocity is below the threshold, there is no perceived closure and the gap is sufficient to be accepted.

Using the threshold of angular velocity leads to a realistic accept-reject criterion for the gap seeking driver which is generally a more stable decision basis than some other criteria for human control. However, the threshold for a ramp driver is stochastic when he is traveling in the acceleration lane. Consequently, in this study, the threshold to accept a specific gap size for a ramp driver is hypothesized as a function of the number of gaps rejected so far and the location of the ramp vehicle in the acceleration lane. A hypothesized model is given as follows:

$$\omega_{cr}(i, x_i) = \overline{\omega}_{cr} + \alpha(i-1)^{\beta} + \gamma(L-x_i)^{\delta} + \varepsilon_i \qquad (3.77)$$

Where

$\omega_{cr}(i, x_i)$ = the critical angular velocity of a ramp driver randomly chosen from the population when facing the i-th gap in sequence and at the position x_i;

$\overline{\omega}_{cr}$ = the theoretical mean critical angular velocity when a ramp driver runs to the end of the acceleration lane and still faces the first lag, i.e. for i=1 and x_i=L;

L = the length of the acceleration lane;

x_i = the distance that the ramp driver has traveled when facing the i-th gap;

$L - x_i$ = the remaining length to the acceleration lane end when facing the i-th gap

ε_i = disturbance term which varies across drivers and gaps,
$\varepsilon_i \sim$ iid $N(0,\sigma^2)$;

α, β, γ, and δ are parameters to be estimated.

Following the specification of Eq.(3.77), the mean critical angular velocity when a ramp driver just arrives at the merging end, or in other words the driver just enters the acceleration lane, is readily given as

$$\begin{aligned} \omega_{cr}(1, 0) &= \overline{\omega}_{cr}^{0} \\ &= \hat{\overline{\omega}}_{cr} + \hat{\gamma} L^{\hat{\delta}} \end{aligned} \qquad (3.78)$$

Where

$\overline{\omega}_{cr}^{0}$ = the mean critical angular velocity when a ramp driver just arrives at the merging end, i.e. for i=1 and x_i=0;

$\hat{\bar{\omega}}_{cr}$, $\hat{\gamma}$, and $\hat{\delta}$ are the estimated values of parameter $\bar{\omega}_{cr}$, γ, and δ respectively. The $\bar{\omega}_{cr}^{0}$ is just a constant since L is a known constant and $\hat{\bar{\omega}}_{cr}$, $\hat{\gamma}$, and $\hat{\delta}$ are all estimated values.

Note that this formulation cannot distinguish between the distribution across ramp drivers and within gaps. The unit of observation is the i-th angular velocity associated with the i-th gap of the j-th ramp driver and all the normal variates are assumed to be independent and identically distributed.

Maximum Likelihood Estimation

The gap acceptance model is given by the probability that a certain ramp driver would accept a given gap. The gaps are characterized by their associated angular velocity, ω_i, sequential number, i, and the location of the ramp driver when facing such a gap in the acceleration lane, x. Thus the gap acceptance function is given by the probit function:

$$
\begin{aligned}
& pr(\text{accept gap i} \mid \bar{\omega}_{cr},\ i,\ \omega_i,\ L,\ x_i,\ \alpha,\ \beta,\ \gamma,\ \delta) \\
&= pr[\ \omega_i < \omega_{cr}(i,\ x_i)\ ] \\
&= pr[\ \omega_i < \bar{\omega}_{cr} + \alpha(i-1)^{\beta} + \gamma(L-x_i)^{\delta} + \varepsilon_i\ ] \\
&= pr[\ \omega_i - \bar{\omega}_{cr} - \alpha(i-1)^{\beta} - \gamma(L-x_i)^{\delta} < \varepsilon_i\ ] \\
&= 1 - pr[\ \varepsilon_i < \omega_i - \bar{\omega}_{cr} - \alpha(i-1)^{\beta} - \gamma(L-x_i)^{\delta}\ ] \\
&= 1 - \Phi\left[\frac{\omega_i - \bar{\omega}_{cr} - \alpha(i-1)^{\beta} - \gamma(L-x_i)^{\delta}}{\sigma}\right]
\end{aligned}
\qquad (3.79)
$$

Where $\Phi[\ \bullet\ ]$ denotes the standard cumulative normal distribution.

The maximum likelihood method can be used to estimate the parameters in Eq.(3.79). In order to construct a proper likelihood function for this model let the superscript j refer to an observation from a simple random sample of size N. Let k_j denote the sequential number of the gap accepted by ramp driver j; j = 1, 2, ..., N. The probability that the j-th driver would accept the k-th gap, $p_{k_j}^{j}$, is given by:

$$p^{j}_{k_j} = pr[\omega^{j}_{k} \leq \omega^{j}_{cr}(k, x_k)] \cdot \prod_{i=1}^{k-1} pr[\omega^{j}_{i} > \omega^{j}_{cr}(i, x_i)] \quad (3.80)$$

since accepting the k-th gap means that all preceding gaps were rejected. The likelihood function of this model for a given sample size, N, is:

$$L(\overline{\omega}_{cr}, \alpha, \beta, \gamma, \delta \mid \omega_{\cdot}, k_{\cdot}) = \prod_{j=1}^{N} p^{j}_{k_j} \quad (3.81)$$

Solving the likelihood function gives the solutions to the parameters of $\overline{\omega}_{cr}$, α, β, γ, and δ. Equivalently, the original critical angular velocity distribution, Eq.(3.77), can also be obtained. A new multinomial probit (MNP) estimation procedure originally developed by Lam (1991) and recently revised by Liu (1996) is proposed to solve for the likelihood function.

SUMMARY

The freeway merge maneuver is complex and may involve a lane change, continuous acceleration, possibly deceleration, and finally a gap acceptance. This chapter has presented the methodologies used in this study to collect and reduce field data, analyze freeway merge behavior data, calibrate a ramp vehicle acceleration-deceleration model, and develop a ramp vehicle critical angular velocity distribution for merging.

The probability density function of speed estimation measurement error through video image techniques was developed. Mathematical derivation of the probability function which incorporates the effect of imbedded video camera time-base resolution, fiducial mark interval, and actual vehicle speed was presented. A Monte Carlo simulation was applied to verify the developed probability function. Both graphical comparison and goodness-of-fit tests demonstrated very good agreement between the theoretical probability function and simulation. Obviously, time-base resolution, actual vehicle speed, and fiducial mark intervals have a joint effect in determining measurement error and cannot be considered individually. Among them, the time-base resolution was found to have the most significant speed measurement error effect. Using a video camera that features κ=10 frames/second, one cannot expect to obtain accurate speed estimates. The higher the vehicle speed, the higher the probability of producing large measurement errors. For a given time-base resolution, the faster the actual vehicle speed and the shorter the fiducial mark intervals, the higher the probability of having a large measurement error. The probability function presented in this paper provides a very useful tool for it allows traffic

engineers to evaluate in advance the probability of occurrence of certain measurement error magnitudes and to adjust the data collection plan accordingly.

Primary data capturing a wide range of information were collected using manual and video tape methods and manually reduced through image processing techniques. Comprehensive traffic surveys were conducted at several entrance ramps in the Austin and Houston areas. This freeway merge traffic data provides fundamental information for use in investigating ramp driver freeway merge behavior. Ramp vehicle merging position in conjunction with freeway and ramp flow levels was analyzed for both parallel and taper type entrance ramps. At the Houston location where vehicle trajectory data was available, merging position with respect to ramp vehicle speed, as well as relative speed and time gap between a ramp vehicle and corresponding freeway lag and lead vehicles were examined respectively. Both graphical presentations and contingency table independence tests show that ramp vehicle merging position is not significantly related to any single traffic parameter. Driver-vehicle behavior during merge maneuvers can only be modeled using combinations of the above traffic parameters.

To develop an in-depth understanding of freeway merge gap acceptance behavior, this study also investigated the gap structure elements, i.e. acceleration rate, speed, relative speed, time gap, distance gap, and angular velocity between ramp vehicles and corresponding freeway lag and lead vehicles, associated with the location where ramp drivers accepted a gap and performed a merge. Although almost all gap structure elements, except merge acceleration rate, have insignificant mean differences across fiducial marks, Figures 3.22 to 3.29 show significant scatter spread and skewing which limits the usage of the statistical mean equality test results. These data characteristics suggest that freeway merge gap acceptance behavior should be examined using disaggregate rather than aggregate data.

A theoretical framework for modeling freeway merge ramp vehicle acceleration-deceleration behavior was presented. This methodology used the stimulus-response concept as a fundamental rule and was formulated as a modified form of conventional car-following models. The classical time-based car-following model was expanded to a nonlinear distance-based stimulus-response equation to capture the characteristics of the collected traffic data. Recognizing the potential serial correlation problems associated with the collected acceleration data, a generalized least-squares technique is proposed as a tool to calibrate the freeway merge acceleration-deceleration model. Formulations for deriving consistent and unbiased GLS estimators assuming the within vehicle disturbance follows a first-order autoregressive scheme were developed. Procedures for using the proposed methods to calibrate this specific ramp driver acceleration-deceleration behavior were also presented.

A discrete choice analysis method was adopted as a tool to calibrate a ramp driver gap acceptance behavior model. This study hypothesized that most ramp drivers operate at some angular velocity threshold level during the gap search process. The threshold to accept a specific gap size, characterized by the angular velocity, for a ramp driver is hypothesized as a function of the number of gaps rejected so far and the location of the ramp vehicle in the acceleration lane. The probability of accepting a given gap, or namely gap acceptance function, is specified as a probit functional form. The maximum likelihood method was proposed to estimate the parameters in the gap acceptance function.

The methodologies presented in this chapter are proposed as hypotheses to be examined and refined. A pilot study performed on a small number of field observations will be described in the next chapter.

CHAPTER 4. RESULTS OF THE PILOT STUDY

INTRODUCTION

In the previous chapter, a conceptual methodology to model ramp driver acceleration-deceleration as well as gap acceptance behavior in the acceleration lane is described. Due to the sophisticated nature of this problem, performing a pilot study to investigate the feasibility of the conceptual methodology is desired before major efforts are undertaked. To calibrate the models, a small amount of data were collected at one freeway entrance ramp for use in initial model development. These data provided preliminary indications of the characteristics of certain key variables and identified additional data needs. Potential problems detected through the pilot study enhance the applicability of the proposed methodology. Conclusions drawn from the pilot study serve as a basis for later detailed model calibration.

LOCATION OF THE PILOT STUDY

An entrance ramp of southbound IH-35 at Oltorf Street in Austin was chosen to perform pilot study data collection. This location has a short one-lane entrance ramp where the acceleration lane is approximately 300 feet in length and merges with three freeway through lanes. The freeway upstream of the entrance ramp has a slight upgrade, however, the section near the merging area is almost flat. Freeway geometrics around the merging area are expected to have limited impacts on vehicle operations.

The video camera was set up on the roof of a nearby four-floor building from where the whole acceleration lane operation was visible. Fiducial marks, starting from the merging end, were made by putting wide and long white tape on the grass beside the acceleration lane shoulder. All fiducial marks were perpendicular to the pavement edge. Each set of fiducial marks represented a 30 feet speed trap. The videotaping was performed at four o'clock in the afternoon when the peak traffic was beginning. The weather was clear and the pavement was dry. The freeway right lane carried approximately 1500 vph while the entrance ramp had 350 vph during the recording period. Five and a half percent of the freeway right lane vehicles were trucks while the ramp vehicles contained no trucks. This middle to high freeway flow level is appropriate for the purpose of this study. Thirty-one ramp vehicle merging trajectory data were collected. These data were used to gain a better understanding of the entry process, calibrate certain parameters identified in the mathematical framework, and test the validity of proposed methodology.

GENERAL BEHAVIOR OF RAMP VEHICLES IN ACCELERATION LANE

A ramp driver in the acceleration lane must perform many different tasks in a timesharing mode before merging into the freeway stream. Interaction with freeway vehicles and variability within drivers make the observed behavior different from driver to driver. The outcomes of these variations depict the fundamental aspects of entrance ramp operations. The following sections contain discussions of the fundamental phenomena of merging operations obtained from field data analysis.

Speed Data

The primary data of interest was the speed of vehicles traveling through speed traps in the acceleration lane and entering the freeway. These speeds provided a vehicle speed change profile during transition, indicating where and with what magnitude vehicles were accelerating or decelerating, the speed at which vehicles were entering the freeway, and the accepted merge angular velocities for each ramp vehicle along the merging area. Speeds of freeway vehicles were also collected in order to determine speed differentials and associated angular velocities at which ramp vehicles were entering the freeway right lane.

Speed data was calculated for each trap by measuring the travel time required by the vehicle to move from one fiducial mark to the next. Therefore, the resulting speed was actually space mean travel speed within one trap. Intuitively, the shorter the length of each trap, the more closely the space means approach spot or instantaneous speeds. Figures 3.3 and 3.4, however, indicate that the shorter the length of each trap, the larger the errors associated with measurement. Figure 4.1 shows calculated ramp vehicle average speed profiles based upon 30 feet and 60 feet trap lengths respectively.

The curve representing successive 30 feet trap speeds shows much greater speed fluctuation than the 60 feet speeds. However, experience indicates that a driver will not change acceleration or deceleration magnitude continuously within such a short distance. This fact demonstrates that it is not appropriate to use the 30 feet trap length to calculate vehicle speeds. Because, under such a circumstance, a small time measurement error will have great contribution to the resulting speed measurement error. The curve using the 60 feet trap length, on the other hand, shows a reasonable result. This curve depicts that on average a ramp driver will decelerate first after he or she enters the acceleration lane because the driver starts to search for an acceptable gap. Soon after the driver detects an angular velocity below his or her threshold of acceptance, the driver will accelerate to accept the gap and enter the freeway stream. For the case of a short acceleration lane, the above analysis results are expected. The length constraint restricts the possibility of a ramp vehicle continuously alternating between acceleration and

deceleration. Comparison of speed profiles of a ramp vehicle and a corresponding freeway lag vehicle is shown in Figure 4.2. For this specific location, freeway lag vehicles, on average, have a higher speed in the first quarter of the acceleration lane. For the rest of the acceleration lane, ramp vehicles have a higher speed than freeway lag vehicles.

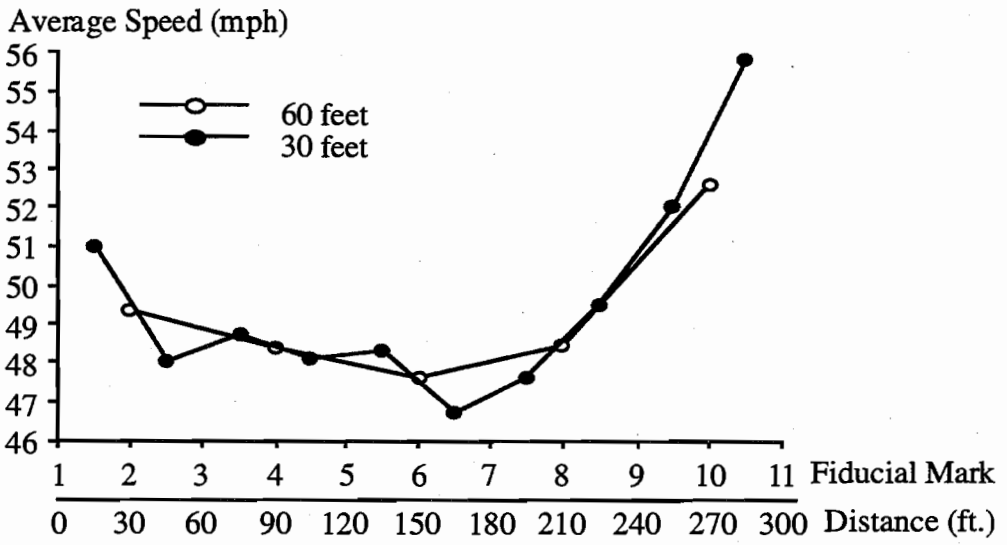

Figure 4.1 Ramp vehicle speed profile for different fiducial mark distance

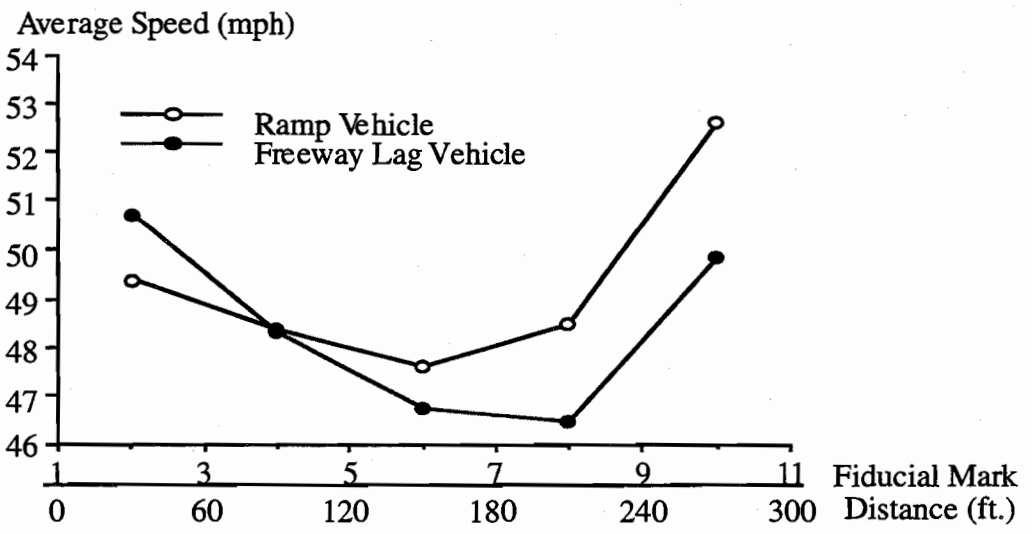

Figure 4.2 Comparison of average speed of ramp vehicle and freeway lag vehicle

Acceleration-Deceleration Data

The calculations of acceleration-deceleration, using speed data, are straightforward. A pair of speeds can be used to calculate average acceleration-deceleration rate with the following expression,

average acceleration-deceleration rate over traps i and i+1

$$= \frac{\text{average speed over trap } (i+1) \text{ - average speed over trap } i}{\text{average travel time of trap i and trap } (i+1)} \quad (4.1)$$

Figure 4.3 shows the acceleration-deceleration profiles of ramp vehicles and their corresponding freeway lag vehicles. The trends indicate that the freeway lag vehicle apparently decelerates with a greater magnitude than the ramp vehicle to accommodate the merging ramp vehicles. This result is reasonable because with a short acceleration lane, ramp drivers do not have many chances to search for acceptable gaps. Therefore, as soon as an acceptable gap is detected, ramp drivers will accelerate with a greater magnitude than that of corresponding freeway lag vehicles in order to position himself opposite a freeway gap and maneuver into it before reaching the acceleration lane terminus. Failing to merge before reaching the acceleration lane end will cause a sudden stop or illegal driving on the freeway shoulder. Knowing the ramp vehicle acceleration-deceleration performance in the merging area is important in simulating freeway merging operations, designing acceleration lane length, evaluating freeway entrance ramps operations, and estimating merging area fuel consumption and emissions.

Speed Differential at Merge

The speed differential, measured at the position where a ramp vehicle was performing a merge maneuver, was defined as the speed difference between a merging ramp vehicle and its corresponding freeway lag vehicle. The equation shown in section 3.4.2.3 was used to calculate the speed differential magnitudes. Figure 4.4 presents a speed differential distribution observed at this pilot study site. AASHTO (1990) has suggested 5 mph as a reasonable speed differential criterion to design acceleration lane lengths. The distribution shown in Figure 4.4 indicates that, at their merge positions, 50% of the ramp vehicles have at least a 3.5 mph greater speed than their corresponding freeway lag vehicles. Thirty percent of the ramp vehicles have a lower speed, or positive speed differential, than their corresponding freeway lag vehicles during the merge maneuver. Very few have a speed differential greater than 5 mph. Evidence shown in Figure 4.4 supports the AASHTO criterion suggesting an acceleration lane length based upon 85% of the

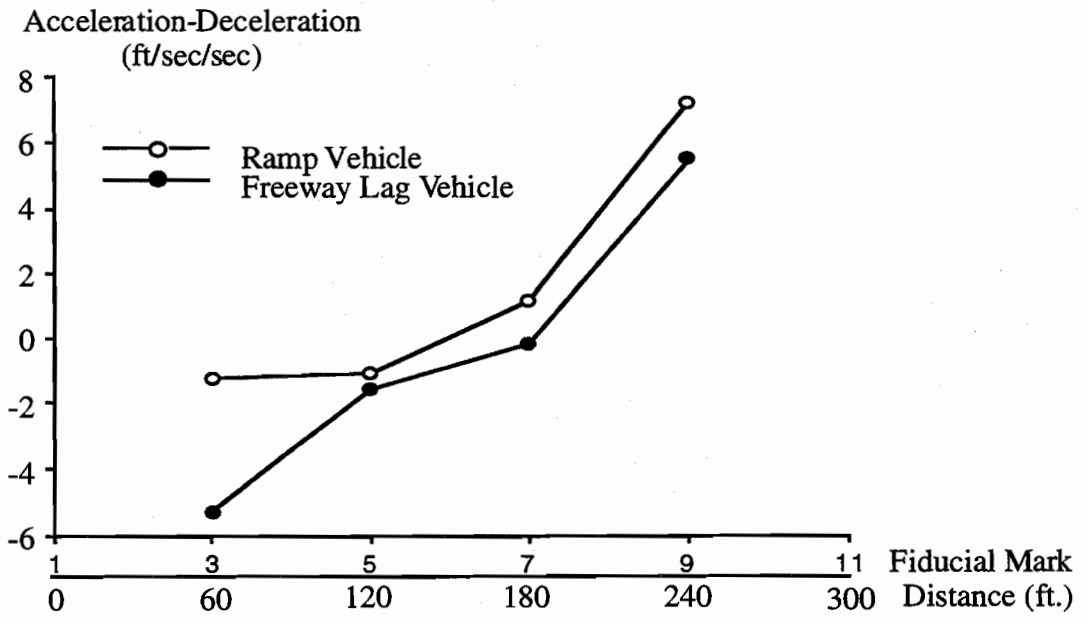

Figure 4.3 Comparison of acceleration-deceleration profile of ramp vehicle and freeway lag vehicle

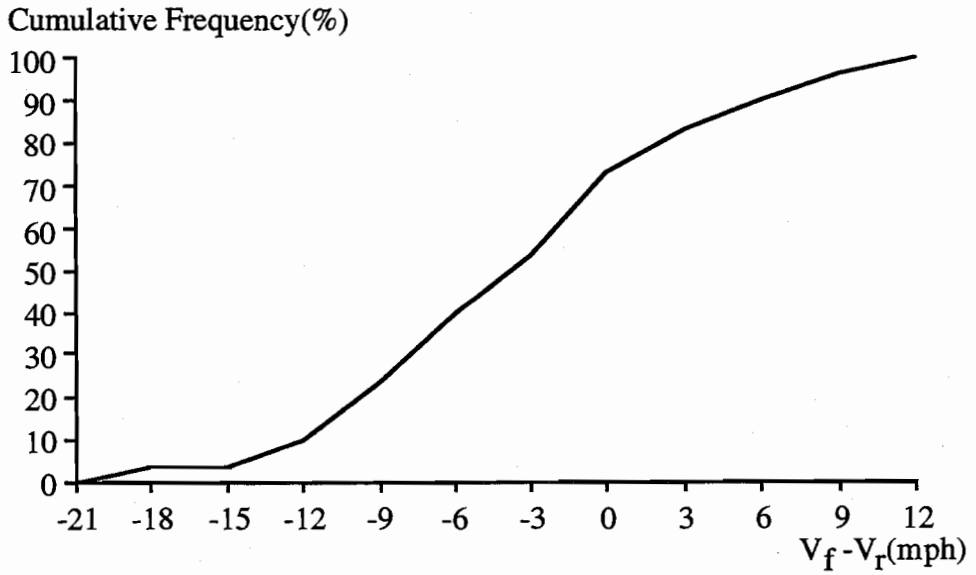

Figure 4.4 Distribution of merge speed differential between freeway lag vehicle and ramp vehicle

ramp vehicles having a merge speed differential of less than 5 mph. However, the minimum required acceleration lane length (excluding taper) recommended in Table X-4 of AASHTO (1990) is longer than the real acceleration lane length of this pilot study site, implying that the AASHTO recommendations using speed differential as the sole design criterion might depart somewhat from reality.

Figure 4.5 shows the speed differential data from a different perspective, the speed difference between freeway and ramp vehicles at merge versus the merge maneuver location. Almost all the observed ramp vehicles merge in the later portion of the acceleration lane. This vehicle merge trajectory is reasonable for a short acceleration lane. Similar to that of Figure 3.22, Figure 4.5 also shows that the dispersion of the merge speed differential is large. This provides more evidence that ramp drivers might not merge in response to some threshold speed differential as assumed by AASHTO. Rather, ramp drivers will merge at any speed differential, possibly responding to the freeway right lane vehicle angular velocity or other traffic parameter combinations.

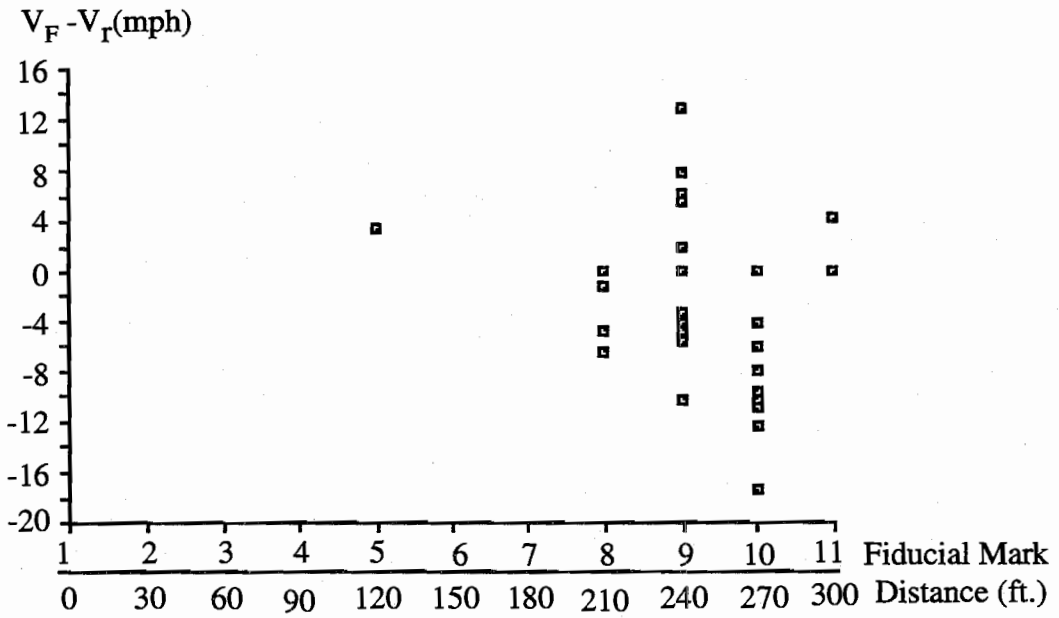

Figure 4.5 Scatter of speed differential at merge vs. merge location

Angular Velocity at Merge

As previously discussed, the angular velocity created by a freeway lag vehicle and viewed by a ramp driver might be the critical criterion used by a ramp driver to determine whether a gap is sufficient. Figure 4.6 shows, based upon field measurement of individual drivers, the distribution of angular velocity accepted by ramp drivers to complete a merge. Many ramp vehicles contained in the data set merged with a speed higher than the freeway lag vehicles, resulting in a corresponding negative accepted angular velocity. Fifty percent of the ramp drivers have an accepted angular velocity approximately equal to or less than -0.01 rads/sec which is smaller than the magnitudes found by Michaels and Fazio (1989) where the median angular velocity at beginning of the merge was 0.0043 rads/sec for a loop ramp and 0.0034 rads/sec for a diamond ramp. This phenomenon might be partially due to the fact that ramp drivers will accelerate rapidly to merge into the freeway as soon as possible when entering a short acceleration lane. It may also be because when approaching a short acceleration lane merge area, freeway lag vehicles will slightly reduce speeds to yield the right of way to merging ramp vehicles in order to avoid a potential forced merge situation. There is a potential advantage of using angular velocity rather than either time gap or distance gap alone as a freeway merge predictor. If time gap is the sole gap acceptance criterion, speed differential effects are ignored, many ramp drivers would appear to accept unrealisticly small time gaps.

By removing negative angular velocities from the data set, Figure 4.7 shows the cumulative frequency distribution of the positive angular velocities only. Among the ramp drivers who accept a gap with positive angular velocity, about 50 percent accept an angular velocity below 0.004 rads/sec. This tends to support the theoretical assumption of an angular velocity threshold on the order of 0.001 to 0.01 rads/sec (Michaels, 1963). This result, however, is inconclusive since only a small quantity of positive angular velocity observations were obtained.

Figures 4.6 and 4.7 provide no information that can be directly used to construct a driver behavior model but only demonstrate general phenomena in order to gain more understanding about the freeway merge process. Most drivers rejected no gaps before merging into the freeway stream, partially because of the short acceleration lane at the site studied. The critical, or threshold, angular velocities for merging therefore cannot be determined from this analysis because gap rejection information is not available.

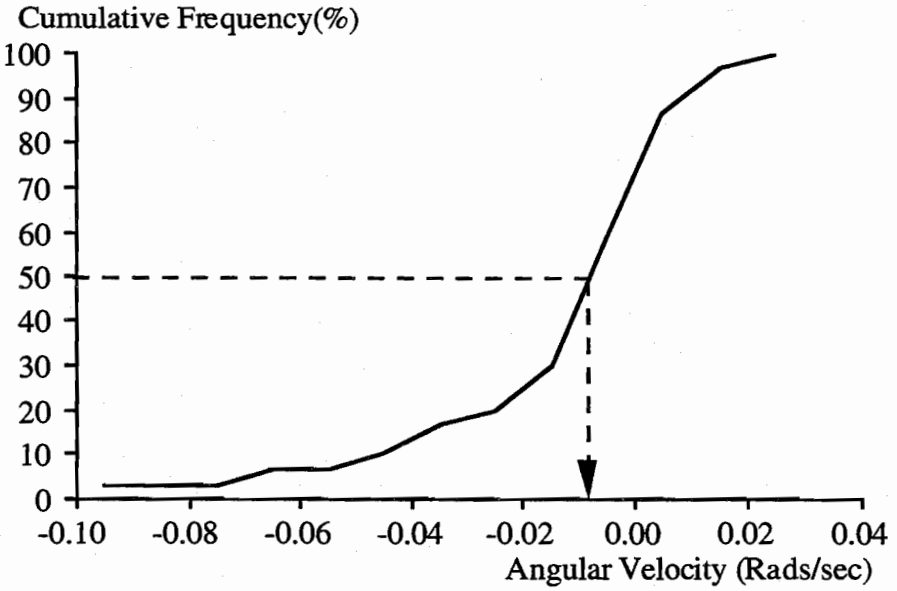

Figure 4.6 Distribution of accepted angular velocity at merge

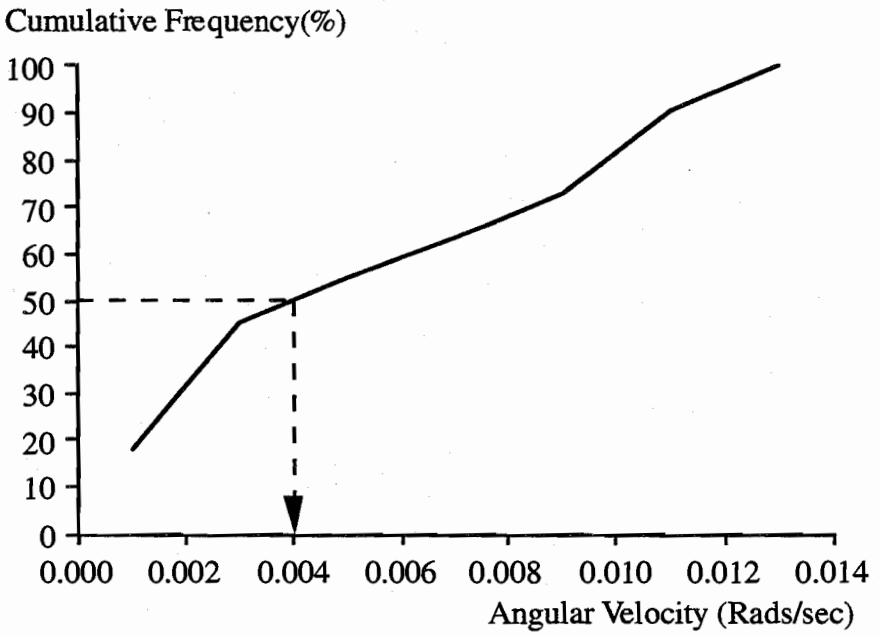

Figure 4.7 Distribution of positive accepted angular velocity at merge

ACCELERATION-DECELERATION MODELS

The quantity of data collected in this pilot study for use in developing methodologies for ramp vehicle acceleration-deceleration models is not large enough to cover all the scenarios described in section 3.4.2. Instead, only two scenarios which have comparatively larger observation quantities are analyzed to calibrate the associated acceleration-deceleration models. These two scenarios are:

Scenario 1: Single vehicle or the leader of a ramp platoon with both of its corresponding freeway lag and lead vehicles;

Scenario 2: Single vehicle or the leader of a ramp platoon with only a corresponding freeway lag vehicle.

The linear and nonlinear methodologies used to calibrate the acceleration-deceleration models for these two scenarios are discussed in the following sections.

Linear Methodology for Calibrating Acceleration-Deceleration Models

The basic specifications used to calibrate linear acceleration-deceleration models for scenarios 1 and 2 respectively are shown as follows:

Scenario 1

$$\begin{aligned}\ddot{X}_r(d + D) = \beta_0 &+ \beta_1 \dot{X}_r^{\gamma}(d + D)\omega_{rflag}(d) \\ &+ \beta_2 \dot{X}_r^{\gamma}(d + D)\omega_{rflead}(d) \\ &+ \beta_3 \dot{X}_r^{\gamma}(d + D)\omega_{rend}(d) \end{aligned} \quad (4.2)$$

Scenario 2

$$\begin{aligned}\ddot{X}_r(d + D) = \beta_0 &+ \beta_1 \dot{X}_r^{\gamma}(d + D)\omega_{rflag}(d) \\ &+ \beta_2 \dot{X}_r^{\gamma}(d + D)\omega_{rend}(d) \end{aligned} \quad (4.3)$$

Where

$\ddot{X}_r(\bullet)$ in ft/sec/sec;
$\dot{X}_r^{\gamma}(\bullet)$ in ft/sec; and
$\omega_{rflag}(\bullet)$, $\omega_{rflead}(\bullet)$, and $\omega_{rend}(\bullet)$ in rads/sec

The definitions of variables are the same as those defined in Chapter 3. In order to be calibrated using a linear regression technique, the magnitudes of γ in Eqs.(4.2) and (4.3) should be given. In this pilot study, the magnitudes of those angular velocity components, $\omega_{\text{rflag}}(\bullet)$, $\omega_{\text{rflead}}(\bullet)$, and $\omega_{\text{rend}}(\bullet)$, for each ramp vehicle at each fiducial mark are calculated from field data assuming the lateral distances, W_{rflag}, W_{rflead}, and W_{rend}, equal to 12 feet, 5 feet, and 7 feet respectively. In order not to omit any possible specifications that could be used to predict ramp vehicle acceleration-deceleration rates, all the possible combinations of the angular velocity components of Eqs.(4.2) and (4.3) respectively are investigated exhaustively. The results of applying OLS on Eqs.(4.2) and (4.3) and their associated specifications for the cases of D equal to 0 feet, 60 feet, and 120 feet respectively, as well as, γ equal to 0, 0.5, 1.0, and 1.5 respectively are shown in Tables 4.1 to 4.3 for scenario 1, and Tables 4.4 to 4.6 for scenario 2. For each scenario, the model that has the highest adjusted R-squared value and has statistically significant regression coefficients is chosen as the best model. The adjusted R-square, $\overline{R}^2$, is defined as follows:

$$\overline{R}^2 = 1 - (1 - R^2)\frac{N - 1}{N - k} \tag{4.4}$$

Where

R^2 is known as the coefficient of determination

N is the sample size

k is the number of parameters in the model including the intercept term

The term *adjusted* means adjusted for the degrees of freedom associated with the sum of squares. It is good to use $\overline{R}^2$ rather than R^2, particularly when comparing regression models with the same dependent variable but different numbers of independent variables, because R^2 is a nondecreasing function of the number of explanatory variables in the models and tends to give an overly optimistic picture of the regression fit.

TABLE 4.1 SUMMARY OF LINEAR ACCELERATION-DECELERATION MODEL FOR SCENARIO 1 (D=0 feet)

Model #	speed factor	β_0 (t-value)	β_1 (t-value)	β_2 (t-value)	β_3 (t-value)	R-squared (adj. R-squared)	*Durbin-Watson d*
1	γ=0.0	-4.028 (-3.815)	7.603 (1.240)*	0.637 (1.692)	139.285 (3.846)	0.33 (0.281)	2.06 (no correlation)
	γ=0.5	-4.163 (-3.834)	0.947 (1.264)*	0.08 (1.623)*	17.457 (3.838)	0.332 (0.283)	2.004 (no correlation)
	γ=1.0	-4.264 (-3.819)	0.119 (1.295)*	0.01 (1.549)*	2.159 (3.797)	0.331 (0.282)	2.025 (no correlation)
	γ=1.5	-4.319 (-3.766)	0.015 (1.336)*	0.001 (1.472)*	0.263 (3.718)	0.327 (0.278)	2.005 (no correlation)
2	γ=0.0	-1.048 (-1.372)*	10.796 (1.540)*			0.052 (0.030)	2.283 (no correlation)
	γ=0.5	-1.04 (-1.363)*	1.363 (1.594)*			0.056 (0.034)	2.284 (no correlation)
	γ=1.0	-1.031 (-1.355)*	0.172 (1.650)*			0.06 (0.038)	2.285 (no correlation)
	γ=1.5	-1.023 (-1.346)*	0.022 (1.708)*			0.064 (0.042)	2.285 (no correlation)
3	γ=0.0	-1.154 (-1.509)*		0.514 (1.165)*		0.031 (0.008)	2.102 (no correlation)
	γ=0.5	-1.154 (-1.508)*		0.067 (1.165)*		0.031 (0.008)	2.101 (no correlation)
	γ=1.0	-1.153 (-1.507)*		0.009 (1.166)*		0.031 (0.008)	2.101 (no correlation)
	γ=1.5	-1.153 (-1.506)*		0.001 (1.166)*		0.031 (0.008)	2.101 (no correlation)

TABLE 4.1 (CONT.) SUMMARY OF LINEAR ACCELERATION-DECELERATION MODEL FOR SCENARIO 1 (D=0 feet)

Model #	speed factor	β_0 (t-value)	β_1 (t-value)	β_2 (t-value)	β_3 (t-value)	R-squared (adj. R-squared)	*Durbin-Watson d*
4	γ=0.0				22.029 (0.808)*	0.015 (0.00)	1.911 (no correlation)
	γ=0.5				2.49 (0.746)*	0.012 (0.00)	1.922 (no correlation)
	γ=1.0				0.277 (0.681)*	0.01 (0.00)	1.935 (no correlation)
	γ=1.5				0.03 (0.613)*	0.008 (0.00)	1.948 (no correlation)
5	γ=0.0	-0.881 (-1.146)*	11.432 (1.640)*	0.564 (1.300)*		0.089 (0.046)	2.174 (no correlation)
	γ=0.5	-0.873 (-1.137)*	1.439 (1.692)	0.074 (1.303)*		0.092 (0.049)	2.174 (no correlation)
	γ=1.0	-0.864 (-1.128)*	0.181 (1.747)	0.01 (1.307)*		0.096 (0.053)	2.174 (no correlation)
	γ=1.5	-0.855 (-1.118)*	0.023 (1.804)	0.001 (1.311)*		0.1 (0.058)	2.174 (no correlation)
6	γ=0.0	-4.146 (-3.851)	6.972 (1.115)*		136.17 (3.684)	0.284 (0.250)	1.961 (no correlation)
	γ=0.5	-4.299 (-3.896)	0.872 (1.143)*		17.22 (3.716)	0.289 (0.256)	1.95 (no correlation)
	γ=1.0	-4.42 (-3.909)	0.11 (1.180)*		2.148 (3.716)	0.292 (0.258)	1.94 (no correlation)
	γ=1.5	-4.494 (-3.885)	0.014 (1.225)*		0.264 (3.678)	0.292 (0.258)	1.932 (no correlation)

TABLE 4.1 (CONT.) SUMMARY OF LINEAR ACCELERATION-DECELERATION MODEL FOR SCENARIO 1 (D=0 feet)

Model #	speed factor	β_0 (t-value)	β_1 (t-value)	β_2 (t-value)	β_3 (t-value)	R-squared (adj. R-squared)	*Durbin-Watson d*
7	γ=0.0	-4.369 (-4.260)		0.609 (1.609)*	146.579 (4.076)	0.305 (0.272)	1.984 (no correlation)
	γ=0.5	-4.528 (-4.298)		0.076 (1.537)*	18.441 (4.086)	0.306 (0.273)	1.97 (no correlation)
	γ=1.0	-4.656 (-4.297)		0.009 (1.458)*	2.291 (4.062)	0.304 (0.271)	1.955 (no correlation)
	γ=1.5	-4.74 (-4.258)		0.001 (1.375)*	0.28 (3.999)	0.298 (0.264)	1.937 (no correlation)
Note: * means the coefficient is not significant at 90% level Number of observation : 45							

TABLE 4.2 SUMMARY OF LINEAR ACCELERATION-DECELERATION MODEL FOR SCENARIO 1 (D=60 feet)

Model #	speed factor	β_0 (t-value)	β_1 (t-value)	β_2 (t-value)	β_3 (t-value)	R-squared (adj. R-squared)	*Durbin-Watson d*
1	γ=0.0	-5.535 (-3.223)	6.269 (0.963)*	-0.476 (-1.161)*	424.078 (4.251)	0.484 (0.431)	2.283 (no correlation)
	γ=0.5	-5.334 (-3.266)	0.742 (0.921)*	-0.074 (-1.447)*	48.274 (4.379)	0.497 (0.444)	2.312 (no correlation)
	γ=1.0	-5.097 (-3.275)	0.089 (0.894)*	-0.011 (-1.709)	5.45 (4.477)	0.506 (0.455)	2.336 (no correlation)
	γ=1.5	-4.839 (-3.256)	0.011 (0.879)*	-0.002 (-1.941)	0.611 (4.549)	0.513 (0.462)	2.355 (no correlation)
2	γ=0.0	1.254 (1.194)*	11.932 (1.427)*			0.062 (0.031)	2.354 (no correlation)
	γ=0.5	1.252 (1.193)*	1.496 (1.433)*			0.062 (0.032)	2.355 (no correlation)
	γ=1.0	1.249 (1.191)*	0.187 (1.438)*			0.062 (0.032)	2.356 (no correlation)
	γ=1.5	1.246 (1.189)*	0.023 (1.444)*			0.063 (0.033)	2.357 (no correlation)
3	γ=0.0	0.56 (0.554)*		-0.996 (-1.994)		0.114 (0.085)	1.909 (no correlation)
	γ=0.5	0.559 (0.553)*		-0.128 (-1.994)		0.114 (0.085)	1.91 (no correlation)
	γ=1.0	0.558 (0.552)*		-0.016 (-1.995)		0.114 (0.085)	1.91 (no correlation)
	γ=1.5	0.558 (0.551)*		-0.002 (-1.995)		0.114 (0.085)	1.91 (no correlation)

TABLE 4.2 (CONT.) SUMMARY OF LINEAR ACCELERATION-DECELERATION MODEL FOR SCENARIO 1 (D=60 feet)

Model #	speed factor	β_0 (t-value)	β_1 (t-value)	β_2 (t-value)	β_3 (t-value)	R-squared (adj. R-squared)	*Durbin-Watson d*
4	γ=0.0				154.58 (2.851)	0.202 (0.178)	2.022 (no correlation)
	γ=0.5				18.501 (2.928)	0.211 (0.187)	2.043 (no correlation)
	γ=1.0				2.202 (3.003)	0.22 (0.195)	2.066 (no correlation)
	γ=1.5				0.261 (3.076)	0.228 (0.204)	2.091 (no correlation)
5	γ=0.0	0.88 (0.857)*	10.734 (1.333)*	-0.945 (-1.908)		0.163 (0.107)	2.085 (no correlation)
	γ=0.5	0.877 (0.855)*	1.348 (1.341)*	-0.121 (-1.911)		0.164 (0.108)	2.086 (no correlation)
	γ=1.0	0.874 (0.853)*	0.169 (1.350)*	-0.016 (-1.913)		0.164 (0.109)	2.088 (no correlation)
	γ=1.5	0.871 (0.850)*	0.021 (1.358)*	-0.002 (-1.916)		0.165 (0.109)	2.089 (no correlation)
6	γ=0.0	-5.83 (-3.413)	6.502 (0.993)*		455.178 (4.710)	0.46 (0.424)	2.497 (no correlation)
	γ=0.5	-5.547 (-3.349)	0.786 (0.959)*		51.626 (4.705)	0.46 (0.424)	2.569 (no correlation)
	γ=1.0	-5.198 (-3.240)	0.097 (0.942)*		5.778 (4.660)	0.456 (0.420)	2.627 (no correlation)
	γ=1.5	-4.818 (-3.102)	0.012 (0.939)*		0.64 (4.589)	0.449 (0.413)	2.671 (correlation)

TABLE 4.2 (CONT.) SUMMARY OF LINEAR ACCELERATION-DECELERATION MODEL FOR SCENARIO 1 (D=60 feet)

Model #	speed factor	β_0 (t-value)	β_1 (t-value)	β_2 (t-value)	β_3 (t-value)	R-squared (adj. R-squared)	*Durbin-Watson d*
7	γ=0.0	-5.951 (-3.585)		-0.488 (-1.192)*	439.564 (4.470)	0.468 (0.432)	2.171 (no correlation)
	γ=0.5	-5.729 (-3.643)		-0.076 (-1.487)*	50.021 (4.618)	0.482 (0.447)	2.213 (no correlation)
	γ=1.0	-5.472 (-3.664)		-0.011 (-1.757)	5.645 (4.730)	0.492 (0.458)	2.247 (no correlation)
	γ=1.5	-5.197 (-3.650)		-0.002 (-1.997)	0.633 (4.811)	0.5 (0.466)	2.274 (no correlation)

Note: * means the coefficient is not significant at 90% level
Number of observation : 33

TABLE 4.3 SUMMARY OF LINEAR ACCELERATION-DECELERATION MODEL FOR SCENARIO 1 (D=120 feet)

Model #	speed factor	β_0 (t-value)	β_1 (t-value)	β_2 (t-value)	β_3 (t-value)	R-squared (adj. R-squared)	*Durbin-Watson d*
1	γ=0.0	-6.271 (-1.146)*	13.765 (1.539)*	16.466 (0.506)*	973.583 (1.931)	0.367 (0.232)	2.118 (no correlation)
	γ=0.5	-5.823 (-1.177)*	1.631 (1.429)*	1.905 (0.494)*	108.804 (2.055)	0.387 (0.256)	2.186 (no correlation)
	γ=1.0	-5.252 (-1.170)*	0.197 (1.350)*	0.223 (0.488)*	11.957 (2.147)	0.403 (0.274)	2.242 (no correlation)
	γ=1.5	-4.639 (-1.133)*	0.024 (1.299)*	0.026 (0.485)*	1.301 (2.214)	0.415 (0.289)	2.288 (no correlation)
2	γ=0.0	3.596 (2.469)	16.581 (1.823)			0.172 (0.120)	2.077 (no correlation)
	γ=0.5	3.586 (2.470)	2.141 (1.842)			0.175 (0.123)	2.08 (no correlation)
	γ=1.0	3.575 (2.470)	0.276 (1.862)			0.178 (0.127)	2.084 (no correlation)
	γ=1.5	3.562 (2.470)	0.036 (1.884)			0.182 (0.130)	2.087 (no correlation)
3	γ=0.0	3.09 (1.924)		11.156 (0.301)*		0.006 0	2.14 (no correlation)
	γ=0.5	3.098 (1.927)		1.403 (0.315)*		0.006 0	2.138 (no correlation)
	γ=1.0	3.105 (1.930)		0.176 (0.328)*		0.007 0	2.135 (no correlation)
	γ=1.5	3.112 (1.934)		0.022 (0.340)*		0.007 0	2.132 (no correlation)

TABLE 4.3 (CONT.) SUMMARY OF LINEAR ACCELERATION-DECELERATION MODEL FOR SCENARIO 1 (D=120 feet)

Model #	speed factor	β_0 (t-value)	β_1 (t-value)	β_2 (t-value)	β_3 (t-value)	R-squared (adj. R-squared)	*Durbin-Watson d*
4	γ=0.0				347.753 (2.602)	0.285 (0.243)	2.213 (no correlation)
	γ=0.5				42.017 (2.731)	0.305 (0.264)	2.225 (no correlation)
	γ=1.0				5.045 (2.858)	0.325 (0.285)	2.239 (no correlation)
	γ=1.5				0.602 (2.982)	0.344 (0.305)	2.256 (no correlation)
5	γ=0.0	3.929 (2.529)	17.932 (1.900)	24.692 (0.704)*		0.198 (0.092)	1.97 (no correlation)
	γ=0.5	3.923 (2.534)	2.311 (1.919)	3.002 (0.714)*		0.202 (0.096)	1.972 (no correlation)
	γ=1.0	3.916 (2.538)	0.298 (1.940)	0.364 (0.723)*		0.206 (0.100)	1.974 (no correlation)
	γ=1.5	3.906 (2.541)	0.038 (1.962)	0.044 (0.732)*		0.21 (0.104)	1.974 (no correlation)
6	γ=0.0	-6.838 (-1.310)*	12.737 (1.500)*		1006.97 (2.067)	0.356 (0.270)	2.148 (no correlation)
	γ=0.5	-6.357 (-1.352)*	1.502 (1.387)*		112.428 (2.201)	0.376 (0.293)	2.206 (no correlation)
	γ=1.0	-5.756 (-1.353)*	0.18 (1.306)*		12.348 (2.300)	0.392 (0.311)	2.254 (no correlation)
	γ=1.5	-5.117 (-1.322)*	0.022 (1.254)*		1.343 (2.373)	0.405 (0.326)	2.292 (no correlation)

TABLE 4.3 (CONT.) SUMMARY OF LINEAR ACCELERATION-DECELERATION MODEL FOR SCENARIO 1 (D=120 feet)

Model #	speed factor	β_0 (t-value)	β_1 (t-value)	β_2 (t-value)	β_3 (t-value)	R-squared (adj. R-squared)	*Durbin-Watson d*
7	γ=0.0	-8.836 (-1.624)*		5.099 (0.154)*	1160.61 (2.271)	0.26 (0.161)	2.484 (no correlation)
	γ=0.5	-8.321 (-1.739)		0.65 (0.168)*	130.725 (2.495)	0.297 (0.204)	2.553 (no correlation)
	γ=1.0	-7.596 (-1.787)		0.083 (0.181)*	14.388 (2.659)	0.325 (0.235)	2.606 (no correlation)
	γ=1.5	-6.815 (-1.783)		0.01 (0.192)*	1.565 (2.777)	0.344 (0.257)	2.645 (no correlation)

Note: * means the coefficient is not significant at 90% level
Number of observation : 18

TABLE 4.4 SUMMARY OF LINEAR ACCELERATION-DECELERATION MODEL FOR SCENARIO 2 (D=0 feet)

Model #	speed factor	β_0 (t-value)	β_1 (t-value)	β_2 (t-value)	R-squared (adj. R-squared)	*Durbin-Watson d*
1	γ=0.0	-2.29 (-1.601)*	-0.297 (-0.501)*	150.664 (2.479)	0.221 (0.159)	2.164 (no correlation)
	γ=0.5	-2.254 (-1.612)*	-0.034 (-0.653)*	17.428 (2.521)	0.226 (0.164)	2.163 (no correlation)
	γ=1.0	-2.196 (-1.607)*	-0.004 (-0.417)*	1.997 (2.549)	0.23 (0.168)	2.161 (no correlation)
	γ=1.5	-2.119 (-1.588)*	-0.0004 (-0.385)*	0.227 (2.565)	0.232 (0.170)	2.158 (no correlation)
2	γ=0.0	0.771 (0.977)*	-0.573 (-0.897)		0.03 (0.001)	2.242 (no correlation)
	γ=0.5	0.77 (0.976)*	-0.071 (-0.893)		0.03 (0.001)	2.242 (no correlation)
	γ=1.0	0.77 (0.975)*	-0.009 (-0.889)*		0.03 (0.001)	2.24 (no correlation)
	γ=1.5	0.769 (0.974)*	-0.001 (-0.885)*		0.029 (0.001)	2.24 (no correlation)
3	γ=0.0			61.029 (1.962)	0.125 (0.092)	2.056 (no correlation)
	γ=0.5			7.271 (2.013)	0.13 (0.098)	2.058 (no correlation)
	γ=1.0			0.862 (2.060)	0.136 (0.104)	2.062 (no correlation)
	γ=1.5			0.102 (2.105)	0.141 (0.109)	2.065 (no correlation)

Note: * means the coefficient is not significant at 90% level
Number of observation : 28

TABLE 4.5 SUMMARY OF LINEAR ACCELERATION-DECELERATION MODEL FOR SCENARIO 2 (D=60 feet)

Model #	speed factor	β_0 (t-value)	β_1 (t-value)	β_2 (t-value)	R-squared (adj. R-squared)	*Durbin-Watson d*
1	γ=0.0	-3.751 (-2.135)	-1.142 (-1.783)	396.27 (4.519)	0.572 (0.529)	1.658 (no correlation)
	γ=0.5	-3.663 (-2.113)	-0.13 (-1.588)*	45.703 (4.538)	0.572 (0.529)	1.666 (no correlation)
	γ=1.0	-3.554 (-2.074)	-0.015 (-1.410)*	5.248 (4.535)	0.569 (0.526)	1.675 (no correlation)
	γ=1.5	-3.428 (-2.020)	-0.002 (-1.252)*	0.6 (4.513)	0.565 (0.522)	1.684 (no correlation)
2	γ=0.0	3.162 (2.638)	-1.587 (-1.807)		0.134 (0.093)	2.396 (no correlation)
	γ=0.5	3.157 (2.626)	-0.2 (-1.778)		0.131 (0.089)	2.38 (no correlation)
	γ=1.0	3.15 (2.613)	-0.025 (-1.746)		0.127 (0.085)	2.363 (no correlation)
	γ=1.5	3.14 (2.597)	-0.003 (-1.712)*		0.122 (0.081)	2.347 (no correlation)
3	γ=0.0			208.88 (4.189)	0.444 (0.418)	1.876 (no correlation)
	γ=0.5			24.762 (4.296)	0.456 (0.432)	1.866 (no correlation)
	γ=1.0			2.923 (4.390)	0.467 (0.443)	1.859 (no correlation)
	γ=1.5			0.344 (4.471)	0.476 (0.452)	1.853 (no correlation)

Note: * means the coefficient is not significant at 90% level
Number of observation : 23

TABLE 4.6 SUMMARY OF LINEAR ACCELERATION-DECELERATION MODEL FOR SCENARIO 2 (D=120 feet)

Model #	speed factor	β_0 (t-value)	β_1 (t-value)	β_2 (t-value)	R-squared (adj. R-squared)	*Durbin-Watson d*
1	γ=0.0	-12.314 (-2.916)	0.936 (1.271)*	1479.01 (4.043)	0.643 (0.583)	1.869 (no correlation)
	γ=0.5	-11.797 (-3.116)	0.148 (1.725)*	168.362 (4.386)	0.677 (0.624)	1.936 (no correlation)
	γ=1.0	-10.979 (-3.166)	0.022 (2.107)	18.761 (4.565)	0.694 (0.644)	1.997 (no correlation)
	γ=1.5	-10.016 (-3.086)	0.003 (2.381)	2.062 (4.595)	0.698 (0.648)	2.039 (no correlation)
2	γ=0.0	4.042 (2.263)	1.639 (1.550)*		0.156 (0.091)	2.659 (no correlation)
	γ=0.5	4.021 (2.254)	0.206 (1.575)*		0.16 (0.096)	2.65 (no correlation)
	γ=1.0	4.004 (2.249)	0.026 (1.596)*		0.164 (0.099)	2.644 (no correlation)
	γ=1.5	3.993 (2.246)	0.003 (1.613)*		0.167 (0.103)	2.641 (no correlation)
3	γ=0.0			533.791 (4.464)	0.587 (0.558)	2.898 (no correlation)
	γ=0.5			63.656 (4.554)	0.597 (0.568)	2.908 (no correlation)
	γ=1.0			7.553 (4.626)	0.604 (0.576)	2.916 (no correlation)
	γ=1.5			0.892 (4.678)	0.61 (0.582)	2.922 (no correlation)

Note: * means the coefficient is not significant at 90% level
Number of observation : 15

The best linear acceleration-deceleration model for scenario 1 is given by

$$\ddot{X}_r(d + 60) = -5.197 - 0.002\dot{X}_r^{1.5}(d + 60)\omega_{rflead}(d) + 0.633\dot{X}_r^{1.5}(d + 60)\omega_{rend}(d) \quad (4.5)$$

with $\overline{R}^2$ equal to 0.466.

Alternatively, Eq. (4.5) may be rewritten

$$\ddot{X}_r(d + 60) = -5.197 - 0.01\frac{\dot{X}_r^{1.5}(d + 60)}{[X_{flead}(d) - X_r(d)]^2}[\dot{X}_r(d) - \dot{X}_{flead}(d)] + 4.431\frac{\dot{X}_r^{1.5}(d + 60)}{[L - X_r(d)]^2}[\dot{X}_r(d)] \quad (4.6)$$

by substituting Eqs.(3.24) and (3.25) in Eq.(4.5).

The evidence that the best model is obtained when D, the distance response lag, is equal to 60 feet supports the intuitive knowledge that there does exist a distance lag, or equivalently time lag, between the time a ramp driver detects the stimuli and the time he/she begins to perform acceleration or deceleration. In addition, the $\overline{R}^2$ values for those cases of D is equal to 60 feet are, in general, larger than their corresponding specifications when D is equal to 0 feet. This evidence further confirms the time lag response rule. The freeway lag vehicle angular velocity component is statistically insignificant in scenario 1. This result indicates that the relative movement between the ramp vehicle and its corresponding freeway lead vehicle and the relative ramp vehicle position to the acceleration lane terminus contribute more information to explain ramp vehicle acceleration-deceleration behavior than the freeway lag vehicle.

The signs of the regression coefficients all have reasonable explanations. The negative sign of the coefficient of $\omega_{rflead}(d)$ in Eq.(4.5) depicts, assuming all other things remain constant, as the ramp vehicle approaches its corresponding freeway lead vehicle, or more precisely detects a positive angular velocity with respect to the freeway lead vehicle, the ramp vehicle will decelerate in order to create sufficient space to be able to merge. The positive sign of the coefficient of $\omega_{rend}(d)$, on the other hand, indicates that the closer the ramp vehicle is to the acceleration lane terminus, the larger the magnitude of its acceleration rate. This result is consistent with the phenomenon demonstrated in Figure 4.3. The reason may partially result from

the fact that no ramp vehicle in the data set decelerated to a stop while approaching the acceleration lane terminus.

The inclusion of ramp vehicle current speed as one of the explanatory variables is necessary because its regression coefficient is statistically significant. However, the improvement of the explanatory ability of the fitted models after adding speed as an independent variable is not significant producing little change in the R-squared values. In general, the larger the value of the parameter g, the better the model explanatory ability.

The best linear model for scenario 2 is shown as follows:

$$\ddot{X}_r(d + 120) = -10.016 + 0.003\dot{X}_r^{1.5}(d + 120)\omega_{rflag}(d) + 2.062\dot{X}_r^{1.5}(d + 120)\omega_{rend}(d) \quad (4.7)$$

$\overline{R}^2 = 0.648$.

It follows immediately that Eq.(4.7) can be rewritten as

$$\ddot{X}_r(d + 120) = -10.016 + 0.036\frac{\dot{X}_r^{1.5}(d+120)}{[\,X_r(d) - X_{flag}(d)\,]^2}[\,\dot{X}_{flag}(d) - \dot{X}_r(d)\,] + 14.434\frac{\dot{X}_r^{1.5}(d+120)}{[\,L - X_r(d)\,]^2}[\,\dot{X}_r(d)\,] \quad (4.8)$$

The best model for scenario 2 is obtained when D is equal to 120 feet. indicating that a little longer time lag is needed than for scenario 1. This probably results from the fact that in scenario 2, a ramp driver views the angular velocities produced by a freeway lag vehicle through the mirror or by turning his head; therefore more body movements are involved in the decision process. As a consequence, the ramp driver needs to take a longer time to respond to the stimulus. The best model of scenario 1, on the other hand, suggests that a ramp driver directly views the angular velocities produced by a freeway lead vehicle without turning his head; therefore potentially a shorter response time lag is needed.

The positive coefficient of the second term of Eq.(4.7) is reasonable in the sense that when a ramp driver detects a positive angular velocity relative to the corresponding freeway lag

vehicle, he/she intends to accelerate creating a smaller angular velocity for the freeway merge. This result is consistent with the finding presented in Figure 4.3 that ramp vehicles normally accelerate with a larger magnitude than corresponding freeway lag vehicles.

Due to the special structure of the data set for use in OLS applications, it is desirable to examine the magnitude of serial correlation associated with the data. The Durbin-Watson d test has been adopted to investigate the serial correlation of disturbance terms with regard to all observations. The results are shown in the last column of Tables 4.1 to 4.6. The d statistic is computed from the vector of OLS residuals and is defined as

$$d = \frac{\sum_{i=2}^{N}(e_t - e_{t-1})^2}{\sum_{i=1}^{N} e_t^2} \tag{4.9}$$

The results indicate that there is no serial correlation between successive observations. Part of the reason is that the site studied has a short acceleration lane; therefore only a few observations of each ramp vehicle are available. This evidence does not imply that the serial correlation problem can be ignored. It can be expected that for data collected from a long acceleration lane the serial correlation of the observations associated with each ramp vehicle will become more significant and cannot be ignored. Furthermore, even though no serial correlation is found from the perspective of the whole data set, developing a methodology that can explicitly incorporate into the calibration process a serial correlation problem solution is highly desirable.

Nonlinear Methodology for Calibrating Acceleration-Deceleration Models

In the previous section, the linear methodology for calibrating the ramp vehicle acceleration-deceleration model which manually assigned specific constant values to some parameters simplifying model specifications was described. Although that approach simplified the specifications for the OLS procedure, it may not produce the "statistically best" model. Discussions in this section will describe relaxation of the constraints imposed on those linear model parameters. In other words, no values will be manually assigned. The best values for each parameter are estimated using a nonlinear regression procedure such that the sum of the squared residuals is a minimum. The basic nonlinear specifications for calibrating acceleration-deceleration models for scenarios 1 and 2 are given respectively in Eqs.(4.10) and (4.11).

Scenario 1

$$\ddot{X}_r(d+D) = \beta_0 + \beta_1 \frac{\dot{X}_r^{\gamma}(d+D)}{[X_r(d) - X_{flag}(d)]^{\alpha_1}}[\dot{X}_{flag}(d) - \dot{X}_r(d)]$$

$$+ \beta_2 \frac{\dot{X}_r^{\gamma}(d+D)}{[X_{flead}(d) - X_r(d)]^{\alpha_2}}[\dot{X}_r(d) - \dot{X}_{flead}(d)]$$

$$+ \beta_3 \frac{\dot{X}_r^{\gamma}(d+D)}{[\,L - X_r(d)\,]^{\alpha_3}}[\,\dot{X}_r(d)\,] \qquad (4.10)$$

Scenario 2

$$\ddot{X}_r(d+D) = \beta_0 + \beta_1 \frac{\dot{X}_r^{\gamma}(d+D)}{[X_r(d) - X_{flag}(d)]^{\alpha_1}}[\dot{X}_{flag}(d) - \dot{X}_r(d)]$$

$$+ \beta_2 \frac{\dot{X}_r^{\gamma}(d+D)}{[\,L - X_r(d)\,]^{\alpha_2}}[\,\dot{X}_r(d)\,] \qquad (4.11)$$

The parameters to be estimated are β_0, β_1, β_2, β_3, α_1, α_2, α_3, and γ for scenario 1 and β_0, β_1, β_2, α_1, α_2, and γ for scenario 2. In order not to omit any possible specifications that potentially could describe ramp vehicle acceleration-deceleration behavior during the freeway merge maneuver, all possible combinations of the explanatory variable components of Eqs.(4.10) and (4.11) were examined individually. The statistical analysis software, SPSS, was used to solve the nonlinear regression problems. SPSS adopts the sequential quadratic programming algorithm to search for the best parameter estimators which minimize the sum of squared residuals. The results for a D of 0 feet, 60 feet, and 120 feet respectively are shown in Tables 4.7 through 4.9 for scenario 1 and Tables 4.10 through 4.12 for scenario 2, respectively. The model that has the largest R-squared value is chosen as the best model.

For scenario 1, the best nonlinear acceleration-deceleration models should be

$$\ddot{X}_r(d+60) = -5.419$$

$$- 0.005 \frac{\dot{X}_r^{1.311}(d+60)}{[X_{flead}(d) - X_r(d)]^{0.455}}[\dot{X}_r(d) - \dot{X}_{flead}(d)]$$

$$+ 4.123 \frac{\dot{X}_r^{1.311}(d+60)}{[\,L - X_r(d)\,]^{1.828}}[\,\dot{X}_r(d)\,] \qquad (4.12)$$

with R-squared value equal to 0.55.

However, there is another specification has an R-squared value which is almost equal to that of Eq.(4.12). That model specification is given by Eq.(4.13).

$$\ddot{X}_r(d+60) = -7.79 - 1.058\frac{\dot{X}_r^{0.716}(d+60)}{[X_r(d) - X_{flag}(d)]^{1.884}}[\dot{X}_{flag}(d) - \dot{X}_r(d)] - 0.053\frac{\dot{X}_r^{0.716}(d+60)}{[X_{flead}(d) - X_r(d)]^{0.379}}[\dot{X}_r(d) - \dot{X}_{flead}(d)] + 8.727\frac{\dot{X}_r^{0.716}(d+60)}{[L - X_r(d)]^{1.416}}[\dot{X}_r(d)] \quad (4.13)$$

R-squared value is 0.545

For scenario 2, the best nonlinear model is

$$\ddot{X}_r(d+120) = -8.278 + 0.009\frac{\dot{X}_r^{2.316}(d+120)}{[X_r(d) - X_{flag}(d)]^{3.0}}[\dot{X}_{flag}(d) - \dot{X}_r(d)] + 0.454\frac{\dot{X}_r^{2.316}(d+120)}{[L - X_r(d)]^{2.03}}[\dot{X}_r(d)] \quad (4.14)$$

with R-squared value equal to 0.66.

TABLE 4.7 SUMMARY OF NONLINEAR ACCELERATION-DECELERATION MODEL FOR SCENARIO 1 (D=0 feet)

Model	β_0	β_1	β_2	β_3	α_1	α_2	α_3	γ	R-Squared
1	-4.51	0.152	0.052	76.04	0.715	0.558	2.118	0.768	0.387
2	-1.207	0.003			1.102			1.939	0.102
3	-1.157		0.045			3.00		1.206	0.032
4				1.00			-0.734	-0.986	0.012
5	-1.112	0.024	0.021		0.991	2.809		1.39	0.145
6	-3.826	0.004		6.294	0.93		2.471	1.68	0.329
7	-4.548		0.286	90.52		2.082	1.999	0.584	0.306
Sample Size: 45									

TABLE 4.8 SUMMARY OF NONLINEAR ACCELERATION-DECELERATION MODEL FOR SCENARIO 1 (D=60 feet)

Model	β_0	β_1	β_2	β_3	α_1	α_2	α_3	γ	R-Squared
1	-7.79	-1.058	-0.053	8.727	1.884	0.379	1.416	0.716	0.545
2	0.506	2.12			0.57			0.00	0.125
3	0.335		-0.001			0.347		1.632	0.269
4				348.9			3.00	1.457	0.301
5	0.261	-0.248	-0.002		2.812	0.334		1.569	0.269
6	-6.951	0.011		47.97	0.147		1.838	0.796	0.528
7	-5.419		-0.005	4.123		0.455	1.828	1.311	0.55
Sample Size: 33									

TABLE 4.9 SUMMARY OF NONLINEAR ACCELERATION-DECELERATION MODEL FOR SCENARIO 1 (D=120 feet)

Model	β_0	β_1	β_2	β_3	α_1	α_2	α_3	γ	R-Squared
1	-4.714	0.021	0.013	50.79	0.645	0.584	2.185	1.293	0.465
2	2.934	0.022			1.073			1.56	0.216
3	3.15		0.052			3.00		2.354	0.013
4				12.44			3.00	2.5	0.287
5	2.414	0.023	0.009		0.76	0.601		1.423	0.296
6	-2.454	0.002		14.05	1.5		2.818	2.338	0.437
7	-3.701		0.01	4.647		2.953	2.711	2.50	0.366
Sample Size: 18									

TABLE 4.10 SUMMARY OF NONLINEAR ACCELERATION-DECELERATION MODEL FOR SCENARIO 2 (D=0 feet)

Model	β_0	β_1	β_2	α_1	α_2	γ	R-Squared
1	-1.25	-0.002	4.811	3.00	3.00	2.313	0.255
2	0.795	-2.187		3.00		0.755	0.049
3			1.378		3.00	2.50	0.17
Sample Size: 28							

TABLE 4.11 SUMMARY OF NONLINEAR ACCELERATION-DECELERATION MODEL FOR SCENARIO 2 (D=60 feet)

Model	β_0	β_1	β_2	α_1	α_2	γ	R-Squared
1	-3.682	-2.849	59.538	3.00	1.945	0.829	0.598
2	3.1	-9.258		3.00		0.619	0.152
3			4.665		3.00	2.50	0.471
Sample Size: 23							

TABLE 4.12 SUMMARY OF NONLINEAR ACCELERATION-DECELERATION MODEL FOR SCENARIO 2 (D=120 feet)

Model	β_0	β_1	β_2	α_1	α_2	γ	R-Squared
1	-8.278	0.009	0.454	3.00	2.030	2.316	0.66
2	3.983	7.059		3.00		0.612	0.098
3			1.00		0.649	-0.820	0.429
Sample Size: 14							

Comparisons between Linear and Nonlinear Methodologies for Acceleration-Deceleration Models

In general, the results of linear and nonlinear acceleration-deceleration models show good consistency in both sign and magnitude. For example, both the best models for scenario 1, Eqs.(4.6) and (4.12), are found when D is equal to 60 feet; and the freeway lag vehicle component does not enter into the best models. Furthermore, when D is equal to 120 feet, scenario 2 also produces the best models, Eqs.(4.8) and (4.14), for both linear and nonlinear approaches. The signs of the coefficients of the best models obtained from the linear and nonlinear approaches for both scenario 1 and scenario 2 are identical.

If the comparison is made based strictly on R-squared values, the nonlinear models, as expected, are slightly better than the linear models for both scenarios. The difference, however, is not significant. For instance, 0.55 is just slightly over 0.466 for the case of scenario 1; and for scenario 2, 0.66 is almost equal to 0.648. The reason that the nonlinear approach is statistically better than the linear approach is straightforward since the former approach imposes no constraints on any of the parameters and therefore leaves more freedom allowing the procedure to search for the optimal solutions. Nevertheless, the insignificant difference between the linear and nonlinear approaches does indicate that the best linear acceleration-deceleration model is still a good approximation.

A comparison from another perspective, however, may support that the linear model is better in the sense that it has better capability to interpret acceleration-deceleration behavior than the nonlinear approach. This recommendation is desirable since the linear model implicitly treats angular velocity components as stimuli, and it is believed that this kind of approach might be more consistent with real dynamic driving behavior.

Combination of Linear and Nonlinear Models

Evidence of the above discussion indicates that it is desirable to develop a compromise model which contains the advantages of each of the two approaches. In other words, the angular velocity components are treated as explanatory variables like the linear approach and the remaining parameters are estimated using a nonlinear regression procedure. Stated more precisely, Eqs.(4.2) and (4.3) are given as the basic models. Instead of assigning specific values to the parameter γ in order that OLS can be used, a nonlinear regression procedure is applied to estimate the parameters β_0, β_1, β_2, β_3, and γ. The results for the cases of D equal to 0 feet, 60 feet, and 120 feet respectively are shown in Tables 4.13 through 4.15 for scenario 1 and Tables 4.16 through 4.18 for scenario 2. A negative R-squared value obtained in model 4 of Table 4.13 is

unusual but is possible for the nonlinear regression procedure. R-squared values in nonlinear models may be interpreted as the proportion of the total variance of the dependent variable about its mean that is explained by the fitted model. If the selected model fits worse than the mean, a negative R-squared value can be obtained(SPSS® 1990).

TABLE 4.13 SUMMARY OF NONLINEAR ACCELERATION-DECELERATION MODEL FOR SCENARIO 1(ANGULAR VELOCITY COMPONENTS ARE TREATED AS EXPLANATORY VARIABLES) (D=0 feet)

Model	β_0	β_1	β_2	β_3	γ	R-Square
1	-4.191	6.943	0.244	74.768	0.618	0.332
2	-0.954	0.0003			3.122	0.077
3	-1.153		0.044		1.00	0.031
4				154.354	0	-0.05
5	-0.87	0.0068	0.0002		2.378	0.108
6	-4.451	0.619		7.018	1.182	0.292
7	-4.52		0.388	129.984	0.498	0.306
Sample Size: 45						

TABLE 4.14 SUMMARY OF NONLINEAR ACCELERATION-DECELERATION MODEL FOR SCENARIO 1(ANGULAR VELOCITY COMPONENTS ARE TREATED AS EXPLANATORY VARIABLES) (D=60 feet)

Model	β_0	β_1	β_2	β_3	γ	R-Square
1	-4.768	0.106	-0.006	3.438	1.548	0.512
2	1.253	0.036			1.996	0.063
3	0.562		-0.040		1.432	0.114
4				0.084	2.217	0.221
5	0.877	0.142	-0.0056		1.640	0.166
6	-5.477	7.981		288.981	0.549	0.459
7	-5.114		-0.0044	2.243	1.654	0.501
Sample Size: 33						

TABLE 4.15 SUMMARY OF NONLINEAR ACCELERATION-DECELERATION MODEL FOR SCENARIO 1(ANGULAR VELOCITY COMPONENTS ARE TREATED AS EXPLANATORY VARIABLES) (D=120 feet)

Model	$\beta 0$	$\beta 1$	$\beta 2$	$\beta 3$	γ	R-Square
1	-4.661	0.157	0.076	4.915	1.642	0.42
2	3.558	0.0176			2.278	0.188
3	3.126		0.0017		2.486	0.008
4				0.0014	3.370	0.272
5	3.874	0.022	0.01		2.240	0.216
6	-5.077	0.101		3.449	1.730	0.413
7	-6.704		0.017	2.830	1.811	0.357
Sample Size: 18						

TABLE 4.16 SUMMARY OF NONLINEAR ACCELERATION-DECELERATION MODEL FOR SCENARIO 2 (ANGULAR VELOCITY COMPONENTS ARE TREATED AS EXPLANATORY VARIABLES) (D=0 FEET)

Model	β_0	β_1	β_2	γ	R-Square
1	-2.098	-0.0042	1.206	1.562	0.232
2	0.766	-4.167		0.119	0.03
3			0.001	3.025	0.137
Sample Size: 28					

TABLE 4.17 SUMMARY OF NONLINEAR ACCELERATION-DECELERATION MODEL FOR SCENARIO 2 (ANGULAR VELOCITY COMPONENTS ARE TREATED AS EXPLANATORY VARIABLES) (D=60 feet)

Model	β_0	β_1	β_2	γ	R-Square
1	-3.65	-0.752	157.721	0.663	0.57
2	3.161	-19.039		0.000	0.134
3			0.018	2.636	0.392
Sample Size: 23					

TABLE 4.18 SUMMARY OF NONLINEAR ACCELERATION-DECELERATION MODEL FOR SCENARIO 2 (ANGULAR VELOCITY COMPONENTS ARE TREATED AS EXPLANATORY VARIABLES) (D=120 feet)

Model	β_0	β_1	β_2	γ	R-Square
1	-10.336	0.043	15.74	1.484	0.654
2	4.013	13.953		0.000	0.064
3			0.069	2.530	0.34
Sample Size: 14					

The best specification of the compromise model for each scenario is

Scenario 1

$$\ddot{X}_r(d+60) = -4.768 + 0.106\frac{\dot{X}_r^{1.548}(d+60)}{[X_r(d) - X_{flag}(d)]^2}[\dot{X}_{flag}(d) - \dot{X}_r(d)] - 0.006\frac{\dot{X}_r^{1.548}(d+60)}{[X_{flead}(d) - X_r(d)]^2}[\dot{X}_r(d) - \dot{X}_{flead}(d)] + 3.438\frac{\dot{X}_r^{1.548}(d+60)}{[L - X_r(d)]^2}[\dot{X}_r(d)] \quad (4.15)$$

R-squared = 0.512

Scenario 2

$$\ddot{X}_r(d+120) = -10.336 + 0.043\frac{\dot{X}_r^{1.484}(d+120)}{[X_r(d) - X_{flag}(d)]^2}[\dot{X}_{flag}(d) - \dot{X}_r(d)] + 15.74\frac{\dot{X}_r^{1.484}(d+120)}{[L - X_r(d)]^2}[\dot{X}_r(d)] \quad (4.16)$$

R-squared = 0.645

For both scenarios the best acceleration-deceleration specifications obtained from the compromise approach are identical to those derived from the linear and nonlinear approaches alone. Comparisons of the calibration approaches from the perspectives of statistical properties and interpretation capability are summarized in the following table. Evidence shown in Table 4.19 indicates that the nonlinear approach is the best model in terms of statistical properties because of its high R-squared value. The compromise approach, on the other hand, is superior to other approaches subject to model interpretation capability; because it implicitly treats the angular velocity with respect to surrounding freeway vehicles as a major variable in determining acceleration-deceleration rates. Both the nonlinear and compromise models have their own

advantages and deserve further examination using larger data sets. The results obtained in this pilot study are only tentative.

TABLE 4.19 COMPARATIVE SUMMARY BETWEEN CALIBRATION APPROACHES

Calibration Approach	R-squared Value		Explanatory Variables	Interpretation Capability
	Scenario 1	Scenario 2		
Linear Model	0.466	0.648	angular velocity absolute speed	easy straightforward
Nonlinear Model	0.55	0.66	relative speed, distance absolute speed	complicated
Compromise Model	0.512	0.654	angular velocity absolute speed	easy straightforward

GAP ACCEPTANCE MODELS

To calibrate the critical gap distribution presented in Eq.(3.77), a large quantity of data involving gap acceptance as well as rejection is desirable. The limited quantity of data collected for use in this pilot study made such a calibration difficult. However, using this limited data set, preliminary analyses of ramp vehicle gap acceptance behavior may be performed.

In previous discussions, angular velocity was hypothesized as a criterion that a ramp driver may use to determine whether an oncoming freeway gap is acceptable. This hypothesis is believed to be closer to real driving behavior in the sense that angular velocity implicitly incorporates the distance gap and relative speed into one simple decision criterion. Table 4.20 demonstrates some fundamental information of the collected data with regard to the merging gap acceptance phenomena.

On the average, a ramp vehicle merges with a faster speed than the corresponding freeway lag vehicle and a lower speed than a corresponding freeway lead vehicle. This evidence is reasonable since merging with a higher speed than the freeway lag vehicle can insure a safe merge and a lower speed than the freeway lead vehicle can avoid a collision. In general, at the merge point, ramp vehicles usually have a shorter distance and time gap from their freeway lead

vehicle than from their freeway lag vehicle indicating that the ramp drivers are more attentive to freeway lag vehicle movement. This phenomenon is quite reasonable because a ramp driver, a follower in this situation, can easily observe leading vehicle movements and respond accordingly. Observation to the freeway lag vehicles, on the other hand, involves more body movement and a longer reaction time. In other words, the freeway lag vehicle is more critical for the ramp driver gap acceptance decision.

TABLE 4.20 STATISTICAL SUMMARY OF GAP ACCEPTANCE PHENOMENA AT MERGE

	with respect to freeway lag vehicle				with respect to freeway lead vehicle			
	gap size (sec)	V_{flag}-V_r (mph)	dist. (ft)	ω (rads/sec)	gap size (sec)	V_r-V_{flead} (mph)	dist. (ft)	ω (rads/sec)
Mean	2.22	-1.70	145.8	-0.0099	1.21	-3.56	92.24	-0.0088
Std Dev	1.72	6.56	121.9	0.0246	0.68	4.61	50.49	0.0159
Obs no	30				19			

The gap acceptance behavior essentially is a binary decision process. For every gap, the ramp driver will either accept it and merge into the freeway stream or reject it and stay in the acceleration lane to wait for a later acceptable gap. Consequently, gap acceptance behavior, or more precisely the gap acceptance function, is readily modeled as a binary choice model. Due to the data quantity limitation, instead of directly calibrating Eq.(3.77), a simple binary probit model was adopted as a preliminary tool to calibrate the ramp driver gap acceptance behavior during a freeway merge.

The binary probit model is specified as follows

$$prob(\text{accept}) = \Phi\left(\frac{V_a - V_r}{\sigma}\right) \tag{4.17}$$

Where

V_a is the systematic component of the utility of accepting a specific gap;

V_r is the systematic component of the utility of rejecting a specific gap;

σ^2 is defined as $\text{var}(\varepsilon_r - \varepsilon_a)$;

ε_a is the disturbance term of the utility of accepting a specific gap;

ε_r is the disturbance term of the utility of rejecting a specific gap;

$\Phi(\bullet)$ is the standardized cumulative normal distribution.

Eq.(4.17) indicates that only the difference of the systematic components determines the probability of accepting a gap. Several alternatives can be used to specify the systematic component difference, namely $V_a - V_r$.

$$V_a - V_r = \alpha_0 + \alpha_1(\text{time gap size}) \tag{4.18}$$

$$V_a - V_r = \alpha_0 + \alpha_1(\text{time gap size}) + \alpha_2(\text{distance to the acceleration lane end}) \tag{4.19}$$

$$V_a - V_r = \alpha_0 + \alpha_1(\text{time gap size}) + \alpha_2(\text{distance to the acceleration lane end}) + \alpha_3(\text{speed differential to the freeway lag vehicle}) \tag{4.20}$$

$$V_a - V_r = \beta_0 + \beta_1(\text{angular velocity of freeway lag vehicle}) \tag{4.21}$$

$$V_a - V_r = \beta_0 + \beta_1(\text{angular velocity of freeway lag vehicle}) + \beta_2(\text{distance to the acceleration lane end}) \tag{4.22}$$

Of the alternatives, only for Eq.(4.21) can a solution be found at convergence due to the small data quantity. The results are summarized in Table 4.21.

The informal goodness-of-fit index, ρ^2, measures the fraction of an initial log likelihood value explained by the model. ρ^2 is analogous to R^2 used in regression. The value of ρ^2 is 0.80, which indicates that the interpretation capability of estimated model is fairly satisfactory. However, the t - statistic of angular velocity, -1.2053, shows that the coefficient is not significant at any acceptable significance level. The reason may partially be due to only 32 observations being involved in the calibration and only two of them are related to gap rejection. Nevertheless, the above results do demonstrate that angular velocity might be the most appropriate criterion to describe ramp driver gap acceptance behavior. Using gap size or speed differential alone as a gap acceptance criterion is not desirable.

TABLE 4.21 SUMMARY OF BINARY PROBIT ESTIMATIONS

Independent Variable	Estimation Coefficient	Standard Error	t-Statistic
Constant	1.7912	0.4536	3.9486
Angular Velocity	-21.8633	18.1391	-1.2053
Log likelihood at initial, $L(0)$		-22.181	
Log likelihood at convergence, $L(\hat{\beta})$		-4.3176	
Percent correctly predicted (%)		96.875	
Number of observations		32	

$$\rho^2 = 1 - \frac{L(\hat{\beta})}{L(0)} \approx 0.80 \qquad (4.23)$$

SUMMARY

Data collected at a short acceleration lane were used to calibrate the hypothesized ramp vehicle acceleration-deceleration models. Results indicate that a time gap before ramp drivers respond to stimuli does exist. The angular velocity components of freeway lag, lead vehicles and the acceleration lane terminus were found to have significant effects on ramp vehicle acceleration-deceleration behavior. The nonlinear functional form is the best model in terms of statistical properties because of its high R-squared value. The compromise model which implicitly treats the angular velocity components and ramp vehicle absolute speed as explanatory variables seems to be the most appropriate methodology subject to model interpretation capability. Both the nonlinear and compromise models have advantages and deserve further examination using larger data sets.

Due to the data quantity limitation, Eq.(3.77) was not directly calibrated in this pilot study. A simplified binary probit model, however, has been used to calibrate the ramp vehicle gap acceptance function. The results, although statistically insignificant, reveal that ramp drivers may use angular velocity as a gap acceptance criterion. Using either gap size or speed differential alone as a gap acceptance criterion is found to be not desirable.

Although the results obtained from this pilot study are encouraging, the limited quantity of data used in the calibration process makes the conclusions drawn only tentative. In addition, the

potential serial correlation problem associated with successive acceleration-deceleration data is not incorporated in this pilot study. In the following chapters, more freeway merge behavior data will be collected and used to calibrate the proposed acceleration-deceleration and gap acceptance behavior models. Necessary revisions of the proposed methodologies will be made to best describe ramp driver behavior during the freeway merge maneuver.

CHAPTER 5. CALIBRATION OF RAMP VEHICLE ACCELERATION-DECELERATION MODELS

INTRODUCTION

In the previous chapter, a pilot study using observations collected at a short acceleration lane were presented. The results, although encouraging, are only tentative due to the small number of data. In this chapter, more freeway merge observation data were collected from a taper type entrance ramp on Loop 610 in Houston Texas. A sketch of this site can be found in Figure 3.9. Presentation of this chapter starts with a general ramp vehicle merge behavior data analysis. Ramp vehicle speed and acceleration profiles along an acceleration lane were graphically examined to capture merge trajectory information. Distributions of speed differentials as well as angular velocity viewed by ramp drivers during the merge maneuver with respect to their corresponding freeway vehicles were also examined. Calibration of the methodologies for modeling ramp vehicle acceleration-deceleration behavior using the collected data is the major task of this chapter. A revised mathematical framework incorporating dummy variables to generalize the proposed models, as shown in Eqs.(3.18) and (3.19), was developed to involve all possible merge traffic vehicle situations. Nonlinear regression techniques were directly applied to calibrate the new model. Modifications to the mathematical framework and calibration procedure due to unsatisfied calibration objectives were made to best capture traffic data characteristics. These modifications include incorporating longitudinal distance weighting factors to the model specifications capturing distance effects on driver behavior, splitting data into subgroups based on the existence of corresponding freeway and ramp vehicles, and further splitting the observations into subgroups based upon longitudinal distance separation between ramp and corresponding freeway vehicles. The modifications simplify the mathematical model form by reducing the number of parameters to be estimated. The potential drawback of the nonlinear regression calibration approach was discussed leading to the exclusion of further Generalized Least Squared calibration procedures. The discouraging nonlinear regression results led to the development of bi-level calibration procedures which involve solving the discrete choice behavior models and then the continuous regression models. The discrete choice behavior model aims to estimate the probability of acceleration, deceleration, or constant speed operation under prevailing traffic conditions, while the continuous model predicts the corresponding acceleration or deceleration rates. Better calibration results were obtained from the revised bi-level calibration procedures. The developed methodologies for modeling ramp vehicle acceleration-deceleration

behavior are useful in revising microscopic freeway simulation model entrance ramp merge components.

DATA ANALYSIS

The freeway merge traffic data used in this calibration task were collected from a taper type entrance ramp located on Loop 610 in Houston. Loop 610, a divided 8 lane freeway system, is one of the busiest highways in the Houston Metropolitan area. This southbound entrance ramp, between San Felipl Rd. and Westheimer Rd., is near the Post Oak business district and the Galleria shopping mall. Due to the location characteristics, this section of Loop 610 carries consistently high traffic volumes. No significant traffic volume difference was observed during daytime peak and off-peak periods. One mile downstream of this entrance ramp is U.S. 59 and Loop 610 interchange, one of the busiest freeway interchanges in the nation. Vast traffic volumes intersect in this interchange resulting in stop-and-go traffic flows frequently propagating to the upstream entrance ramp even during off-peak periods.

The video camera was set up on the roof of a 17 story office building beside Loop 610 from where the merge area, 880 feet in length from painted nose to ramp terminus, could be viewed. Long and wide white fiducial marks were painted every 50 feet on the grass beside the ramp shoulder along the acceleration lane and could be clearly seen from the video camera site. The distance between fiducial marks was determined partially by distance from the video camera and partially by the required measurement accuracy. All fiducial marks were perpendicular to the pavement edge and were invisible to drivers. Traffic data for use in this calibration procedure were recorded on May 17, 1995 morning peak hours using a S-VHS video camcorder. During the data reduction process, fiducial marks were lines drawn across the acceleration lane and freeway lanes directly on a transparency superimposed on the video monitor. The desirable freeway merge fundamental data for 236 ramp vehicles were manually reduced from the videotapes at 0.03-sec. interval (30 frames/sec) resolution. The primary data reduced from the videotapes were a set of times for each ramp vehicle, with corresponding (if any) times which freeway lag, freeway lead, and ramp lead vehicles, crossed each fiducial mark. For each ramp vehicle, only those corresponding freeway lag, freeway lead, and ramp lead vehicles that were respectively within 400 feet, 300 feet, and 300 feet were reduced from the video image. Associated speed, acceleration-deceleration, and angular velocity magnitudes were calculated accordingly using these time-space trajectory data. Due to the inevitable parallax effect, the further down the acceleration lane the vehicle proceeded, the less the data accuracy. In the following sections, ramp vehicle speed and

acceleration profiles along the acceleration lane are discussed, followed by examination of merge speed differential and merge angular velocity characteristics.

Speed Profile Data

Historically, acceleration lanes have been designed as a safe facility to allow a ramp vehicle to accelerate to a desired speed in order to perform a safe merge. AASHTO (1990) stated "a speed-change lane should, as a minimum requirement, have sufficient length to enable a driver to make the necessary change between the speed of operation on the highway and the speed on the turning roadway in a safe and comfortable manner." Consequently, one can intuitively expect an increasing speed profile of a ramp vehicle during a freeway merge maneuver. Figure 5.1 demonstrates the speed scatter of all observed ramp vehicles along with corresponding means and standard deviations calculated for each fiducial mark.

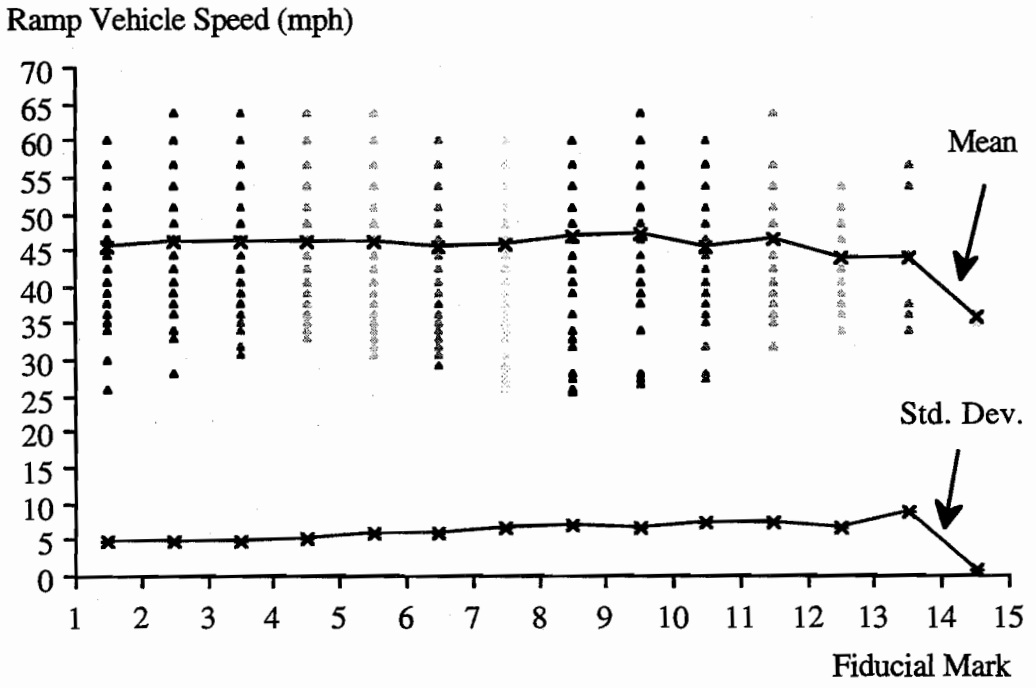

Figure 5.1 Ramp vehicle speed scatter vs. fiducial marks

Except near the ramp end, the mean speed profile does not visibly show any significant trend change throughout the acceleration lane. Table 5.1 shows the statistical test result for equality of means across fiducial marks excluding the last one which represented a limited sample. The statistic r is calculated using Eq.(3.5). According to the result, one cannot reject the null hypothesis that all means are statistically equal at the 0.05 significance level. This statistic value, however, is almost significant at the 0.1 significance level revealing that mean speeds across fiducial marks are statistically different.

TABLE 5.1 RESULT OF STATISTICAL TEST FOR EQUALITY OF SPEED MEANS

r	k	n	$F_{(k-1, n-k, 5\%)}$	$F_{(k-1, n-k, 10\%)}$
1.54	13	1847	1.75	1.55

The mean speeds have a greater variation at the later portion of the acceleration lane because of decreasing merge chances. Aggressive drivers may make greater speed changes taking advantage of possible gaps to complete freeway merge while passive drivers may not. On average, according to the observations, ramp vehicles have fairly constant speeds during freeway merge maneuvers. The scatter plots, on the other hand, illustrate very wide scatter indicating that each ramp vehicle might have a different speed profile in the acceleration lane. This result, however, is not surprising since each ramp vehicle faces a totally different traffic structure during the freeway merge; and the traffic parameters including speed differential, distance separation, and existence of freeway vehicles, that influence ramp driver speed change decisions. This phenomenon can be examined from another perspective. The standard deviation curve shown in Figure 5.1 has a slightly increasing trend that implicitly reveals vehicles had a more uniform speed when entering the acceleration lane. Further down the acceleration lane, stronger interaction with freeway vehicles produces larger ramp vehicle speed variations. This speed data analysis result implies that the ramp driver speed change decision is dynamic and varies greatly among drivers. Methodologies, such that proposed by Sullivan, E. C. et al. (1995), that simply estimate ramp vehicle speed magnitudes as a function of the time or distance a ramp vehicle travels in the acceleration lane might not be adequate for ramp vehicle speed change predictions.

The mean speed profile shown in Figure 5.1 is different from that of Figure 4.2 due to geometric difference of these two locations. At the short acceleration lane location, in general, the

length constraint prohibits ramp drivers from having much time and room to search for acceptable gaps. Therefore, ramp drivers have to respond quickly and accelerate or decelerate with great magnitude to complete the merge maneuver before reaching the acceleration lane terminus. At the long acceleration lane location, on the other hand, ramp drivers have many chances to comfortably adjust their speeds and positions with respect to freeway vehicles in order to create acceptable merge gaps. Nevertheless, in spite of the mean equality property, speed change decisions in the acceleration lane are strongly subject to individual ramp driver behavior and are expected to have great variations among drivers.

Acceleration-deceleration Profile Data

The expression for acceleration-deceleration rate calculations, using speed data, is shown in Eq(4.1). Figure 5.2 shows the acceleration-deceleration scatter points of each observed ramp vehicle along with the means and standard deviations calculated for each fiducial mark. Statistical test results for equality of acceleration-deceleration mean across fiducial marks is shown in Table 5.2.

Both the graphical presentation and statistical test show significant mean acceleration-deceleration differences across fiducial marks. The mean acceleration-deceleration trend reveals that ramp drivers, in general, tended to decelerate slightly when entering the acceleration lane in order to search for freeway gaps. Then they accelerate to make a freeway merge near the middle portion of the acceleration lane. Great acceleration-deceleration variations were found in the later portions of the acceleration lane reflecting the pressure of decreasing distance to ramp terminus on driver behavior. Normally, in order not to be forced to stop, most ramp drivers accelerated to take advantage of any possible chances to complete a freeway merge when they were approaching the acceleration lane end. Many positive acceleration rates observed from the later portions of the acceleration lane supported this hypothesis. In addition, during the data collection period when freeway traffic flow ranged from moderate to heavy, only one ramp vehicle was found to stop at the acceleration lane end. This implies that ramp drivers would prefer to make a risky merge rather than to stop at the ramp end. Similar to those of Figure 5.1, the scatter plot shown in Figure 5.2 also illustrates very wide dispersion indicating that each ramp driver had a different acceleration-deceleration profile during the freeway merge maneuver. One must note that, this mean equality test only provides aggregate information. Except for the mean and standard deviation, other distribution information are not incorporated in the test statistic.

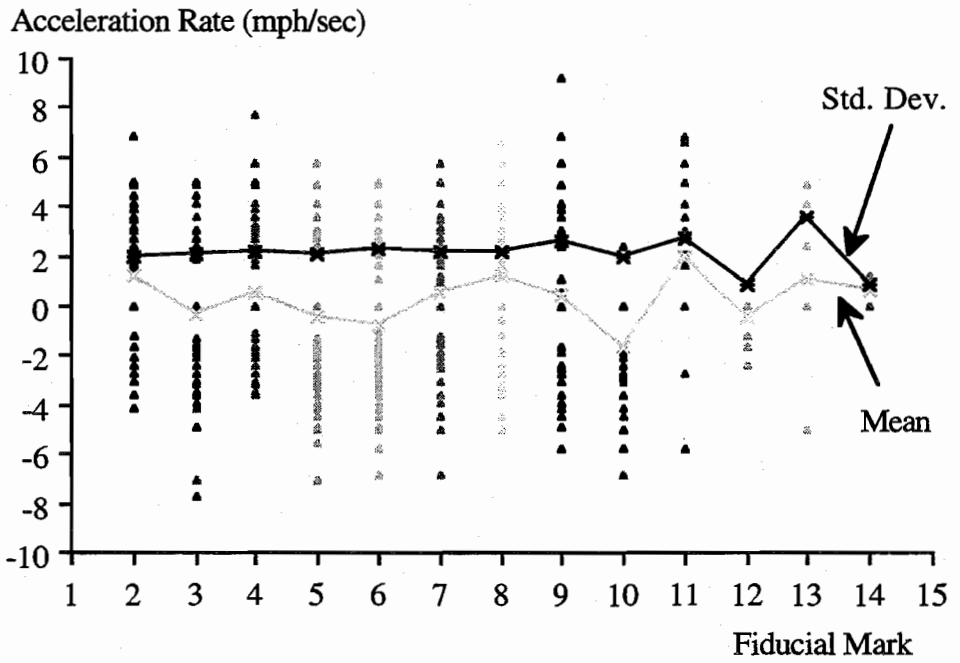

Figure 5.2 Ramp vehicle acceleration rate scatter vs. fiducial marks

TABLE 5.2 RESULT OF STATISTICAL TEST FOR EQUALITY OF ACCELERATION-DECELERATION MEANS

r	k	n	$F_{(k-1, n-k, 5\%)}$	$F_{(k-1, n-k, 10\%)}$
19.996	12	1612	1.79	1.57

Speed Differential at Merge

Speed differential is defined as the speed difference between a freeway lag vehicle and a merging vehicle. Figure 5.3 presents a merge speed differential distribution observed at the Loop 610 site. The distribution illustrates that, at their merge point, 50% of the ramp vehicles have a similar or slightly smaller speed than their corresponding freeway lag vehicles. This characteristic is different from that demonstrated in Figure 4.4 where 50% of the ramp vehicles have a 3.5 mph merge speed greater than their corresponding freeway lag vehicles. This driver behavior difference is reasonable due to the entrance ramp geometry difference. At the short acceleration

lane location, most ramp drivers accelerated with a greater magnitude in order to merge before reaching the acceleration lane end resulting in ramp vehicles have a higher merge speed than their corresponding freeway lag vehicles. At the long acceleration lane location, on the other hand, ramp drivers have many chances to adjust speeds and positions with respect to freeway vehicles to comfortably complete a merge. At the Loop 610 site, 80% of the ramp vehicles have a speed differential at merge of less than 5 mph.

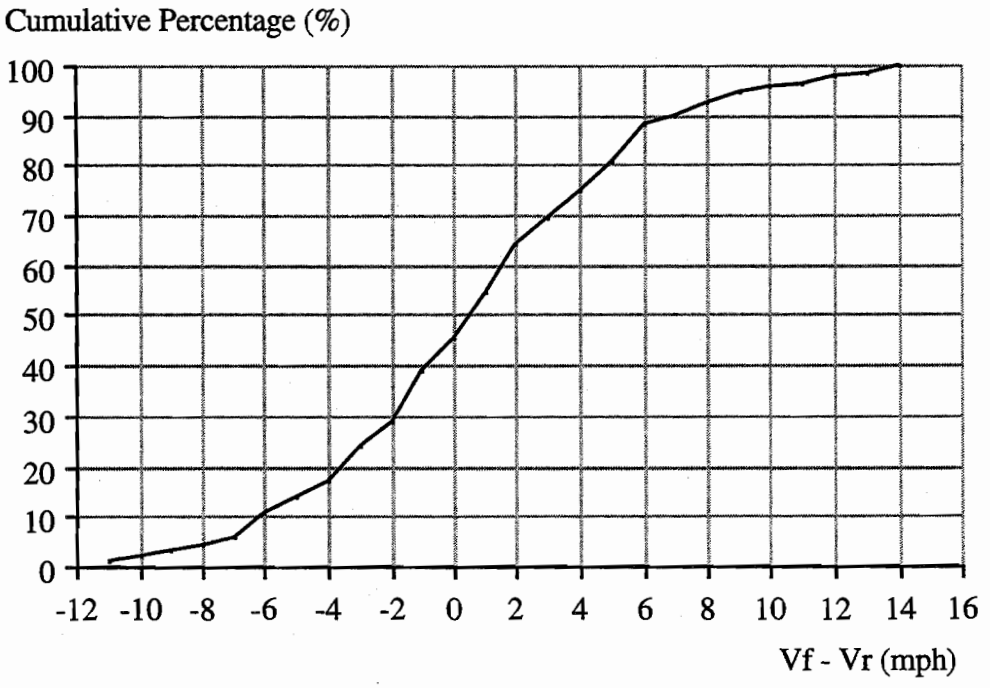

Figure 5.3 Distribution of merge speed differential between ramp vehicle and freeway lag vehicle

Angular Velocity at Merge

Angular velocity is defined as the rate of change of the angle bounded by the path of the freeway lag vehicle and the imaginary line connecting the gap seeking driver's eye and the corresponding freeway lag vehicle. Historically (Drew, 1971; Gordon and Michaels, 1963; Michaels and Cozan, 1963; Michaels and Fazio, 1989; Reilly, et al., 1989), the angle being used to calculate angular velocity is the angle θ shown in Figure 2.3. Through an extensive discussion

with Dr. Robert Herman, one argues that angle θ is the one that is viewed by the freeway vehicles with respect to ramp vehicles or roadside objectives. The actual angle evaluated by the gap seeking drivers with respect to freeway lag vehicles during freeway merge process should be the angles, θ_1 and θ_2, illustrated in Figure 5.4. The angular velocity formulation, based upon the new argument, can be derived as follows.

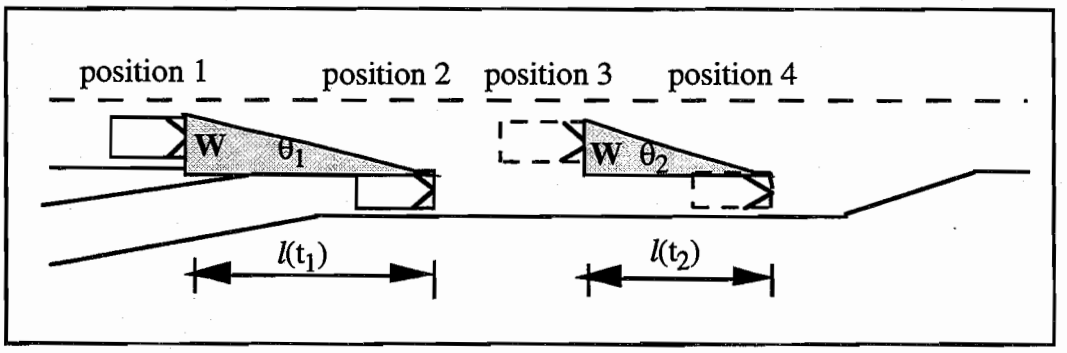

Figure 5.4 Sketch of viewed angle with respect to freeway lag vehicle during freeway merge process

At time t_1, a freeway lag vehicle and a ramp vehicle are located at positions 1 and 2 respectively. At time t_2, they have moved to positions 3 and 4 respectively. The angles evaluated by the ramp vehicle with respect to the freeway lag vehicle at t_1 and t_2 are θ_1 and θ_2 respectively.

$$\tan\theta_1 = \frac{W}{l(t_1)} \quad \Rightarrow \quad \theta_1 = \tan^{-1}\left[\frac{W}{l(t_1)}\right] \tag{5.1}$$

$$\tan\theta_2 = \frac{W}{l(t_2)} \quad \Rightarrow \quad \theta_2 = \tan^{-1}\left[\frac{W}{l(t_2)}\right] \tag{5.2}$$

Where

W : total of freeway lag vehicle width and lateral offset between freeway lag vehicle and ramp vehicle;

$l(t_1)$: longitudinal distance between ramp vehicle and freeway lag vehicle at t_1;

$l(t_2)$: longitudinal distance between ramp vehicle and freeway lag vehicle at t_2.

The magnitude of change of viewed angles from times t_1 to t_2 is

$$\Delta\theta = \theta_2 - \theta_1 = \tan^{-1}[\frac{W}{l(t_2)}] - \tan^{-1}[\frac{W}{l(t_1)}] \tag{5.3}$$

Let $$\Delta t = t_2 - t_1 \tag{5.4}$$

By definition, angular velocity is obtained using Eq.(5.5).

$$\frac{\Delta\theta}{\Delta t} = \frac{1}{\Delta t}\{ \tan^{-1}[\frac{W}{l(t_2)}] - \tan^{-1}[\frac{W}{l(t_1)}] \} \tag{5.5}$$

If Δt approach a very small time interval, Eq.(5.5) is readily rewritten as follows,

$$\omega = \lim_{\Delta t \to 0} \frac{\Delta\theta}{\Delta t} = \frac{d\theta}{dt}$$

$$= \frac{d}{dt}[\tan^{-1}(\frac{W}{l(t)})]$$

$$= \frac{d}{d[l(t)]}[\tan^{-1}(\frac{W}{l(t)})]\frac{d[l(t)]}{dt}$$

$$= \frac{1}{1 + [\frac{W}{l(t)}]^2} \cdot \frac{-W}{l^2(t)} \cdot (V_r - V_f)$$

$$= \frac{W}{l^2(t) + W^2} \cdot (V_f - V_r) \tag{5.6}$$

$l(t)$ is the longitudinal distance between ramp vehicle and freeway lag vehicle at time t. Generally, ω can be respecified as Eq.(5.7) by replacing $l(t)$ with L

$$\omega = \frac{W}{L^2 + W^2} \cdot (V_f - V_r) \tag{5.7}$$

When $W^2 << L^2$, Eq.(5.7) is simply approximated as

$$\omega \cong \frac{W}{L^2} \cdot (V_f - V_r) \tag{5.8}$$

Numerically, Eq.(5.8) is exactly identical to Eq.(2.8). Strictly speaking, however, the W's are not always significantly smaller than L in the freeway merge case. On the contrary, L would play a more and more important role in terms of angular velocity magnitude as the freeway lag vehicles are closing on the gap seeking drivers. Approximating angular velocity calculations using Eq.(5.8), although simple, might bias the true magnitudes. Consequently, in order to obtain more precise results, Eq.(5.7) was used to calculate angular velocity magnitudes hereafter in this study. The same arguments are also applied to the angular velocity components, as shown in Figure 3.33, with respect to freeway lead vehicles and ramp lead vehicles respectively.

Figure 5.5 shows, based upon field measurement of individual drivers, the distribution of angular velocity, with respect to freeway lag vehicles, accepted by ramp drivers completing a merge. Fifty percent of the ramp drivers have an accepted angular velocity approximately equal to or less than 0.00 rads/sec. The median accepted angular velocity was found to be 0.00088 rads/sec which is smaller than the nominal threshold value of 0.004 rads/sec proposed by Michaels (1963). About 70% of the ramp drivers accepted an angular velocity ranging between -0.01 rads/sec and 0.01 rads/sec. The distribution shown in Figure 5.5, however, is different from those obtained by Michaels and Fazio (1989) and the pilot study conducted in this research where only approximately 45% ~ 50% of the ramp drivers have an accepted angular velocity that falls within that range. This difference might be partially due to different data collection locations or to the involvement of W in angular velocity calculations. The latter is expected to have a significant effect.

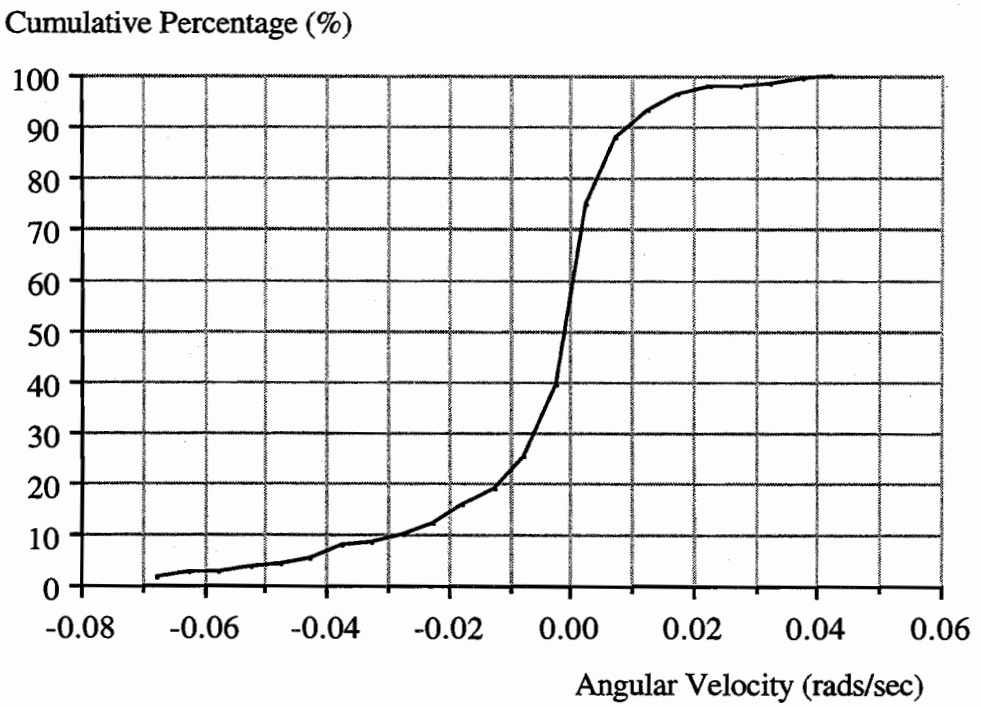

Figure 5.5 Distribution of merge angular velocity between ramp vehicle and freeway lag vehicle

CALIBRATION OF NONLINEAR ACCELERATION-DECELERATION MODEL

The pilot study results discussed in the previous chapter illustrate that the nonlinear methodology framework, as shown in Eqs.(3.18) and (3.19), has a potential for use in modeling ramp driver acceleration-deceleration behavior during freeway merge. Those two equations, however, were respectively specified for only one particular freeway merge situation. Equation (3.18), for example, is only suitable for the case when the ramp vehicle is a single vehicle or is the leader of a platoon of ramp vehicles in the acceleration lane, and both freeway lag and lead vehicles are present within a specific distance to the ramp vehicle. If either of the traffic situations change, the specification must be modified accordingly. The same shortcoming also happens to Eq.(3.19). This inflexibility associated with the previously proposed specifications limits their practical applications in modeling various freeway merge traffic situations. To overcome this restriction, a more sophisticated framework incorporating dummy variables to generalize the model specification was developed. The framework, as specified in Eq.(5.9), should be able to

model ramp vehicle acceleration-deceleration behavior under all possible freeway merge situations.

$$\ddot{X}_{r_i}(d_j + D) = \beta_0$$

$$+ \delta_1 D_{1j} + \beta_1 D_{1j} \dot{X}_{r_i}(d_j + D)^{\gamma} \frac{\dot{X}_{flag_i}(d_j) - \dot{X}_{r_i}(d_j)}{[(X_{r_i}(d_j) - X_{flag_i}(d_j))^2 + W^2_{rflag_i}(d_j)]^{\alpha_1}}$$

$$+ \delta_2 D_{2j} + \beta_2 D_{2j} \dot{X}_{r_i}(d_j + D)^{\gamma} \frac{\dot{X}_{r_i}(d_j) - \dot{X}_{flead_i}(d_j)}{[(X_{flead_i}(d_j) - X_{r_i}(d_j))^2 + W^2_{rflead_i}(d_j)]^{\alpha_2}}$$

$$+ \delta_3 D_{3j} + \beta_3 D_{3j} \dot{X}_{r_i}(d_j + D)^{\gamma} \frac{\dot{X}_{r_i}(d_j) - \dot{X}_{rlead_i}(d_j)}{[(X_{rlead_i}(d_j) - X_{r_i}(d_j))^2 + W^2_{rrlead_i}(d_j)]^{\alpha_3}}$$

$$+ \delta_4 (1 - D_{3j}) D_{4j} + \beta_4 (1 - D_{3j}) D_{4j} \dot{X}_{r_i}(d_j + D)^{\gamma} \frac{\dot{X}_{r_i}(d_j)}{[(L - X_{r_i}(d_j))^2 + W^2_{rend_i}(d_j)]^{\alpha_4}}$$

$$+ u_{r_i d_j} \qquad (5.9)$$

Where

$X_{r_i}(d_j)$, $X_{flag_i}(d_j)$, $X_{flead_i}(d_j)$, $\dot{X}_{r_i}(d_j)$, $\dot{X}_{flag_i}(d_j)$, $\dot{X}_{flead_i}(d_j)$, $\ddot{X}_{r_i}(d_j + D)$, $u_{r_i d_j}$, d_j, L, and D, are the same variables as defined in Eq.(3.18). The new variables appearing in Eq.(5.9) are defined as follows,

- $X_{rlead_i}(d_j)$: location of ramp vehicle i's corresponding ramp lead vehicle when vehicle i passed fiducial mark j;
- $\dot{X}_{rlead_i}(d_j)$: velocity of ramp vehicle i's corresponding ramp lead vehicle when vehicle i passed fiducial mark j;
- $W_{rflag_i}(d_j)$: lateral offset between ramp vehicle i and its corresponding freeway lag vehicle when vehicle i passed fiducial mark j;
- $W_{rflead_i}(d_j)$: lateral offset between ramp vehicle i and its corresponding freeway lead vehicle when vehicle i passed fiducial mark j;
- $W_{rrlead_i}(d_j)$: lateral offset between ramp vehicle i and its corresponding ramp lead vehicle when vehicle i passed fiducial mark j;

$W_{rend_i}(d_j)$: lateral offset of ramp vehicle i relative to the ramp end when vehicle i passed fiducial mark j;

D_{1j}, D_{2j}, D_{3j}, and D_{4j} are dummy variables and are defined as follows

$$D_{1j} = \begin{cases} 1 & \text{if there are freeway lag vehicles when vehicle i passed fiducial mark j} \\ 0 & \text{otherwise} \end{cases}$$

$$D_{2j} = \begin{cases} 1 & \text{if there are freeway lead vehicles when vehicle i passed fiducial mark j} \\ 0 & \text{otherwise} \end{cases}$$

$$D_{3j} = \begin{cases} 1 & \text{if there are ramp lead vehicles when vehicle i passed fiducial mark j} \\ 0 & \text{otherwise} \end{cases}$$

$$D_{4j} = \begin{cases} 1 & \text{if ramp vehicle is within 300 feet to the ramp end when vehicle i passed fiducial mark j} \\ 0 & \text{otherwise} \end{cases}$$

β_0, β_1, β_2, β_3, β_4, α_1, α_2, α_3, α_4, δ_1, δ_2, δ_3, δ_4, and γ are parameters to be estimated.

Introduction of dummy variables, namely D_{1j}, D_{2j}, D_{3j}, and D_{4j}, makes Eq.(5.9) become a more general model that could incorporate all possible traffic situations in one expression. Specifying dummy variables, namely D_{1j}, D_{2j}, D_{3j}, and D_{4j}, with subscript j enables Eq.(5.9) to account for dynamic traffic relationships. This consideration is particularly essential in modeling freeway merge traffic flow, for ramp vehicles and freeway vehicles are continuously changing their relative positions due to the maneuvers of merge, lane change, or overtaking. For example, a ramp vehicle's freeway lag vehicle will turn out to be its freeway lead

vehicle after a freeway overtaking. The ninth term of Eq.(5.9) reflects the effect of the acceleration lane terminus on the ramp vehicle's acceleration-deceleration behavior. It should be noted that this term is only valid when there are no ramp lead vehicles, D_{3j}=0, and the remaining distance to the acceleration lane terminus is less than 300 feet, D_{4j}=1. Once there are ramp lead vehicles, the following ramp vehicle will only pay attention to the relative movements of the leading vehicles. The acceleration lane terminus, in this case, should not be considered as an effect on ramp driver decision making. By the same token, even if no ramp vehicles are present, a ramp driver will pay no, or negligible, attention to the acceleration lane terminus if he/she is not within the effective zone. The effective zone, however, is difficult to define due to driver behavior variation and measurement technique limitations. The three hundred feet effective zone assumed in this study was adopted from the experimental results of Levin (1970). Although Levin's work, investigations of the freeway lane changing process, is not directly related to this study, 300 feet is believed to be a reasonable distance from which drivers can start to detect relative movement of an object.

Similar to the procedures derived in section 3.5.2, Eq.(5.9) can be rewritten as a special formulation implicitly taking angular velocities, with respect to surrounding freeway and ramp vehicles, into account as acceleration-deceleration decision stimuli.

$$\begin{aligned}\ddot{X}_{r_i}(d_j + D) = {} & \beta_0' \\ & + \delta_1' D_{1j} + \beta_1' D_{1j} \dot{X}_{r_i}(d_j + D)^{\gamma'} \omega_{rflag_i}(d_j) \\ & + \delta_2' D_{2j} + \beta_2' D_{2j} \dot{X}_{r_i}(d_j + D)^{\gamma'} \omega_{rflead_i}(d_j) \\ & + \delta_3' D_{3j} + \beta_3' D_{3j} \dot{X}_{r_i}(d_j + D)^{\gamma'} \omega_{rrlead_i}(d_j) \\ & + \delta_4' (1 - D_{3j}) D_{4j} + \beta_4' (1 - D_{3j}) D_{4j} \dot{X}_{r_i}(d_j + D)^{\gamma'} \omega_{rend_i}(d_j) \\ & + u_{r_i d_j} \end{aligned} \tag{5.10}$$

$\omega_{rflag_i}(d_j)$ is the angular velocity viewed by ramp vehicle i with respect to its corresponding freeway lag vehicle when vehicle i passed fiducial mark j;

$$\omega_{rflag_i}(d_j) = \frac{W_{rflag_i}(d_j)[\dot{X}_{flag_i}(d_j) - \dot{X}_{r_i}(d_j)]}{[X_{r_i}(d_j) - X_{flag_i}(d_j)]^2 + W^2_{rflag_i}(d_j)} \quad (5.11)$$

$\omega_{rflead_i}(d_j)$ is the angular velocity viewed by ramp vehicle i with respect to its corresponding freeway lead vehicle when vehicle i passed fiducial mark j;

$$\omega_{rflead_i}(d_j) = \frac{W_{rflead_i}(d_j)[\dot{X}_{r_i}(d_j) - \dot{X}_{flead_i}(d_j)]}{[X_{flead_i}(d_j) - X_{r_i}(d_j)]^2 + W^2_{rflead_i}(d_j)} \quad (5.12)$$

$\omega_{rrlead_i}(d_j)$ is the angular velocity viewed by ramp vehicle i with respect to its corresponding ramp lead vehicle when vehicle i passed fiducial mark j;

$$\omega_{rrlead_i}(d_j) = \frac{W_{rrlead_i}(d_j)[\dot{X}_{r_i}(d_j) - \dot{X}_{rlead_i}(d_j)]}{[X_{rlead_i}(d_j) - X_{r_i}(d_j)]^2 + W^2_{rrlead_i}(d_j)} \quad (5.13)$$

$\omega_{rend_i}(d_j)$ is the angular velocity viewed by ramp vehicle i with respect to the acceleration lane terminus when vehicle i passed fiducial mark j;

$$\omega_{rend_i}(d_j) = \frac{W_{rend_i}(d_j)\dot{X}_{r_i}(d_j)}{[L - X_{r_i}(d_j)]^2 + W^2_{rend_i}(d_j)} \quad (5.14)$$

Basically, Eqs.(5.9) and (5.10) are applicable to any variable units. However, the calibration results will be meaningful only when the same variable units are consistently used throughout the data set. Hereafter, the variable units used in the calibration procedures are

defined as follows: $\ddot{X}_{\bullet}(\bullet)$ in mph/sec; $\dot{X}_{\bullet}(\bullet)$ in mph; $X_{\bullet}(\bullet)$ in feet; $W_{\bullet}(\bullet)$ in feet; and $\omega_{\bullet}(\bullet)$ in rads/sec. In the following sections, a nonlinear regression technique will be used to calibrate the revised acceleration-deceleration models, Eqs.(5.9) and (5.10), using pooled or partial the data collected from Houston Loop 610 site, respectively. Calibration procedures and the mathematical expression will be modified accordingly to find the best fit models.

Calibration on Pooled Data

In an attempt to develop a general methodology that is applicable to model ramp vehicle acceleration-deceleration behavior under most freeway traffic situations, calibrations were performed using all vehicle trajectory data. The D's were parameters reflecting distance gaps (or equivalent time gaps) between stimuli ramp drivers detected and the location where they responded. As a consequence, the developed models, similar to those conventional car following models, should have a capability to directly predict ramp vehicle acceleration-deceleration rates under prevailing traffic conditions. The nonlinear regression procedures imbedded in SPSS statistical software were used to calibrate the proposed models for the cases of D equal to 0 feet, 50 feet, and 100 feet respectively. The results are shown in Tables 5.3 and 5.4 respectively for the general nonlinear model, Eq.(5.9), and the angular velocity model, Eq.(5.10).

TABLE 5.3 CALIBRATION RESULTS OF NONLINEAR ACCELERATION-DECELERATION MODEL

	D = 0 feet	D = 50 feet	D = 100 feet
β_0	0.9696	0.7494	0.7517
β_1	-0.1234	-10.8276	-2.2693
β_2	-0.0774	-0.0087	-0.0678
β_3	76.3482	-0.6891	-5.9612
β_4	44.1312	15.0025	-14.8151
α_1	0.1145	1.2394	0.7980
α_2	0.0000	0.0000	0.0000
α_3	1.2128	0.4525	0.4282
α_4	4.6131	0.7776	0.6533
δ_1	0.3318	0.4991	0.4247
δ_2	-1.1424	-1.3381	-1.3385
δ_3	-0.4287	-0.5481	-0.3179
δ_4	-0.9781	-1.7956	1.9348
γ	0.0002	0.6248	0.0438
R-squared	0.0562	0.1254	0.1160

TABLE 5.4 CALIBRATION RESULTS OF ANGULAR VELOCITY ACCELERATION-DECELERATION MODEL

	D = 0 feet	D = 50 feet	D = 100 feet
β_0'	0.8871	0.6471	0.6778
β_1'	-0.1610	-0.0007	0.4277
β_2'	-0.1008	-0.0004	-0.2511
β_3'	1.3653	-0.0048	-27.9055
β_4'	-21.7438	0.1079	-75.0185
δ_1'	0.3121	0.6340	0.5770
δ_2'	-0.9436	-1.2291	-1.2640
δ_3'	-0.4676	-0.6225	-0.3948
δ_4'	-0.6681	-1.4354	1.8420
γ'	0.0000	1.8411	0.0000
R-squared	0.0297	0.0602	0.0608

Generally, the nonlinear acceleration-deceleration models have better results than the angular velocity models in terms of R-squared values. This conclusion is not surprising due to the former has less limitations on the estimated parameters allowing greater freedom for the nonlinear search algorithm to search for optimal solutions. The results depicted in both Table 5.3 and Table 5.4, however, show low R-squared values for all cases revealing that these two models statistically have little ability to explain ramp vehicle acceleration-deceleration rate variations. Several reasons may cause this unsatisfactory result including: large variations embedded in the observations, incorrect model specifications (too complicated or lack of important parameters), or inappropriate calibration techniques.

Learning from ones daily driving experience, one can reasonably hypothesize that ramp drivers will pay unequal attention to their surrounding freeway or ramp vehicles depending on their physical separation distance. More specifically, drivers will be more responsive to relative movements of closer vehicles than far away vehicles. The specifications illustrated in Eqs.(5.9) and (5.10), however, do not implicitly take this effect into account. In the next section, weighting factors will be incorporated in the model specifications to more precisely capture dynamic driver behavior.

Calibration Involving Weighting Factors

According to previous discussion, Eqs.(5.9) and (5.10) should be specified so that the relative importance of surrounding freeway and ramp vehicles to the gap seeking vehicle can be automatically reflected. In other words, one should add weighting factors to the explanatory variables to capture such characteristics. It was hypothesized that the shorter the distance separation the greater the relative stimulus magnitude. Consequently, distance separation was used as an index to derive weighting factors and are shown as follows:

$$\Psi_{rflag_i}(d_j) = \frac{D_{1j} / \sqrt{[X_{r_i}(d_j) - X_{flag_i}(d_j)]^2 + W^2_{rflag_i}(d_j)}}{A} \tag{5.15}$$

$$\Psi_{rflead_i}(d_j) = \frac{D_{2j} / \sqrt{[X_{flead_i}(d_j) - X_{r_i}(d_j)]^2 + W^2_{rflead_i}(d_j)}}{A} \tag{5.16}$$

$$\Psi_{rrlead_i}(d_j) = \frac{D_{3j} / \sqrt{[X_{rlead_i}(d_j) - X_{r_i}(d_j)]^2 + W^2_{rrlead_i}(d_j)}}{A} \tag{5.17}$$

$$\Psi_{rend_i}(d_j) = \frac{D_{4j} / \sqrt{[L - X_{r_i}(d_j)]^2 + W^2_{rend_i}(d_j)}}{A} \tag{5.18}$$

Certainly,

$$\Psi_{rflag_i}(d_j) + \Psi_{rflead_i}(d_j) + \Psi_{rrlead_i}(d_j) + \Psi_{rend_i}(d_j) = 1 \tag{5.19}$$

Where

$$A = \frac{D_{1j}}{\sqrt{[X_{r_i}(d_j) - X_{flag_i}(d_j)]^2 + W^2_{rflag_i}(d_j)}} + \frac{D_{2j}}{\sqrt{[X_{flead_i}(d_j) - X_{r_i}(d_j)]^2 + W^2_{rflead_i}(d_j)}}$$

$$+ \frac{D_{3j}}{\sqrt{[X_{rlead_i}(d_j) - X_{r_i}(d_j)]^2 + W^2_{rrlead_i}(d_j)}}$$

$$+ \frac{D_{4j}}{\sqrt{[L - X_{r_i}(d_j)]^2 + W^2_{rend_i}(d_j)}} \qquad (5.20)$$

$\Psi_{rflag_i}(d_j)$: weighting factor associated with freeway lag vehicle stimulus;
$\Psi_{rflead_i}(d_j)$: weighting factor associated with freeway lead vehicle stimulus;
$\Psi_{rrlead_i}(d_j)$: weighting factor associated with ramp lead vehicle stimulus;
$\Psi_{rend_i}(d_j)$: weighting factor associated with acceleration lane end stimulus;

Incorporating dummy variables in weighting factor specifications enables different traffic situations to be exhaustively considered. Substituting $\Psi_{rflag_i}(d_j)$, $\Psi_{rflead_i}(d_j)$, $\Psi_{rrlead_i}(d_j)$, and $\Psi_{rend_i}(d_j)$ in Eqs.(5.9) and (5.10) respectively, one obtains

$$\ddot{X}_{r_i}(d_j + D) = \beta_0$$

$$+ \delta_1 D_{1j} + \beta_1 D_{1j} \dot{X}_{r_i}(d_j + D)^{\gamma} \frac{\Psi_{rflag_i}(d_j)[\dot{X}_{flag_i}(d_j) - \dot{X}_{r_i}(d_j)]}{[(X_{r_i}(d_j) - X_{flag_i}(d_j))^2 + W^2_{rflag_i}(d_j)]^{\alpha_1}}$$

$$+ \delta_2 D_{2j} + \beta_2 D_{2j} \dot{X}_{r_i}(d_j + D)^{\gamma} \frac{\Psi_{rflead_i}(d_j)[\dot{X}_{r_i}(d_j) - \dot{X}_{flead_i}(d_j)]}{[(X_{flead_i}(d_j) - X_{r_i}(d_j))^2 + W^2_{rflead_i}(d_j)]^{\alpha_2}}$$

$$+ \delta_3 D_{3j} + \beta_3 D_{3j} \dot{X}_{r_i}(d_j + D)^{\gamma} \frac{\Psi_{rrlead_i}(d_j)[\dot{X}_{r_i}(d_j) - \dot{X}_{rlead_i}(d_j)]}{[(X_{rlead_i}(d_j) - X_{r_i}(d_j))^2 + W^2_{rrlead_i}(d_j)]^{\alpha_3}}$$

$$+ \delta_4(1 - D_{3j})D_{4j} + \beta_4(1 - D_{3j})D_{4j} \dot{X}_{r_i}(d_j + D)^{\gamma} \frac{\Psi_{rend_i}(d_j)\dot{X}_{r_i}(d_j)}{[(L - X_{r_i}(d_j))^2 + W^2_{rend_i}(d_j)]^{\alpha_4}}$$

$$+ u_{r_i d_j} \qquad (5.21)$$

and

$$\ddot{X}_{r_i}(d_j + D) = \beta_0'$$

$$+ \delta_1' D_{1j} + \beta_1' D_{1j} \dot{X}_{r_i}(d_j + D)^{\gamma'} \Psi_{rflag_i}(d_j)\omega_{rflag_i}(d_j)$$

$$+ \delta_2' D_{2j} + \beta_2' D_{2j} \dot{X}_{r_i}(d_j + D)^{\gamma'} \Psi_{rflead_i}(d_j)\omega_{rflead_i}(d_j)$$

$$+ \delta_3' D_{3j} + \beta_3' D_{3j} \dot{X}_{r_i}(d_j + D)^{\gamma'} \Psi_{rrlead_i}(d_j)\omega_{rrlead_i}(d_j)$$

$$+ \delta_4' (1 - D_{3j}) D_{4j} + \beta_4' (1 - D_{3j}) D_{4j} \dot{X}_{r_i}(d_j + D)^{\gamma'} \Psi_{rend_i}(d_j)\omega_{rend_i}(d_j)$$

$$+ u_{r_i d_j} \qquad (5.22)$$

The weighting factors are inversely proportional to the distance separation so the model will automatically incorporate more weight for stimulus due to closer vehicles. Implicitly, those stimulus magnitudes will have greater contributions toward the nonlinear optimization solution search reflecting driver behavior more reasonably. The calibration results of Eqs.(5.21) and (5.22) using all observations are shown in Tables (5.5) and (5.6) respectively.

The calibration results of Eqs.(5.21) and (5.22) still show very low R-squared values. This unsuccessful attempt leads to the recognition that complex freeway merge traffic flow might not be described well by such sophisticated formulations, e.g. Eqs.(5.9) and (5.10) as well as (5.21) and (5.22). An intuitive approach would be to split all observations into homogeneous subgroups based upon traffic criteria. For instance, a subgroup might contain only observations in which freeway lag and lead vehicles were present, while another subgroup might contain observations in which only freeway lag vehicles were present. Then, there would be no need to use dummy variables in the specifications; because there would be only one unique specification associated with each subgroup. Calibrations using homogeneous subgroup data are expected to obtain better results with a disadvantage that each specification represents only one special freeway merge case. The following section will present calibrations performed on data subgroups distinguished by the presence of freeway or other ramp vehicles.

TABLE 5.5 CALIBRATION RESULTS OF NONLINEAR ACCELERATION-DECELERATION MODEL

(WEIGHTING FACTORS INVOLVED)

	D = 0 feet	D = 50 feet	D = 100 feet
β_0	0.8785	0.5648	0.5319
β_1	4.6321	-11.6926	0.0191
β_2	0.0209	-0.0032	-0.0469
β_3	3.8113	133.2030	2.9729
β_4	2.8065	60.5363	0.0817
α_1	5.3198	1.5767	0.0000
α_2	5.9399	0.0000	0.0000
α_3	5.8238	1.9207	5.6656
α_4	4.1954	0.9027	0.0000
δ_1	0.3068	0.6246	0.5155
δ_2	-0.9033	-1.3161	-1.2475
δ_3	-0.4709	-0.5559	-0.2974
δ_4	-0.8302	-0.9941	0.7533
γ	6.0000	0.9800	0.1928
R-squared	0.0342	0.1052	0.0871

TABLE 5.6 CALIBRATION RESULTS OF ANGULAR VELOCITY ACCELERATION-DECELERATION MODEL
(WEIGHTING FACTORS INVOLVED)

	D = 0 feet	D = 50 feet	D = 100 feet
β_0'	0.8665	0.5942	0.6180
β_1'	-0.0001	-0.0013	0.0004
β_2'	-0.0001	-0.0006	-0.0004
β_3'	0.0055	0.0049	-0.0194
β_4'	0.1320	0.6831	0.7807
δ_1'	0.3186	0.6571	0.5951
δ_2'	-0.9200	-1.1934	-1.2126
δ_3'	-0.4715	-0.6261	-0.4018
δ_4'	-0.9808	-0.9540	0.8708
γ'	1.8102	1.7587	1.7300
R-squared	0.0300	0.0614	0.0558

Calibration Using Data Subgroups Identified by the Presence of Corresponding Freeway and Ramp Vehicles

All observations were split into ten homogeneous subgroups having uncontrolled sample sizes using the presence of corresponding freeway lag, freeway lead, or ramp lead vehicles as subgroup identification criteria. The acceleration-deceleration model for each subgroup can be specified as one special case of Eqs.(5.9) or (5.10). For example, if only freeway lag and lead vehicles are present and the remaining distance to the acceleration lane end is more than 300 feet, the acceleration-deceleration model is specified as either Eq.(5.23) for the general nonlinear framework or Eq.(5.24) for the angular velocity framework. As a matter of fact, one should note that Eqs.(5.23) and (5.24) are similar to specifications presented in Chapters 3 and 4. The specifications, namely Eqs.(5.21) and (5.22), that incorporated weighting factors can be respecified using the same procedures as well.

$$\ddot{X}_{r_i}(d_j + D) = \beta_0$$

$$+ \beta_1 \dot{X}_{r_i}(d_j + D)^{\gamma} \frac{\dot{X}_{flag_i}(d_j) - \dot{X}_{r_i}(d_j)}{[(X_{r_i}(d_j) - X_{flag_i}(d_j))^2 + W^2_{rflag_i}(d_j)]^{\alpha_1}}$$

$$+ \beta_2 \dot{X}_{r_i}(d_j + D)^{\gamma} \frac{\dot{X}_{r_i}(d_j) - \dot{X}_{flead_i}(d_j)}{[(X_{flead_i}(d_j) - X_{r_i}(d_j))^2 + W^2_{rflead_i}(d_j)]^{\alpha_2}}$$

$$+ u_{r_i d_j} \qquad (5.23)$$

$$\ddot{X}_{r_i}(d_j + D) = \beta_0'$$

$$+ \beta_1' \dot{X}_{r_i}(d_j + D)^{\gamma'} \omega_{rflag_i}(d_j)$$

$$+ \beta_2' \dot{X}_{r_i}(d_j + D)^{\gamma'} \omega_{rflead_i}(d_j)$$

$$+ u_{r_i d_j} \qquad (5.24)$$

Each subgroup data set was used to calibrate the nonlinear and angular velocity acceleration-deceleration models. For comparison, calibrations were performed on the specifications with and without weighting factors. The calibration results, in terms of R-squared values, of each subgroup are summarized in Tables 5.7 to 5.9 for the cases of D equal to 0 feet, 50 feet, and 100 feet respectively. The row showing $D_{1\bullet}$=1, $D_{2\bullet}$=1, $D_{3\bullet}$=1, and $D_{4\bullet}$=0, for example, is for the subgroup that has corresponding freeway lag, freeway lead and ramp lead vehicles, and the traced ramp vehicle is more than 300 feet from the acceleration lane terminus.

In general, the results imply that incorporating weighting factors, as specified in Eqs.(5.15) to (5.18), does not actually provide any contribution to model development and therefore they are excluded from further consideration. Although not all statistically significant, the results of Tables 5.8 and 5.9 are better overall than their Table 5.7 counterparts. This implies that a driver responding to a stimulus does have a minimum acceptance time gap. R-squared values of

all cases are small except for a few subgroups that have very small sample sizes. Unfortunately, the small sample size makes the resulting high R-squared values less meaningful. Obviously, calibrations using homogeneous subgroup data, split based upon the presence of corresponding freeway and ramp vehicles, did not obtain satisfactory results. In the next section, each homogeneous subgroup data set is further split into even more homogeneous sub-subgroups based on the distance separations between the ramp vehicle and corresponding freeway and ramp vehicles. Calibration using more homogeneous subgroup data is hypothesized as a means of providing better results.

TABLE 5.7 SUMMARY OF R-SQUARED VALUES FOR SUBGROUPS IDENTIFIED BY THE PRESENCE OF CORRESPONDING FREEWAY AND RAMP VEHICLES

(D = 0 feet)

Subgroup				W/ weighting factor		W/O weighting factor		Obs.
$D_{1\bullet}$	$D_{2\bullet}$	$D_{3\bullet}$	$D_{4\bullet}$	Nonlinear	Ang. Vel.	Nonlinear	Ang. Vel.	No.
1	1	1	0	0.0592	0.0274	0.0673	0.0240	347
1	1	0	1	0.0698	0.0613	0.0823	0.0505	81
1	1	0	0	0.0074	0.0007	0.0074	0.0007	819
1	0	1	0	0.0168	0.0095	0.0165	0.0087	217
0	1	1	0	0.0175	0.2743	0.0174	0.3337	13
1	0	0	1	0.0284	0.0129	0.0899	0.0301	4
0	1	0	1	0.0000	0.0781	0.0000	0.0798	5
1	0	0	0	0.0392	0.0000	0.0392	0.0000	49
0	1	0	0	0.0246	0.0032	0.0246	0.0032	54
0	0	1	0	0.0000	0.0392	0.0000	0.0392	6

TABLE 5.8 SUMMARY OF R-SQUARED VALUES FOR SUBGROUPS IDENTIFIED BY THE PRESENCE OF CORRESPONDING FREEWAY AND RAMP VEHICLES

(D = 50 feet)

Subgroup				W/ weighting factor		W/O weighting factor		Obs.
$D_{1\bullet}$	$D_{2\bullet}$	$D_{3\bullet}$	$D_{4\bullet}$	Nonlinear	Ang. Vel.	Nonlinear	Ang. Vel.	No.
1	1	1	0	0.0710	0.0479	0.0751	0.0688	316
1	1	0	1	0.2600	0.2446	0.2690	0.2345	81
1	1	0	0	0.0301	0.0292	0.0291	0.0272	675
1	0	1	0	0.0727	0.0192	0.0521	0.0168	181
0	1	1	0	0.5201	0.6213	0.5435	0.6378	12
1	0	0	1	0.6128	0.5974	0.5963	0.5326	4
0	1	0	1	0.0000	0.1482	0.3548	0.4728	6
1	0	0	0	0.0434	0.0337	0.0434	0.0337	40
0	1	0	0	0.1165	0.0299	0.1165	0.0299	42
0	0	1	0	0.0000	0.2010	0.0000	0.2010	5

TABLE 5.9 SUMMARY OF R-SQUARED VALUES FOR SUBGROUPS IDENTIFIED BY THE PRESENCE OF CORRESPONDING FREEWAY AND RAMP VEHICLES

(D = 100 feet)

Subgroup				W/ weighting factor		W/O weighting factor		Obs.
$D_{1\bullet}$	$D_{2\bullet}$	$D_{3\bullet}$	$D_{4\bullet}$	Nonlinear	Ang. Vel.	Nonlinear	Ang. Vel.	No.
1	1	1	0	0.0893	0.0363	0.0918	0.0557	283
1	1	0	1	0.2416	0.2493	0.2471	0.2184	37
1	1	0	0	0.0417	0.0017	0.0500	0.0026	576
1	0	1	0	0.0161	0.0036	0.0087	0.0109	146
0	1	1	0	0.5565	0.6822	0.8836	0.7525	10
1	0	0	1	0.2860	0.6952	0.0270	0.7327	3
0	1	0	1	1.0000	1.0000	1.0000	1.0000	2
1	0	0	0	0.0691	0.0575	0.0691	0.0575	32
0	1	0	0	0.0109	0.0131	0.0109	0.0131	35
0	0	1	0	0.0000	0.3559	0.0000	0.3559	5

Calibration Using Data Subgroups Identified by Distance Separations between Ramp Vehicle and Corresponding Freeway and Ramp Vehicles

In the original data set, a ramp vehicle's corresponding freeway lag, lead, and ramp lead vehicles were defined as those vehicles that were within 400 feet, 300 feet, and 300 feet respectively. These distance separations might be too long for a ramp driver to be stimulated by those vehicles' movements. Ramp drivers, on the other hand, may only pay attention to those freeway and ramp vehicles that are nearer. To investigate this hypothesis, the homogeneous subgroups defined in the previous section were further split into 48 sub-subgroups based upon distance separation between a ramp vehicle and its corresponding freeway lag, lead, and ramp lead vehicles. For example, a sub-subgroup might contain only observations that freeway lag and lead vehicles are present and the associated distance separations between the traced ramp vehicle and these corresponding freeway vehicles are less than 200 feet. It is hoped that better calibration results can be obtained through splitting data into more homogenous subgroups.

However, one must point out that the more constraints the data have, the less the practical applications of the calibrated models.

Both nonlinear and angular velocity acceleration-deceleration models were calibrated using each of these sub-subgroup data sets. The resulting R-squared values are summarized in Tables 5.10 to 5.17. It is worth of noting that in each table, the subgroup of D_{rflag}, D_{rflead}, and D_{rrlead} less than 250 feet respectively, for example, is just a subset of the subgroup of D_{rflag}, D_{rflead}, and D_{rrlead} less than 300 feet. More specificly, a row, representing one subgroup, is a subset of preceding rows, or subgroups. As usual, the R-squared values of all cases are small except for a few small sample size subgroups indicating that this approach is not successful, either. Up to now, one is trying to calibrate models that are capable of directly predicting ramp vehicle acceleration or deceleration rates given freeway merge traffic conditions. Neither of the efforts, however, produces encouraging results leading to the recognition that developing a global formulation for all acceleration or deceleration rate predictions might not be feasible. In the next section, the observation data will be split into three subgroups containing observations of positive, negative, and zero acceleration rates respectively. A separate model will be developed for each subgroup.

TABLE 5.10 SUMMARY OF R-SQUARED VALUES FOR SUBGROUPS IDENTIFIED BY THE PRESENCE OF CORRESPONDING FREEWAY AND RAMP VEHICLES AND ASSOCIATED DISTANCE SEPARATIONS

$(D_{1\bullet} = 1,\ D_{2\bullet} = 1,\ D_{3\bullet} = 1,\ D_{4\bullet} = 0)$

D_{rflag}	D_{rflead}	D_{rrlead}	D_{rend}	D = 0 feet			D = 50 feet			D = 100 feet		
(≤)	(≤)	(≤)	(≤)	Nonlinear	Ang. Vel.	Obs	Nonlinear	Ang. Vel.	Obs	Nonlinear	Ang. Vel.	Obs
400	300	300	-	0.0673	0.0240	348	0.0751	0.0688	317	0.0918	0.0557	284
300	300	300	-	0.0692	0.0255	338	0.1145	0.0687	307	0.0889	0.0555	274
250	250	250	-	0.0772	0.0230	305	0.0983	0.0655	276	0.0945	0.0567	245
200	200	200	-	0.0610	0.0208	244	0.1528	0.0733	221	0.1061	0.0604	197
150	150	150	-	0.0434	0.0185	178	0.1367	0.0654	162	0.1133	0.0421	145
100	100	100	-	0.0428	0.0218	73	0.2473	0.0994	68	0.1017	0.0525	62
50	50	50	-	0.6251	0.4292	9	0.3692	0.0940	9	0.8596	0.8362	9

TABLE 5.11 SUMMARY OF R-SQUARED VALUES FOR SUBGROUPS IDENTIFIED BY THE PRESENCE OF CORRESPONDING FREEWAY AND RAMP VEHICLES AND ASSOCIATED DISTANCE SEPARATIONS

($D_{1\bullet} = 1$, $D_{2\bullet} = 1$, $D_{3\bullet} = 0$, $D_{4\bullet} = 1$)

D_{rflag}	D_{rflead}	D_{rrlead}	D_{rend}	D = 0 feet			D = 50 feet			D = 100 feet		
(≤)	(≤)	(≤)	(≤)	Nonlinear	Ang. Vel.	Obs	Nonlinear	Ang. Vel.	Obs	Nonlinear	Ang. Vel.	Obs
400	300	-	300	0.0823	0.0505	82	0.2690	0.2345	82	0.2471	0.2184	38
300	300	-	300	0.0700	0.0505	80	0.2695	0.2390	80	0.2584	0.2260	37
250	250	-	250	0.1487	0.1384	39	0.2276	0.1894	39	0.5327	0.5107	15
200	200	-	200	0.4993	0.3608	14	0.7259	0.6717	14	1.0000	0.9775	5
150	150	-	150	0.9975	0.9995	5	1.0000	0.9596	5	-	-	1

TABLE 5.12 SUMMARY OF R-SQUARED VALUES FOR SUBGROUPS IDENTIFIED BY THE PRESENCE OF CORRESPONDING FREEWAY AND RAMP VEHICLES AND ASSOCIATED DISTANCE SEPARATIONS

$(D_{1\bullet} = 1,\ D_{2\bullet} = 1,\ D_{3\bullet} = 0,\ D_{4\bullet} = 0)$

D_{rflag}	D_{rflead}	D_{rrlead}	D_{rend}	D = 0 feet			D = 50 feet			D = 100 feet		
(≤)	(≤)	(≤)	(≤)	Nonlinear	Ang. Vel.	Obs	Nonlinear	Ang. Vel.	Obs	Nonlinear	Ang. Vel.	Obs
400	300	-	-	0.0074	0.0007	820	0.0291	0.0272	676	0.0500	0.0026	577
300	300	-	-	0.0080	0.0007	758	0.0312	0.0281	624	0.0466	0.0026	534
250	250	-	-	0.0089	0.0015	678	0.0376	0.0334	557	0.0478	0.0031	478
200	200	-	-	0.0106	0.0020	593	0.0284	0.0253	485	0.0453	0.0013	412
150	150	-	-	0.0120	0.0017	479	0.0365	0.0316	393	0.0356	0.0026	335
100	100	-	-	0.0043	0.0033	288	0.0281	0.0059	235	0.0334	0.0089	200
50	50	-	-	0.0111	0.0083	54	0.1070	0.0400	42	0.2248	0.1436	35

TABLE 5.13 SUMMARY OF R-SQUARED VALUES FOR SUBGROUPS IDENTIFIED BY THE PRESENCE OF CORRESPONDING FREEWAY AND RAMP VEHICLES AND ASSOCIATED DISTANCE SEPARATIONS

$(D_{1\bullet} = 1,\ D_{2\bullet} = 0,\ D_{3\bullet} = 1,\ D_{4\bullet} = 0)$

D_{rflag}	D_{rflead}	D_{rrlead}	D_{rend}	D = 0 feet			D = 50 feet			D = 100 feet		
(≤)	(≤)	(≤)	(≤)	Nonlinear	Ang. Vel.	Obs	Nonlinear	Ang. Vel.	Obs	Nonlinear	Ang. Vel.	Obs
400	-	300	-	0.0165	0.0087	218	0.0521	0.0168	182	0.0087	0.0109	147
300	-	300	-	0.0171	0.0091	210	0.0612	0.0182	175	0.0077	0.0105	141
250	-	250	-	0.0178	0.0093	203	0.0574	0.0178	169	0.0083	0.0107	136
200	-	200	-	0.0201	0.0098	175	0.0512	0.0181	145	0.0140	0.0125	116
150	-	150	-	0.0266	0.0088	133	0.0655	0.0222	110	0.1586	0.1440	88
100	-	100	-	0.0270	0.0245	92	0.1789	0.1789	76	0.0307	0.0917	61
50	-	50	-	0.0021	0.0146	18	0.3677	0.3570	15	0.1013	0.0946	12

TABLE 5.14 SUMMARY OF R-SQUARED VALUES FOR SUBGROUPS IDENTIFIED BY THE PRESENCE OF CORRESPONDING FREEWAY AND RAMP VEHICLES AND ASSOCIATED DISTANCE SEPARATIONS

$(D_{1\bullet} = 0,\ D_{2\bullet} = 1,\ D_{3\bullet} = 1,\ D_{4\bullet} = 0)$

D_{rflag}	D_{rflead}	D_{rrlead}	D_{rend}	D = 0 feet			D = 50 feet			D = 100 feet		
(≤)	(≤)	(≤)	(≤)	Nonlinear	Ang. Vel.	Obs	Nonlinear	Ang. Vel.	Obs	Nonlinear	Ang. Vel.	Obs
-	300	300	-	0.0174	0.3337	14	0.5435	0.6378	13	0.8836	0.7525	11
-	250	250	-	0.0103	0.4029	13	0.6023	0.7278	12	0.6119	0.7485	10
-	200	200	-	0.0422	0.4572	11	0.6263	0.7179	10	0.5914	0.7371	8
-	150	150	-	0.0342	0.3606	10	0.6234	0.7670	9	0.5274	0.6245	7
-	100	100	-	1.0000	0.4269	4	0.5473	0.9476	4	1.0000	1.0000	3

TABLE 5.15 SUMMARY OF R-SQUARED VALUES FOR SUBGROUPS IDENTIFIED BY THE PRESENCE OF CORRESPONDING FREEWAY AND RAMP VEHICLES AND ASSOCIATED DISTANCE SEPARATIONS

($D_{1\bullet} = 1$, $D_{2\bullet} = 0$, $D_{3\bullet} = 0$, $D_{4\bullet} = 0$)

D_{rflag}	D_{rflead}	D_{rrlead}	D_{rend}	D = 0 feet			D = 50 feet			D = 100 feet		
(≤)	(≤)	(≤)	(≤)	Nonlinear	Ang. Vel.	Obs	Nonlinear	Ang. Vel.	Obs	Nonlinear	Ang. Vel.	Obs
300	-	-	-	0.0166	0.0000	55	0.0318	0.0230	46	0.0705	0.0661	37
250	-	-	-	0.0166	0.0000	55	0.0318	0.0230	46	0.0705	0.0661	37
200	-	-	-	0.0409	0.0006	45	0.0420	0.0325	37	0.0835	0.0767	29
150	-	-	-	0.0409	0.0001	45	0.0420	0.0325	37	0.0835	0.0767	29
100	-	-	-	0.0402	0.0000	44	0.0405	0.0298	36	0.0814	0.0688	28
50	-	-	-	0.1038	0.0198	18	0.1588	0.1407	16	0.1695	0.1116	14

TABLE 5.16 SUMMARY OF R-SQUARED VALUES FOR SUBGROUPS IDENTIFIED BY THE PRESENCE OF CORRESPONDING FREEWAY AND RAMP VEHICLES AND ASSOCIATED DISTANCE SEPARATIONS

($D_{1\bullet} = 0$, $D_{2\bullet} = 1$, $D_{3\bullet} = 0$, $D_{4\bullet} = 0$)

D_{rflag}	D_{rflead}	D_{rrlead}	D_{rend}	D = 0 feet			D = 50 feet			D = 100 feet		
(≤)	(≤)	(≤)	(≤)	Nonlinear	Ang. Vel.	Obs	Nonlinear	Ang. Vel.	Obs	Nonlinear	Ang. Vel.	Obs
-	300	-	-	0.0184	0.0014	61	0.1182	0.0356	50	0.0897	0.0938	39
-	250	-	-	0.0184	0.0014	61	0.1182	0.0356	50	0.0897	0.0938	39
-	200	-	-	0.0251	0.0014	59	0.1292	0.0349	48	0.0892	0.0935	38
-	150	-	-	0.0138	0.0012	58	0.1292	0.0349	48	0.0892	0.0935	38
-	100	-	-	0.0200	0.0009	53	0.1738	0.0352	45	0.0917	0.0965	37
-	50	-	-	0.0342	0.0017	16	0.3318	0.1170	13	0.4447	0.4477	10

TABLE 5.17 SUMMARY OF R-SQUARED VALUES FOR SUBGROUPS IDENTIFIED BY THE PRESENCE OF CORRESPONDING FREEWAY AND RAMP VEHICLES AND ASSOCIATED DISTANCE SEPARATIONS

$(D_{1\bullet} = 0, D_{2\bullet} = 0, D_{3\bullet} = 1, D_{4\bullet} = 0)$

D_{rflag}	D_{rflead}	D_{rrlead}	D_{rend}	D = 0 feet			D = 50 feet			D = 100 feet		
(≤)	(≤)	(≤)	(≤)	Nonlinear	Ang. Vel.	Obs	Nonlinear	Ang. Vel.	Obs	Nonlinear	Ang. Vel.	Obs
-	-	300	-	0.0000	0.0392	7	0.0000	0.1966	6	0.0000	0.3559	6
-	-	250	-	0.0000	0.0392	7	0.0000	0.1966	6	0.0000	0.3559	6
-	-	200	-	0.0000	0.0392	7	0.0000	0.1966	6	0.0000	0.3559	6
-	-	150	-	0.0000	0.0392	7	0.0000	0.1966	6	0.0000	0.3559	6
-	-	100	-	0.3597	0.2175	3	1.0000	1.0000	2	1.0000	1.0000	2

Calibration Using Subgroups of Positive and Negative Acceleration Data

Preceding sections described attempts to calibrate global formulations that are capable of predicting both positive and negative acceleration rate magnitudes given freeway merge traffic flow situations using only one equation. If one combines all ramp vehicle acceleration-deceleration observations in one data set and sequentially numbers the observations, the scatter plot of the acceleration-deceleration rate versus the sequential observation number is shown in Figure 5.6. These scatter plots illustrate three very distinct acceleration rate corridors. The patterns of Figure 5.6, indicate why developing a good global model using pooled positive, negative, and zero acceleration rate observations is difficult. However, one might be able to develop separate positive and negative acceleration-deceleration models respectively. Calibrations were performed on Eq.(5.9) for the cases of D equal to 0 feet, 50 feet, and 100 feet respectively using the subgroups of positive and negative acceleration rate observations. The calibration results are shown in the first row of Table 5.18 for the positive acceleration model and Table 5.19 for the negative acceleration model.

Although they are still not good enough, the results are better, in terms of R-squared values, than the preceding calibration results implying that developing separate positive and negative acceleration models seems to be a right approach. In addition, in order not to omit any possible chance of obtaining better results, calibrations were also performed using subsets of positive and negative acceleration observations respectively. The resulting R-squared values are also summarized in Tables 5.18 and 5.19. Overall, the evidence shown in Tables 5.18 and 5.19 is not strong enough, none of the R-squared values is greater than 0.30, to conclude that Eq.(5.9) is a good ramp vehicle acceleration-deceleration formulation. Disadvantages of the nonlinear regression calibration procedures will be discussed in the next section, and an alternative calibration procedure will be proposed.

The proposed GLS calibration procedures were not applied in the previous model calibrations, because the nonlinear calibration results using classical least square techniques are so poor. R-squared values are hardly greater than 0.150 for large sample size subgroups indicating that one cannot expect to obtain significant improvements by implementing GLS calibration procedures.

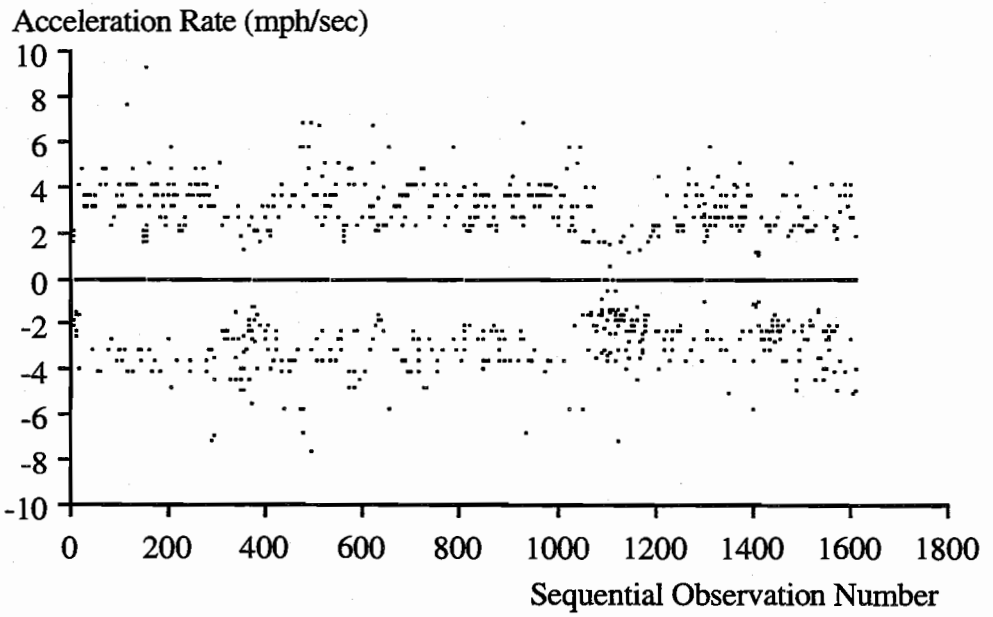

Figure 5.6 Scatter plot of acceleration-deceleration rate observations

TABLE 5.18 SUMMARY OF R-SQUARED VALUES FOR MODELS CALIBRATED USING POSITIVE ACCELERATION OBSERVATIONS ONLY

Acceleration Rate	D=0 feet		D=50 feet		D=100 feet	
(mph/sec)	Nonlinear	Obs	Nonlinear	Obs	Nonlinear	Obs
0 ≤	0.1407	426	0.1461	322	0.1283	286
1.0 ≤	0.1560	424	0.1349	320	0.1143	284
1.5 ≤	0.1585	418	0.1311	315	0.1360	279
2.0 ≤	0.1756	390	0.1750	296	0.1778	263
2.5 ≤	0.1930	307	0.1961	235	0.1746	211
3.0 ≤	0.1933	251	0.1695	193	0.1603	176
3.5 ≤	0.1335	186	0.1378	146	0.1419	134
4.0 ≤	0.0840	91	0.0782	72	0.0889	68

TABLE 5.19 SUMMARY OF R-SQUARED VALUES FOR MODELS CALIBRATED USING NEGATIVE ACCELERATION OBSERVATIONS ONLY

Acceleration Rate	D=0 feet		D=50 feet		D=100 feet	
(mph/sec)	Nonlinear	Obs	Nonlinear	Obs	Nonlinear	Obs
≤ 0	0.1484	348	0.1523	311	0.1428	272
≤ -1.0	0.1406	343	0.1453	325	0.1332	268
≤ -1.5	0.1326	324	0.1477	308	0.1424	255
≤ -2.0	0.1654	292	0.1872	278	0.1988	227
≤ -2.5	0.2286	216	0.2268	208	0.2376	169
≤ -3.0	0.2016	168	0.2228	161	0.2229	128
≤ -3.5	0.1805	115	0.2409	112	0.3000	87
≤ -4.0	0.1721	57	0.2349	56	0.2224	48

Comments on Nonlinear Regression Calibration Approach

The major purpose of this chapter is describing efforts to calibrate general formulations for predicting ramp vehicle acceleration-deceleration rates given freeway merge traffic conditions. Acceleration-deceleration rate was specified as a dependent variable, and other traffic parameters or combinations, such as speed differentials, distance separations, or angular velocities, were specified as independent variables. Basically, all calibration procedures performed so far used a nonlinear regression technique as the tool to calibrate candidate nonlinear specifications, such as Eqs.(5.9), (5.10), and other modified forms, using data subsets. Unfortunately, no acceptable calibration results have been found. Although a few high R-squared values were obtained, fairly small sample sizes associated with those cases make these calibration results less meaningful. In fact, the high R-squared values obtained in the preceding pilot study might also be the direct result of small sample sizes. Nevertheless, experience and knowledge learned from these painful calibration efforts are valuable.

Several reasons might lead to these discouraging situations. The proposed nonlinear specifications, although theoretically attractive, may be too sophisticated to predict dynamic ramp vehicle acceleration-deceleration rates. In other words, traffic parameters, such as speed differentials, distance separations, or angular velocities, are not good acceleration-deceleration

rate predictors. There is no doubt that ramp driver acceleration-deceleration "decisions" are jointly affected by these traffic parameters. The acceleration-deceleration "rates", however, might be determined by other very simple factors. To investigate this hypothesis, the variance-covariance matrices of all collected traffic parameters for the positive acceleration rate subset are shown in Table 5.20, and in Table 5.21 for the negative acceleration rate subset. Variables having a high correlation coefficient with the dependent variable have potential as predictors.

The following definitions are good only for Tables 5.20 and 5.21.. One should not confuse them with other variable definitions.

Accel : ramp vehicle acceleration-deceleration rate magnitude;

Vr : ramp vehicle speed;

Vflagr : speed differential between ramp vehicle and its corresponding freeway lag vehicle, Vflagr = Vflag - Vr;

Dflagr : distance separation between ramp vehicle and its corresponding freeway lag vehicle;

Wflagr : angular velocity viewed by the ramp driver with respect to its corresponding freeway lag vehicle;

Vrflead : speed differential between ramp vehicle and its corresponding freeway lead vehicle, Vrflead = Vr - Vflead;

Drflead : distance separation between ramp vehicle and its corresponding freeway lead vehicle;

Wrflead : angular velocity viewed by the ramp driver with respect to its corresponding freeway lead vehicle;

Vrrlead : speed differential between ramp vehicle and its corresponding ramp lead vehicle, Vrflead = Vr - Vrlead;

Drrlead : distance separation between ramp vehicle and its corresponding ramp lead vehicle;

Wrflead : angular velocity viewed by the ramp driver with respect to its corresponding ramp lead vehicle;

Drend : remaining distance to acceleration lane end;

Wrend : angular velocity viewed by the ramp driver with respect to acceleration lane end.

TABLE 5.20 VARIANCE-COVARIANCE MATRIX FOR POSITIVE ACCELERATION RATE OBSERVATIONs

	Accel	Vr	Vflagr	Dflagr	Wflagr	Vrflead	Drflead	Wrflead	Vrrlead	Drrlead	Wrrlead	Drend	Wrend
Accel	1.0000												
Vr	0.7409	1.0000											
Vflagr	-0.3005	-0.4001	1.0000										
Dflagr	0.0139	0.0586	0.0253	1.0000									
Wflagr	-0.1123	-0.1154	0.4044	-0.0513	1.0000								
Vrflead	0.1977	0.2726	-0.4855	-0.0363	-0.2510	1.0000							
Drflead	-0.0066	-0.0965	0.0991	-0.0462	0.0516	0.2869	1.0000						
Wrflead	0.1212	0.1930	-0.2126	-0.0057	-0.0441	0.5064	0.2380	1.0000					
Vrrlead	0.1276	0.2564	-0.1586	0.0278	-0.0959	0.1422	-0.0137	0.0778	1.0000				
Drrlead	0.1594	0.2191	-0.0829	0.0043	0.0520	-0.1457	-0.4795	-0.0695	0.1202	1.0000			
Wrrlead	0.0669	0.0097	0.0723	-0.0093	-0.0084	0.0352	0.1179	0.0262	0.1550	-0.0901	1.0000		
Drend	-0.0201	-0.0460	0.0502	0.0409	0.0492	0.0133	0.0762	0.0828	-0.0187	-0.1440	0.0107	1.0000	
Wrend	0.0366	0.0657	-0.0671	-0.0462	-0.0463	0.0041	-0.0550	-0.0539	0.0172	0.1327	-0.0098	-0.9426	1.0000

TABLE 5.21 VARIANCE-COVARIANCE FOR NEGATIVE ACCELERATION RATE OBSERVATIONS

	Accel	Vr	Vflagr	Dflagr	Wflagr	Vrflead	Drflead	Wrflead	Vrrlead	Drrlead	Wrrlead	Drend	Wrend
Accel	1.0000												
Vr	-0.5656	1.0000											
Vflagr	0.2864	-0.2192	1.0000										
Dflagr	-0.1786	0.1136	0.0025	1.0000									
Wflagr	0.1439	-0.1412	0.4027	-0.0528	1.0000								
Vrflead	-0.1565	0.0758	-0.5288	0.0011	-0.2832	1.0000							
Drflead	0.1309	-0.0653	0.1123	-0.0508	0.0376	0.0731	1.0000						
Wrflead	0.0103	-0.0486	-0.2819	-0.0361	-0.0240	0.5529	0.1393	1.0000					
Vrrlead	-0.2067	0.1053	-0.2240	0.2797	-0.2098	0.2109	0.0090	0.0584	1.0000				
Drrlead	-0.1692	0.3032	0.0150	0.0523	-0.0630	0.0139	-0.3160	-0.0806	-0.0582	1.0000			
Wrrlead	-0.0139	-0.1050	-0.0608	0.0560	-0.0465	0.0300	0.1727	0.0407	0.4385	-0.1783	1.0000		
Drend	0.0593	-0.0301	0.1167	0.0628	0.0124	-0.0018	0.1006	0.0669	0.0141	-0.2503	0.0398	1.0000	
Wrend	-0.0732	0.0008	-0.0581	-0.0455	-0.0289	-0.0176	-0.0846	-0.1549	-0.0110	0.1950	-0.0310	-0.8150	1.0000

In both tables, ramp vehicle speed, Vr, is the only variable that has a high correlation coefficient, 0.7409 in Table 5.20 and -0.5656 in Table 5.21, with acceleration-deceleration rate magnitude, Accel. The rest of the variables have very poor correlation with acceleration-deceleration rate. This result is intuitively reasonable because, by definition, acceleration-deceleration is the rate of change of speed. Consequently, there is no doubt that speed is the major element that determines acceleration-deceleration rate magnitudes. This evidence implicitly shows that all variables except ramp vehicle speed have little capability to explain ramp vehicle acceleration-deceleration rate changes. It is therefore not surprising that one cannot calibrate a good nonlinear acceleration-deceleration rate prediction model using the collected observations. The evidence that acceleration-deceleration rate magnitude has poor correlation with speed differentials, distance separations, and angular velocities does not imply that ramp drivers make acceleration-deceleration decisions regardless of the presence of surrounding freeway and ramp vehicles. On the contrary, ramp drivers must continuously pay close attention to surrounding freeway and ramp vehicles to make proper acceleration-deceleration decisions in order to safely and efficiently accomplish the required lateral and longitudinal positioning.

Essentially, no matter what the circumstance, ramp drivers can only perform one of three maneuvers, namely acceleration, deceleration, or constant speed, at any given time instant. Therefore, one should be able to calibrate a discrete choice model using collected traffic vehicle observations as attributes to predict ramp driver acceleration-deceleration decision choice behavior. Furthermore, using ramp vehicle speed as an explanatory variable, one can calibrate a continuous model to predict ramp vehicle acceleration-deceleration rate magnitudes. From a practical application perspective, one can conjoin a discrete decision choice model with a continuous magnitude prediction model to form a bi-level ramp vehicle acceleration-deceleration behavior framework. This bi-level approach is practically superior to the originally proposed nonlinear acceleration-deceleration magnitude prediction model, and is believed to be closer to true driver behavior. Based on the original nonlinear model framework, given certain traffic conditions, one obtains the acceleration-deceleration rate predictions. Given the same freeway merge traffic conditions, the nonlinear model always predicts ramp drivers will apply the same acceleration-deceleration rate magnitudes. This assumption, however, does not correspond with true driver behavior. Even facing exactly the same traffic relationships, a ramp driver might demonstrate different acceleration-deceleration choices, needless to say, different acceleration-deceleration rate magnitudes. The bi-level approach, on the other hand, does not directly predict acceleration-deceleration rate magnitudes. Instead, it predicts, given freeway merge traffic conditions, ramp driver acceleration-deceleration choice probability using a discrete choice

model, and acceleration-deceleration rate magnitude using a corresponding continuous model. Practically, this bi-level approach is more appropriate to model dynamic ramp driver acceleration-deceleration behavior for it does not always predict the same acceleration-deceleration decision choices and magnitudes given the same traffic conditions. Just like true driver behavior, one is not expected to behave identically even under the same vehicle relationships, e.g. same speed differentials or distance separations with respect to surrounding freeway vehicles. An overview of the acceleration-deceleration behavior model calibration procedures is illustrated in Figure 5.7. The tasks above the dashed line have been presented in the previous sections. Details of the calibration procedure below the dashed line will be discussed in the following sections.

BI-LEVEL DISCRETE-CONTINUOUS APPROACH

This study intends to develop a methodology capable of describing true driver behavior during the ramp driver freeway merge acceleration-deceleration process. The bi-level calibration concept described in the preceding section is proposed to fulfill the modeling requirements. Ramp driver acceleration-deceleration rate magnitudes during freeway merge maneuvers are variable and have been shown to be difficult to predict using a singular global equation. From a practical application perspective, the bi-level approach provides the opportunity to model dynamic freeway merge driver acceleration-deceleration behavior through combining a probabilistic discrete choice behavior framework with a continuous magnitude prediction formulation. This concept can be easily implemented in existing microscopic freeway simulation models by incorporating a random number generation technique. In the following sections, calibration of discrete choice acceleration-deceleration models using pooled traffic data are presented. Data structures associated with no response lag, one fiducial mark response lag, and two fiducial marks response lag are examined respectively as a first step to identify the best data set for use in further discrete choice model calibrations. Continuous magnitude prediction models, however, are developed using acceleration data or deceleration data subsets respectively.

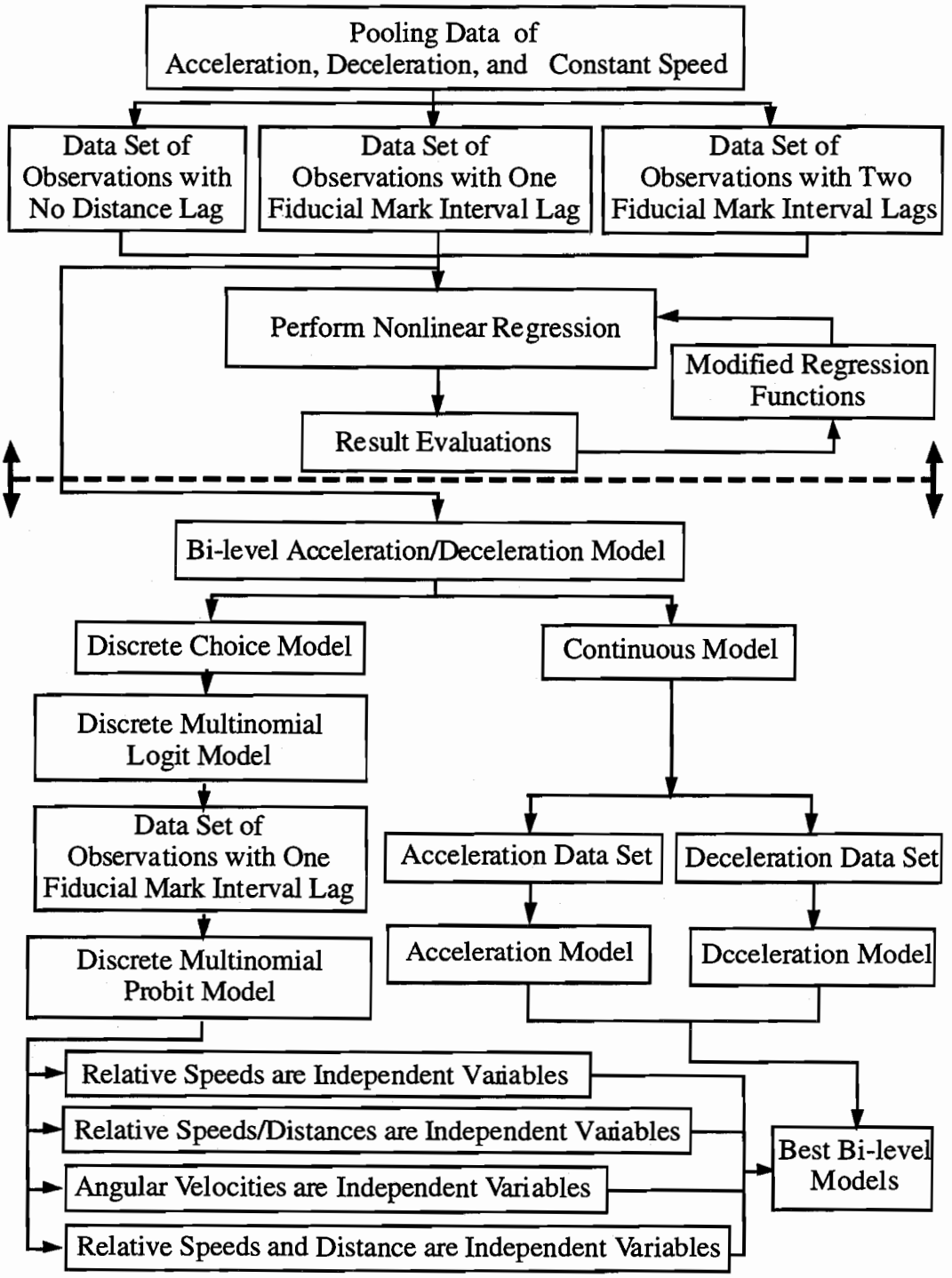

Figure 5.7 Flowchart of calibrating ramp vehicle acceleration-deceleration models

Discrete Acceleration-deceleration Choice Behavior Model

The methods of discrete choice analysis have been used largely in travel demand modeling during the past few decades. Early discrete choice model transportation applications were made for the binary choice of travel mode. During the early 1970's, discrete choice methods were further applied in mode choice models with more than two alternatives, trip destination, trip frequency, car ownership, residential, and housing (Ben-Akiva and Lerman 1989). Recently, more advanced discrete choice methods were developed to overcome barriers due to interdependencies among related choices, practical and theoretical problems posed by a choice from a large number of choice alternatives, and time dynamic choice decisions (Jou 1994; Lam 1991; Tong 1990). There is, however, no application in the driver speed change decision area.

It is assumed that an individual decision maker who, faced with a set of feasible discrete alternatives, selects the one that yields greatest utility. If one views the utility of any alternative as a random variable, it leads directly to the notion of random utility models in which the probability of any alternative *i* being selected by person *n* from a mutually exclusive and collectively exhaustive choice set C_n is given by the following:

$$P(i|C_n) = P_r(U_{in} \geq U_{jn}, \forall j \in C_n) \tag{5.25}$$

Where

U_{in} is the utility individual *n* gains by selecting alternative *i*

U_{jn} is the utility individual *n* gains by selecting alternative *j*

Recalling that U_{in} and U_{jn} are random variables, one can accordingly specify them as follows:

$$U_{in} = V_{in} + \varepsilon_{in} \tag{5.26}$$

$$U_{jn} = V_{jn} + \varepsilon_{jn} \tag{5.27}$$

Where V_{in} and V_{jn} are called the systematic components of the utility of *i* and*j*; ε_{in} and ε_{jn} are called random disturbances. To make random utility theory operate, one specifies the systematic components, $V_{\bullet n}$, which are functions characterized by a vector of attributes, and the random disturbances, $\varepsilon_{\bullet n}$. Detailed discussion of random utility theory can be found in any standard discrete choice analysis text book.

Stemming from the theories behind discrete choice methods, ramp driver acceleration-deceleration choice behavior during the freeway merge maneuver should be a good application.

Ramp drivers, at any time instant, have only three discrete speed change choices, acceleration, constant speed, or deceleration, forming a mutually exclusive and collectively exhaustive choice set. In any case, only one of these three choices will be made. The attributes that affect ramp driver choice behavior are various ranging from internal attributes such as age, gender, personality, or trip purpose to external attributes such as speed differential and distance separation with surrounding vehicles, entrance ramp geometric configurations, or vehicle performance characteristics. Consequently, the systematic components of utility functions can be specified in many different ways depending on the information one can possibly obtain. Unlike conventional transportation applications of discrete choice models in which only one observation is normally obtained for each individual, more than one acceleration-deceleration choice observation is associated with each ramp vehicle. This advantage allows one to take into account the time related data characteristics in the discrete choice modeling framework. Consideration of time related elements is essential for this particular driver behavior modeling because drivers' acceleration-deceleration decisions could be dominated by previous stimuli or attributes. One can write the utility functions of alternative 1, deceleration, alternative 2, constant speed, and alternative 3, acceleration, respectively as the following general forms where ramp driver *n* was at the location $d_j + D$.

$$U_{1n}(d_j + D) = V_{1n}(d_j) + \varepsilon_{1n}(d_j + D) \tag{5.28}$$

$$U_{2n}(d_j + D) = V_{2n}(d_j) + \varepsilon_{2n}(d_j + D) \tag{5.29}$$

$$U_{3n}(d_j + D) = V_{3n}(d_j) + \varepsilon_{3n}(d_j + D) \tag{5.30}$$

Where

d_j : position of fiducial mark j measured from the merging end;

D : distance lag.

The notations of Eqs.(5.28) to (5.30) implicitly demonstrate that the utilities of each alternative at position $d_j + D$ are characterized by attributes collected at position d_j. In other words, the speed change decision that the ramp driver will make at position $d_j + D$ is assumed to be based on the traffic situation he/she experienced at position d_j. If D is equal to 0 feet, this implies that the ramp driver acceleration-deceleration decision is made according to the concurrent traffic situation. There are many possible combinations of systematic component

specifications and time related data sets. The effort that would be involved in calibrating all possible combinations would be very large. To determine which time related data set contains the best information for describing ramp driver speed change behavior, a preliminary experiment was designed. As a first step, the data sets of D equal to 0 feet, 50 feet, and 100 feet were used respectively to calibrate discrete choice models for three different systematic component specifications. The results of this preliminary calibration served as criteria to identify the best data set for further use. For this purpose, a multinomial logit model was adopted as a preliminary screening tool due to its simplicity. Details of the multinomial logit model calibration will be discussed in the following section.

Preliminary Multinomial Logit Model Calibration for Data Set Screening. By assuming that $\varepsilon_{1n}(\bullet)$, $\varepsilon_{2n}(\bullet)$, and $\varepsilon_{3n}(\bullet)$ are independent and identically Gumble distributed, one can write the choice probability, at position $d_j + D$, for alternative i as the following logistical form.

$$P_n^{d_j+D}(i) = \frac{e^{V_{in}(d_j)}}{\sum_{k=1}^{3} e^{V_{kn}(d_j)}} \tag{5.31}$$

Where

alternative 1 ($i=1$): deceleration
alternative 2 ($i=2$): constant speed
alternative 3 ($i=3$): acceleration

The major issue of calibrating a multinomial logit model is how to specify those systematic components of each utility function. In other words, one should determine what types of variables can enter those functions? In this study, all traffic observations were collected through video image techniques. As a consequence, a set of vehicle time-position trajectory observations was obtained. The magnitudes of speeds, speed differentials, acceleration-deceleration rates, distance separations, and angular velocities were calculated using this basic data set. However, other attributes such as age, sex, aggressiveness, occupation, vehicle performance, comfort, and safety that are also believed to have strong effects on driver behavior are unknown.

In this preliminary experiment, three different systematic component specifications were considered. They are characterized respectively by speed differentials, angular velocities, and speed differential distance/separation ratios between ramp vehicle and surrounding vehicles as

well as acceleration lane terminus. The specifications are tabulated respectively in Tables 5.22 to 5.24. The three rows correspond to deceleration, constant speed, and acceleration utilities, and the columns correspond to the fourteen coefficients labeled β_1 to β_{14}. The entries in the tables define the variables that enter into the models. The variables under the first two columns are termed *alternative-specific constants*. It is redundant to specify three alternative-specific constants because all that matters is their difference. The third to fourteen coefficients correspond to the attributes of relative vehicle relationships, such as speed differentials, angular velocities, or speed differential/distance separation ratios, between the ramp vehicle and surrounding vehicles as well as acceleration lane terminus. These variables are defined as *alternative specific variables*. It should be noted that ramp drivers respond to the same traffic vehicle attribute differently when making different speed change decisions. For instance, a ramp driver might be more cautious of the speed differential corresponding to a freeway lead vehicle when making acceleration decisions compared to deceleration decisions. If this ramp vehicle has a considerably higher speed than its corresponding freeway lead vehicle, if "all else is equal", the utilities that would result from choosing acceleration, deceleration, or constant speed would obviously be different. Choosing the acceleration maneuver, under such a circumstance, might have an adverse utility effect due to an increasing collision potential while choosing deceleration or constant speed might not. More precisely, for each alternative, each traffic attribute, speed differential to freeway lead vehicle in this example, should have different marginal effects. This property can only be reflected by specifying those traffic attributes as *alternative specific variables*. It makes no sense to specify those attributes as *generic* variables because this implicitly forces, for each alternative, identical marginal utilities.

TABLE 5.22 SPECIFICATION CHARACTERIZED BY SPEED DIFFERENTIALS BETWEEN RAMP VEHICLE AND SURROUNDING VEHICLES

Alternative	β_1	β_2	β_3	β_4	β_5	β_6
Deceleration	1	0	Speed Differential to Freeway Lag Vehicle	0	0	Speed Differential to Freeway Lead Vehicle
Constant Speed	0	1	0	Speed Differential to Freeway Lag Vehicle	0	0
Acceleration	0	0	0	0	Speed Differential to Freeway Lag Vehicle	0

Alternative	β_7	β_8	β_9	β_{10}
Deceleration	0	0	Speed Differential to Ramp Lead Vehicle	0
Constant Speed	Speed Differential to Freeway Lead Vehicle	0	0	Speed Differential to Ramp Lead Vehicle
Acceleration	0	Speed Differential to Freeway Lead Vehicle	0	0

Alternative	β_{11}	β_{12}	β_{13}	β_{14}
Deceleration	0	Speed Differential to Acceleration Lane End	0	0
Constant Speed	0	0	Speed Differential to Acceleration Lane End	0
Acceleration	Speed Differential to Ramp Lead Vehicle	0	0	Speed Differential to Acceleration Lane End

TABLE 5.23 SPECIFICATION CHARACTERIZED BY ANGULAR VELOCITY BETWEEN RAMP VEHICLE AND SURROUNDING VEHICLES

Alternative	β_1	β_2	β_3	β_4	β_5	β_6
Deceleration	1	0	Angular Velocity to Freeway Lag Vehicle	0	0	Angular Velocity to Freeway Lead Vehicle
Constant Speed	0	1	0	Angular Velocity to Freeway Lag Vehicle	0	0
Acceleration	0	0	0	0	Angular Velocity to Freeway Lag Vehicle	0

Alternative	β_7	β_8	β_9	β_{10}
Deceleration	0	0	Angular Velocity to Ramp Lead Vehicle	0
Constant Speed	Angular Velocity to Freeway Lead Vehicle	0	0	Angular Velocity to Ramp Lead Vehicle
Acceleration	0	Angular Velocity to Freeway Lead Vehicle	0	0

Alternative	β_{11}	β_{12}	β_{13}	β_{14}
Deceleration	0	Angular Velocity to Acceleration Lane End	0	0
Constant Speed	0	0	Angular Velocity to Acceleration Lane End	0
Acceleration	Angular Velocity to Ramp Lead Vehicle	0	0	Angular Velocity to Acceleration Lane End

TABLE 5.24 SPECIFICATION CHARACTERIZED BY SPEED DIFFERENTIAL/DISTANCE BETWEEN RAMP VEHICLE AND SURROUNDING VEHICLES

Alternative	β_1	β_2	β_3	β_4	β_5	β_6
Deceleration	1	0	Speed Differential/Dist. to Freeway Lag Vehicle	0	0	Speed Differential/Dist. to Freeway Lead Vehicle
Constant Speed	0	1	0	Speed Differential/Dist. to Freeway Lag Vehicle	0	0
Acceleration	0	0	0	0	Speed Differential/Dist. to Freeway Lag Vehicle	0

	β_7	β_8	β_9	β_{10}
Deceleration	0	0	Speed Differential/Dist. to Ramp Lead Vehicle	0
Constant Speed	Speed Differential/Dist. to Freeway Lead Vehicle	0	0	Speed Differential/Dist. to Ramp Lead Vehicle
Acceleration	0	Speed Differential/Dist. to Freeway Lead Vehicle	0	0

	β_{11}	β_{12}	β_{13}	β_{14}
Deceleration	0	Speed Differential/Dist. to Acceleration Lane End	0	0
Constant Speed	0	0	Speed Differential/Dist. to Acceleration Lane End	0
Acceleration	Speed Differential/Dist. to Ramp Lead Vehicle	0	0	Speed Differential/Dist. to Acceleration Lane End

Statistical Software Tools (SST) was used to estimate the coefficients of these multinomial logit models for three, D=0 feet, D=50 feet, and D=100 feet, data sets respectively. The results are shown in Tables 5.25 to 5.27. The purpose of this experiment is to choose a best data set for use in further calibration. Therefore, all that matters is the relative goodness of each calibration result, not the absolute magnitudes of estimated coefficients. Below each figure is a group of summary statistics for the entire estimation run. $L(0)$ is the value of the log likelihood function when all the parameters are zero. $L(\hat{\beta})$ is the value of the log likelihood function at its maximum. An informal goodness-of-fit index, ρ^2, measures the fraction of an initial log likelihood value explained by the model and is defined as $1 - L(\hat{\beta}) / L(0)$. Another informal goodness-of-fit index, $\overline{\rho}^2$, is similar to ρ^2 but is corrected for the number of parameters estimated and is defined as $1 - [L(\hat{\beta}) - K] / L(0)$. Both have been extensively used in discrete choice analysis as criteria to evaluate calibrated models. Their true meanings illustrated by their magnitudes, however, are not clear. In other words, one is not sure of how high an index magnitude is good. ρ^2 and $\overline{\rho}^2$ are most useful in comparing different specifications developed on the same data and with the same set of alternatives. As a rule of thumb, the higher the index magnitude, the better the fit; and without other better choices, ρ^2 and $\overline{\rho}^2$ are adopted here as model selection criteria.

The results of Tables 5.25 to 5.27 show that calibrations on the data set with fiducial mark interval D=50 feet have the highest ρ^2 and $\overline{\rho}^2$ values. This fact indicates that the utility functions used to calculate speed change choice probability are best characterized by traffic attributes 50 feet ahead of the driver. This conclusion coincides with that suggested by conventional car-following that a small time lag exists between driver response, in terms of acceleration-deceleration magnitude, and the stimuli, characterized by driver perceived speed differential or distance separation.

In the multinomial logit model calibrations, data correlation neither across alternatives nor within individual ramp drivers were taken into consideration. These correlations, however, are likely embedded in the collected traffic data and should not be ignored in model calibration. The multinomial logit model, although simple, is not capable of incorporating the cross alternative correlation effects in the model calibration procedures. In the following section, multinomial probit models featuring the capability of incorporating cross alternative correlation, by specifying a disturbance variance-covariance matrix, are presented. Within driver correlations are implicitly captured by introducing dynamic dummy Markov indexes in the systematic component specifications. In comparison, the multinomial probit model allows more flexible model specifications and more realistic correlation structures for dynamic discrete choice analysis.

TABLE 5.25 ESTIMATION RESULTS OF SPECIFICATIONS CHARACTERIZED BY SPEED DIFFERENTIALS BETWEEN RAMP VEHICLES AND SURROUNDING VEHICLES

Parameter	D = 0 feet		D = 50 feet		D = 100 feet	
	Estimates	t statistic	Estimates	t statistic	Estimates	t statistic
β_1	-0.1817	-2.034	0.3994	3.862	0.3930	3.616
β_2	0.8592	11.830	1.2607	13.812	1.1229	11.485
β_3	0.3512	9.928	0.2418	7.683	0.1863	6.184
β_4	0.0714	4.511	0.0715	4.092	0.0719	3.693
β_5	0.1303	5.718	0.2337	7.667	0.2100	7.043
β_6	0.0959	3.205	0.1412	4.730	0.1033	3.446
β_7	-0.0642	-3.809	-0.0745	-3.945	-0.0988	-4.609
β_8	-0.2199	-8.032	-0.3108	-7.797	-0.2876	-6.792
β_9	0.1304	3.167	0.2295	4.416	0.2798	4.416
β_{10}	0.0691	2.722	0.0425	1.507	0.0372	1.154
β_{11}	-0.0161	-0.370	-0.1707	-2.238	-0.1393	-2.102
β_{12}	0.3620	0.149	0.3385	0.1286	0.3518	0.0458
β_{13}	0.3056	0.133	0.3090	0.1286	0.3191	0.0962
β_{14}	0.2910	0.095	0.3212	0.1323	0.3246	0.1422
$L(0)$	-1773.2		-1515		-1257.9	
$L(\hat{\beta})$	-1308.4		-1033.5		-901.33	
ρ^2	0.2621		0.3178		0.2835	
$\bar{\rho}^2$	0.2542		0.3086		0.2723	

TABLE 5.26 ESTIMATION RESULTS OF SPECIFICATIONS CHARACTERIZED BY ANGULAR VELOCITIES BETWEEN RAMP VEHICLES AND SURROUNDING VEHICLES

Parameter	D = 0 feet		D = 50 feet		D = 100 feet	
	Estimates	t statistic	Estimates	t statistic	Estimates	t statistic
β_1	-0.2384	-2.915	0.0018	0.019	-0.0470	-0.486
β_2	0.7426	11.207	0.9375	12.260	0.8148	10.022
β_3	3.4229	2.564	3.5898	3.193	0.8778	0.965
β_4	0.5326	1.041	0.6476	1.189	0.7227	1.362
β_5	1.2998	1.962	0.7178	0.956	2.9089	2.894
β_6	-2.7076	-6.313	-2.3245	-5.476	-2.6908	-5.643
β_7	-1.4109	-5.231	-1.2934	-4.998	-1.3906	-4.923
β_8	-6.4754	-5.041	-10.9998	-4.291	-2.5090	-5.110
β_9	107.432	3.736	286.443	5.959	360.166	6.022
β_{10}	36.2329	2.215	36.3164	1.910	23.7762	1.331
β_{11}	15.1292	1.354	2.3298	0.341	-31.7616	-1.471
β_{12}	2834.64	0.132	3098.25	0.090	2030.66	0.067
β_{13}	2502.82	0.099	2420.42	0.097	2409.45	0.122
β_{14}	2542.20	0.062	1819.51	0.077	2371.56	0.131
$L(0)$	-1773.2		-1515		-1257.9	
$L(\hat{\beta})$	-1397.6		-1147.8		-1004.7	
ρ^2	0.2118		0.2424		0.2013	
$\bar{\rho}^2$	0.2039		0.2331		0.1902	

TABLE 5.27 ESTIMATION RESULTS OF SPECIFICATIONS CHARACTERIZED BY SPEED DIFFERENTIAL AND DISTANCE SEPARATION RATIOS BETWEEN RAMP VEHICLES AND SURROUNDING VEHICLES

Parameter	D = 0 feet		D = 50 feet		D = 100 feet	
	Estimates	t statistic	Estimates	t statistic	Estimates	t statistic
β_1	-0.1716	-2.018	0.2565	2.610	0.1583	1.551
β_2	0.7953	11.412	1.1324	13.253	0.9522	10.703
β_3	6.2396	4.346	4.0527	3.726	1.1582	1.237
β_4	0.7602	1.367	0.8726	1.442	1.1342	1.819
β_5	1.4645	1.776	2.6174	2.655	5.7247	4.182
β_6	-2.8364	-5.797	-2.0087	-4.353	-2.6248	-4.977
β_7	-2.3372	-6.078	-2.1069	-5.583	-2.2797	-5.458
β_8	-9.3454	-7.113	-15.6542	-7.059	-4.8251	-5.713
β_9	19.6610	4.406	34.6717	6.423	42.5624	6.284
β_{10}	6.8238	2.391	4.3118	1.254	2.1251	0.563
β_{11}	1.1895	0.284	-28.7183	-4.570	-26.7855	-4.065
β_{12}	93.8090	0.174	100.05	0.125	85.2575	0.060
β_{13}	78.0193	0.142	78.4501	0.118	88.1130	0.096
β_{14}	77.3435	0.099	72.0587	0.116	88.5262	0.125
$L(0)$	-1773.2		-1515		-1257.9	
$L(\hat{\beta})$	-1347.1		-1082.4		-956.74	
ρ^2	0.2403		0.2855		0.2394	
$\overline{\rho}^2$	0.2324		0.2763		0.2283	

Multinomial Probit Model Calibration Incorporating Cross Alternative and Within Individual Correlations. The traffic observation data used in this study were collected and calculated on a fiducial mark basis. Consequently, for each individual ramp vehicle, it is very likely that serial correlation is associated with successive observations of the same vehicle. Cross alternative correlation, on the other hand, results from the fact that ramp drivers do not usually jump directly from acceleration to deceleration and *vice versa* during very short time intervals. Instead, they are likely to perform smooth speed transitions. This hypothesis can be characterized by specifying a cross alternative correlation matrix with the correlation coefficients as parameters to be estimated. In the multinomial logit model, the calibration procedures are performed under the assumptions that there are neither within vehicle nor across alternative correlation. To make the developed discrete acceleration-deceleration choice models more precisely reflect dynamic driver choice behavior, both within driver and across alternative correlation should be considered. This desire can be achieved by specifying utility functions that implicitly incorporate the unobservable within driver serial correlation in the systematic components and by using the Multinomial Probit Model as a calibration tool. Four model specifications, denoted as model 1, 2, 3, and 4 respectively, were developed. The only difference between these specifications is the traffic attributes that go into the systematic components. The utility functions for each models are demonstrated as follows:

Model 1: (speed differentials between ramp vehicle and surrounding freeway and ramp vehicles as well as acceleration lane end are attributes)

$$\begin{aligned} U_{1n}(d_j+50) = {} & \alpha_1 + \alpha_3 D_{1j} V_{1n}^{flagr}(d_j) + \alpha_6 D_{2j} V_{1n}^{rflead}(d_j) \\ & + \alpha_9 D_{3j} V_{1n}^{rrlead}(d_j) + \alpha_{12}(1-D_{3j}) D_{4j} V_{1n}^{rend}(d_j) \\ & + \alpha_{15}\delta_{1n}(d_j) + \xi_{1n}(d_j+50) \end{aligned} \tag{5.32}$$

$$\begin{aligned} U_{2n}(d_j+50) = {} & \alpha_2 + \alpha_4 D_{1j} V_{2n}^{flagr}(d_j) + \alpha_7 D_{2j} V_{2n}^{rflead}(d_j) \\ & + \alpha_{10} D_{3j} V_{2n}^{rrlead}(d_j) + \alpha_{13}(1-D_{3j}) D_{4j} V_{2n}^{rend}(d_j) \\ & + \alpha_{16}\delta_{2n}(d_j) + \xi_{2n}(d_j+50) \end{aligned} \tag{5.33}$$

$$\begin{aligned} U_{3n}(d_j+50) = {} & \alpha_5 D_{1j} V_{3n}^{flagr}(d_j) + \alpha_8 D_{2j} V_{3n}^{rflead}(d_j) \\ & + \alpha_{11} D_{3j} V_{3n}^{rrlead}(d_j) + \alpha_{14}(1-D_{3j}) D_{4j} V_{3n}^{rend}(d_j) \\ & + \alpha_{17}\delta_{3n}(d_j) + \xi_{3n}(d_j+50) \end{aligned} \tag{5.34}$$

Where

$V_{in}^{flagr}(d_j)$: speed differential measured at position d_j (or fiducial mark j) between ramp vehicle and corresponding freeway lag vehicle, specified for alternative *i*, *i* = 1, 2, 3;

$V_{in}^{rflead}(d_j)$: speed differential measured at position d_j (or fiducial mark j) between ramp vehicle and corresponding freeway lead vehicle, specified for alternative *i*, *i* = 1, 2, 3;

$V_{in}^{rrlead}(d_j)$: speed differential measured at position d_j (or fiducial mark j) between ramp vehicle and corresponding ramp lead vehicle, specified for alternative *i*, *i* = 1, 2, 3;

$V_{in}^{rend}(d_j)$: speed differential measured at position d_j (or fiducial mark j) between ramp vehicle and acceleration lane terminus, specified for alternative *i*, *i* = 1, 2, 3;

$\delta_{in}(d_j)$: alternative specific dummy variable to capture successive observation correlation, *i* = 1, 2, 3;

$\delta_{in}(d_j)$ = 1 if ramp driver *n* chooses alternative *i* at both positions d_j and d_j+50 (or fiducial marks j and j+1)

= 0 Otherwise

$\xi_{in}(\bullet)$: disturbance term for alternative *i*, *i* = 1, 2, 3;

D_{1j}, D_{2j}, D_{3j}, and D_{4j} are the same as those defined in Eq.(5.9)

The use of d_j+50 in the left side of utility functions reflects the fact that only the data set that contains observations with one fiducial mark interval will be used in this analysis. Similar to those specified in Tables 5.22 to 5.24, all traffic attributes are defined as alternative specific variables. The alternative specific dummy variable, $\delta_{in}(\bullet)$, is termed a Markov index for it implicitly captures the unobservable serial correlation between current and preceding observations in the systematic component. Addition of these Markov indexes in the utility functions are important because ramp drivers are not expected to change speed dramatically during short time intervals. In other words, if a ramp driver was accelerating, or decelerating, at the fiducial mark j, with very

high likelihood he/she will still be accelerating, or decelerating, at the fiducial mark j+1. By specifying these Markov indexes in the systematic components, one can capture this serial correlation problem in the calibration procedures.

In addition to speed differentials, distance separations between ramp vehicle and corresponding freeway and ramp vehicles are another important attribute that should be considered. However, joint effects of these two attributes on ramp driver speed change decisions is not certain. In models 2, 3, and 4, different combination forms of speed differentials and distance separations will be specified in the systematic components. The model that achieves the best calibration results will be suggested as the ramp driver discrete acceleration-deceleration decision model.

Model 2: (speed differential and distance separation ratios between ramp vehicle and surrounding freeway and ramp vehicles as well as acceleration lane terminus are attributes)

$$\begin{aligned} U_{1n}(d_j+50) = {} & \alpha_1 + \alpha_3 D_{1j} X_{1n}^{flagr}(d_j) + \alpha_6 D_{2j} X_{1n}^{rflead}(d_j) \\ & + \alpha_9 D_{3j} X_{1n}^{rrlead}(d_j) + \alpha_{12}(1-D_{3j}) D_{4j} X_{1n}^{rend}(d_j) \\ & + \alpha_{15}\delta_{1n}(d_j) + \xi_{1n}(d_j+50) \end{aligned} \tag{5.35}$$

$$\begin{aligned} U_{2n}(d_j+50) = {} & \alpha_2 + \alpha_4 D_{1j} X_{2n}^{flagr}(d_j) + \alpha_7 D_{2j} X_{2n}^{rflead}(d_j) \\ & + \alpha_{10} D_{3j} X_{2n}^{rrlead}(d_j) + \alpha_{13}(1-D_{3j}) D_{4j} X_{2n}^{rend}(d_j) \\ & + \alpha_{16}\delta_{2n}(d_j) + \xi_{2n}(d_j+50) \end{aligned} \tag{5.36}$$

$$\begin{aligned} U_{3n}(d_j+50) = {} & \alpha_5 D_{1j} X_{3n}^{flagr}(d_j) + \alpha_8 D_{2j} X_{3n}^{rflead}(d_j) \\ & + \alpha_{11} D_{3j} X_{3n}^{rrlead}(d_j) + \alpha_{14}(1-D_{3j}) D_{4j} X_{3n}^{rend}(d_j) \\ & + \alpha_{17}\delta_{3n}(d_j) + \xi_{3n}(d_j+50) \end{aligned} \tag{5.37}$$

$$X_{in}^{flagr}(d_j) = \frac{V_{in}^{flagr}(d_j)}{S_{in}^{flagr}(d_j)} \tag{5.38}$$

$$X_{in}^{rflead}(d_j) = \frac{V_{in}^{rflead}(d_j)}{S_{in}^{rflead}(d_j)} \tag{5.39}$$

$$X_{in}^{\text{rrlead}}(d_j) = \frac{V_{in}^{\text{rrlead}}(d_j)}{S_{in}^{\text{rrlead}}(d_j)} \tag{5.40}$$

$$X_{in}^{\text{rend}}(d_j) = \frac{V_{in}^{\text{rend}}(d_j)}{S_{in}^{\text{rend}}(d_j)} \tag{5.41}$$

Where

$S_{in}^{\text{flagr}}(d_j)$: distance separation measured at position d_j (or fiducial mark j) between ramp vehicle and corresponding freeway lag vehicle, specified for alternative *i*, $i = 1, 2, 3$;

$S_{in}^{\text{rflead}}(d_j)$: distance separation measured at position d_j (or fiducial mark j) between ramp vehicle and corresponding freeway lead vehicle, specified for alternative *i*, $i = 1, 2, 3$;

$S_{in}^{\text{rrlead}}(d_j)$: distance separation measured at position d_j (or fiducial mark j) between ramp vehicle and corresponding ramp lead vehicle, specified for alternative *i*, $i = 1, 2, 3$;

$S_{in}^{\text{rend}}(d_j)$: distance separation measured at position d_j (or fiducial mark j) between ramp vehicle and acceleration lane terminus, specified for alternative *i*, $i = 1, 2, 3$;

Model 3: (angular velocities viewed by ramp drivers with respect to surrounding freeway and ramp vehicles as well as acceleration lane terminus are attributes)

$$\begin{aligned} U_{1n}(d_j + 50) = {} & \alpha_1 + \alpha_3 D_{1j} \omega_{1n}^{\text{flagr}}(d_j) + \alpha_6 D_{2j} \omega_{1n}^{\text{rflead}}(d_j) \\ & + \alpha_9 D_{3j} \omega_{1n}^{\text{rrlead}}(d_j) + \alpha_{12}(1 - D_{3j}) D_{4j} \omega_{1n}^{\text{rend}}(d_j) \\ & + \alpha_{15} \delta_{1n}(d_j) + \xi_{1n}(d_j + 50) \end{aligned} \tag{5.42}$$

$$\begin{aligned} U_{2n}(d_j + 50) = {} & \alpha_2 + \alpha_4 D_{1j} \omega_{2n}^{\text{flagr}}(d_j) + \alpha_7 D_{2j} \omega_{2n}^{\text{rflead}}(d_j) \\ & + \alpha_{10} D_{3j} \omega_{2n}^{\text{rrlead}}(d_j) + \alpha_{13}(1 - D_{3j}) D_{4j} \omega_{2n}^{\text{rend}}(d_j) \\ & + \alpha_{16} \delta_{2n}(d_j) + \xi_{2n}(d_j + 50) \end{aligned} \tag{5.43}$$

$$U_{3n}(d_j+50) = \alpha_5 D_{1j}\omega_{3n}^{flagr}(d_j) + \alpha_8 D_{2j}\omega_{3n}^{rflead}(d_j) + \alpha_{11} D_{3j}\omega_{3n}^{rrlead}(d_j) + \alpha_{14}(1-D_{3j})D_{4j}\omega_{3n}^{rend}(d_j) + \alpha_{17}\delta_{3n}(d_j) + \xi_{3n}(d_j+50) \quad (5.44)$$

Where

$\omega_{in}^{flagr}(d_j)$: angular velocity viewed by ramp driver at position d_j (or fiducial mark j) with respect to corresponding freeway lag vehicle, specified for alternative *i*, *i* = 1, 2, 3;

$\omega_{in}^{rflead}(d_j)$: angular velocity viewed by ramp driver at position d_j (or fiducial mark j) with respect to corresponding freeway lead vehicle, specified for alternative *i*, *i* = 1, 2, 3;

$\omega_{in}^{rrlead}(d_j)$: angular velocity viewed by ramp driver at position d_j (or fiducial mark j) with respect to corresponding ramp lead vehicle, specified for alternative *i*, *i* = 1, 2, 3;

$\omega_{in}^{rend}(d_j)$: angular velocity viewed by ramp driver at position d_j (or fiducial mark j) with respect to acceleration lane terminus, specified for alternative *i*, *i* = 1, 2, 3;

Model 4: (speed differentials and distance separations between ramp vehicle and surrounding freeway and ramp vehicles as well as acceleration lane terminus are attributes)

$$U_{1n}(d_j+50) = \alpha_1 + \alpha_3 D_{1j}V_{1n}^{flagr}(d_j) + \alpha_6 D_{2j}V_{1n}^{rflead}(d_j) + \alpha_9 D_{3j}V_{1n}^{rrlead}(d_j) + \alpha_{12}(1-D_{3j})D_{4j}V_{1n}^{rend}(d_j) + \alpha_{15}S_{1n}^{flagr}(d_j) + \alpha_{18}S_{1n}^{rflead}(d_j) + \alpha_{21}S_{1n}^{rrlead}(d_j) + \alpha_{24}S_{1n}^{rend}(d_j) + \alpha_{27}\delta_{1n}(d_j) + \xi_{1n}(d_j+50) \quad (5.45)$$

$$U_{2n}(d_j+50) = \alpha_2 + \alpha_4 D_{1j}V_{2n}^{flagr}(d_j) + \alpha_7 D_{2j}V_{2n}^{rflead}(d_j) + \alpha_{10} D_{3j}V_{2n}^{rrlead}(d_j) + \alpha_{13}(1-D_{3j})D_{4j}V_{2n}^{rend}(d_j) + \alpha_{16}S_{2n}^{flagr}(d_j) + \alpha_{19}S_{2n}^{rflead}(d_j) + \alpha_{22}S_{2n}^{rrlead}(d_j) + \alpha_{25}S_{2n}^{rend}(d_j) + \alpha_{28}\delta_{2n}(d_j) + \xi_{2n}(d_j+50) \quad (5.46)$$

$$
\begin{aligned}
U_{3n}(d_j + 50) = \quad & \alpha_5 D_{1j} V_{3n}^{flagr}(d_j) + \alpha_8 D_{2j} V_{3n}^{rflead}(d_j) \\
& + \alpha_{11} D_{3j} V_{3n}^{rrlead}(d_j) + \alpha_{14}(1 - D_{3j}) D_{4j} V_{3n}^{rend}(d_j) \\
& + \alpha_{17} S_{3n}^{flagr}(d_j) + \alpha_{20} S_{3n}^{rflead}(d_j) \\
& + \alpha_{23} S_{3n}^{rrlead}(d_j) + \alpha_{26} S_{3n}^{rend}(d_j) \\
& + \alpha_{29} \delta_{3n}(d_j) + \xi_{3n}(d_j + 50)
\end{aligned} \tag{5.47}
$$

The multinomial probit model is established by assuming that the vector of disturbances is multivariate normal distributed with a vector of means **0** and a variance-covariance matrix, $\sum_{\xi}$. If $\sum_{\xi}$ is not a function of the attribute matrix, it can have at most I(I-1)/2 estimable parameters that do not appear in utility specifications(Mahmassani, 1996). I is the number of choice alternatives. For a three choice alternatives case, the maximum number of parameters that can be specified in $\sum_{\xi}$ is 3. Although the exact specifications of the structure of this matrix is ultimately empirical, a hypothetical structure of the variance-covariance matrix of this analysis is specified as follows:

$$
\sum_{\xi} = \begin{bmatrix} \sigma^2 & \eta & \rho \\ \eta & \sigma^2 & \eta \\ \rho & \eta & \sigma^2 \end{bmatrix} \tag{5.48}
$$

η is the covariance of alternatives 1(deceleration) and 2(constant speed) as well as alternatives 2 and 3(acceleration). ρ is the covariance of alternatives 1 and 3. These parameters can be estimated through entire multinomial probit runs. In the multinomial logit model, η and ρ are implicitly forced to be 0 while σ is set to be 1.

The multinomial probit model estimation program, MNP, originally developed by Lam (1991) and later revised by Liu (1996), was applied in this study to estimate the discrete acceleration-deceleration choice model parameters, and the calibration results for Models 1, 2, 3, and 4 are shown in Tables 5.28 to 5.31 respectively. This new MNP estimation tool, based on a VMC (Vectorized Monte Carlo) simulation procedure and new implementations of quasi-Newton BFGS (Broyden-Fletcher-Goldfarb-Shanno) nonlinear procedures, had been successfully applied to calibrate Multinomial Probit Models with general specifications and relatively large numbers of choice alternatives (Jou 1994; Lam 1991).

TABLE 5.28 MULTINOMIAL PROBIT MODEL CALIBRATION RESULTS FOR MODEL 1

Parameter	Variable	Description	Estimates	t statistic
α_1		constant, specified for alternative 1	0.3541	7.751
α_2		constant, specified for alternative 2	1.0038	3.447
α_3	V_{1n}^{flagr}	speed differential to freeway lag vehicle, specified for alternative 1	0.2712	2.915
α_4	V_{2n}^{flagr}	speed differential to freeway lag vehicle, specified for alternative 2	0.1802	2.128
α_5	V_{3n}^{flagr}	speed differential to freeway lag vehicle, specified for alternative 3	0.1921	8.023
α_6	V_{1n}^{rflead}	speed differential to freeway lead vehicle, specified for alternative 1	0.1036	3.818
α_7	V_{2n}^{rflead}	speed differential to freeway lead vehicle, specified for alternative 2	-0.0658	-1.367
α_8	V_{3n}^{rflead}	speed differential to freeway lead vehicle, specified for alternative 3	-0.2501	-2.959
α_9	V_{1n}^{rrlead}	speed differential to ramp lead vehicle, specified for alternative 1	0.2719	5.494
α_{10}	V_{2n}^{rrlead}	speed differential to ramp lead vehicle, specified for alternative 2	0.0352	0.625
α_{11}	V_{3n}^{rrlead}	speed differential to ramp lead vehicle, specified for alternative 3	-0.1216	-2.230
α_{12}	V_{1n}^{rend}	speed differential to acceleration lane end, specified for alternative 1	0.3954	2.435
α_{13}	V_{2n}^{rend}	speed differential to acceleration lane end, specified for alternative 2	0.3203	3.849
α_{14}	V_{3n}^{rend}	speed differential to acceleration lane end, specified for alternative 3	0.1920	2.099

TABLE 5.28 (CONT.) MULTINOMIAL PROBIT MODEL CALIBRATION RESULTS FOR MODEL 1

Parameter	Variable	Description	Estimates	t statistic
α_{15}	δ_{1n}	Markov index, specified for alternative 1	14.8173	10.649
α_{16}	δ_{2n}	Markov index, specified for alternative 2	14.4900	9.477
α_{17}	δ_{3n}	Markov index, specified for alternative 3	15.0430	4.575
σ^2		variance	1.3824	8.107
η		covariance	0.0740	2.918
ρ		covariance	-0.0717	-1.689
$L(0)$			-1515	
$L(\hat{\beta})$			-724.08	
ρ^2			0.5221	
$\overline{\rho}^2$			0.5089	
# of obs.			1379	

TABLE 5.29 MULTINOMIAL PROBIT MODEL CALIBRATION RESULTS FOR MODEL 2

Parameter	Variable	Description	Estimates	t statistic
α_1		constant, specified for alternative 1	0.1609	5.920
α_2		constant, specified for alternative 2	0.8052	6.606
α_3	X_{1n}^{flagr}	speed differential/distance separation to freeway lag vehicle, alternative 1	4.0227	6.877
α_4	X_{2n}^{flagr}	speed differential/distance separation to freeway lag vehicle, alternative 2	0.6247	5.498
α_5	X_{3n}^{flagr}	speed differential/distance separation to freeway lag vehicle, alternative 3	2.5480	5.192
α_6	X_{1n}^{rflead}	speed differential/distance separation to freeway lead vehicle, alternative 1	-1.9684	-5.038
α_7	X_{2n}^{rflead}	speed differential/distance separation to freeway lead vehicle, alternative 2	-2.2434	-5.496
α_8	X_{3n}^{rflead}	speed differential/distance separation to freeway lead vehicle, alternative 3	-15.6629	-4.751
α_9	X_{1n}^{rrlead}	speed differential/distance separation to ramp lead vehicle, alternative 1	34.6648	7.366
α_{10}	X_{2n}^{rrlead}	speed differential/distance separation to ramp lead vehicle, alternative 2	4.3049	7.361
α_{11}	X_{3n}^{rrlead}	speed differential/distance separation to ramp lead vehicle, alternative 3	-28.7096	-5.944
α_{12}	X_{1n}^{rend}	speed differential/distance separation to acceleration lane end, alternative 1	100.0499	5.815
α_{13}	X_{2n}^{rend}	speed differential/distance separation to acceleration lane end, alternative 2	78.4504	5.507
α_{14}	X_{3n}^{rend}	speed differential/distance separation to acceleration lane end, alternative 3	72.0581	5.213

TABLE 5.29 (CONT.) MULTINOMIAL PROBIT MODEL CALIBRATION RESULTS FOR MODEL 2

Parameter	Variable	Description	Estimates	t statistic
α_{15}	δ_{1n}	Markov index, specified for alternative 1	14.8155	4.666
α_{16}	δ_{2n}	Markov index, specified for alternative 2	14.4801	4.585
α_{17}	δ_{3n}	Markov index, specified for alternative 3	15.0400	4.772
σ^2		variance	1.5326	4.460
η		covariance	-0.1981	-7.672
ρ		covariance	-0.2526	-8.892
$L(0)$			-1515	
$L(\hat{\beta})$			-741.20	
ρ^2			0.5108	
$\overline{\rho}^2$			0.4976	
# of obs.			1379	

TABLE 5.30 MULTINOMIAL PROBIT MODEL CALIBRATION RESULTS FOR MODEL 3

Parameter	Variable	Description	Estimates	t statistic
α_1		constant, specified for alternative 1	0.0060	1.513
α_2		constant, specified for alternative 2	0.5620	6.244
α_3	$\omega_{1n}^{\text{flagr}}$	angular velocity w. r. t. freeway lag vehicle, specified for alternative 1	3.5865	7.301
α_4	$\omega_{2n}^{\text{flagr}}$	angular velocity w. r. t. freeway lag vehicle, specified for alternative 2	0.5508	6.038
α_5	$\omega_{3n}^{\text{flagr}}$	angular velocity w. r. t. freeway lag vehicle, specified for alternative 3	0.6285	6.458
α_6	$\omega_{1n}^{\text{rflead}}$	angular velocity w. r. t. freeway lead vehicle, specified for alternative 1	-2.3426	-6.374
α_7	$\omega_{2n}^{\text{rflead}}$	angular velocity w. r. t. freeway lead vehicle, specified for alternative 2	-1.2418	-4.901
α_8	$\omega_{3n}^{\text{rflead}}$	angular velocity w. r. t. freeway lead vehicle, specified for alternative 3	-11.0084	-4.174
α_9	$\omega_{1n}^{\text{rrlead}}$	angular velocity w. r. t. ramp lead vehicle, specified for alternative 1	286.442	5.846
α_{10}	$\omega_{2n}^{\text{rrlead}}$	angular velocity w. r. t. ramp lead vehicle, specified for alternative 2	36.3143	4.293
α_{11}	$\omega_{3n}^{\text{rrlead}}$	angular velocity w. r. t. ramp lead vehicle, specified for alternative 3	2.3271	6.642
α_{12}	$\omega_{1n}^{\text{rend}}$	angular velocity w. r. t. acceleration lane end, specified for alternative 1	309.820	6.308
α_{13}	$\omega_{2n}^{\text{rend}}$	angular velocity w. r. t. acceleration lane end, specified for alternative 2	242.042	5.227
α_{14}	$\omega_{3n}^{\text{rend}}$	angular velocity w. r. t. acceleration lane end, specified for alternative 3	181.951	4.696

TABLE 5.30 (CONT.) MULTINOMIAL PROBIT MODEL CALIBRATION RESULTS FOR MODEL 3

Parameter	Variable	Description	Estimates	t statistic
α_{15}	δ_{1n}	Markov index, specified for alternative 1	14.8224	5.552
α_{16}	δ_{2n}	Markov index, specified for alternative 2	14.4948	5.212
α_{17}	δ_{3n}	Markov index, specified for alternative 3	15.0367	5.586
σ^2		variance	1.1360	4.636
η		covariance	0.1580	7.976
ρ		covariance	-0.3927	-5.008
$L(0)$			-1515	
$L(\hat{\beta})$			-799.62	
ρ^2			0.4722	
$\overline{\rho}^2$			0.4590	
# of obs.			1379	

TABLE 5.31 MULTINOMIAL PROBIT MODEL CALIBRATION RESULTS FOR MODEL 4

Parameter	Variable	Description	Estimates	t statistic
α_1		constant, specified for alternative 1	0.0047	0.802
α_2		constant, specified for alternative 2	0.0003	0.212
α_3	V_{1n}^{flagr}	speed differential to freeway lag vehicle, specified for alternative 1	0.2410	5.747
α_4	V_{2n}^{flagr}	speed differential to freeway lag vehicle, specified for alternative 2	0.0710	3.119
α_5	V_{3n}^{flagr}	speed differential to freeway lag vehicle, specified for alternative 3	0.2329	5.649
α_6	V_{1n}^{rflead}	speed differential to freeway lead vehicle, specified for alternative 1	0.1410	4.396
α_7	V_{2n}^{rflead}	speed differential to freeway lead vehicle, specified for alternative 2	-0.0739	-3.184
α_8	V_{3n}^{rflead}	speed differential to freeway lead vehicle, specified for alternative 3	-0.3098	-6.519
α_9	V_{1n}^{rrlead}	speed differential to ramp lead vehicle, specified for alternative 1	0.2290	5.602
α_{10}	V_{2n}^{rrlead}	speed differential to ramp lead vehicle, specified for alternative 2	0.0420	2.400
α_{11}	V_{3n}^{rrlead}	speed differential to ramp lead vehicle, specified for alternative 3	-0.1699	-4.828
α_{12}	V_{1n}^{rend}	speed differential to acceleration lane end, specified for alternative 1	0.3380	6.807
α_{13}	V_{2n}^{rend}	speed differential to acceleration lane end, specified for alternative 2	0.3090	6.508
α_{14}	V_{3n}^{rend}	speed differential to acceleration lane end, specified for alternative 3	0.3210	6.633

TABLE 5.31 (CONT.) MULTINOMIAL PROBIT MODEL CALIBRATION RESULTS FOR MODEL 4

Parameter	Variable	Description	Estimates	t statistic
α_{15}	S_{1n}^{flagr}	distance separation to freeway lag vehicle, specified for alternative 1	0.0121	1.286
α_{16}	S_{2n}^{flagr}	distance separation to freeway lag vehicle, specified for alternative 2	0.0040	0.745
α_{17}	S_{3n}^{flagr}	distance separation to freeway lag vehicle, specified for alternative 3	0.0152	1.442
α_{18}	S_{1n}^{rflead}	distance separation to freeway lead vehicle, specified for alternative 1	0.0071	0.985
α_{19}	S_{2n}^{rflead}	distance separation to freeway lead vehicle, specified for alternative 2	-0.0021	-0.541
α_{20}	S_{3n}^{rflead}	distance separation to freeway lead vehicle, specified for alternative 3	-0.0036	-0.705
α_{21}	S_{1n}^{rrlead}	distance separation to ramp lead vehicle, specified for alternative 1	0.0113	1.244
α_{22}	S_{2n}^{rrlead}	distance separation to ramp lead vehicle, specified for alternative 2	0.0032	0.663
α_{23}	S_{3n}^{rrlead}	distance separation to ramp lead vehicle, specified for alternative 3	0.0051	0.838
α_{24}	S_{1n}^{rend}	distance separation to acceleration lane end, specified for alternative 1	0.0179	1.567
α_{25}	S_{2n}^{rend}	distance separation to acceleration lane end, specified for alternative 2	0.0175	1.547
α_{26}	S_{3n}^{rend}	distance separation to acceleration lane end, specified for alternative 3	0.0322	2.100

TABLE 5.31 (CONT.) MULTINOMIAL PROBIT MODEL CALIBRATION RESULTS FOR MODEL 4

Parameter	Variable	Description	Estimates	t statistic
α_{27}	δ_{1n}	Markov index, specified for alternative 1	14.8200	9.014
α_{28}	δ_{2n}	Markov index, specified for alternative 2	14.4900	8.913
α_{29}	δ_{3n}	Markov index, specified for alternative 3	15.0400	9.081
σ^2		variance	1.0000	4.677
η		covariance	0.2000	5.236
ρ		covariance	-0.1000	-3.703
$L(0)$			-1515	
$L(\hat{\beta})$			-7.170	
ρ^2			0.9953	
$\overline{\rho}^2$			0.9741	
# of obs.			1379	

All four models were calibrated using the same data with the same set of alternatives. The only difference is the utility function specifications. At first sight, model 4 appears to be the best model since it has the highest $\overline{\rho}^2$ value. Unfortunately, many variables, especially those related to the attributes of distance separations, are insignificant at any reasonable significance level. This significant drawback rules out model 4 from further consideration. Generally speaking, the other three models are almost equally good. It is a challenge to make a firm conclusion. Model 1 is best in terms of the $\overline{\rho}^2$ value, however, it is not appropriate to compare models solely based on $\overline{\rho}^2$ when all the $\overline{\rho}^2$ values have similar magnitudes. Model 2 has a slightly smaller $\overline{\rho}^2$ than model 1, but unlike model 1 has a parameter, α_7, that is insignificant at any reasonable significance level. Model 2 outshines model 1 through the fact that all of its parameters are significant at a 5% significance level. Model 2 is also superior in $\overline{\rho}^2$ value to model 3 even though all of its parameters are significant. All these considerations suggest model 2 is most appropriate for modeling ramp driver discrete acceleration-deceleration choice behavior. This result also supports the hypothesis that both speed differentials and distance separations have a joint effect on ramp driver acceleration-deceleration behavior, although it is still not clear how drivers combine these two attributes into one singular decision criterion. In the following discussions, all attention will be given to model 2.

The parameter α_3 has a larger value than α_5 implying that when the freeway lag vehicle has a higher speed than the ramp vehicle, a positive speed differential, the smaller the distance separation between these two vehicles, the higher the probability that the ramp driver will make a deceleration decision. This result corresponds with one's driving experience. When a freeway vehicle is closing on a ramp vehicle, most likely the ramp driver will reduce speed so as to provide a better position for later acceptable gaps, however, some drivers will choose acceleration to merge before the freeway lag vehicle. Maintaining constant speeds, under such a circumstance, will enjoy least utility. On the contrary, when a ramp vehicle has a higher speed than its corresponding freeway lag vehicle, a negative speed differential, then the ramp driver will probably accelerate or maintain constant speed. Deceleration, under this circumstance, will be less attractive.

Parameters, α_6, α_7, and α_8, that relate to freeway lead vehicles have negative signs indicating that when a ramp vehicle is closing, with a higher speed, on its corresponding freeway lead vehicle, negative utility will be experienced no matter which alternative is chosen. This result might be due to the fact that the ramp driver is uncomfortable and feels unsafe being forced to adjust speeds to avoid a potential collision. However, with the highest likelihood, the ramp driver, under such a circumstance, will choose deceleration due to its comparatively smaller negative utility. Choosing acceleration is rare, as indicated by the fairly large negative α_8 coefficient, unless

the ramp driver can confidently overtake the freeway lead vehicle and safely merge before reaching the acceleration lane end.

It is reasonable to argue that when a ramp vehicle has a higher speed than its corresponding ramp lead vehicle, a positive speed differential, with very high probability the ramp driver will choose deceleration. The shorter the distance separation, the larger the probability would be. This argument is strongly supported by the fact that α_9 has a positive sign. It is very unlikely that under such a circumstance, the ramp driver will choose acceleration due to the negative coefficient of parameter α_{11}. The opposite signs of α_9 and α_{11} reveal that, in any case, a ramp driver would tend to favor only one alternative. This is true because a ramp driver cannot overtake its corresponding ramp lead vehicle without making an early merge. Therefore, when a ramp driver senses a positive speed differential to its ramp lead vehicle, the best choice alternative will be to reduce his/her speeds. The acceleration lane terminus is a final decision point where ramp drivers must either risk a forced merge or stop before reaching the ramp end. The calibration results show that the parameter α_{12} has the largest positive value among α_{12}, α_{13}, and α_{14} implying that ramp drivers, with highest probability, will decelerate while he/she is approaching the acceleration lane terminus. These three parameters, however, are not significantly different from each other in magnitudes revealing that many ramp drivers will be predicted to choose the alternatives of acceleration or maintaining constant speed when they are closing on the ramp end. These conclusions correspond with those discussed in Sections 3.4.2.1 and 3.4.2.2.

The calibrated results of the three Markov index parameters, namely α_{15}, α_{16}, and α_{17}, are impressive. They all have positive signs and almost equal magnitudes. This result confirms the expectation that ramp drivers will have the largest utility if they choose the same alternative at successive fiducial marks. In other words, continuously switching from one alternative to another is not likely to be predicted by this model unless some traffic attributes have strong joint utility contributions favoring switching. This argument can be justified by the fact that the magnitudes of traffic attributes, namely speed differential and distance separation ratios, are comparatively small and in turn their utility contributions are small. The Markov indexes, on the other hand, will have large utility contributions as long as ramp drivers stay with the same choice alternative. The inclusion of the Markov indexes in the systematic components is a great success for it not only effectively captures dynamic driver choice behavior but also allows the model to make robust predictions.

Continuous Acceleration-deceleration Model

Tables 5.20 and 5.21 illustrated that ramp vehicle speed is the only variable that has a high correlation coefficient with both vehicle acceleration and deceleration rates. Recalling that acceleration, by definition, is the time-rate-change of speed, one would not be surprised by that result. Consequently, one should be able to expect fairly reliable acceleration-deceleration rate estimations using instantaneous vehicle speed as a sole explanatory variable. Unlike the one fiducial mark interval data set used in the discrete acceleration-deceleration choice analysis, the data set that contains instantaneous acceleration-deceleration and speed observations will be used in this analysis. The scatter plots of acceleration and deceleration rates *versus* ramp vehicle speeds are shown in Figures 5.8 and 5.9 respectively. Impressively, there exists a family of curves in both figures. In Figure 5.8, one can visibly identify a family of two distinct curves, denoted as curves 1 and 2 respectively. While in Figure 5.9, a family of three distinguishable curves, denoted as curves 1, 2, and 3 respectively, are clearly seen. A few outliers in Figure 5.9 seems to form a forth curve, however, due to the small quantity, these outliers were incorporated into curve 3. It is not surprising that drivers who have the same driving speeds adopt different acceleration or deceleration rates. This phenomenon might be caused by vehicle performance, driver aggressiveness, or other unobservable driver vehicle factors. Fortunately, the trends illustrated in Figures 5.8 and 5.9 confirm that vehicle speed should be a good explanatory variable to capture most of the effects causing acceleration-deceleration variations. Historically, ramp vehicle acceleration-deceleration issues have been oversimplified in most research and practical engineering works. Therefore, the finding of families of acceleration as well as deceleration curves should be able to provide a great opportunity to enhance practical applications. The scatter diagram was extensively examined and traced to identify the vehicle that each point represents. However, there is no significant evidence to guarantee that a certain driver's acceleration or deceleration observations will always fall on the same curve. In other words, even running at the same speed, a ramp driver might show different acceleration or deceleration rates. For practical applications, this randomness can be accommodated by introducing probabilistic random numbers to determine which curve should be applied to estimate acceleration-deceleration rate magnitudes.

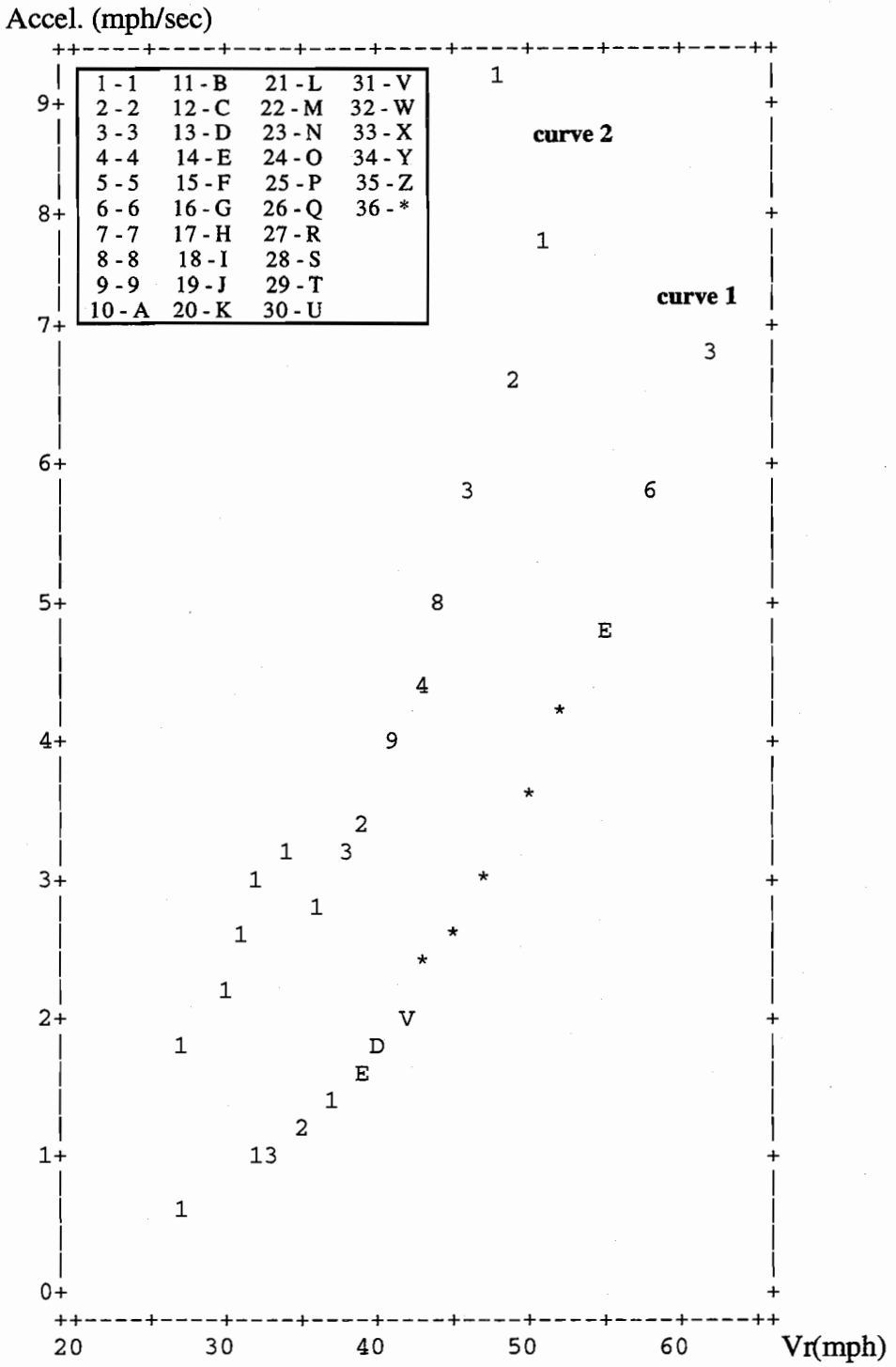

Figure 5.8 Scatter plot of acceleration rates vs. ramp vehicle speeds

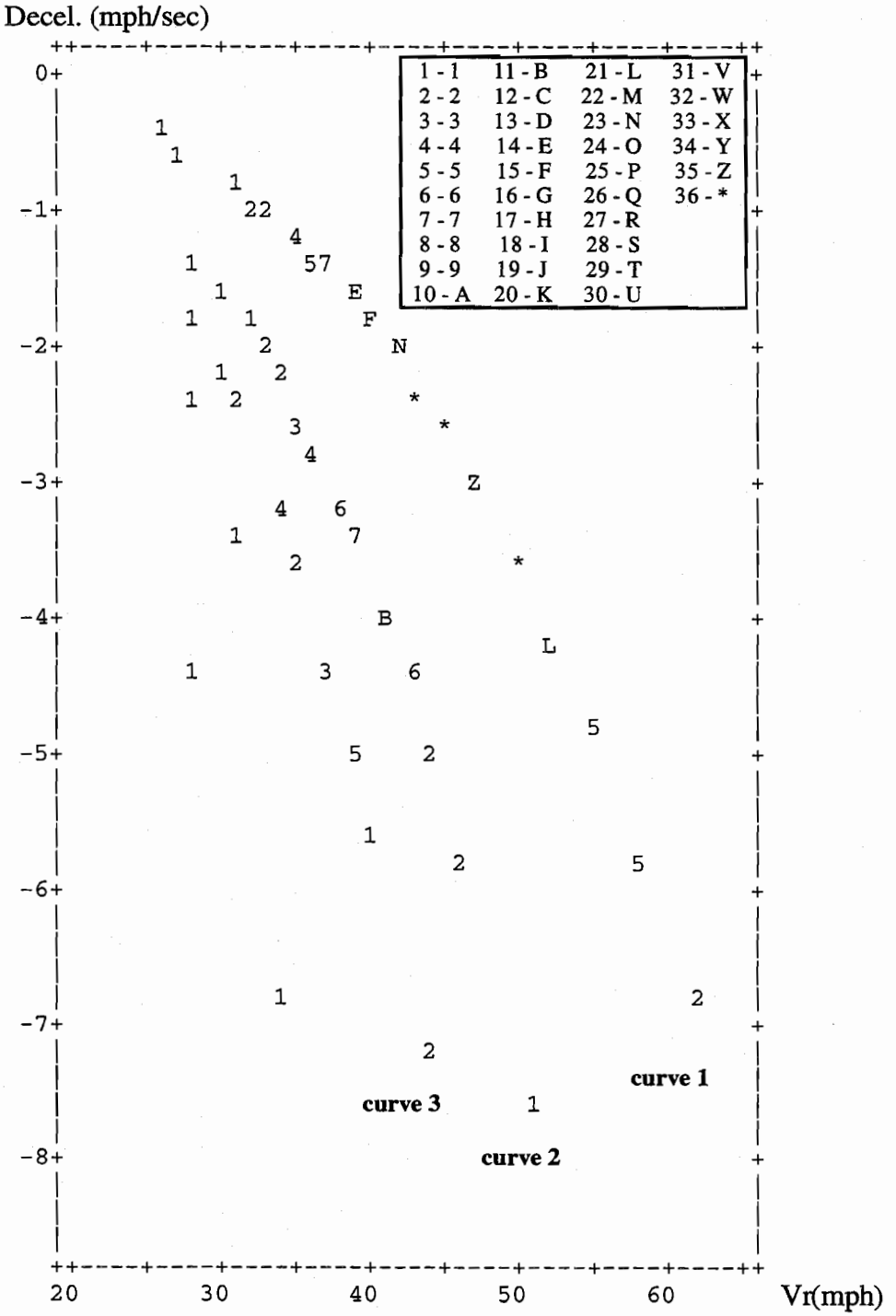

Figure 5.9 Scatter plot of deceleration rates vs. ramp vehicle speeds

Instead of having a linear relationship, all the curves shown in Figures 5.8 and 5.9 visibly have exponential trends. The hypothetical expressions of continuous acceleration and deceleration models are shown as follows:

Acceleration model

$$\text{Accel} = e^{a + bV_r} \tag{5.49}$$

Deceleration model

$$\text{Decel} = -e^{a + bV_r} \tag{5.50}$$

All curves were calibrated respectively using their own data sets. With simple transformations, all cases can be easily estimated using conventional linear regression procedures. The results are shown in Tables 5.32 and 5.33 for acceleration models and Tables 5.34 to 5.36 for deceleration models. The calibration results of each curve are promising with significant coefficients in all parameters and high adjusted R-squared values. Surprisingly, simple models even perform much better in ramp vehicle acceleration-deceleration rate prediction than those complicated nonlinear models, such as Eqs.(5.9) and (5.10). Of the acceleration rate observations, 386 (91.04%) observations were incorporated into curve 1 indicating that ramp drivers follow a somewhat more uniform pattern in terms of acceleration maneuvers. Of the deceleration rate observations, 273 (79.13%) and 48 (13.91%) observations were incorporated into curves 1 and 2 respectively revealing that there are more random variations associated with deceleration maneuvers. This phenomenon might be due to the fact that ramp drivers do not intend to decelerate during freeway merge maneuvers unless it is necessary. Consequently, some drivers might occasionally make stronger deceleration maneuvers resulting in greater deceleration rate variations. The calibrated models should not be extrapolated when ramp vehicle speeds are less than 25 mph or greater than 65 mph that is the observed data range.

TABLE 5.32 CALIBRATION RESULTS FOR ACCELERATION MODEL - CURVE 1

Multiple R	.99539	Analysis of Variance			
R Square	.99081		DF	Sum of Squares	
Adjusted R Square	.99078	Regression	1	40.08353	
Standard Error	.03108	Residual	385	.37185	
		F = 41500.75251		Signif F = .0000	

Variable	B	SE B	Beta	T	Sig T
VR	.065382	3.2094E-04	.995394	203.717	.0000
(Constant)	-1.995106	.015173		-131.487	.0000

TABLE 5.33 CALIBRATION RESULTS FOR ACCELERATION MODEL - CURVE 2

Multiple R	.95817	Analysis of Variance			
R Square	.91808		DF	Sum of Squares	
Adjusted R Square	.91587	Regression	1	3.76857	
Standard Error	.09533	Residual	37	.33626	
		F = 414.67291		Signif F = .0000	

Variable	B	SE B	Beta	T	Sig T
VR	.059879	.002940	.958166	20.364	.0000
(Constant)	-1.039153	.122534		-8.481	.0000

TABLE 5.34 CALIBRATION RESULTS FOR DECELERATION MODEL - CURVE 1

Multiple R	.99394	Analysis of Variance			
R Square	.98792		DF	Sum of Squares	
Adjusted R Square	.98787	Regression	1	39.41053	
Standard Error	.04210	Residual	272	.48202	
		F = 22239.18991		Signif F = .0000	
Variable	B	SE B	Beta	T	Sig T
VR	.068264	4.5775E-04	.993940	149.128	.0000
(Constant)	-2.131431	.020872		-102.117	.0000

TABLE 5.35 CALIBRATION RESULTS FOR DECELERATION MODEL - CURVE 2

Multiple R	.99612	Analysis of Variance			
R Square	.99225		DF	Sum of Squares	
Adjusted R Square	.99209	Regression	1	5.32108	
Standard Error	.02973	Residual	47	.04155	
		F = 6019.25152		Signif F = .0000	
Variable	B	SE B	Beta	T	Sig T
VR	.077906	.001004	.996119	77.584	.0000
(Constant)	-1.830672	.039501		-46.345	.0000

TABLE 5.36 CALIBRATION RESULTS FOR DECELERATION MODEL - CURVE 3

Multiple R	.84088	Analysis of Variance			
R Square	.70707		DF	Sum of Squares	
Adjusted R Square	.69434	Regression	1	2.24718	
Standard Error	.20119	Residual	23	.93096	
		F = 55.51806		Signif F = .0000	
Variable	B	SE B	Beta	T	Sig T
VR	.067192	.009018	.840877	7.451	.0000
(Constant)	-.988289	.318402		-3.104	.0050

Conceptual Integration of Bi-level Acceleration-deceleration Model in Microscopic Freeway Simulation

The bi-level acceleration-deceleration models have some potential applications. Among them, integration in existing microscopic freeway simulation models is the most promising one. This application is straightforward and can be easily implemented through incorporating random number generation. A conceptually logical diagram of integration in microscopic freeway simulation models is demonstrated in Figure 5.10. The threshold values suggested in this diagram to determine which curve should be used to estimate acceleration-deceleration rates are calculated based on the collected observations. These values, however, are subject to change if local data are available. The tasks of computing alternative choice probabilities under the multinomial probit framework are somewhat cumbersome and ought to be evaluated numerically. Using the freeway simulation model, the entrance ramp delay problem, queuing length estimation, ramp metering control strategy, acceleration lane geometric configuration, and merge area level of service can be evaluated.

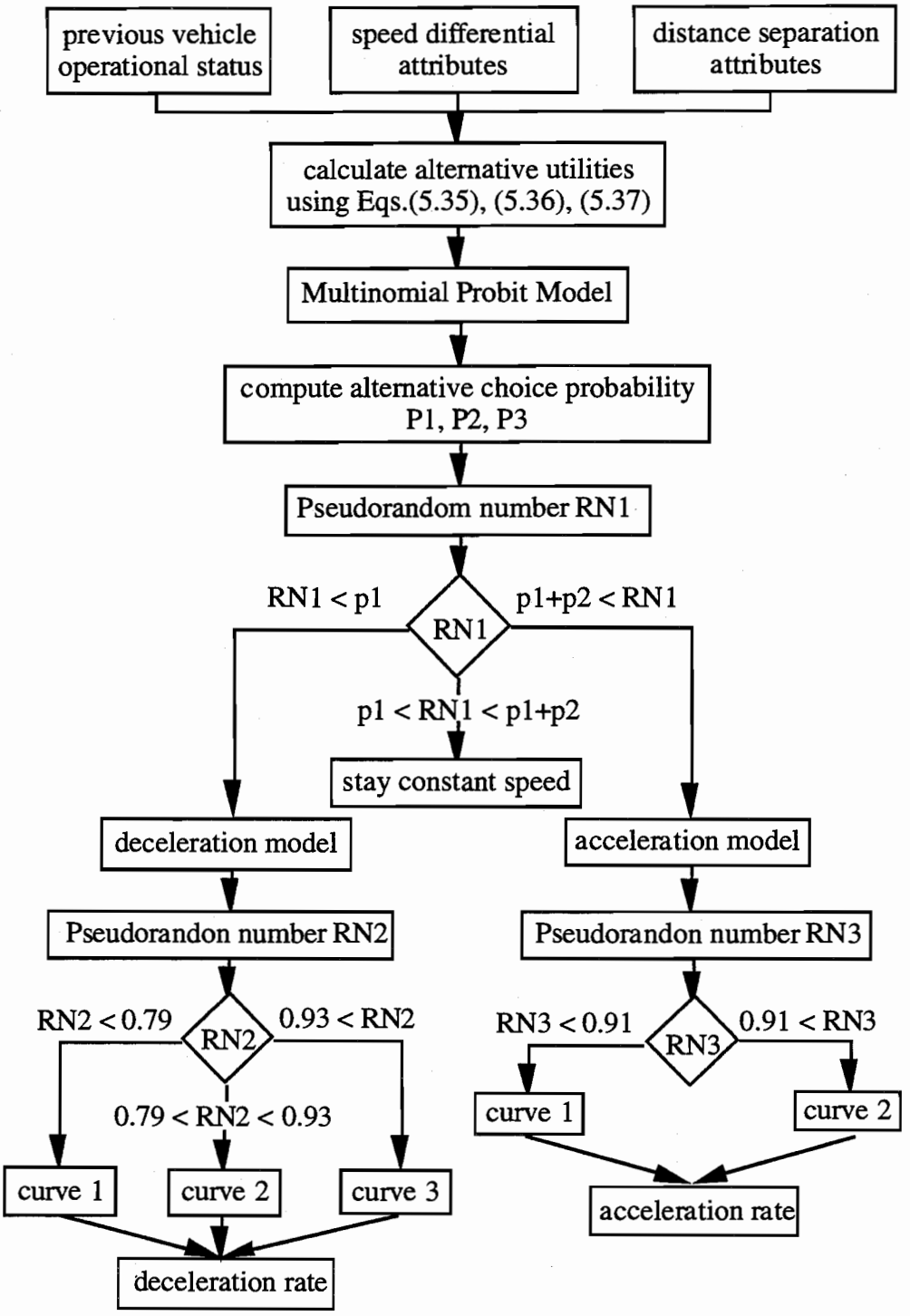

Figure 5.10 Conceptual diagram for microscopic simulation applications

SUMMARY

This chapter has presented the results of freeway merge traffic characteristics analyses and ramp vehicle acceleration-deceleration model calibrations. Freeway merge observations were collected from a taper type entrance ramp on Loop 610 in Houston, Texas. A revised nonlinear mathematical framework incorporating dummy variables to generalize models proposed in chapter 3 was developed to involve all possible freeway merge traffic vehicle situations. Calibrations using this revised nonlinear model on different data subsets were performed. Unsatisfactory calibration results lead to the development of bi-level calibration procedures which involve solving discrete choice behavior models to predict decision choice probabilities and then continuous regression models to estimate acceleration-deceleration rates. Several findings drawn from these analyses are summarized as follows:

1. Mean ramp vehicle speeds calculated between each fiducial mark pair are not significantly different across all fiducial marks while the mean acceleration-deceleration rates are. The speed scatter plots, however, illustrate very wide spread indicating that each ramp vehicle has a considerably different acceleration lane speed history.

2. The distribution of speed differential illustrates that, at their merge point, approximately 50% of the ramp vehicles have a similar or higher speed than their corresponding freeway lag vehicles. Fifty percentage of the ramp drivers have an accepted angular velocity approximately equal to or less than 0.00 rads/sec. The median accepted angular velocity was found to be 0.00088 rads/sec which is smaller than the nominal threshold value of 0.004 rads/sec proposed by Michaels (1963). About 70% of the ramp drivers accepted an angular velocity ranging between -0.01 rads/sec and 0.01 rads/sec.

3. As a first step, calibrations were performed using all vehicle trajectory observation data covering a wide variety of situations. The results, however, show low R-squared values for all cases revealing that the nonlinear and angular velocity models statistically have very poor ability to explain ramp vehicle acceleration-deceleration rate variations.

4. Based on the hypothesis that drivers pay more attention to closer vehicles than to fara way vehicles, weighting factors characterized by the longitudinal distances between ramp vehicles and surrounding vehicles were specified. The calibration results still showed very low R-squared values. This unsuccessful attempt lead to the recognition that complex freeway merge traffic flow might not be well described using such sophisticated formulations.

5. All observations were split into ten homogeneous subgroups having uncontrolled sample sizes based on the presence of corresponding freeway lag, freeway lead, or ramp lead vehicles. Nonlinear models were calibrated using each subgroup. The R-squared values of all cases are

small except for several subgroups that have very small sample sizes. Unfortunately, small sample sizes makes the resulting high R-squared values less meaningful.

6. Each homogeneous subgroup data set was further split into even more homogeneous sub-subgroups based on distance separations between ramp vehicles and corresponding freeway and ramp vehicles. As before, R-squared values of all cases were small except for several small sample size subgroups indicating that this approach was not successful, either.

7. All data were split into three subgroups containing observations of positive, negative, and zero acceleration rates, respectively. The resulting R-squared values were still not good enough. None of the R-squared values was greater than 0.30.

8. Correlation analysis shows that ramp vehicle speed is the only variable that demonstrates high correlation coefficient with acceleration-deceleration rate. Other traffic variables have very poor correlation coefficients; and this explains why good calibration results cannot be obtained using the proposed sophisticated nonlinear models.

9. Although traffic attributes, such as speed differential, distance separation, and angular velocity, cannot be shown to be good predictors for ramp vehicle acceleration-deceleration "rates", they are believed to be important factors affecting ramp driver acceleration-deceleration "decisions". This hypothesis leads to the development of a bi-level calibration framework that uses discrete choice methods to predict acceleration-deceleration choice probabilities and a continuous model to estimate acceleration-deceleration rates.

10. Preliminary multinomial logit calibration showed that the data set with one fiducial mark interval, D=50 feet, had the highest ρ^2 and $\overline{\rho}^2$ values suggesting this data set's potential for calibrating ramp driver acceleration-deceleration choice behavior.

11. A multinomial probit calibration result suggested that the model characterized by ratios of speed differential and distance separation between ramp vehicles and corresponding freeway and ramp vehicles is most appropriated for modeling ramp driver discrete acceleration-deceleration choice behavior. It is, however, still not clear how drivers combine these two attributes into one singular decision criterion.

12. Markov indexes, attributes specified in the multinomial probit model systematic components, were shown to have large utility contributions because ramp drivers tend to stay with the same choice alternative. The inclusion of Markov indexes was impressive for it not only effectively captured dynamic driver choice behavior but also allowed the model to make robust predictions.

13. Scatter plots of acceleration and deceleration rates *versus* ramp vehicle speeds demonstrated that a family of curves exists in both figures. In the acceleration case, one can visibly

identify a family of two distinct curves. While in deceleration case, a family of three distinguishable curves are clearly seen. This phenomenon perfectly corresponds to dynamic driver behavior for it is true that drivers might apply different acceleration or deceleration rates even though they are running at the same speeds.

14. This chapter described successful calibration of both discrete acceleration-deceleration choice models and continuous acceleration-deceleration rate prediction models. Integration of the bi-level models in existing microscopic freeway simulation models is promising.

CHAPTER 6. CALIBRATION OF RAMP DRIVER GAP ACCEPTANCE MODEL

INTRODUCTION

In chapter 3, a conceptual freeway merge critical gap distribution model was proposed. To calibrate that critical gap distribution, a large quantity of data involving gap acceptance as well as rejection is desirable. The limited quantity of data collected for use in the previously presented pilot study, however, make it difficult to perform such a calibration. In this chapter, freeway merge observation data collected from a taper type entrance ramp in Houston Texas, as presented in chapter 5, were used. This data set contains a considerably larger quantity of freeway merge observations which is believed to be a reasonable magnitude for model development. The proposed model, as shown in Eq.(3.77), specified gap acceptance threshold, characterized by corresponding angular velocity, as a function of the number of gaps previously rejected and the remaining distance to the acceleration lane terminus. To expect a statistically significant coefficient for the parameter describing the number of gaps being rejected, one should have a comparatively large quantity of gap rejection observations. In addition, the gap sizes accepted by ramp drivers who had rejected gaps are expected to follow different trends from those of drivers who rejected no gaps before merging.

Presentation of this chapter starts with the investigation of gap acceptance characteristics differences between drivers who had rejected at least one gap and who rejected no gaps before merging. The investigation results lead to a revision of the proposed critical gap distribution model by eliminating the term regarding rejected gap number. Without emphasizing the sequential gaps being rejected, one can simply calibrate the ramp driver gap acceptance function using a binary choice model. Several systematic component specifications characterized by both freeway lag and lead vehicle parameters have been tested to determine the best model. All freeway lead vehicle related parameters were found to insignificant indicating that ramp drivers are more attentive to corresponding freeway lag vehicle movements during the gap search process. Before closing, the developed gap acceptance function is transformed into a critical gap distribution and the remaining distance to acceleration lane terminus effect on ramp driver gap acceptance behavior is discussed.

GAP ACCEPTANCE-REJECTION ANALYSIS

Of the observed ramp drivers, only 6.39% and 0.46% had rejected one and two gaps respectively before merging. For the observed cases of medium to high freeway right lane traffic

volume, this finding is not surprising. At the entrance ramp under study, most ramp drivers spent approximately 4 - 7 seconds in the acceleration lane before merging. During such a short time, there is only a small chance that ramp vehicles will be overtaken by corresponding freeway lag vehicles because of a speed differential effect. This situation, however, will be different when freeway traffic volume becomes larger. Knowing whether the number of rejected gap has a significant effect upon gap acceptance behavior is very desirable. If this effect does exist, one should be able to observe a gap acceptance trend difference between reject-no-gap and reject-gap driver groups. For instance, those ramp drivers who had rejected gaps might be consistently found to accept small time gaps due to decreasing merge chances. To illustrate this difference, graphical presentations of gap acceptance parameters *versus* merge positions for both reject-no-gap and reject-gap driver groups are given respectively in Figures 6.1 to 6.10.

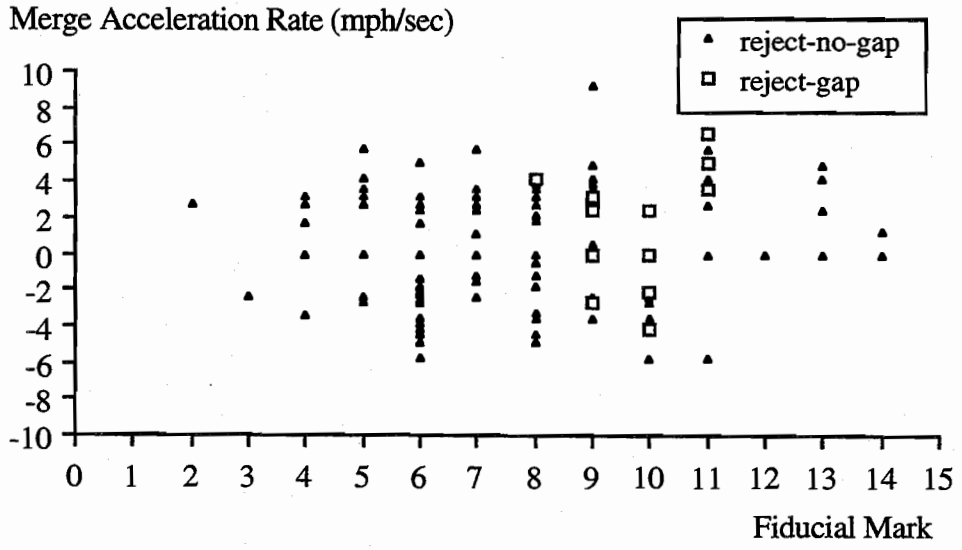

Figure 6.1 Ramp vehicle merge acceleration rate vs. merge position for reject-no-gap and reject-gap driver groups

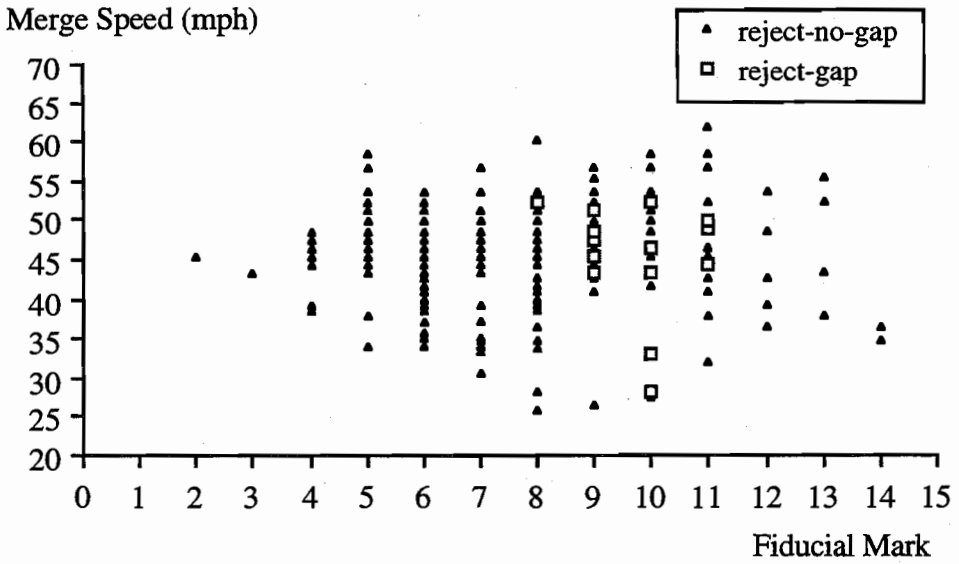

Figure 6.2 Ramp vehicle merge speed vs. merge position for reject-no-gap and reject-gap driver groups

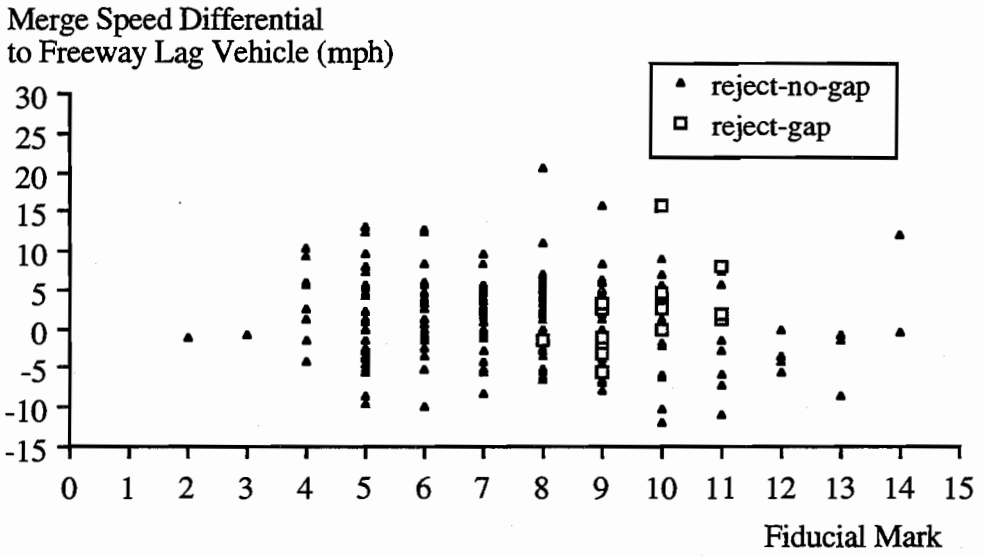

Figure 6.3 Merge speed differential to freeway lag vehicle vs. merge position for reject-no-gap and reject-gap driver groups

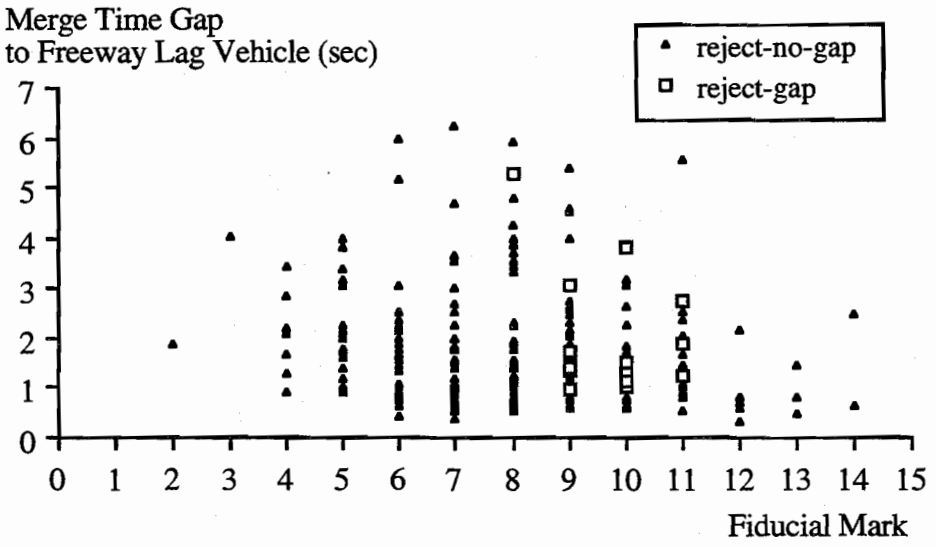

Figure 6.4 Merge time gap to freeway lag vehicle vs. merge position for reject-no-gap and reject-gap driver groups

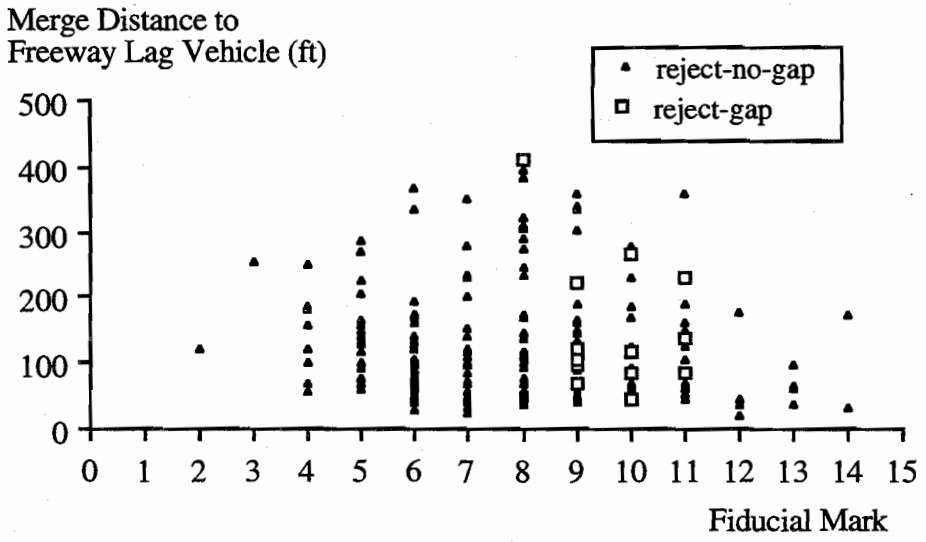

Figure 6.5 Merge distance to freeway lag vehicle vs. merge position for reject-no-gap and reject-gap driver groups

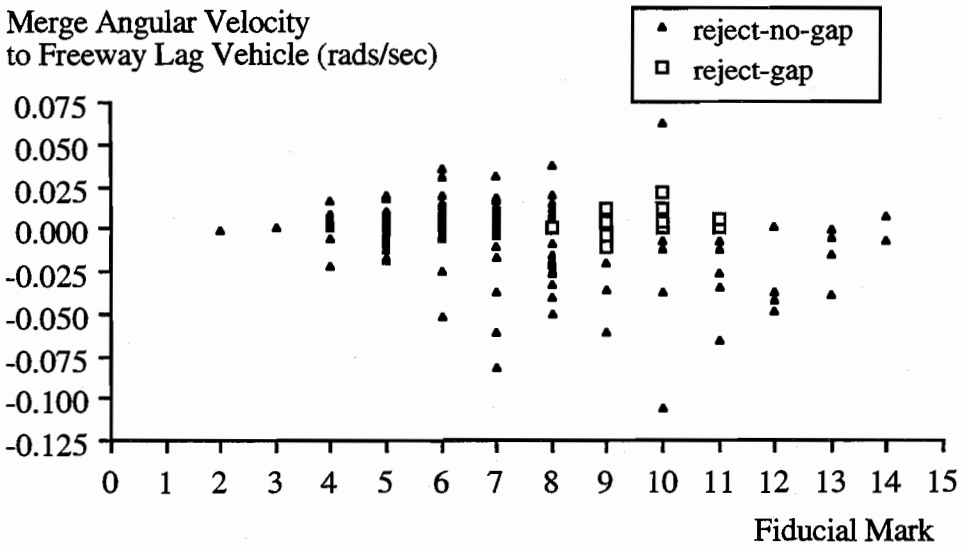

Figure 6.6 Merge angular velocity to freeway lag vehicle vs. merge position for reject-no-gap and reject-gap driver groups

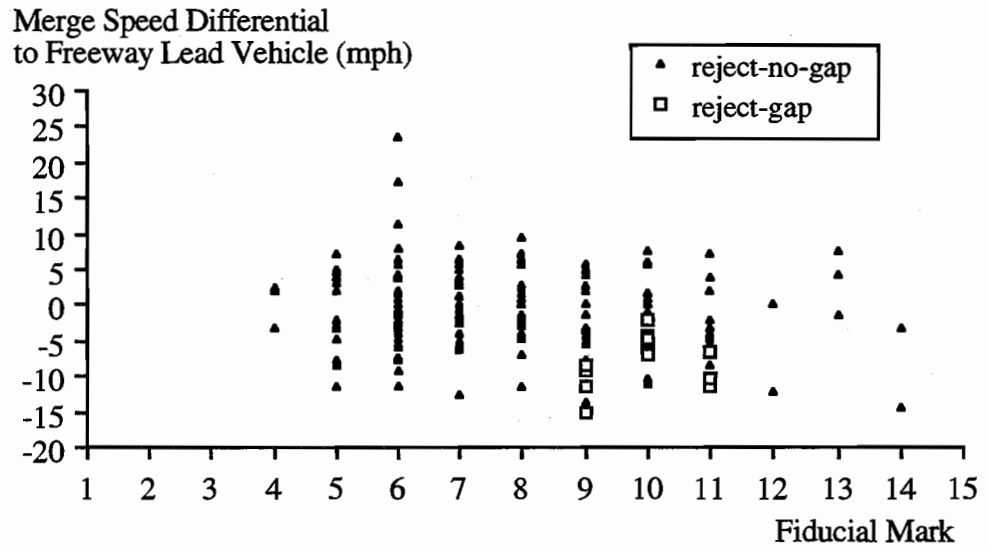

Figure 6.7 Merge speed differential to freeway lead vehicle vs. merge position for reject-no-gap and reject-gap driver groups

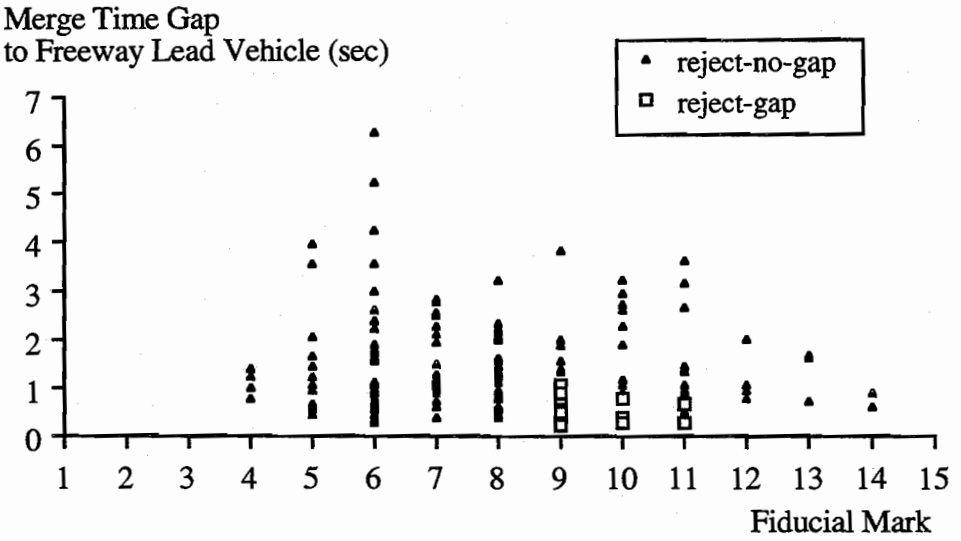

Figure 6.8 Merge time gap to freeway lead vehicle vs. merge position for reject-no-gap and reject-gap driver groups

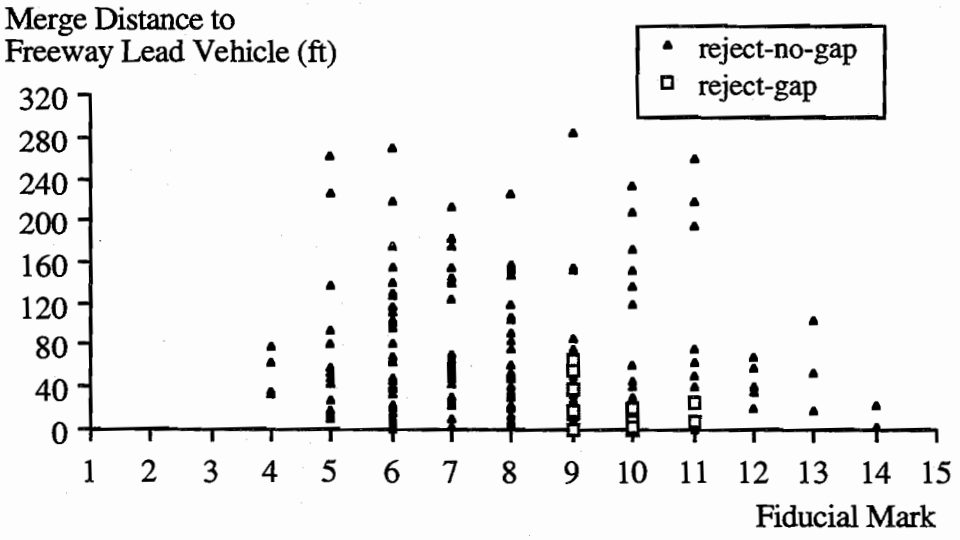

Figure 6.9 Merge distance to freeway lead vehicle vs. merge position for reject-no-gap and reject-gap driver groups

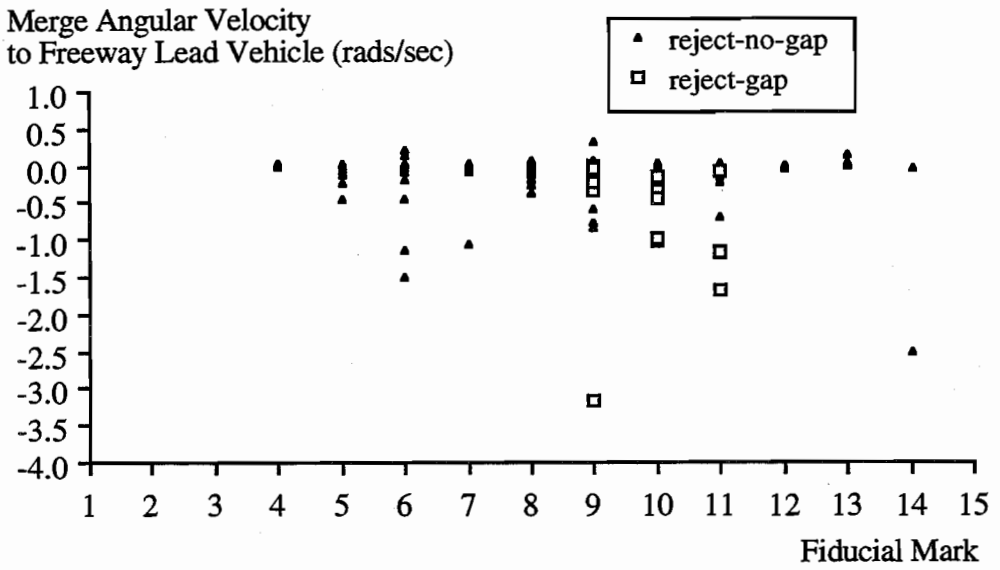

Figure 6.10 Merge angular velocity to freeway lead vehicle vs. merge position for reject-no-gap and reject-gap driver groups

Essentially, Figures 6.1 to 6.10 are respectively identical to Figures 3.20 to 3.29 except that reject-no-gap and reject-gap driver groups are illustrated using different symbols. As expected, all reject-gap drivers merged to freeway stream from the later portion of the acceleration lane. In general, except for figures related to the freeway lead vehicle, the scatter of each figure is wide and they show no significant gap acceptance trend difference between reject-no-gap and reject-gap driver groups. Whenever ramp vehicles were overtaken by their corresponding freeway lag vehicles, which become the freeway lead vehicles thereafter, the ramp vehicles merged immediately taking advantage of the freeway lag vehicle gap resulting in small accepted freeway lead gaps. This phenomenon, however, was believed to be triggered by instinct because under such a circumstance, ramp drivers need to pay little attention to their corresponding freeway lead vehicles, or formerly the overtaking vehicles, due to large speed differentials. Consequently, one should be cautious of interpreting these observations in gap acceptance model calibrations.

In short, very few ramp vehicles rejected gaps before merging; and none of the evidences shown in the previous figures supports the comment that reject-gap drivers have significantly different gap acceptance trends from those of the reject-no-gap drivers. This conclusion leads to revision of the proposed gap acceptance model that hypothesizes the gap

acceptance threshold is a function of the number of gaps rejected and the location of the ramp vehicle in the acceleration lane. The term associated with the number of gaps rejected was eliminated from the model specification. The probability of accepting a specific gap size is then no longer characterized by the sequential number of the rejected gap, and each gap acceptance/rejection observation is implicitly treated as an independent trial. This modification simplifies the likelihood function of the gap acceptance model allowing conventional binary logit and probit models to be directly applied. Calibrations of the revised gap acceptance models are detailed in the following section.

GAP ACCEPTANCE FUNCTION CALIBRATION

Freeway merge gap acceptance behavior is essentially a binary choice process. Stemming from the assumption that ramp drivers always choose utility-maximizing alternatives, the gap acceptance function is readily defined as follows:

$$P_r(\text{ accept a gap }) = P_r(\, U_a > U_r \,) \tag{6.1}$$

Where

U_a is the utility of accepting a gap

U_r is the utility of rejecting a gap

Denote V_a and V_r as the systematic components of U_a and U_r respectively. The systematic component difference, namely $V_a - V_r$, determines the probability of accepting a gap. Table 6.1 summarizes the binary logit model calibration results using various $V_a - V_r$ specifications for the gap acceptance function. Except for the top row which corresponds to variable notations, each row represents one $V_a - V_r$ specification. The entries in the table implicitly define the variables that enter into the specification. For example, the row that has no-blank cells associate with Const, V_{flagr}, G_{flagr}, V_{rflead}, and G_{rflead} demonstrates the calibration results obtained from the following $V_a - V_r$ specification.

$$V_a - V_r = \alpha_0 + \alpha_1 V_{flagr} + \alpha_2 G_{flagr} + \alpha_3 V_{rflead} + \alpha_4 G_{rflead} \tag{6.2}$$

The notations used in Table 6.1 are defined as follows:

V_{flagr} : speed differential between ramp vehicle and freeway lag vehicle measured at ramp vehicle merge, $V_{flagr} = V_{flag} - V_r$;

G_{flagr} : time gap between ramp vehicle and freeway lag vehicle measured at ramp vehicle merge;

D_{flagr} : distance separation between ramp vehicle and freeway lag vehicle measured at ramp vehicle merge;

V/D_{flagr} : speed differential and distance separation ratio, $V/D_{flagr} = V_{flagr} / D_{flagr}$;

ω_{flagr} : angular velocity viewed by the ramp driver with respect to freeway lag vehicle at ramp vehicle merge;

V_{rflead} : speed differential between ramp vehicle and freeway lead vehicle measured at ramp vehicle merge, $V_{rflead} = V_r - V_{flead}$;

G_{rflead} : time gap between ramp vehicle and freeway lead vehicle measured at ramp vehicle merge;

D_{rflead} : distance separation between ramp vehicle and freeway lead vehicle measured at ramp vehicle merge;

V/D_{rflead} : speed differential and distance separation ratio, $V / D_{rflead} = V_{rflead} / D_{rflead}$;

ω_{rflead} : angular velocity viewed by the ramp driver with respect to freeway lead vehicle at ramp vehicle merge;

D_{rend} : remaining distance to the acceleration lane end measured at ramp vehicle merge.

Throughout the calibration results, all freeway lead vehicle related attributes are found to be insignificant at any reasonable significance level revealing that these attributes provide little explanatory power to the gap acceptance model and should be removed from further consideration. The first model estimation outputs to be examined are the signs of the coefficient estimates and the significance of individual coefficients. Table 6.2 shows the models having all parameters significant at the 0.05 significance level. Both the speed differential and distance separation to a freeway lag vehicle have significant individual or joint effects on ramp driver gap acceptance behavior. All parameters have reasonable signs. Statistically, all gap acceptance models shown in Table 6.2 are almost equally good, however, the specification with the largest $\bar{\rho}^2$ magnitude is considered to be the best. In other words, the specification characterized by angular velocity and remaining distance to the acceleration lane terminus merits further attention.

TABLE 6.1 SUMMARY OF BINARY LOGIT MODEL CALIBRATION RESULTS FOR GAP ACCEPTANCE FUNCTION

Const	V_{flagr}	G_{flagr}	D_{flagr}	V/D_{flagr}	ω_{flagr}	V_{rflead}	G_{rflead}	D_{rflead}	V/D_{rflead}	ω_{rflead}	D_{rend}	$\bar{\rho}^2$
-1.880	-0.904	12.837				0.036	-0.607					0.916
(-1.086)	(-2.838)	(2.865)				(0.253)	(-1.138)					
-2.161	-0.919	11.048										0.924
(-1.405)	(-3.038)	(3.051)										
4.184	-0.244					0.078						0.725
(7.400)	(-4.218)					(1.333)						
-2.397	-0.933	11.284				-0.048						0.918
(-1.422)	(-3.048)	(3.030)				(-0.386)						
3.998	-0.269											0.726
(7.630)	(-4.845)											
68.778	-1.013										-0.107	0.954
(1.631)	(-1.476)										(-1.633)	
-1.744		5.458					-0.156					0.767
(-1.862)		(4.200)					(-0.748)					
-2.037		5.406										0.771
(-2.365)		(4.179)										

Note : the value in the parentheses is the t statistic

TABLE 6.1 (CONT.) SUMMARY OF BINARY LOGIT MODEL CALIBRATION RESULTS FOR GAP ACCEPTANCE FUNCTION

Const	V_{flagr}	G_{flagr}	D_{flagr}	V/D_{flagr}	ω_{flagr}	V_{rflead}	G_{rflead}	D_{rflead}	V/D_{rflead}	ω_{rflead}	D_{rend}	$\bar{\rho}^2$
40.083		16.786									-0.100	0.963
(1.198)		(0.933)									(-1.110)	
-1.940	-1.109		0.191			-0.0069		-0.0078				0.917
(-1.104)	(-2.925)		(2.824)			(-0.049)		(-1.024)				
-1.953	-1.117		0.172									0.926
(-1.275)	(-2.997)		(2.839)									
-2.088	-1.058	3.392	0.120									0.920
(-1.325)	(-2.788)	(0.419)	(0.916)									
5.713				-43.465					-1.044			0.873
(5.662)				(-4.594)					(-0.784)			
47.185				-47.452					0.0286		-0.074	0.959
(1.705)				(-1.775)					(0.154)		(-1.675)	
1.377		3.648		-34.187					-0.892			0.890
(0.798)		(2.096)		(-3.423)					(-0.577)			
5.872				-42.911								0.876
(5.716)				(-4.493)								

Note : the value in the parentheses is the t statistic

TABLE 6.1 (CONT.) SUMMARY OF BINARY LOGIT MODEL CALIBRATION RESULTS FOR GAP ACCEPTANCE FUNCTION

Const	V_{flagr}	G_{flagr}	D_{flagr}	V/D_{flagr}	ω_{flagr}	V_{rflead}	G_{rflead}	D_{rflead}	V/D_{rflead}	ω_{rflead}	D_{rend}	$\bar{\rho}^2$
47.016				-47.474							-0.0738	0.965
(1.705)				(-1.770)							(-1.674)	
1.391		3.633		-32.711								0.895
(0.818)		(2.164)		(-3.453)								
4.753					-103.13					-0.571		0.870
(6.574)					(-4.512)					(-0.365)		
60.403					-52.118					9.045	-0.0949	0.959
(1.052)					(-1.520)					(0.888)	(-1.067)	
2.013		2.065			-75.431					-0.0555		0.872
(1.129)		(1.311)			(-3.083)					(-0.034)		
4.786					-101.09							0.876
(6.662)					(-4.597)							
30.857					-94.877						-0.0489	0.957
(2.368)					(-2.312)						(-2.260)	
2.002		2.071			-75.027							0.878
(1.137)		(1.337)			(-3.311)							

Note : the value in the parentheses is the t statistic

For comparison purposes, a binary probit model was also applied to calibrate the specifications shown in Table 6.2. The results are presented in Table 6.3. With only small coefficient magnitude differences, the estimation outputs obtained from binary logit and probit calibrations are almost identical. The best specification suggested by binary probit calibration is the same as that drawn from the logit model. Generally speaking, binary logit calibration results are slightly superior to their binary probit counterparts in terms of $\overline{\rho}^2$ values. Furthermore, due to its computational attractiveness, the binary logit model is suggested for the gap acceptance function. The best gap acceptance function obtained from this study is

$$P_r(\text{ accept a specific gap size } | \ \omega_{flagr}, \mathrm{D}_{rend}\ ) = \frac{1}{1 + e^{-30.857 + 94.877\omega_{flagr} + 0.0489\mathrm{D}_{rend}}} \tag{6.3}$$

Reflecting upon the psychological literature which claimed that ramp drivers are only capable of processing a first order motion vector when analyzing an adjacent freeway vehicle, angular velocity has been proven to be an important criterion for the gap acceptance decision. The larger the viewed angular velocity magnitude with respect to an oncoming freeway lag vehicle, all else equal, the smaller the probability of accepting that gap, according to Eq.(6.3). Drivers have an obvious tendency to force a merge when approaching the acceleration lane terminus. The inclusion of the remaining distance to the acceleration lane end as an explanatory variable, with proper sign, reflects this tendency. Application of Eq.(6.3) is straightforward and can be easily implemented in existing freeway simulation models.

TABLE 6.2 MODELS WITH PARAMETERS SIGNIFICANT AT 0.05 LEVEL

(BINARY LOGIT MODEL)

Const.	V_{flagr}	G_{flagr}	D_{flagr}	V/D_{flagr}	ω_{flagr}	D_{rend}	$\bar{\rho}^2$
3.998	-0.269						0.726
(7.630)	(-4.845)						
-2.037		5.406					0.771
(-2.365)		(4.179)					
5.872				-42.911			0.876
(5.716)				(-4.493)			
4.786					-101.09		0.876
(6.662)					(-4.597)		
30.857					-94.877	-0.0489	0.957
(2.368)					(-2.312)	(-2.260)	

TABLE 6.3 MODELS WITH PARAMETERS SIGNIFICANT AT 0.05 LEVEL

(BINARY PROBIT MODEL)

Const.	V_{flagr}	G_{flagr}	D_{flagr}	V/D_{flagr}	ω_{flagr}	D_{rend}	$\bar{\rho}^2$
3.548	-0.257						0.712
(6.824)	(-6.009)						
-2.215		5.285					0.738
(-5.392)		(6.572)					
5.572				-42.681			0.868
(6.228)				(-9.340)			
4.767					-101.12		0.872
(6.308)					(-5.114)		
31.029					-94.878	-0.049	0.951
(6.687)					(-7.783)	(-2.228)	

DISCUSSION ON CRITICAL GAP DISTRIBUTION TRANSFORMATION

Essentially, a gap acceptance function is equivalent to a critical gap distribution although the mechanism interpretations are different. For example, the probability of a randomly chosen driver accepting an angular velocity of size ω is the same as the probability of that driver having a critical angular velocity greater than ω. By removing the term relating to the number of rejected gaps and by setting d equal to 1, one can simplify Eq.(3.77) as follows:

$$\omega_{cr}(x) = \overline{\omega}_{cr} + \gamma(L-x) + \varepsilon \tag{6.4}$$

Thus, the gap acceptance function is

$$\begin{aligned} & P_r(\text{ accept a gap featuring an angular velocity } \omega_x) \\ = \; & P_r(\omega_x < \omega_{cr}(x)) \\ = \; & P_r(\omega_x < \overline{\omega}_{cr} + \gamma(L-x) + \varepsilon) \\ = \; & P_r(\varepsilon^* < \overline{\omega}_{cr} - \omega_x + \gamma(L-x)) \end{aligned} \tag{6.5}$$

Assuming ε^* is logistically distributed, one obtains

$$\begin{aligned} & P_r(\text{ accept a gap featuring an angular velocity } \omega_x) \\ = \; & \frac{1}{1 + e^{-[\overline{\omega}_{cr} - \omega_x + \gamma(L-x)]}} \end{aligned} \tag{6.6}$$

The best gap acceptance function suggested in this study is

$$\begin{aligned} & P_r(\text{ accept a gap featuring an angular velocity } \omega_x) \\ = \; & \frac{1}{1 + e^{-[\beta_0 + \beta_1\omega_x + \beta_2(L-x)]}} \end{aligned} \tag{6.7}$$

Comparing Eqs.(6.6) and (6.7), one can argue that the former is only a special case of the latter by forcing β_1 equal to -1.

By specifying a gap acceptance probability threshold, α, one can express the critical angular velocity, ω^*_{flagr}, as a function of D_{rend} and α. Let

$$\alpha = \frac{1}{1 + e^{-30.857 + 94.877\omega^{*}_{flagr} + 0.0489 D_{rend}}} \quad (6.8)$$

Rewriting Eq.(6.8), one get

$$\frac{1 - \alpha}{\alpha} = e^{-30.857 + 94.877\omega^{*}_{flagr} + 0.0489 D_{rend}} \quad (6.9)$$

Taking the natural logarithm of both sides of Eq.(6.9),

$$\ln(\frac{1 - \alpha}{\alpha}) = -30.857 + 94.877\omega^{*}_{flagr} + 0.0489 D_{rend} \quad (6.10)$$

Dividing both sides of Eq.(6.10) by 94.877 and rearranging, one obtains

$$\omega^{*}_{flagr} = 0.3252 - 0.000515 D_{rend} + 0.01054 \ln(\frac{1 - \alpha}{\alpha}) \quad (6.11)$$

One should note that the critical angular velocity, ω^{*}_{flagr}, is defined over gap acceptance threshold, α. For example, if one defines ω^{*}_{flagr} as the angular velocity associated with a randomly chosen gap that will be accepted 50% of the time, α is equal to 0.5. For a given gap acceptance threshold magnitude, α=0.5, the graphical presentation of ω^{*}_{flagr} and D_{rend} is illustrated in Figure 6.11. The shorter the remaining distance of the gap seeking driver to the acceleration lane end, the larger the critical angular velocity of the driver, according to Figure 6.11. This trend corresponds with one's intuitive hypothesis that ramp drivers tend to accept a smaller gap, or equivalently a larger angular velocity, while they are approaching the acceleration lane end.

SUMMARY

The gap acceptance observation data have been graphically examined. Very few ramp vehicles, less than 7%, were found to reject gaps before merging. Those ramp vehicles that had rejected gaps before merging do not visibly demonstrate significant gap acceptance trend differences from those that had not. In other words, rejecting gaps or not does not influence the final gap acceptance decision. This conclusion led to revision of the previously proposed critical

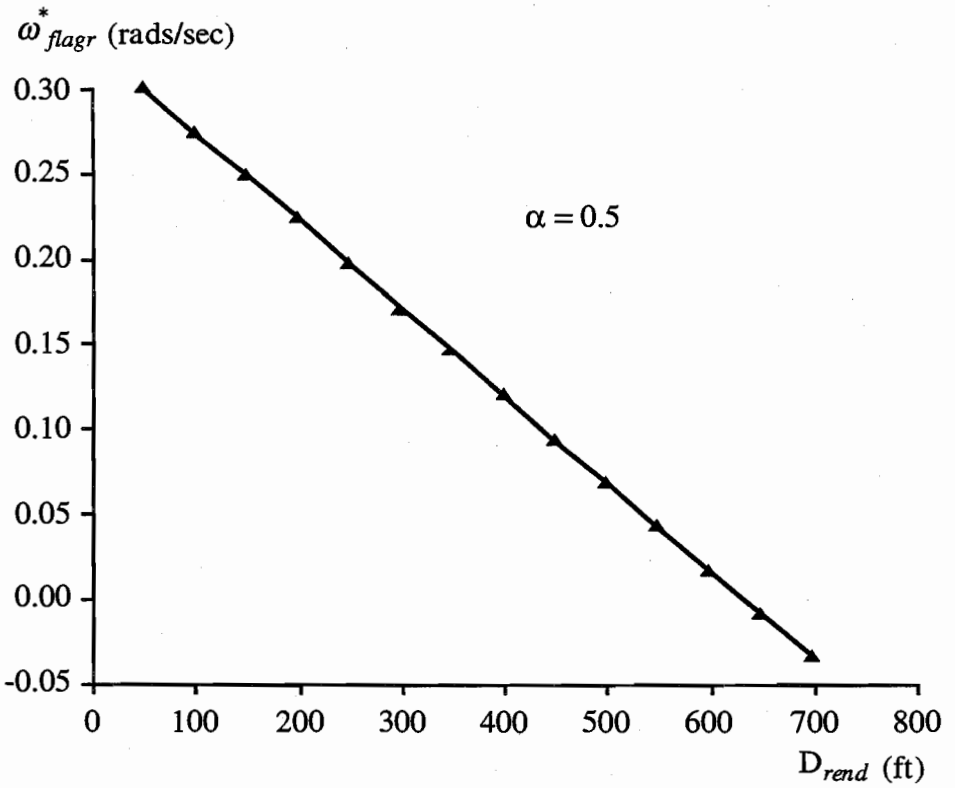

Figure 6.11 Critical angular velocity vs. remaining distance to the acceleration lane end (α=0.5)

angular velocity distribution, as shown in chapter 3, by removing the term describing the rejected gap number from the model specification. Instead of calibrating the critical angular velocity distribution, this study estimated the gap acceptance function using discrete binary choice models. Respective calibration results of various model specifications from binary logit and probit models are similar with the former slightly superior to the latter. The gap acceptance function characterized by angular velocity to the freeway lag vehicle and remaining distance to the acceleration lane end was found to be the best gap acceptance model. This result corresponds with the psychological literature which argued that ramp drivers use the first order vehicle motion, e.g. angular velocity, as a gap acceptance decision criterion.

The revised form of the previously proposed critical angular velocity distribution was transformed to a gap acceptance function form and compared with the best model obtained from this study. The evidence shows that the previous model is a special case of the suggested gap acceptance function. By specifying a gap acceptance probability threshold, this study derived the

critical angular velocity as a function of the remaining distance to the acceleration lane terminus and the probability threshold. The critical angular velocity was found to be a decreasing function of the remaining distance to the acceleration lane end.

CHAPTER 7. CONCLUSIONS AND RECOMMENDATIONS

This chapter includes a brief summary of the tasks performed in this study, a conclusion and potential contributions drawn from the major findings, and a highlight of the avenues for future research.

SUMMARY

The acceleration and merging process from an acceleration lane to the freeway lanes constitute an important aspect of freeway traffic operation and ramp junction geometric design. Ramp drivers continuously change speed in response to the relative movement of surrounding freeway and ramp vehicles to create a chance for making a safe merge before reaching the acceleration lane terminus. This merge process is complex and dynamic in nature. The complexity is a result of the fact that driver psychological components have multiple dimensions affecting freeway merge decisions. Traffic, roadway, and driver variability effects jointly contribute to the driver decision complexity. Very rich mathematically oriented studies have been done on gap acceptance behavior in the last few decades, while very few articles address ramp vehicle acceleration characteristics. Both the acceleration and gap acceptance issues, unfortunately, have been oversimplified in literature. Constant acceleration rates or even constant speeds with zero acceleration rate, were normally assumed for ramp vehicles traveling in acceleration lanes, while constant critical gaps were assumed for gap acceptance. Dynamic freeway merge driver-vehicle interactions were not well reflected in previous studies. The major objective of this study is to develop empirical methodologies for modeling ramp vehicle acceleration-deceleration and gap acceptance behavior during freeway merge maneuvers. Solidly understand the detailed driver-vehicle interaction mechanism is essential for developing sophisticated freeway merge behavior models. Real freeway merge driver-vehicle observation data, undoubtedly, are the best resources for capturing such fundamental knowledge.

In this study, considerable efforts were devoted to data collection and reduction. Freeway merge traffic data were collected from several entrance ramps including both parallel and taper type acceleration lanes. Traffic data were collected by either manual or videotaping methods depending on the data attributes to be collected. These surveys covered both off-peak and peak periods capturing a wide traffic flow range suiting different analysis purposes. Conditions in which demand exceeds capacity were not included because these conditions induce very different driver behavior such as forced merging into stop-and-go freeway flow and were not the issues of this study. At locations where ramp vehicle freeway merge trajectory data were collected, a high

resolution video camcorder was set up at a vantage point near the entrance ramp from which the operation of the entire merge area was videotaped. White lines which were used as fiducial marks were placed, at regular distance intervals, on the grass beside the ramp shoulder along the acceleration lane. During data reduction procedure, fiducial marks are lines drawn across the acceleration lane and freeway lanes directly on a transparency superimposed on the video monitor. The videotapes were played back, using a video camera recorder which featured a jog-shuffle function, at slow speed, or frame-by-frame, to ensure precise tracking of the time vehicles crossed each fiducial mark. Nevertheless, measurement errors occurred due to the video camera's embedded time-code resolution limitation and parallax and human data reduction errors. The primary data reduced from the videotapes were a set of time codes for each ramp vehicle, with corresponding (if any) freeway lag, freeway lead, and ramp lead vehicles, crossing each fiducial mark. Almost all traffic characteristic parameters used in later freeway merge behavior analyses and model calibrations were calculated from the time-based data set.

Traffic data provide the best information for investigating fundamental ramp vehicle freeway merge behavior. Comprehensive freeway merge traffic characteristic analyses were conducted using the collected data to examine effects of freeway merge area traffic flow conditions on ramp vehicle merge position, ramp vehicle acceleration-deceleration performance in the acceleration lane, and gap acceptance behavior. All freeway merge related traffic parameters such as merge speed, merge acceleration rate, speed differential, time gap, distance gap, and angular velocity were incorporated in the traffic data analyses. These data analysis results provided not only an in-depth understanding of the complex freeway merge mechanism but also valuable information for developing freeway merge behavior model frameworks. The conceptual methodology for modeling ramp vehicle acceleration-deceleration behavior used the stimulus-respond equation as a fundamental rule and was formulated as an extended form of the conventional car-following models. In other words, speed differentials between the ramp vehicle and its corresponding freeway and ramp vehicles were the stimuli and the associated responses were the ramp vehicle acceleration-deceleration rates. The respective sensitivity term was a nonlinear function of the ramp vehicle speed and the perspective distance separation between the ramp vehicle and corresponding freeway and ramp vehicles. As a pilot study, freeway merge data collected at a short parallel type acceleration lane were used to calibrate the conceptual nonlinear acceleration-deceleration models. Although encouraging, the calibration results were only tentative due to fairly small numbers of observations. As for the conceptual gap acceptance model, it was assumed that most ramp drivers operate at some threshold, or critical, level of angular velocity. The threshold to accept a specific gap size, characterized by the angular velocity,

for a ramp driver was hypothesized as a function of the number of gaps rejected and the remaining distance to the acceleration lane terminus. The small quantity of observations collected from the pilot study site, however, made it impossible to calibrate this critical angular velocity distribution.

A sufficiently large quantity of freeway merge data were later collected from a long taper type acceleration lane and were used to calibrate the proposed nonlinear acceleration-deceleration model. Several modified forms of the model specification such as including weighting factors to emphasize distance effects and splitting whole data sets into homogeneous subsets to simplify model specifications were also applied. Neither of the calibration efforts obtained satisfactory results. This indicated that it was infeasible to directly estimate acceleration-deceleration rates using one comprehensive equation. From the practical application point of view, a bi-level calibration approach was developed. The discrete choice behavior model, the first level, estimates the respective probability of acceleration, deceleration, or constant speed under prevailing traffic conditions. While the continuous model, the second level, estimates the perspective acceleration or deceleration rates. Applausive calibration results were obtained from this bi-level approach. At the field survey site, very few gap rejections were observed. Ramp drivers who did reject gaps before merging did not visibly demonstrate significantly different gap acceptance behavior from those that had not. Binary choice methods were applied respectively to calibrate the gap acceptance models.

Major findings of this study and potential contributions are described in the next section.

CONCLUSIONS AND POTENTIAL APPLICATIONS

The findings of this study are abundant and have a wide range of application. This study serves an important purpose by pointing to the limitations of current freeway merge models which treat the ramp driver acceleration-deceleration and gap acceptance behavior as deterministic phenomena. In addition, the interdependence of freeway merge behavior and surrounding traffic conditions has been proven to be significant indicating that one should not ignore the linkage of driver behavior and traffic dynamics. Successful calibration of methodologies for modeling freeway merge driver behavior makes this study a valuable asset for further applications. The major conclusions are discussed as follows.

1. Although known as a key element in freeway entrance ramp geometric design and freeway merge simulation models, ramp vehicle acceleration-deceleration behavior has not received proper attention. This study, devoted to the empirical analysis of fundamental freeway merge behavior, is one of the most comprehensive freeway merge studies in recent years.

Furthermore, this study is probably the only study that links such traffic parameters as speed differential, distance separation, and travel speed with vehicle acceleration-deceleration behavior.

2. Video recording technique has been extensively used by traffic engineers to estimate vehicle speed data. Accuracy in estimating actual speeds and associated measurement errors, however, have not been quantitatively examined. In this study, the probability density function (PDF) of measurement error for estimating speed through video image techniques was successfully developed. This PDF incorporates the effect of an embedded video camera time-base resolution, fiducial mark interval, and actual vehicle speed. These three parameters have a joint effect in determining speed measurement error, and cannot be considered individually. Among them, the time-base resolution was found to have the most significant speed measurement error effect. The developed PDF has a great contribution to practical traffic engineering works. It can be applied, in advance, either to estimate the probability of occurrence of a certain magnitude of speed measurement error or to determine the best traffic survey scheme given a data quality requirement. Application of the model is straightforward. Two hypothetical examples dealing with frequently raised speed data survey questions can be found in a recent publication (Kou and Machemehl, 1997b).

The measurement errors investigated in this study are the basic parts of total measurement error. There are many other factors such as data reduction techniques, parallax, and human error that jointly contribute to speed estimation accuracy and are not included in the derived measurement error probability functions.

3. Both graphical presentations and independence tests in contingency tables indicated that ramp vehicle merge position is insignificantly related to any single traffic parameter, such as ramp vehicle approach speeds, freeway flow levels, and speed differentials as well as time or distance gaps between a ramp vehicle and its surrounding freeway and ramp vehicles. In other words, it is not always true that ramp vehicles that had higher approach speeds and larger time gaps to the corresponding freeway lag vehicles merged into the freeway from the former sections of the acceleration lane. Driver-vehicle behavior during the freeway merge maneuver is too dynamic to be precisely predicted using only one traffic parameter. Besides, the observed mean speed profile of ramp vehicles did not show significant variations along the acceleration lane indicating that ramp drivers did not primarily use the acceleration lane as a facility for accelerating. These results make a significant contribution in that they provide strong evidence that the historically used AASHTO acceleration lane length design policy that exclusively uses freeway and entrance ramp design speeds as criteria should be examined.

4. Calibrations of the proposed nonlinear acceleration-deceleration models that incorporated speed differentials and distance separations of corresponding freeway lag and lead vehicles, ramp lead vehicles, and the acceleration lane end in one general formulation were not successful. This discouragement only revealed the message that one cannot predict ramp vehicle acceleration-deceleration rates using such complicated models. It does not, however, mean that those driver-vehicle parameters have no ramp driver acceleration-deceleration decision effect. As a matter of fact, ramp drivers will not make speed change decisions without considering the surrounding freeway as well as ramp vehicles movements and the physical acceleration lane end constraint. The associated acceleration-deceleration rate magnitudes, on the other hand, might be predicted using simple variables.

5. A bi-level calibration procedure has been successfully applied to calibrate a ramp vehicle acceleration-deceleration behavior model. This procedure used a multinomial probit model, as the first level, to predict ramp driver acceleration, deceleration, or constant speed choice behavior. Speed differential and distance separation ratios with respect to freeway lag, freeway lead, ramp lead vehicles, and the acceleration lane terminus were found to be the best explanatory variables. As expected, both speed differentials and distance separations between ramp vehicles and surrounding freeway and ramp vehicles have a joint acceleration-deceleration effect. In addition, the alternative specific markov indexes that capture the unobservable serial correlation between successive observations in the systematic component were also significant. Addition of these markov indexes in the specifications is a great success because ramp drivers are not expected to continuously switch from acceleration to deceleration, or *vice versa*, during short time period. In other words, when a ramp driver was accelerating, or decelerating, at fiducial mark j, with high likelihood he/she will still be accelerating, or decelerating, at fiducial mark j+1. By specifying these Markov indexes in the systematic components, this serial correlation problem was automatically captured. The associated acceleration or deceleration rate magnitudes were predicted, as the second level, by a family of exponential equations that used the ramp vehicle speed as a sole explanatory variable. The finding families of acceleration and deceleration curves reflects true driver acceleration-deceleration behavior. Under the bi-level prediction framework, all decision choice and magnitude prediction procedures are no longer treated as deterministic but as probabilistic phenomena. By incorporating a random number generation technique, this bi-level acceleration-deceleration prediction procedure can be implemented to enhance existing microscopic freeway simulation models.

6. Scatter plots of accepted gap structure elements against merge positions showed a wide spread. However, the scatter ranges became smaller for merge positions near the acceleration

lane end. In other words, ramp drivers who merged from latter sections of the acceleration lane were found to have a higher probability of accepting smaller freeway lag vehicle gaps or larger angular velocities. Although this phenomenon might partially be due to the fact that only small numbers of ramp vehicles merged from the latter sections of the acceleration lane, it also points out that remaining distance to the acceleration lane terminus might have a significant gap acceptance effect. The wide range of scatter indicate that large gap acceptance variations among drivers. This evidence suggested the use of a disaggregate approach for calibrating the ramp driver gap acceptance model.

7. Ramp driver gap acceptance models were successfully calibrated using binary logit models. The angular velocity viewed by the ramp driver to his/her corresponding freeway lag vehicle and the remaining distance to the acceleration lane terminus were found to be the best attributes characterizing the gap acceptance function. The critical angular velocity, for a given gap acceptance threshold, was derived as a decreasing function of the remaining distance to the acceleration lane terminus. This result indicates that ramp drivers are willing to accept a larger angular velocity, or equivalently a smaller gap, while approaching the acceleration lane terminus. The developed gap acceptance function has a variety of applications. It can be used in either freeway simulation or analytical models to evaluate freeway entrance ramp operational performance.

8. This study has provided several useful unique contributions to the body of knowledge on complex freeway merge driver behavior. Among others, this study provides significant evidence suggesting that the AASHTO freeway entrance ramp acceleration lane length design policy requires reexamination to reflect true driver behavior. Another impressive contribution is the successful calibration of the probabilistic ramp vehicle acceleration-deceleration and gap acceptance models allowing the linkage of variable traffic-vehicle parameters and dynamic driver behavior. These probabilistic behavior models could provide great enhancement to existing microscopic freeway simulation models.

RECOMMENDATIONS

The recommendations and the avenues of further research are highlighted as follows.

1. Considerable efforts of this study were devoted to image data reduction. Automatic image processing techniques should be adopted to minimize data reduction work and enhance data quality.

2. There were no driver attributes, such as age, gender, trip purpose, and occupation etc., included in this study. It is believed that these attributes will have great contributions to driver

behavior variations. Studies using experimental vehicles or driver-vehicle simulators as data collection tools are other potentially viable approaches to investigate freeway merge behavior.

3. Due to resource limitations, freeway merge traffic data were collected from only one entrance ramp. To generalize the findings of this study, more data collected from other entrance ramp locations are recommended.

4. Congested freeway merging is another interesting topic that merits further investigation. This kind of merge involves more complicated driver-vehicle interactions, such as forced merging, stop-and-go traffic flow, and frequent lane changing.

5. To complete the freeway merge study, merging area freeway traffic flow should be studied. As a matter of fact, there are strong interactions between merging vehicles and freeway vehicles. Freeway drivers might change lanes before reaching the merging area to avoid potential conflict, or might reduce speed to yield to merging vehicles. Therefore, studies performed from the freeway driver point of view are desirable.

APPENDIX A. DERIVATION OF PROBABILISTIC SPEED MEASUREMENT ERRORS THROUGH VIDEO IMAGES

INTRODUCTION

Traffic speed data can be easily reduced from video images having a digital clock superimposed. The time vehicles cross each fiducial mark, in sequence, is recorded and the average travel speed between fiducial marks is calculated. However, limitations of the video camera's time-base resolution can preclude precise measurements. Both time and distance measurement errors will always be associated with the time readings. Consequently, the time-location errors propagate in the calculation of speeds and other relative parameters. Essentially, the measurement errors are random rather than deterministic variables and are best described from a probabilistic perspective. This appendix focuses on a derivation of the probability density function(pdf) of speed estimation measurement errors that incorporate the effect of imbedded camera time-base resolution, fiducial mark interval, and actual vehicle speed. Mathematical derivation of the measurement error pdf from both time and distance perspectives is described. A Monte Carlo simulation was used to verify the probability function derived mathematically.

MATHEMATICAL DERIVATION OF PROBABILITY FUNCTION

Speed Estimation Errors Due to Time Measurement Error

To precisely read the time vehicles cross fiducial marks, one normally plays back the video image in slow motion or even frame-by-frame. This situation can be best described using Figure A.1. Assume that at time frame i, a vehicle is located at position 1(p1), and at time frame i+1 it moved to position 2(p2). After some time the vehicle approaches mark 2. At time frames j, and j+1 the vehicle is at positions 3(p3) and 4(p4), respectively. Due to time clock resolution limitations, the actual times, t_{act_1} and t_{act_2}, when the vehicle crosses fiducial marks 1 and 2 respectively are not observable. Instead, one records the clock time readings in which the vehicle was visibly nearest the fiducial marks. They are t_{read_1} and t_{read_2} in Figure A.1. Consequently, there are differences between the actual and recorded times that vehicles cross fiducial marks. These time measurement errors will propagate in the calculation of speeds and result in speed estimation measurement errors. Therefore, probabilistic properties of time measurement errors should be investigated before deriving the speed measurement error probability function.

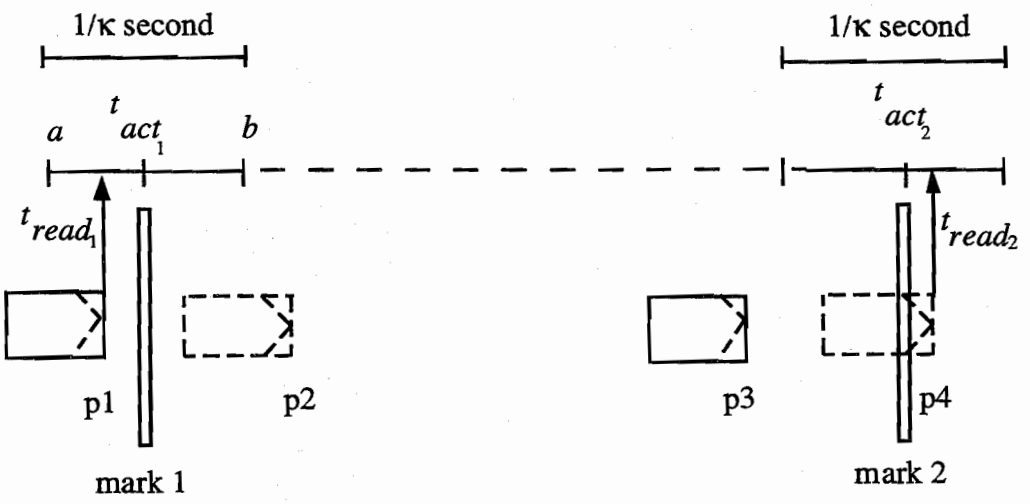

Figure A.1 Sketch of time-location image of vehicles crossing fiducial marks

Derivation of Recorded Time Measurement Errors Probability Function

The recorded time, for example t_{read_1}, of an event can occur anyplace in the time scale region of a to b with equal probability. Thus one can reasonably assume that it is uniformly distributed over the region a to b. The boundaries of the time scale region, namely a and b, are determined by the time-base resolution, κ, in frames/second, of the video camera. Clearly, the region of a to b could be defined as follows:

$$(a, b) = (t_{act_1} - \frac{1}{2\kappa}, t_{act_1} + \frac{1}{2\kappa}) \qquad \text{(A.1)}$$

The mathematical relationships of t_{act_1} and t_{read_1} as well as t_{act_2} and t_{read_2} are

$$t_{read_1} = t_{act_1} + u_1 \qquad -\frac{1}{2\kappa} \le u_1 \le \frac{1}{2\kappa} \qquad \text{(A.2)}$$

$$t_{read_2} = t_{act_2} + u_2 \qquad -\frac{1}{2\kappa} \le u_2 \le \frac{1}{2\kappa} \qquad \text{(A.3)}$$

Where

t_{read_1} and t_{read_2} are the recorded times that vehicles cross marks 1 and 2 respectively ;

t_{act_1} and t_{act_2} are the actual times that vehicles cross marks 1 and 2 respectively;

u_1 and u_2 are uniformly distributed random errors.

The probability density functions of u_1 and u_2 are shown as follows:

$$f(u_1) = \kappa \qquad -\frac{1}{2\kappa} \le u_1 \le \frac{1}{2\kappa} \tag{A.4}$$

$$f(u_2) = \kappa \qquad -\frac{1}{2\kappa} \le u_2 \le \frac{1}{2\kappa} \tag{A.5}$$

Combining Eqs(A.2) and (A.3) gives

$$t_{read_2} - t_{read_1} = (t_{act_2} - t_{act_1}) + (u_2 - u_1) \tag{A.6}$$

$t_{read_2} - t_{read_1}$ is the time duration actually used to calculate average vehicle speeds traveling from mark 1 to mark 2. While $u_2 - u_1$ is the random error.

Let $u = u_2 - u_1 \qquad -\frac{1}{\kappa} \le u \le \frac{1}{\kappa}$ (A.7)

The pdf of u can be derived by means of Eqs(A.4) and (A.5). Since u_1 and u_2 are random errors from two independent time-readings, the joint pdf of u_1 and u_2 is

$$f(u_1, u_2) = f(u_1) f(u_2) = \kappa^2, \qquad -\frac{1}{2\kappa} \le u_1 \le \frac{1}{2\kappa}, \ -\frac{1}{2\kappa} \le u_2 \le \frac{1}{2\kappa} \tag{A.8}$$

$$0, \qquad \text{otherwise}$$

To obtain the pdf of u, one must derive the Cumulative Density Function (CDF) of u, $F_U(u)$. This can be done by integrating the area below line $u = u_2 - u_1$ for those cases of $u \le -\frac{1}{\kappa}, -\frac{1}{\kappa} \le u \le 0, 0 \le u \le \frac{1}{\kappa}$, and $\frac{1}{\kappa} \le u$ respectively. The graphical presentations are shown in Figures A.2 to A.5.

Case 1 : $u \leq -\frac{1}{\kappa}$

$F_U(u) = 0$

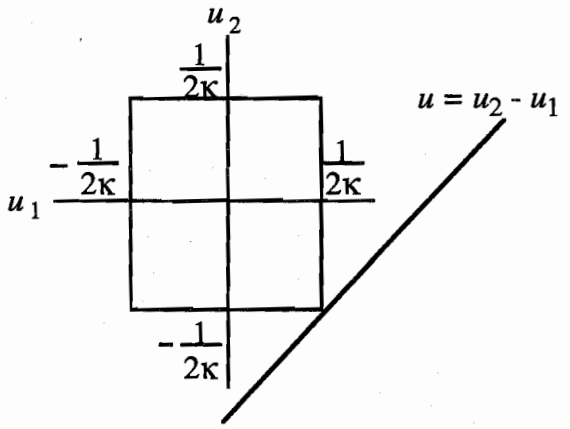

Figure A.2 Derivation of cumulative density function of u(for $u \leq -1/\kappa$)

Case : 2 $\frac{-1}{\kappa} \leq u \leq 0$

$F_U(u)$ = *the area of the shaded triangle*

$$= \int_{\frac{-1}{2\kappa} - u}^{\frac{1}{2\kappa}} \int_{\frac{-1}{2\kappa}}^{u + u_1} f(u_1, u_2)\, du_2\, du_1$$

$$= \int_{\frac{-1}{2\kappa} - u}^{\frac{1}{2\kappa}} \int_{\frac{-1}{2\kappa}}^{u + u_1} \kappa^2\, du_2\, du_1$$

$$= 0.5 + \kappa u + \frac{\kappa^2}{2} u^2$$

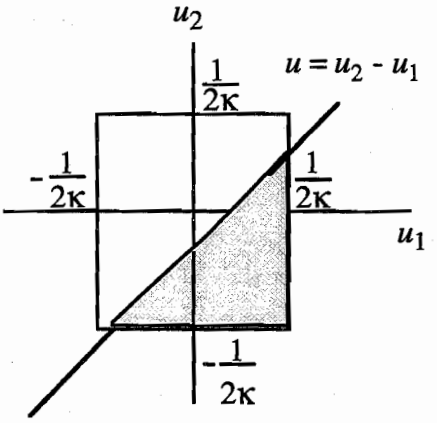

Figure A.3 Derivation of cumulative density function of u (for $-1/\kappa \leq u \leq 0$)

Case 3 : $0 \le u \le \frac{1}{\kappa}$

$F_U(u)$ = *the area of the shaded polygon*

$$= 1 - \int_{\frac{1}{2\kappa} - u}^{\frac{-1}{2\kappa}} \int_{\frac{1}{2\kappa}}^{u + u_1} f(u_1, u_2)\, du_2\, du_1$$

$$= 1 - \int_{\frac{1}{2\kappa} - u}^{\frac{-1}{2\kappa}} \int_{\frac{1}{2\kappa}}^{u + u_1} \kappa^2\, du_2\, du_1$$

$$= 0.5 + \kappa u - \frac{\kappa^2}{2} u^2$$

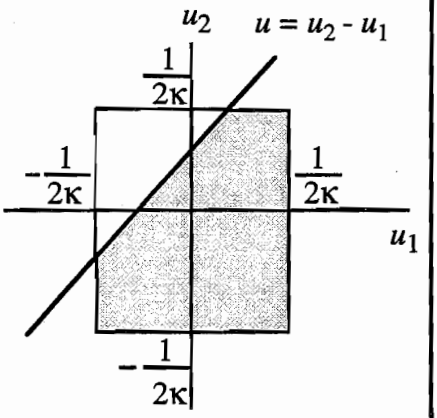

Figure A.4 Derivation of cumulative density function of u (for $0 \le u \le 1/\kappa$)

Case 4 : $\frac{1}{\kappa} \le u$

$F_U(u) = 1$

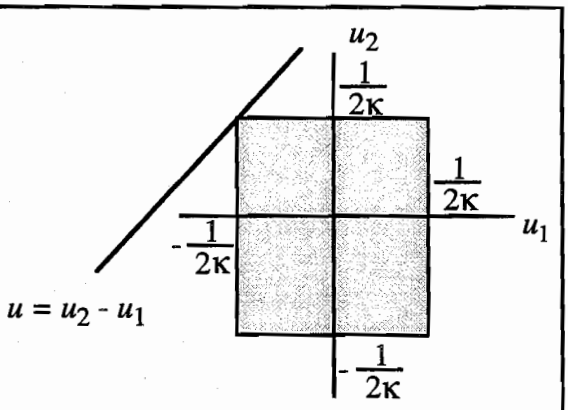

Figure A.5 Derivation of cumulative density function of u (for $1/\kappa \le u$)

In summary, the CDF of u is given as follows:

$$F_U(u) = 0 \qquad u \le -\frac{1}{\kappa} \tag{A.9}$$

$$= 0.5 + \kappa u + \frac{\kappa^2}{2} u^2 \qquad -\frac{1}{\kappa} \le u \le 0 \tag{A.10}$$

$$= 0.5 + \kappa u - \frac{\kappa^2}{2} u^2 \qquad 0 \le u \le \frac{1}{\kappa} \tag{A.11}$$

$$= 1.0 \qquad \frac{1}{\kappa} \le u \tag{A.12}$$

The pdf of u, $f_U(u)$, as shown in Figure A.6, is obtained by differentiating both sides of Eqs(A.9) to (A.12) with respect to u,

$$dF_U(u)/du = f_U(u) = \kappa + \kappa^2 u \qquad -\frac{1}{\kappa} \le u \le 0 \tag{A.13}$$

$$= \kappa - \kappa^2 u \qquad 0 \le u \le \frac{1}{\kappa} \tag{A.14}$$

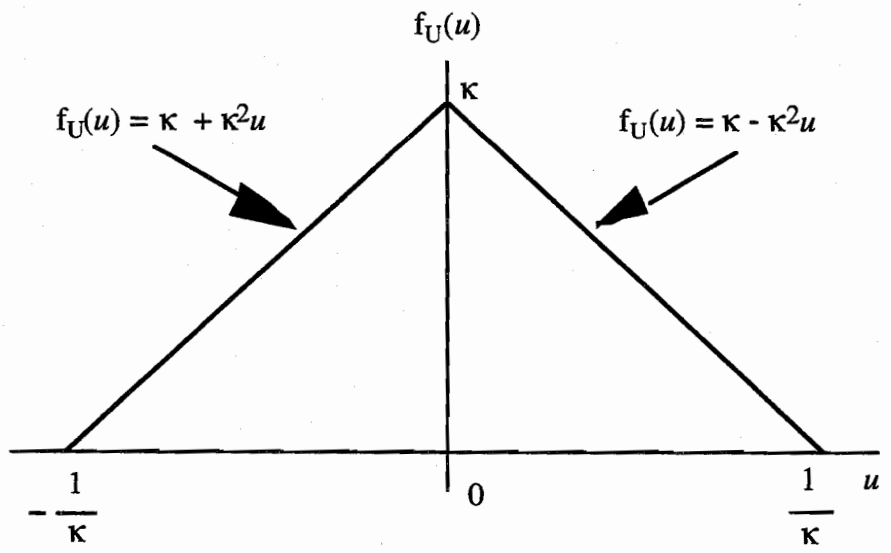

Figure A.6 Probability density function of time measurement error

Derivation of Speed Estimation Measurement Errors Probability Function

The pdf of speed estimation measurement error can be derived by means of the results of Eqs(A.13) and (A.14). The relationship of actual travel speed, v_{act}, and estimated travel speed, v_{est}, can be written as follows:

$$v_{est} = v_{act} + \varepsilon \tag{A.15}$$

Where

ε is the random error associated with the estimated speed.

Let D denote the fiducial mark interval. Then, Eq(A.15) can be rewritten into

$$\frac{D}{t_{read_2} - t_{read_1}} = \frac{D}{t_{act_2} - t_{act_1}} + \varepsilon \tag{A.16}$$

Substituting Eq(A.6) in Eq(A.16), one obtain

$$\frac{D}{(t_{act_2} - t_{act_1}) + (u_2 - u_1)} = \frac{D}{t_{act_2} - t_{act_1}} + \varepsilon \tag{A.17}$$

By substituting Eq(A.7) in Eq(A.17), the expression of ε in terms of v_{act}, D, and u is readily written as follows:

$$\varepsilon = \frac{-v_{act}^2 u}{D + v_{act} u} \tag{A.18}$$

As shown in Figure A.7, Eq(A.18) is a continuous decreasing function of u. Therefore, it is appropriate to apply the variable transformation method to derive the pdf of ε, $f_E(\varepsilon)$, by means of $f_U(u)$. The transformation equation is

$$f_E(\varepsilon) = f_U(u)\left|\frac{du}{d\varepsilon}\right| \tag{A.19}$$

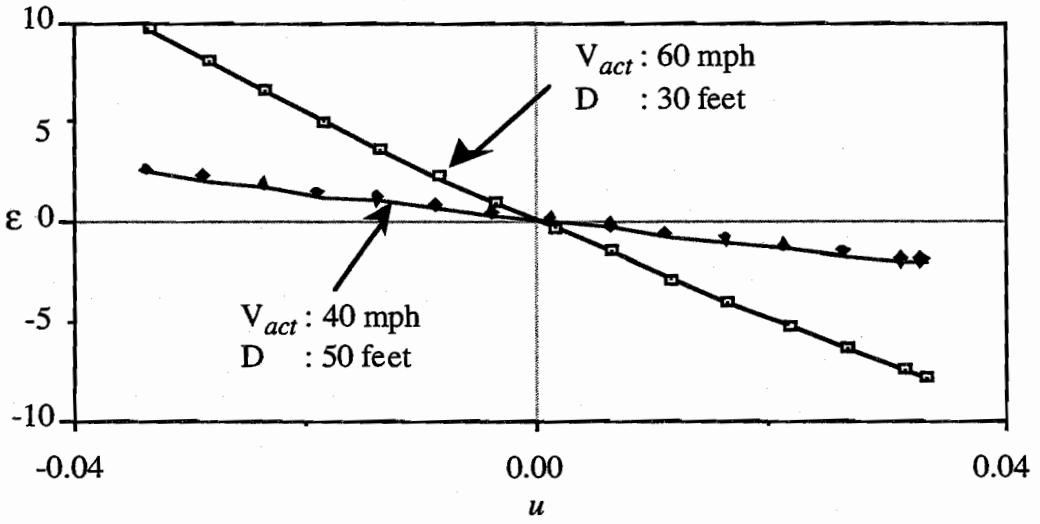

Figure A.7 Relationship between ε and u

Solving Eq(A.18) for u,

$$u = \frac{-\varepsilon D}{v_{act}^2 + \varepsilon v_{act}} \tag{A.20}$$

Differentiating both sides of Eq(A.20) with respect to ε,

$$\frac{du}{d\varepsilon} = \frac{-D}{(v_{act} + \varepsilon)^2} \tag{A.21}$$

The pdf of ε, $f_E(\varepsilon)$, is obtained simply by substituting Eqs(A.13), (A.14), and (A.21) in Eq(A.19),

$$f_E(\varepsilon) = [\kappa - \frac{\kappa^2}{v_{act}}(\frac{\varepsilon D}{v_{act} + \varepsilon})]\frac{D}{(v_{act} + \varepsilon)^2} \tag{A.22}$$

$$\text{for} \quad 0 \le \varepsilon \le \frac{v_{act}^2}{\kappa D - v_{act}}$$

$$f_E(\varepsilon) = [\,\kappa + \frac{\kappa^2}{v_{act}}\left(\frac{\varepsilon D}{v_{act}+\varepsilon}\right)\,]\frac{D}{(v_{act}+\varepsilon)^2} \qquad \text{for} \quad \frac{-v_{act}^2}{\kappa D + v_{act}} \le \varepsilon \le 0 \tag{A.23}$$

The boundary conditions of Eqs(A.22) and (A.23) can be derived by means of the boundary conditions of Eqs(A.13) and (A.14). For the case of Eq(A.22), substituting Eq(A.20) in Eq(A.13),

$$\frac{-1}{\kappa} \le \frac{-\varepsilon D}{v_{act}^2 + \varepsilon v_{act}} \le 0 \tag{A.24}$$

The right inequality, $\frac{-\varepsilon D}{v_{act}^2 + \varepsilon v_{act}} \le 0$, can be further separated into two sets of inequalities:

$$\varepsilon \ge 0 \quad \text{and} \quad \varepsilon + v_{act} \ge 0 \tag{A.25}$$

$$\text{or} \quad \varepsilon \le 0 \quad \text{and} \quad \varepsilon + v_{act} \le 0 \tag{A.26}$$

The only condition that satisfies both Eq(A.25) and Eq(A.26) is

$$\varepsilon \ge 0 \tag{A.27}$$

One can directly solve the left inequality , $\frac{-1}{\kappa} \le \frac{-\varepsilon D}{v_{act}^2 + \varepsilon v_{act}}$, for ε

$$\varepsilon \le \frac{v_{act}^2}{\kappa D - v_{act}} \tag{A.28}$$

The intersection of Eqs(A.27) and (A.28) gives the boundary condition of Eq(A.22).

For the case of Eq(A.23), substituting Eq(A.20) in Eq(A.14),

$$0 \le \frac{-\varepsilon D}{v_{act}^2 + \varepsilon v_{act}} \le \frac{1}{\kappa} \tag{A.29}$$

The left inequality, $0 \leq \frac{-\varepsilon D}{v_{act}^2 + \varepsilon v_{act}}$, can be rewritten using two sets of inequalities

$$\varepsilon \leq 0 \quad \text{and} \quad \varepsilon + v_{act} \geq 0 \tag{A.30}$$

$$\text{or} \quad \varepsilon \geq 0 \quad \text{and} \quad \varepsilon + v_{act} \leq 0 \tag{A.31}$$

The only condition that satisfies both Eq(A.30) and Eq(A.31) is

$$-v_{act} \leq \varepsilon \leq 0 \tag{A.32}$$

The right inequality, $\frac{-\varepsilon D}{v_{act}^2 + \varepsilon v_{act}} \leq \frac{1}{\kappa}$, can be directly solved for ε,

$$\frac{-v_{act}^2}{\kappa D + v_{act}} \leq \varepsilon \tag{A.33}$$

The intersection of Eqs(A.32) and (A.33) gives the boundary condition of Eq(A.23).

Speed Estimation Error Due to Distance Measurement Error

In addition to the above approach, speed estimation errors can be viewed from a totally different prospective. As described in Figure A.8, assume that at time frame i, a vehicle is located at position 1(p1), and at time frame i+1 it moved to position(p2). At time frames j, and j+1 the vehicle is at positions 3(p3) and 4(p4), respectively. The actual distance that a vehicle travels during one time frame is simply the product of vehicle actual speed, v_{act}, and one time frame duration, $\frac{1}{\kappa}$. The distance actually used to calculate the average travel speed is $d_2 - d_1 = D$. However, one can see from Figure A.8 that the actual distance a vehicle travels during time duration $t_{read_2} - t_{read_1}$ is $l_2 - l_1$ rather than D. These distance measurement errors will propagate in the calculation of speeds and result in speed estimation measurement errors.

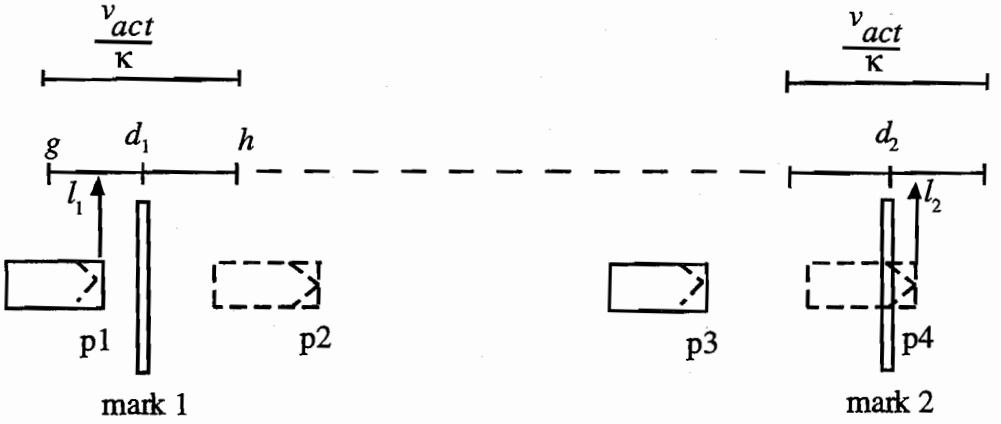

Figure A.8 Sketch of distance-location image of vehicles crossing fiducial marks

The procedures for deriving the speed measurement error pdf are similar to the first approach and are therefore briefly described here. The boundaries of region g and h are defined as

$$(g,h) = \left(d_1 - \frac{1}{2} * \frac{v_{act}}{\kappa},\ d_1 + \frac{1}{2} * \frac{v_{act}}{\kappa} \right) \tag{A.34}$$

l_1 and l_2 can be specified as follows:

$$l_1 = d_1 + \xi_1 \tag{A.35}$$

$$l_2 = d_2 + \xi_2 \tag{A.36}$$

Where

ξ_1 and ξ_2 are uniformly distributed random errors.

$$\xi_1 \sim U(-\frac{v_{act}}{2\kappa}, \frac{v_{act}}{2\kappa}) \tag{A.37}$$

$$\xi_2 \sim U(-\frac{v_{act}}{2\kappa}, \frac{v_{act}}{2\kappa}) \tag{A.38}$$

Rearranging Eqs(A.35) and (A.36) gives

$$l_2 - l_1 = (d_2 - d_1) + (\xi_2 - \xi_1) \tag{A.39}$$

Where

$l_2 - l_1$ is the actual travel distance from mark 1 to mark 2;

$d_2 - d_1$ is the distance actually used to calculate speed;

$\xi_2 - \xi_1$ is the random error associated with $l_2 - l_1$.

Let $\xi = \xi_2 - \xi_1$ $\qquad -\frac{v_{act}}{\kappa} \le \xi \le \frac{v_{act}}{\kappa}$ (A.40)

Similar to those procedures presented in Figures(A.2) to (A.5), the CDF of ξ is summarized as follows:

$$F(\xi) = 0 \qquad \xi \le -\frac{v_{act}}{\kappa} \tag{A.41}$$

$$= 0.5 + \frac{\kappa}{v_{act}}\xi + \frac{\kappa^2}{2v_{act}^2}\xi^2 \qquad -\frac{v_{act}}{\kappa} \le \xi \le 0 \tag{A.42}$$

$$= 0.5 + \frac{\kappa}{v_{act}}\xi - \frac{\kappa^2}{2v_{act}^2}\xi^2 \qquad 0 \le \xi \le \frac{v_{act}}{\kappa} \tag{A.43}$$

$$= 1.0 \qquad \frac{v_{act}}{\kappa} \le \xi \tag{A.44}$$

The pdf of ξ, $f(\xi)$, is then given as

$$dF(\xi)/d\xi = f(\xi) \qquad = \frac{\kappa}{v_{act}} + \frac{\kappa^2}{v_{act}^2}\xi \qquad -\frac{v_{act}}{\kappa} \le \xi \le 0 \tag{A.45}$$

$$= \frac{\kappa}{v_{act}} - \frac{\kappa^2}{v_{act}^2}\xi \qquad 0 \le \xi \le \frac{v_{act}}{\kappa} \tag{A.46}$$

Graphical presentation of $f(\xi)$ is shown in Figure A.9.

Similar to Eq(A.15), the relationship of actual and estimated speed is

$$v_{est} = v_{act} + \varphi \tag{A.47}$$

Where

φ is the random error term associated with estimated speed.

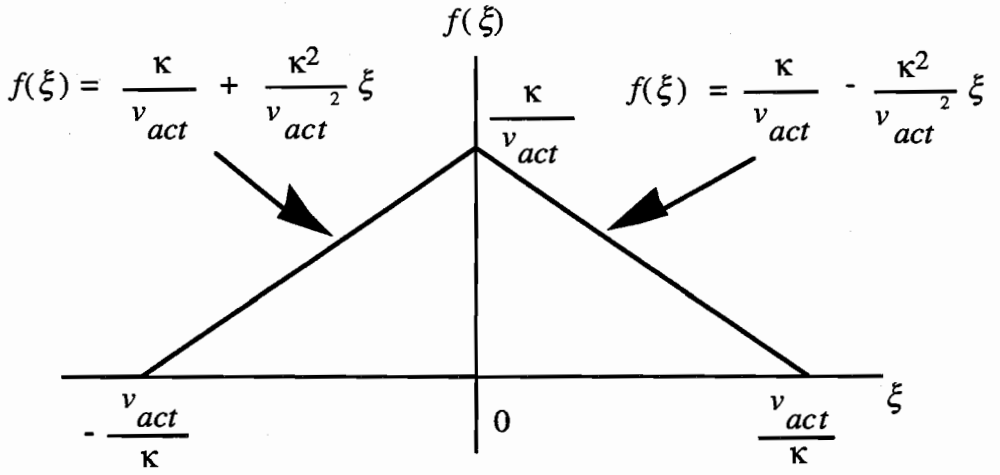

Figure A.9 Probability density function of distance measurement error

By definition, Eq(A.47) can be rewritten as

$$\frac{d_2 - d_1}{t_{read_2} - t_{read_1}} = \frac{(d_2 - d_1) + (\xi_2 - \xi_1)}{t_{read_2} - t_{read_1}} + \varphi \tag{A.48}$$

Replacing $d_2 - d_1$ with D and solving for φ

$$\varphi = \frac{-v_{act}\xi}{D + \xi} \tag{A.49}$$

Since Eq(A.49) is also a decreasing function of ξ, one still can apply the transformation method to obtain the pdf of φ, $f(\varphi)$. The results are shown as follows:

$$\begin{aligned} f(\varphi) &= \left[\frac{\kappa}{v_{act}} + \frac{\kappa^2}{v_{act}^2}\left(\frac{-\varphi D}{\varphi + v_{act}}\right) \right] \frac{D v_{act}}{(\varphi + v_{act})^2} \\ &= \left[\kappa - \frac{\kappa^2}{v_{act}}\left(\frac{\varphi D}{\varphi + v_{act}}\right) \right] \frac{D}{(\varphi + v_{act})^2} \end{aligned} \tag{A.50}$$

$$\text{Where } 0 \le \varphi \le \frac{v_{act}^2}{\kappa D - v_{act}}$$

$$f(\varphi) = [\ \frac{\kappa}{v_{act}} - \frac{\kappa^2}{v_{act}^2}(\frac{-\varphi D}{\varphi + v_{act}})\ ]\frac{Dv_{act}}{(\ \varphi + v_{act}\ )^2}$$

$$= [\ \kappa + \frac{\kappa^2}{v_{act}}(\frac{\varphi D}{\varphi + v_{act}})\ ]\frac{D}{(\ \varphi + v_{act}\ )^2} \qquad \text{(A.51)}$$

$$\text{Where } \frac{-v_{act}^2}{\kappa D + v_{act}} \leq \varphi \leq 0$$

Obviously, Eq(A.50) and (A.51) are identical to Eq(A.22) and (A.23) respectively. The boundaries of Eq(A.50) is derived as follows:

$$-\frac{v_{act}}{\kappa} \leq \xi \leq 0 \qquad \text{(A.52)}$$

Rewriting Eq(A.49) and substituting it to Eq(A.52) gives

$$-\frac{v_{act}}{\kappa} \leq \frac{-\varphi D}{\varphi + v_{act}} \leq 0 \qquad \text{(A.53)}$$

and thus

$$-\frac{1}{\kappa} \leq \frac{-\varphi D}{v_{act}^2 + \varphi v_{act}} \leq 0 \qquad \text{(A.54)}$$

Eq(A.54) is exactly identical to Eq(A.24). Similar procedures are applied for the derivation of the boundaries of Eq(A.51) as well

$$0 \leq \xi \leq \frac{v_{act}}{\kappa} \qquad \text{(A.55)}$$

$$0 \leq \frac{-\varphi D}{\varphi + v_{act}} \leq \frac{v_{act}}{\kappa} \qquad \text{(A.56)}$$

$$0 \leq \frac{-\varphi D}{v_{act}^2 + \varphi v_{act}} \leq \frac{1}{\kappa} \qquad \text{(A.57)}$$

Eq(A.57) is exactly identical to Eq(A.29).

In conclusion, probability density functions of speed estimation measurement errors and their boundary conditions derived from two different approaches are identical. This evidence indicates that the results obtained from mathematical approach are precise.

MONTE CARLO SIMULATION

In this appendix, Monte Carlo simulation was defined as a technique employing random variables to solve certain stochastic problems. In performing this technique to verify the probability function derived mathematically, the random variables, u_1 and u_2, were calculated using random variables generated from U(0, 1). Random variables u_1 and u_2 were further substituted in Eq(A.7) to calculate random variable u. Finally, u was substituted in Eq(A.18) to generate random variable ε. This process was repeated 10 times with 5500 samples for each repetition. Means of the repetitions were used in further analysis. By assuming κ is 30 frames/second; v_{act} is 50 mph; and D is 30 feet, a graphical comparison and a goodness-of-fit chi-square test between the frequency generated from both the theoretical probability function and the Monte Carlo simulation are shown in Figure A.10 and Table A.1, respectively.

The theoretical frequencies were calculated using the following equations.

$$P_r(0 \le \varepsilon \le t) = \frac{\kappa D t}{v_{act}(v_{act}+t)} - \frac{\kappa^2 D^2}{v_{act}}\left[\frac{1}{2v_{act}} - \frac{1}{v_{act}+t} + \frac{v_{act}}{2(v_{act}+t)^2}\right] \quad \text{(A.58)}$$

$$P_r(s \le \varepsilon \le 0) = \frac{-\kappa D s}{v_{act}(v_{act}+s)} - \frac{\kappa^2 D^2}{v_{act}}\left[\frac{1}{2v_{act}} - \frac{1}{v_{act}+s} + \frac{v_{act}}{2(v_{act}+s)^2}\right] \quad \text{(A.59)}$$

$$N(m, n) = \mathrm{N}^*[P_r(0 \le \varepsilon \le n) - P_r(0 \le \varepsilon \le m)] \quad \text{(A.60)}$$

$$N(p, q) = \mathrm{N}^*[P_r(p \le \varepsilon \le 0) - P_r(q \le \varepsilon \le 0)] \quad \text{(A.61)}$$

Where

$N(m, n)$ is the frequency between m and n, $n > m > 0$; and

$N(p, q)$ is the frequency between p and q, $p < q < 0$; and

N is the total sample size

Both graphical comparison and goodness-of-fit chi-square tests demonstrated very good agreement between the theoretical probability function and Monte Carlo simulation. The null hypothesis that there is no difference between theory and simulation output cannot be rejected at any reasonable significant level. These results imply that the derived probability density function of measurement error in estimating speed is precise.

However, time-base resolution, fiducial mark interval, and actual vehicle speed are not the only measurement error causes. The measurement error investigated in this paper is just the basic part of total measurement error. There are other factors such as data reduction techniques, parallax, and human error that jointly contribute to speed estimation accuracy.

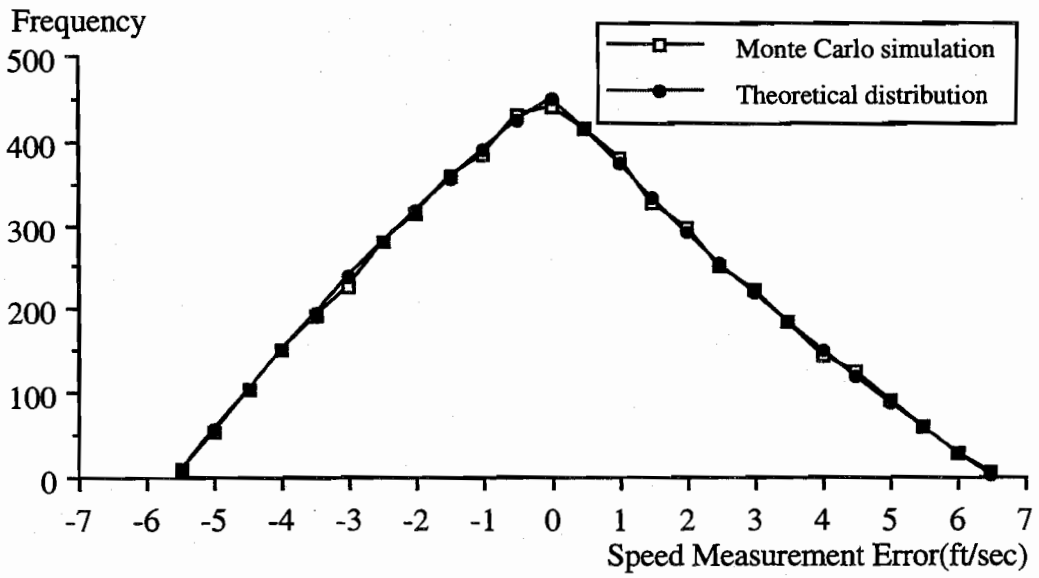

Figure A.10 Frequency curves of monte carlo simulation and theoretical distribution of speed measurement error

TABLE A.1 CHI-SQUARE TEST FOR MONTE CARLO SIMULATION AND THEORETICAL DISTRIBUTION

Number of simulation repetitions	10
Sample size of each repetition	5500
Vact	50 mph
κ	30 frame/sec
D	30 feet

Intervals (ft/sec)	Observations of Monte Carlo Simulation	Observation of Theoretical Distribution	(Nj-nPj)^2/nPj
< -5.25	10.0	9.3	0.053
-5.25 ~ -4.75	54.9	55.9	0.018
-4.75 ~ -4.25	104.0	104.6	0.003
-4.25 ~ -3.75	152.7	151.2	0.015
-3.75 ~ -3.25	191.2	195.8	0.108
-3.25 ~ -2.75	226.7	238.4	0.574
-2.75 ~ -2.25	281.9	279.2	0.026
-2.25 ~ -1.75	314.1	318.2	0.053
-1.75 ~ -1.25	360.4	355.6	0.065
-1.25 ~ -0.75	385.5	391.3	0.086
-0.75 ~ -0.25	432.0	425.4	0.102
-0.25 ~ 0.25	439.0	448.6	0.205
0.25 ~ 0.75	416.2	414.6	0.006
0.75 ~ 1.25	382.4	372.7	0.252
1.25 ~ 1.75	327.8	332.3	0.061
1.75 ~ 2.25	299.6	293.4	0.131
2.25 ~ 2.75	252.6	256.0	0.045
2.75 ~ 3.25	223.4	219.9	0.056
3.25 ~ 3.75	185.5	185.2	0.000
3.75 ~ 4.25	146.5	151.7	0.178
4.25 ~ 4.75	125.6	119.5	0.311
4.75 ~ 5.25	92.8	88.4	0.219
5.25 ~ 5.75	60.8	58.5	0.090
5.75 ~ 6.25	29.2	29.7	0.008
6.25 <	5.2	4.5	0.109
Degree of Freedom = 25 - 1 = 24		Calculated chi-square:	2.777
Critical chi-square value (24, 5%) = 36.415			

Conclusion:

Since 2.777 << 36.415, therefore fail to reject the null hypothseis that there is no significant difference between simulation and theoretical distribution

BIBLIOGRAPHY

Adebisi, O. (1982). "Driver Gap Acceptance Phenomena." Journal of Transportation Engineering Vol. 108, No. TE6, 676-688.

Adebisi, O. and Sama, G. N. (1989). "Influence of Stopped Delay on Driver Gap Acceptance Behavior." Journal of Transportation Engineering Vol. 115, No. 3, 305-315.

American Association of State Highway and Transportation Officials (AASHTO). (1990). A Policy on Geometric Design of Highway and Streets. Washington, D. C..

Ashworth, R. (1968). "A Note on the Selection of Gap Acceptance Criteria for Traffic Simulation Studies." Transportation Research Vol. 2, No. 2, 171-175.

Ashworth, R. (1969). "The Capacity of Priority-Type Intersections with a Non-Uniform Distribution of Critical Acceptance Gaps." Transportation Research Vol. 3, No. 2, 273-278.

Ashworth, R. (1970). "The Analysis and Interpretation of Gap Acceptance Data." Transportation Research Vol. 4, No. 3, 270-280.

Ashworth, R. (1976). "A Videotape-recording System for Traffic Data Collection and Analysis." Traffic Engineering + Control Vol. 17, No. 11, November, 468-470.

Beaket, J. (1938). "Acceleration and Deceleration Characteristics of Private Passenger Vehicles." Proceedings of the 18th Annual Meeting, Highway Research Board, 81-89.

Ben-Akiva, M. and Lerman, S. R. (1989). Discrete Choice Analysis: Theory and Application to Travel Demand. Cambridge: The MIT Press.

Blumenfeld, D. B. and Weiss, G. H. (1970). "On the Robustness of Certain Assumptions in the Merging Delay Problem." Transportation Research Vol. 4, No. 2, 125-139.

Blumenfeld, D. E. and Weiss, G. H. (1971). "Merging from an Acceleration Lane." Transportation Science Vol. 5, No. 2, 161-168.

Blumenfeld, D. B. and Weiss, G. H. (1973). "Gap Stability in the Light of Car-Following Theory." Transportation Research Vol. 7, No. 2, 199-205.

Blunden, W. R., Clissold, C. M., and Fisher, R. B. (1962). "Distribution of Acceptance Gaps for Crossing and Turning Manoeuveres." Proceedings Australian Road Research Board Vol. 1, Part 1, 188-205.

Buhr, J. H. (1966). Traffic Interaction in the Freeway Merging Process. Report 430-5, Texas Transportation Institute, Texas A&M University, College Station, Texas.

Buhr, J. H. (1967). "A Nationwide Study of Freeway Merging Operation." Highway Research Record 202, 76-122.

Cassidy, M. J., et al. (1990). A Proposed Analytical Technique for the Design and Analysis of Major Freeway Weaving Sections. Research Report UCB-ITS-RR-90-16, Institute of Transportation Studies, University of California, Berkeley, CA.

Catchpole, E. A. and Plank, A. W. (1986). "The Capacity of a Priority Intersection." Transportation Research B Vol. 20B, No. 6, 441-456.

Chandler, R. E., Herman, R., and Montroll, E. W. (1958). "Traffic Dynamics: Studies in Car Following." Operations Research Vol. 6, No. 2, 165-184.

Constantine, T. and Young, A. P. (1967). "Traffic Dynamics: Car Following Studies." Traffic Engineering & Control Vol. 8, No. 9, January, 551-554.

Daganzo, C. F. (1981). "Estimation of Gap Acceptance Parameters Within and Across the Population from Direct Roadside Observation." Transportation Research B Vol. 15B, No. 1, 1-15.

Darzentas, J. (1981). "Gap Acceptance: Myth and Reality." in Proceedings of the Eighth International Symposium on Transportation and Traffic Theory, V. F. Hurdle, ed., Toronto, Ontario, Canada, 175-192.

Dawson, R. F. (1964). Analysis of On-Ramp Capacities by Monte Carlo Simulation and Queuing Theory. Ph.D. Dissertation, Purdue University, Lafayette, Indiana.

Drew, D. R. (1967). "Gap Acceptance Characteristics for Ramp-Freeway Surveillance and Control." Highway Research Record 157, 108-143.

Drew, D. R., et al.(1967). "Gap Acceptance in the Freeway Merging Process." Highway Research Record 208, 1-36.

Drew, D. R., et al. (1968). "Determination of Merging Capacity and Its Application to Freeway Design and Control." Highway Research Record 244, 47-68.

Drew, D. R. (1971). Traffic Flow Theory and Control. New York: MaGraw-Hill Book Co.

Dubin, J. A. and Rivers, R. D. (1988). Users Guide of STATISTICAL SOFTWARE TOOLS Version 2.0.

Edie, L. C. (1961). "Car-Following and Steady-State Theory for Noncongestion Traffic." Operations Research Vol. 9, No. 1, 66-76.

Evans, D. H. and Herman, R. (1964). "The Highway Merging and Queuing Problem." Operations Research Vol. 12, No. 6, 832-857.

Fitzpatrick, K. (1991). "Gap Accepted at Stop-Controlled Intersections." Transportation Research Record 1303, 103-112.

Forbes, T. W. (1963). "Human Factor Considerations in Traffic Flow Theory." Highway Research Record 15, 60-66.

Fox, P. and Lehman, F. G. (1967). "A Digital Simulation of Car-Following and Overtaking." Highway Research Record 199, 33-41.

Fukutome, I. and Moskowitz, K. (1959). "Traffic Behavior and On-Ramp Design." Highway Research Board Bulletin 235, 38-72.

Gafarian, A. V. and Walsh, J. E. (1970). "Method for Statistical Validation of a Simulation Model for Freeway Traffic Near an On-Ramp." Transportation Research Vol. 4, No. 4, 379-384.

Gajarati, D. N. (1988). Basic Econometrics. Singapore: McGraw-Hill Book Co..

Gazis, D. C., Herman, R., and Potts, R. B. (1959). "Car-Following Theory of Steady-State Traffic Flow." Operations Research Vol. 7, No. 4, 499-505.

Gazis, D. C., Herman, R., and Rothery, R. W. (1961). "Nonlinear Follow-the Leader Models of Traffic Flow." Operations Research Vol. 9, No. 4, 545-567.

Gerlough, D. L. and Huber, M. J. (1975). Traffic Flow Theory: A monograph. Special Report 165, Transportation Research Board, National Research Council, Washington, D. C..

Gipps, P. G. (1981). "A Behavioural Car-Following Model for Computer Simulation." Transportation Research B Vol. 15B, No. 2, 105-111.

Glickstein, A., Findley, L. D., and Levy, S. L. (1961). "Application of Computer Simulation Techniques to Interchange design Problems." Highway Research Board Bulletin 291, 139-162.

Golias, J. C. (1981). "Waiting to Cross a Major Stream at An Uncontrolled Road Junction." in Proceedings of the Eighth International Symposium on Transportation and Traffic Theory, V. F. Hurdle, ed., Toronto, Ontario, Canada, 292-320.

Golias, J. C. and Kanellaidis, G. C. (1990). "Estimation of Driver Behavior Model Parameters." Journal of Transportation Engineering Vol. 116, No. 2, 153-166.

Gordon, D. A. and Michaels, R. M. (1963). "Static and Dynamic Visual Fields in Vehicular Guidance." Highway Research Record 84, 1-15.

Gourlay, S. M. (1948). "Merging Traffic Characteristics Applied to Acceleration Lane Design." in Studies of Weaving and Merging Traffic: A Symposium. Technical Report No. 4, Bureau of Highway Traffic, Yale University, 61-77.

Haight, F. A., Bisbee, E. F., and Wojcik, C. (1962). "Some Mathematical Aspects of the Problem of Merging." Highway Research Board Bulletin 356, 1-14.

Han, A. F. and Daganzo, C. F. (1982). Estimation of Gap Acceptance Parameters: Sequential vs. Simultaneous Methods in Light Poisson Traffic. Research Report, Institute of Transportation Studies, University of California, Berkeley, CA.

Hanfen, A. F. (1965). A Method and a Model for the Analysis and Description of Car-Following Performance. Report No. 202-B-2, Engineering Experiment Station, The Ohio State University, Columbus, Ohio.

Herman, R. and Rothery, R. W. (1963). "Car Following and Steady State Flow." in Proceedings of the Second International Symposium on the Theory of Road Traffic Flow, J. almond ed., London, published by OECD (1965), Paris, 1-11.

Herman, R. and Weiss, G. (1961). "Comments on the Highway-Crossing Problem." Operations Research Vol. 9, No. 6, 828-840.

Hewitt, R. H. (1983). "Measuring Critical Gap." Transportation Science Vol. 17, No. 1, 87-109.

Hewitt, R. H. (1985). "A Comparison between Some Methods of Measuring Critical Gap." Traffic Engineering + Control Vol. 26, No. 1, January, 13-22.

Heyes, M. P. and Ashworth, R. (1972). "Further Research on Car-Following Models." Transportation Research Vol. 6, No. 3, 287-291.

Highway Capacity Manual (1985). special Report 209, Transportation Research Board, Washington, D. C..

Horowitz, J. L. (1982). "Statistical Estimation of the Parameters of Daganzo's Gap Acceptance Model." Transportation Research Vol. 16B, No. 5, 373-381.

Huberman, M. (1982). "The Development and Evaluation of a Technique for Measuring Vehicle Acceleration on Highway Entrance Ramps." RTAC FORUM Vol. 4, No. 2, 90-96.

Hughes, B. P. (1989). "So You Think You Understand Gap Acceptance!." Australian Road Research 19(3), 195-204.

Hurst, P. M., Perchonok, K., and Seguin, E. L. (1965). Measurement of Subjective Gap Size. Report Number 7, Division of Highway Studies, Institute for Research, State College, Pennsylvania.

Johnston, J. (1991). Econometric Methods. Singapore: McGraw-Hill Book Co..

Jou, R. C. (1994). A Model of Dynamic Commuter Behavior Incorporating Trip-chaining. Ph.D. Dissertation, The University of Texas at Austin.

Kikuchi, S. and Chakroborty, P (1992). "Car-Following Model Based on Fuzzy Inference System." Transportation Research Record 1365, 82-91.

Kimber, R. M. (1989). "Gap-Acceptance and Empiricism in Capacity Prediction." Transportation Science Vol. 23, No. 2, 100-111.

Kita, H. (1993). "Effects of Metering Lane Length on the Merging Behavior at Expressway On-Ramp." in Proceedings of the Twelfth International Symposium on the Theory of Traffic Flow and Transportation, Berkeley, California, 37-51.

Kmenta, J. (1971). Elements of Econom strics. New York: Macmillan Publishing Co., Inc.

Knox, D. W. (1964). "Merging and Weaving Operations in Traffic." Australian Road Research Vol. 2, No. 2, 10-20.

Kou, C. C. and Machemehl, R. B. (1996a). "Modeling Vehicle Acceleration-deceleration Behavior During Merge Maneuvers." in Proceedings of the Canadian Society for Civil Engineering 1st Transportation Specialty Conference, Edmonton, Alberta, Canada, Vol IIIa, 267-279.

Kou, C. C. and Machemehl, R. B. (1996b). "Probabilistic Measurement Errors in Vehicle Speed Estimation Through Video Images." in Proceedings of the Canadian Society for Civil Engineering 1st Transportation Specialty Conference, Edmonton, Alberta, Canada, Vol IIIa, 291-302.

Kou, C. C. and Machemehl, R. B. (1997a). "Probabilistic Aspect of Data Quality in Speed Estimation Through Video Image Technique." in Proceedings of the 9th Conference on the Scientific Use of Statistical Software, Heidelberg, Germany.

Kou, C. C. and Machemehl, R. B. (1997b). "Probabilistic Speed-Estimation Measurement Errors Through Video Images." Journal of Transportation Engineering Vol. 123, No. 2, 136-141.

Lam, S. H. (1991). Multinomial Probit Model Estimation: Computational Procedures and Applications. Ph.D. Dissertation, The University of Texas at Austin.

Lee, J. and Jones, J. H. (1967). "Traffic Dynamics: Visual Angle Car Following Models." Traffic Engineering & Control Vol. 9, No. 7, November, 348-350.

Levin, M. (1970). Some Investigations of the freeway Lane Changing Process. Ph.D. Dissertation, Texas A&M University, College Station, Texas.

Liu, Y. H. (1996). "User's Manual for Multinomial Probit Estimation Tool - Workstation Version." Department of Civil Engineering, The University of Texas at Austin.

Loutzenheiser, D. W. (1938). "Speed-Change Rates of Passenger Vehicles." Proceeding of the 18th Annual Meeting, Highway Research Board, 90-99.

Lyons, T. J., et al. (1988). "Fuel and Time Implications of Merging Traffic at Freeway Entrances." Applied Mathematics Modelling Vol. 12, 226-237.

Madanat, S. M., Cassidy, M. J., and Wang, M. H. (1994). "Probabilistic Delay Model at Stop-Controlled Intersection." Journal of Transportation Engineering Vol. 120, No. 1, 21-36.

Mahmassani, H. S. and Sheffi, Y. (1981). "Using Gap Sequences to Estimate Gap Acceptance Functions." Transportation Research B Vol. 15B, No. 3, 143-148.

Mahmassani, H. S. (1996). "Advances in Transportation Demand Analysis." CE 391E Class Notes, Department of Civil Engineering, The University of Texas at Austin.

Makigami, Y., Adachi, Y., and Sueda, M. (1988). "Merging Lane Length for Expressway Improvement Plan in Japan." Journal of Transportation Engineering Vol. 114, No. 6, 718-734.

Makigami, Y. and Matsuo, T. (1990). "A Merging Probability Calculation Method Considering Multiple Merging Phenomena." in Proceedings of The Eleventh International Symposium of Transportation and Traffic Theory, M. Koshi, ed., Tokyo, Japan, 21-38.

Makigami, Y. and Matsuo, T. (1991). "Evaluation of Outside and Inside Expressway Ramps Based on Merging Probability." Journal of Transportation Engineering Vol. 117, No. 1, 57-70.

May, A. D. and Keller, H. E. M. (1967). "Non-Integer Car-Following Models." Highway Research Record 199, 19-32.

Maze, H.T. (1981). "A Probabilistic Model of Gap Acceptance Behavior." Transportation Research Record 795, 8-13.

McNeil, D. R. and Morgan, J. H. T. (1968). "Estimating Minimum Gap Acceptances for Merging Motorists." Transportation Science Vol. 2, No. 3, 265-277.

McNeil D. R. and Smith, J. T. (1969). "A Comparison of Motorist Delays for Different Merging Strategies." Transportation Science Vol. 3, No. 3, 239-253.

Merrill, Jr., W. J. and Bennett, C. A. (1956). "The Application of Temporal Correlation Techniques in Psychology." The Journal of Applied Psychology Vol. 40, No. 4, 272-280.

Michaels, R. M. and Cozan, L. W. (1963). "Perceptual and Field Factors Causing Lateral Displacement." Highway Research Record 25, 1-13.

Michaels, R. M. (1963). "Perceptual Factors in Car Following." in Proceedings of the Second International Symposium on the Theory of Traffic Flow, J. Almond, ed., London, Published by OECD (1965), Paris, 44-59.

Michaels, R. M. and Fazio, J. (1989). "Driver Behavior Model of Merging." Transportation Research Record 1213, 4-10.

Miller, A. (1972). "Nine Estimators of Gap-Acceptance Parameters." in Proceedings of the Fifth International Symposium on the Theory of Traffic Flow and Transportation, G. F. Newell, ed., 215-235.

Mine, H. and Mimura, T. (1969). "Highway Merging Problem with Acceleration Area." Transportation Science Vol. 3, 205-213.

Olson, P. L., et al. (1984). Parameters Affecting Stopping Sight Distance. NCHRP Report 270, TRB, National Research Council, Washington, D.C.

Pahl, J. (1972). "Gap-Acceptance Characteristics in Freeway Traffic Flow." Highway Research Record 409, 57-63.

Palamarthy, S. (1993). Models of Pedestrian Crossing Behavior at Signalized Intersections. M.S. Thesis, The University of Texas at Austin.

Pant, P. D. and Balakrishnan, P. (1994). "Neural Network for Gap Acceptance at Stop-Controlled Intersections." Journal of Transportation Engineering Vol. 120, N0. 3, 423-446.

Pearson, R. H. and Ferreri, M. G. (1961). "Operational Study-Schuylkill Expressway." Highway Research Board Bulletin 291, 104-123.

Perchonok, P. A. and Levy, S. L. (1960). "Application of Digital Simulation Techniques to Freeway On-Ramp Traffic Operations." Proceedings of the 39th Annual Meeting Highway Research Board Vol. 39, 506-523.

Pinnell, C. (1960). "Driver Requirements in Freeway Entrance Ramp Design." Traffic Engineering Vol. 31, N0. 3, 11-17.

Pipes, L. A. (1967). "Car Following Models and the Fundamental Diagram of Road Traffic." Transportation Research Vol. 1, No. 1, 21-29.

Polus, A., Livneh, M., and Factor, J. (1985). "Vehicle Flow Characteristics on Acceleration Lanes." Journal of Transportation Engineering Vol. 111, No. 6, 595-606.

Polus, A. and Livneh, M. (1987). "Comments on Flow Characteristics on Acceleration Lanes." Transportation Research Vol. 21A, No. 1, 39-46.

Raff, M. S. (1950). A Volume Warrant for Urban Stop Signs. The Eno Foundation for Highway Traffic Control.

Ramsey, J. B. H. and Routledge, I. A. (1973). "A New Approach to the Analysis of Gap Acceptance Time." Traffic Engineering + Control Vol. 15, No. 7, July, 353-357.

Reilly, W. R., et al. (1989). Speed-Change Lanes. Final Report NCHRP 3-35, Transportation Research Board, Washington, D. C..

Rockwell, T. H., Ernst, R. L., and Hanken, A. (1968). "A Sensitivity Analysis of Empirically Derived Car-Following Models." Transportation Research Vol. 2, No. 4, 363-373.

Salter, R. J. and El-Hanna, F. I. H. (1976). "Highway Ramp Merging Examined by Simulation." Australian Road Research Vol. 6, No. 2, 30-39.

Shin, C. H. (1993). The Effect of Acceleration Lanes on Entrance Ramp Operation. Ph.D. Dissertation, Polytechnic University, Brooklyn, New York.

Sinha, K. C. and Dawson, R. F. (1970). "The Development and Validation of a Freeway Traffic Simulator." Highway Research Board 308, 34-47.

Sivak, M. (1987). "Driver Reaction Times in Car-Following Situations." *Public Health Reviews*, 15, 265-274.

Skabardonis, A. (1985). "Modelling the Traffic Behaviour at Grade-Separated Interchanges." Traffic Engineering + Control Vol. 26, No. 9, September, 410-415.

Solberg, P. and Oppenlander, J. D. (1966). "Lag and Gap Acceptance at a Stop-Controlled Intersection." Highway Research Record 118, 48-67.

SPSS® Advanced Statistics User's Guide (1990). Chicago, Illinois: SPSS Inc..

Strickland, R. I. (1948). "A Study of Merging Vehicular Traffic Movements." in Studies of Weaving and Merging Traffic: A Symposium. Technical Report No. 4, Bureau of Highway Traffic, Yale University, 81-101.

Sullivan, E. C., Chatziioanou, A., and Devadoss, N. (1995). "Developing On-Ramp Speed and Acceleration Profiles: Inputs to Estimating Emissions During Metering." presented in Transportation Research Board 74th Annual Meeting, Washington, D.C.

Szwed, N. and Smith, N. M. H. (1972). " Simulation of the Merging Process." Proceeding Australian Road Research Board Vol. 6, Part 3, 77-99.

Szwed, N. and Smith, N. M. H. (1974). " Gap Acceptance and Merging." Proceeding Australian Road Research Board Vol. 7, Part 4, 126-151.

Theophilopoulos, N. A. (1986). A Turbulence Approach at Ramp Junction. Ph.D. Dissertation, Polytechnic University, Brooklyn, New York.

Tong, C. C. (1990). A Study of Dynamic Departure Time and Route Choice Behavior of Urban Commuters. Ph.D. Dissertation, The University of Texas at Austin.

Transportation and Traffic Engineering Handbook (1982). Institute of Transportation Engineers, Englewood Cliffs, New Jersey: Prentice-Hall, Inc..

Uber, C. B. and Hoffmann, E. R. (1988). "Effect of Approaching Vehicle Speed on Gap Acceptance." in Proceedings of 14th ARRB Conference, Part 2, 118-124.

Walker, N. and Catrambone, R. (1993). "Aggregation Bias and the Use of Regression in Evaluating Models of Human Performance." Human Factors 35(3), 397-411.

Wallman, C. G. (1976). "Simulation of Traffic Flow at Grade-Separated Interchanges." Traffic Engineering + Control Vol. 17, No. 10, October, 406-409.

Wattleworth, J. A., et al. (1967). "Operational Effects of Some Entrance Ramp Geometrics on Freeway Merging." Highway Research Record 208, 79-122.

Weiss, G. H. and Maradudin, A. A. (1962). "Some Problems in Traffic Delay." Operations Research Vol. 10, No. 1, 74-104.

Weiss, G. H. (1967). "The Intersection Delay Problem with Gap Acceptance Function Depending on Speed and Time." Transportation Research Vol. 1, No. 4, 367-371.

White, F. S. (1961). Annotated Bibliography on Gap Acceptance and Its Applications, Report 430-7, Texas Transportation Institute, Texas A&M University, College Station, Texas.

Worrall, R. D., et al. (1967). "Merging Behavior at Freeway Entrance Ramps: Some Elementary Empirical Considerations." Highway Research Record 157, 77-106.

Yashiro, A. and Kotani, M. (1986). "The Analysis of Traffic Behaviour Using a Kiteballoon." in Proceedings of the 13th ARRB 5th REAAA Combined Conference Vol. 13, Part 7, 26-33.